This is to certify that the

dissertation entitled

AN EXPERIMENTAL INVESTIGATION OF THE OPTIMUM JOINING AND REPAIR OF COMPOSITE STRUCTURES

presented by

Kristin Beth Zimmerman

has been accepted towards fulfillment
of the requirements for

Ph.D. degree in Engineering Mechanics

Dahsin Liu
Major professor

Date April 15, 1993

AN EXPERIMENTAL INVESTIGATION OF THE OPTIMUM JOINING AND REPAIR OF STRUCTURAL COMPOSITES

By

Kristin Beth Zimmerman

A DISSERTATION

Submitted to

Michigan State University

in partial fulfillment of the requirements

for the degree of

DOCTOR OF PHILOSOPHY

Department of Materials Science and Mechanics

1993

ABSTRACT

AN EXPERIMENTAL INVESTIGATION OF THE OPTIMUM JOINING AND REPAIR OF DAMAGED STRUCTURAL COMPOSITES

By

Kristin Beth Zimmerman

Because of their high stiffness-to-weight and high strength-to-weight ratios, composite materials are rapidly gaining acceptance in today's aerospace industry. As the technology associated with the utilization of composite materials matures, it is transferred to many other industries such as the automotive industry. The primary problems that need to be addressed in composite structure designs include a thorough understanding of the characteristics of composites, as well as the repairability of such materials.

The composite materials under investigation are being developed for the automotive industry, therefore repair techniques must be established to facilitate the expanding use of automotive structural composite components. Current repair techniques involve: (1) determining the damage mode, (2) selecting the joining technique and geometry, (3) choosing an adhesive that is compatible with the matrix material, (4) applying reinforcement patches to both sides of the damaged zone, and (5) assessing the strength of the repaired composites.

Three different types of composite panels are analyzed. They consist of a chopped glass fiber in a polyester matrix, a continuous glass mat in a vinylester matrix, and a cross-woven fabric chemically bonded to randomly oriented glass fibers in a vinylester

matrix. These three samples exemplify most of the composite materials utilized by the automotive industry.

Artificial damage modes created in the laboratory are used to simulate real composite damage. Various repair parameters are explored to repair these artificial damage modes. Results show that by careful selection of geometrical bond line configuration, scarf angle, filler, and reinforcing patch material, 100% of the composite material's strength can be restored. Three-point bending is utilized to assess the restored strengths of the composites. Results show that the bond line geometry between two separated specimen parts plays a critical role in the joining efficiency and repair strength of composite materials.

Based on this research, the fundamental techniques for composite joining and repair are achieved and the development of an optimal design for superior joining efficiency and repair strength becomes possible.

This dissertation is dedicated to my parents John C. and Jacquelyn L. Zimmerman for their relentless, caring, generosity and support throughout my educational career.

There are a few particular phrases that I remember and live by. They state,

> The secret of success in life
> is to be ready when your opportunity comes,
> and do not be afraid to venture, since nothing
> ventured, nothing gained.

Another adage states,

> A mediocre person knows **something** happened
> A brilliant person knows **what** happened, but
> A genius knows **why** it happened.

Thank-you mother and dad for instilling in me that the world is out there just waiting for me. And that I can do whatever I set my mind to.

I'd also like to state a special dedication to my grandfather Lawrence E. Bredahl. A true educational role model, and a true Michigan State University Spartan!

ACKNOWLEDGEMENTS

The author would like to thank Michigan Materials and Processing Institute for their financial support.

The author would also like to thank her Ph.D. committee members, Dr. Gary L. Cloud, Dr. Kalinath Mukherjee, and Dr. Paul M. Parker, for their support and cooperation during this project.

A special acknowledgement goes out to my advisor Dr. Dahsin Liu for his unending time, support, and true friendship...........And for setting off the spark in me to pursue the very challenging research regarding the repairability of composite materials.

TABLE OF CONTENTS

Page

Page

Page

LIST OF TABLES

Page

Page

TABLES CORRESPONDING TO CHAPTER 7:

LIST OF FIGURES

Page

CHAPTER 7

Page

CHAPTER 1

INTRODUCTION

Composite material components are rapidly gaining acceptance in today's aerospace and automotive industries. This is primarily a result of their high stiffness-to-weight and strength-to-weight ratios. The technology associated with the utilization of composite materials is slowly maturing, therefore the need for fundamental knowledge regarding composite materials is pertinent. With the knowledge in hand, many questions regarding the fundamental characteristics of composite materials can be addressed.

1.1 Composite Materials

This introduction is intended to give a very general understanding of composite materials, i.e., what they are, how they work, and how they are used. Subsequent sections will describe the fundamental mechanisms of composite repair in much more detail.

A thorough definition of composite materials is found in volume 1 of the Engineered Materials Handbook on Composite Materials [1], it states, "Composite material is a combination of two or more materials (reinforcing elements, fillers, and composite matrix binder), differing in form or composition on a macro-scale. The constituents retain their identities; that is, they do not dissolve or merge completely into one another although they act in concert. Normally the components can be physically identified and exhibit an interface between one another."

Composites such as cellulose, asbestos, and glass fibers with organic resins have been used since before World War II. These early composites were the precursors to the advanced composites developed today. Advanced composites are similar to their early version, except the reinforcing fiber is much stiffer, i.e., has a higher elastic modulus. A comparative example of typical moduli for unidirectional composites is outlined in Table 1.1 [2].

A unique property of composite materials is their anisotropy. Conventional metals on the other hand are isotropic, meaning their strength and stiffness are independent of the direction of loading. If a metal structure is deformed too far, it stays deformed. A composite's anisotropy means that it can have a strength and stiffness 15 and 30 times greater, respectively, in one direction over another. If it is deformed too far, it breaks. Table 1.2 illustrates the diversity of properties between graphite fiber and epoxy resin which are frequently used for composites [2].

Composites follow what is referred to as the rule of mixtures. For example, if half of the volume is fiber and half resin, the composite properties will be the average of the two individual properties. Therefore, knowing the volume fraction is very important in both the design and repair of composite structures. For example, according to the numbers in Table 1.2, if loading is applied along a sample exclusively made up of fiber, then the tensile strength equals 300,000 psi. However, if half the volume is resin, the tensile strength is approximately:

$$\frac{300{,}000 + 20{,}000}{2} = 160{,}000 \text{ (psi)}$$

Table 1.1 Comparison of Typical Reinforcing Fibers and Their Moduli [2].

REINFORCEMENT	MODULUS, (10^6) PSI
Canvas (cellulose)	0.5
Asbestos	2
Continuous Glass	6
Aramid	10
Graphite	15
Boron	25

Table 1.2 Comparison of Fiber and Matrix Properties [2].

	GRAPHITE FIBER	**EPOXY RESIN**
Tensile Strength (PSI)	300,000	20,000
Tensile Modulus (PSI)	30×10^6	0.5×10^6
Specific Gravity	2.1	1.1
Thermal Expansion (in/in/°F)	-3×10^{-6}	$+400 \times 10^{-6}$
Temperature Limit (°F)	2,000	300

In addition, pulling at 90° to the fibers is the same as pulling on only the resin. Therefore, the tensile strength of the sample is 10,000 psi since half of the volume is fibers.

The purpose of the resin is to hold the fibers in place and to transfer loads from one fiber to another. Since composites exhibit low shear strength properties, they are consequently, designed to minimize shear loading of internal load transfer via shear. Figure 1.1 illustrates the shear strength phenomenon.

The vast difference between the properties of fiber and resin lends to a design flexibility not possible with isotropic metals. For example, the design of a helicopter rotor blade demands very high loads in the blade's length direction because of its need to withstand centripetal forces. Loads across the width are not equally significant. A solid metal blade would have the same strength in all directions, therefore its width direction is overdesigned. To design the same blade out of composite materials, most of the fibers would run the length of the blade and very few across the width. Therefore, the composite blade is tailored to the direction of loading while providing adequate strength and a large reduction of weight [2].

Since polymer composites follow the rule of mixtures, they can be designed to optimize directional stiffnesses. If the same amount of fibers run at both 0° and 90° then the strength will be the same in both directions. Strength at any angle away from the fiber axis will decrease and will be approximately equal to the strength along the axis times a function of the angle [2]. The largest deviation from the fiber axis, for

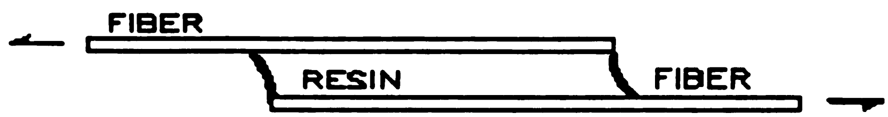

Figure 1.1 Schematic Illustrating Shear Strength Phenomena.

a plane-woven fabric, is 45°. Therefore the strength is reduced from that of the uni-directional fiber direction. Consequently, when designing composites structures, it is most advantageous to identify the direction of loading and strictly design strength and stiffness to that direction.

Continuity of fibers results in anisotropy while discontinuity or random fibers result in stress concentrations. For example, mechanical joints, such as bolt holes, are difficult to design because of the unique free edge effects which do not exist in conventional metals. In addition, any hole cut through fibers will produce a stress concentration or a weakness [2]. Figure 1.2 illustrates the effects of a bolt hole in a bi-directional composite. The result is similar to designing a uni-directional laminate with loads at 90° to the fibers. A common design technique for alleviating the stress concentrations at and around bolted joints is to design and specify fibers at +/- 45° to the load as illustrated in Figure 1.3. Another common technique for designing bolted joints is to move the hole further away from the edge so more fibers can absorb the load before the bolt can pull out. Bolted joints are used frequently, but they often introduce complicated fabrication problems as well as added weight [2]. Also, it should be noted that with bolted joints and riveted joints, the compressive loads developed during torque down and "bucking" often create delamination in the composite material.

The added weight and fabrication problems of bolted joints leads to the introduction of bonded joints. Bonded joints are frequently used and the design and manufacturing procedures are the same as those for bonding metals, except surface preparation is easier. With the introduction of bonded joints comes the introduction of

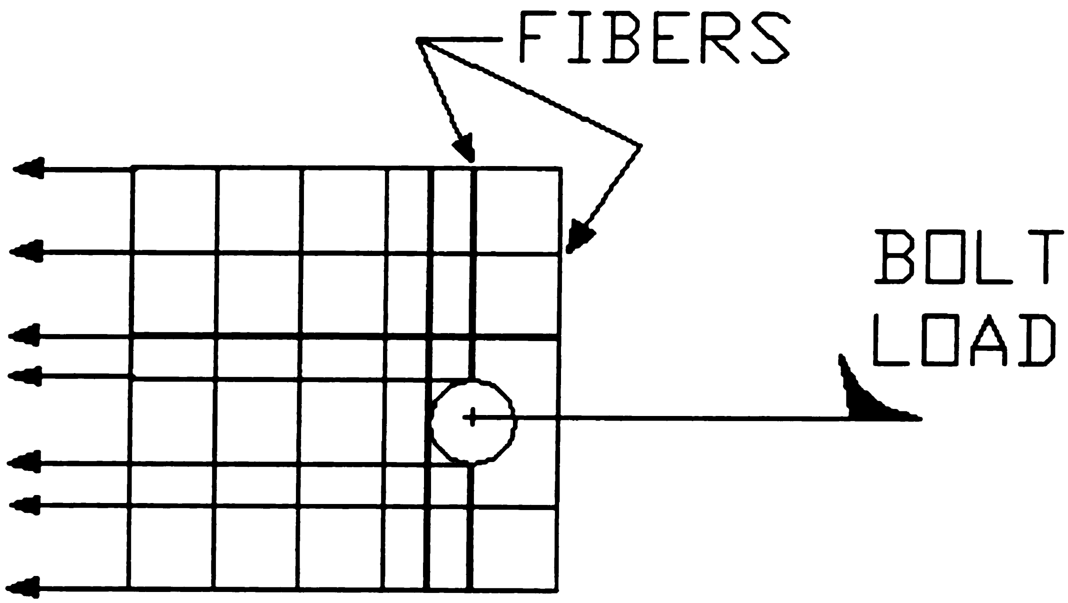

Figure 1.2 A Bolt-Hole in a Bi-Directional Composite Laminate.

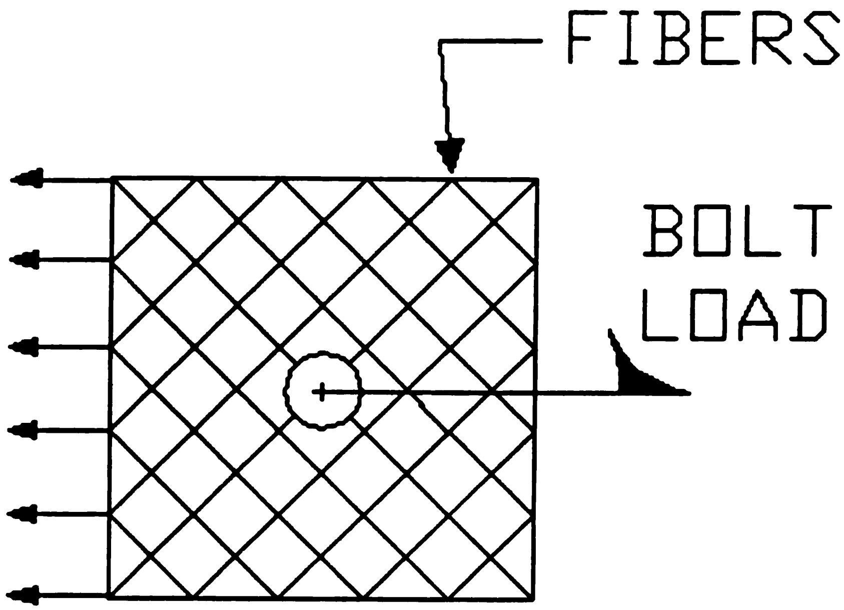

Figure 1.3 Tailoring the Composite Laminate Around a Bolt Hole.

resins and adhesives used during repair. An important parameter to consider when selecting an optimum adhesive system is its temperature usability and capability.

Temperature is a true design constraint in that the resin will degrade if the operating or design temperature is too high. Some temperature regimes for resins are listed below:

1. epoxy - up to 300 °F
2. bismaleimide - up to 450 °F
3. polyimide - up to 600 °F

All three regimes are utilized frequently because of the ever increasing need for more durable adhesives. However, it should be noted that processing sophistication and cost increase with temperature.

The resins listed above are thermosetting resins. They set into a solid and form an infusible mass when properly catalyzed and heated. However, they can encounter difficulties from moisture and other solvents [2]. About 1% by weight of water will diffuse into thermosetting resins. Moisture acts as a plasticizer, therefore reducing the mechanical properties of the resin. It also causes micro-cracking, much like fatigue loading, if the composite is repeatedly heated and cooled. Paint and edge sealants minimize moisture transport into and away from the composite, but nothing completely eliminates the effect [2]. Thermoplastic resins, i.e., PEEK, have been evaluated as substitutes or replacements for epoxy and other thermosetting resins. These resins are currently used for organic matrix composites, and they can be repeatedly heated and reformed. They absorb very little moisture, however they are attacked by hydrocarbon solvents.

Fabrication of organic matrix materials is very important to the overall aspect of composite design and repair. Distinctive features in the fabrication of thermoset composites are the critical processing parameters of time, pressure, and temperature during the cure cycle. All of these parameters determine the mechanical properties of the molded laminate. The same chemical processing takes place during bonded or laminated repair.

Monomers, i.e., small molecular units, are the building blocks of polymers. Resins are created by chemically combining between 50 to 100 monomers into one big chain. These chains are then bonded to dry fiber and presented as the product called "prepreg" [2]. Prepregging is simply the application of resin to dry fiber. It is often available in sheet form and most advanced composite laminate structures are formed through the use of preimpregnated fibers. The fabricators receive prepreg, form it into a shape, and cure it to keep that shape. The polymer changes from a liquid to a solid by forming chemical bonds between polymers. These bonds form in two different ways: by extending the length of the starting polymer chains and by forming bonds between chains. The bonds between the chains, i.e., cross links, determine the temperature resistance and brittleness of the resin.

The cure cycle is also critical since it must allow any entrained air, residual solvent, absorbed water or water produced as part of the chemical processing, to escape or to remain inside as a condensed liquid. Voids, and reduced laminate strength, are the result of not controlling the volatiles. The cure cycle must allow for:

1. trapped air to escape,
2. moisture or other solvents to escape or be kept in the liquid state,
3. excess resin to be squeezed out,
4. the mass of fibers and resin to be compacted, and,
5. the resin polymers, hardeners, catalysts, additives, etc., to chemically react to form a specified solid, dense mass.

Cure cycles are typically specified by time, temperature, and pressure.

The increased use of composites has introduced questions concerning cost effectiveness. Many studies and case histories show a 20% cost reduction in the manufacturing of composite parts over metals. This cost reduction is primarily due to the reduction of assembly time. Assembly time is typically four times greater than fabrication time. This is what makes composites more cost effective compared to metals.

1.2 Composite Repair

One of the primary questions regarding the utilization and implementation of composites is their repairability. Many techniques have already been developed to investigate composite repair [3-12]. However, new composite materials are being developed and employed at a steady pace thus creating the necessity for a systematic repair study to restore the strength of damaged composites. A general sequence of questions to address regarding the repairability of composite structures are:

1. to find the damage,
2. to define the extent of the damage,

3. to calculate damage effects and,
    a) to use as is,
    b) to design a repair scheme,
    c) to scrap the part,

4. to specify the repair method if repair is the option,

5. to accomplish the repair,

6. to evaluate the repaired structure.

Evaluating composite damage follows two modes, that of visual inspection, and that achieved by an overhaul. Visual inspection occurs frequently and with good success, but the visually hidden defects, such as those hidden under paint, grow slowly and can eventually grow to a catastrophic size. However, if the rate of growth is slow, visual inspection will detect the damage before catastrophic damage occurs.

Overhaul maintenance requires the removal of a particular part which is then inspected often by using ultrasonics or x-ray radiography. Repairs made on location, i.e., depot-level repairs, often include both visual inspection and overhaul maintenance [13-17].

The extent of the damage is frequently evaluated using ultrasonic and x-ray radiography inspection [18-22], and the effect of the damage must be critically reviewed by the repair designer. The repair designer must have a comprehensive understanding of not only the fabricated structure but also the processes available for efficient testing of the repair.

Repair techniques developed to date fall into one of the three categories listed: (1) bolt-on patch, (2) bond-on patch, or (3) cut away damaged material and laminate new materials. Most of these repair schemes are depot-level repairs and are individually designed after the extent of damage is determined [23-33]. The major problems in composite repair for which acceptable solutions have not been found are:

1. moisture penetration into the laminate,
2. acceptable, easily stored materials,
3. repairs for high operating temperatures (over 300°F),
4. repair of joints.

1.3 Composite Joining

The repairability of structural composites must be addressed, not only in the realm of repair, but also that of joining. An effective method of joining is the key to a successful and efficient structural repair. Kedward [5] supports this statement, but discusses further that the weight advantage associated with the use of composites frequently becomes eroded at the joint. Therefore, the methodology for joining composite structures, must address the following aspects:

1. the micromechanics level - the fiber-matrix interface phenomenon.
2. the macromechanics level - at the interfaces between layers as characterized by the so-called free edge problem.
3. the structural level - the interfaces between two or more separate components as in the conventional joint.

A unique set of challenges is created by the inability of most composite systems to deform plastically and ultimately reduce the stress concentrations combined with the anisotropy in stiffness and strength properties.

Another parameter to consider during joining is whether or not to incorporate mechanical methods, adhesive methods, or both. There are definite advantages for each. Some are stated in Table 1.3. As a general rule of thumb, bonded joints are more suitable for lightly loaded joints; this is where their high efficiencies can be realized. Mechanical joints, on the other hand, are predominantly used for high-risk, highly loaded joints that are subjected to severe fatigue and environmental conditions. The major disadvantages of the mechanical joints are their increased weight, part count, associated costs, and surface modifications [33].

Adhesive bonding has been an accepted and widely used technique for composite repair in aircraft structures. This is mainly due to the high bonding efficiencies and improved fatigue life. Extensive use of adhesive bonding is utilized in many secondary structures on aircraft as well. Many articles can be cited regarding the repair of aircraft [34-75]. For example, 62% of the Boeing 747 wetted area and 35,000 ft^2 of Lockheed's C5A are adhesively bonded. Some aircraft have even incorporated adhesive bonding of primary structures, i.e. wing stiffeners, fuselage longerons, and fuselage skin panels. The most noteworthy company to employ this technology is Fokker Aircraft Co. in their Fokker F-27.

The use of adhesive bonding has expanded greatly in the past few years to complement the latest technology in advanced composite structures. It is widely agreed that the most efficient adhesively bonded joint is the composite-to-composite or composite-to-metal splice in the form of a scarf or stepped lap joint [76-92]. With the

Table 1.3 The Advantages of both Mechanical and Adhesive Joints [3].

Advantages of Mechanical Joints	**Advantages of Adhesive Joints**
Tolerance to the Effects of Fatigue Loading	High Joint Efficiency Index (relative strength/weight of the joint)
Ease of Inspection	Low Part Count
Capability for Repeated Assembly	No Strength Degradation of Basic Laminate by use of Cutouts
High Reliability	Low Cost Potential
No Special Surface Preparation Required	Potential Corrosion Problems Minimized

increased usage of bonded assemblies, the requirement of a well defined repair method is essential to avoid processing anomalies, mistakes during fabrication, and costly scrapping of large assemblies, etc.

Adhesive joining is an integral factor and procedure in a majority of thin panel repair. Therefore, it is critical to understand the bonding mechanism by which thin to moderately thick structures exhibit. Also, it is important to note the remarkable tolerance for large bond imperfections. However, thicker composite structures exhibit great sensitivity to both large voids and porosity. In thin composites, i.e., those that are 2.5mm or less, the flawed bonds are often strong enough, since in a real structure, in which random bond flaws are surrounded by nominal perfect bonds, any flawed bonds divert some of their share of the load to the adjacent sound bonds. This effect is documented extensively by L.J. Hart-Smith [93]. Hart-Smith also comments that the primary effect of bond flaws is generally a reduction in the thickness, or section modulus, of the members. However, it is important to note that if an adhesive bond, in a thin adherend, is created without bond line pressure during the cure cycle of the resin, then in fact an increase in the section modulus can occur. This increase is primarily due to the air pockets or voids created during resin cure. These voids ultimately reduce the overall strength of the joint. Flaws in thick bonded structures can propagate catastrophically, therefore mechanical fasteners are advocated as a "fail-safe" load path [93]. As a general rule, Hart-Smith states that it is best to restrict the use of adhesive bonding to those applications where there is no possibility for local flaw growth. Also, it is unwise to design or build a purely bonded joint which is weaker than the original adherend [93].

In summary, repair documents have been developed by each manufacturer using their own preferred processing methods and procedures. Depending on the application and environment surrounding the material, very little variation is required to sustain a good repair technique.

A. Adhesive (bonded) Repair using Scarf-Joining

As stated previously, the two general approaches to consider during composite repair are namely bolted or bonded procedures. The factors which determine a particular approach are: the specific component, laminate thickness, damage size, accessibility, load requirements, and repair capability.

When considering bonded repair, it is important to categorize the severity of the damage. For simplicity, three categories of bonded repair are non-structural, secondary structural, and primary structural repair. Non-structural damage includes scratches, dents, and other defects confined to the surface of the laminate, so cosmetic repair is sufficient. Secondary structures usually refer to those components that consist of thin laminate construction (less than 2.5 mm thick). Upon repair, strength is not a critical factor though the restoration of stiffness and stability is. Primary structures are those components that are critical to the operation of, for instance, an aircraft or an automobile. Bonded repair of such structures is much more complicated since the repair must be capable of transferring more load [94-98]. Refer to Figure 1.4.

Two types of bonded repair, for both secondary and primary structures, are an external patch and a flush scarf joint. The bonded flush scarf joint provides maximum

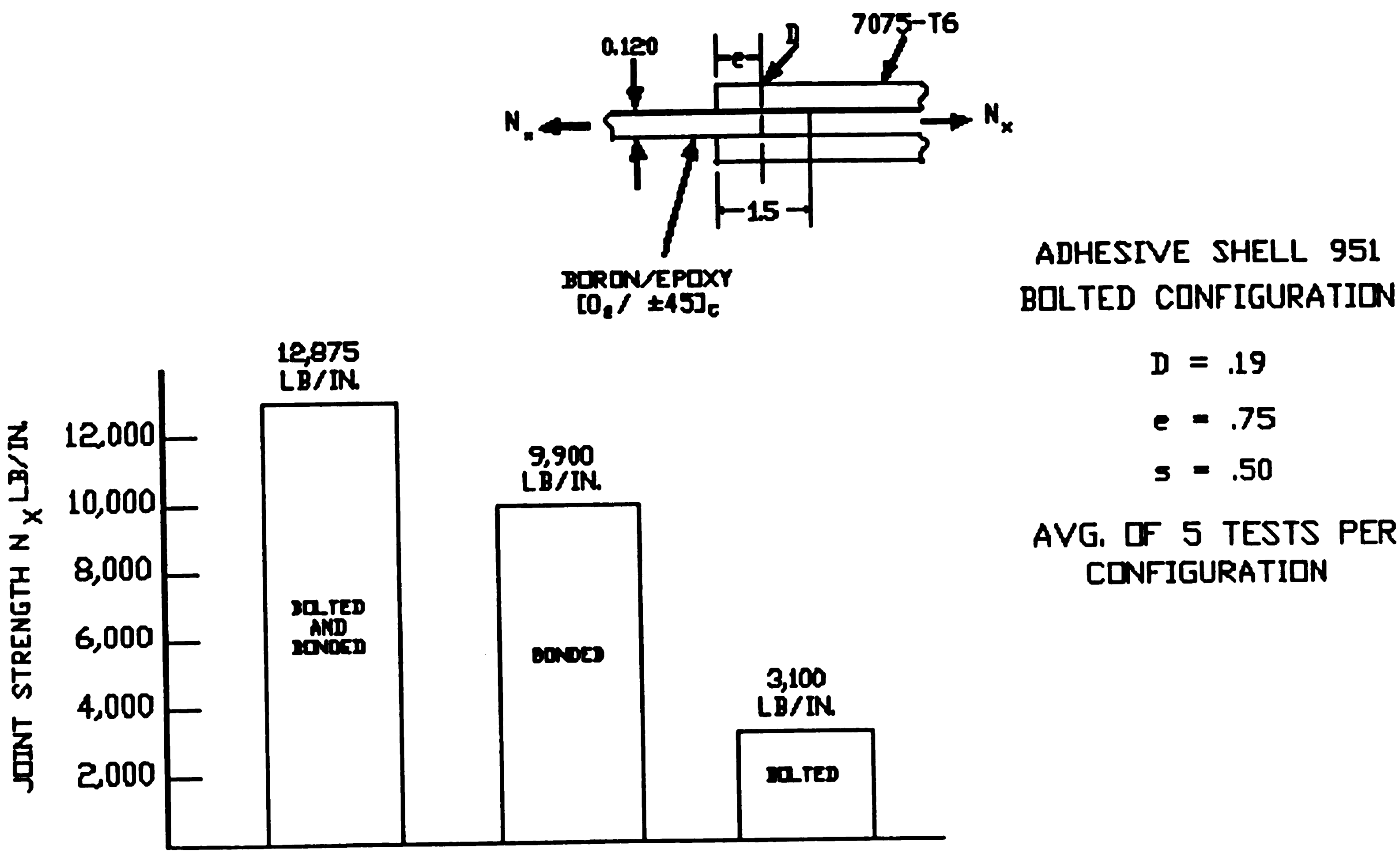

Figure 1.4 Schematic of Bolted vs Bonded Joints [9].

joint efficiency and is applicable where load concentrations and eccentricities must be avoided. The bonded flush-scarf repair has been found to achieve 60% of its unflawed or undamaged strength [10]. These repairs require careful preparation and are very time-consuming regarding machining and application. However, the advantage of scarf repairs is their load carrying capability, which is higher than most other repair schemes.

Scarf bonded repair concepts have been developed for repairing monolithic laminates up to 10 mm thick. These repairs are assumed to be made in place, where no access is available from the back side of the damage. The repair is unique to the particular damage zone and requires the full ultimate design allowable strength of the skin. Figure 1.5 illustrates some variations in bonded scarf joints for monolithic skin repair.

The other major type of bonded repair is the utilization of external patches. In this case, the load is carried over the damaged zone. Patches are applied over the repair zone in a stacking sequence which allows for "fairing-in" of the patch to the adherend [50]. This alleviates large stress concentrations at the patch ends.

Ultimately, scarf-joining with the application of external patches gives the optimum restoration of the original unflawed adherend strength.

A great deal of documentation regarding scarf joining focuses on the repair of thick (more than 2.5 mm) skin laminates and honeycomb structures. This is because, in most cases, thin panel damage is considered non-structural or secondary structural and is not required to maintain large structural loads.

Recently there has been an increased interest in the application of structural

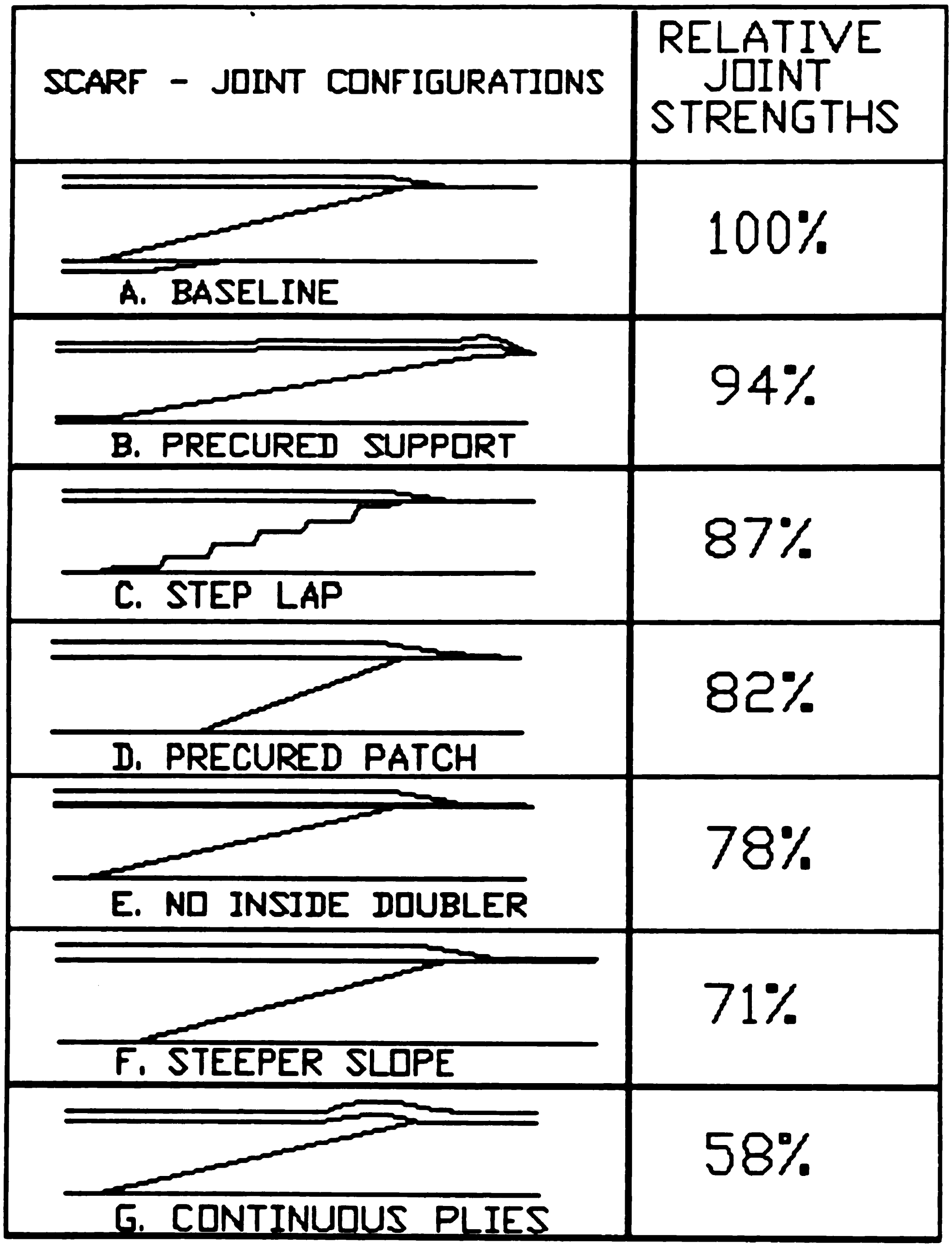

Figure 1.5 Various Bonded Scarf-Joints for Monolithic Skin Repair [5].

composite materials by the automotive industry. Therefore, the topic of thin panel repair must be addressed. The literature is in agreement that scarf joining is sufficient for thick panel repair, but is it the optimum repair design for thin panel repair? This is one of the questions addressed in this research, and will be formally discussed in Chapter 2.

B. Mechanical and Adhesive Joints Combined

The fatigue life of cracked holes is of major interest, especially to the aerospace industry. In the past few years a great deal of effort has been focused on devising an appropriate repair scheme. Full scale fatigue testing of the Royal Australian Air Forces Mirage III was undertaken to address the problem of repairing cracked rivet holes [47]. Steel interference-fit bushings were installed at the bolt holes which virtually inhibited crack initiation from the area of the bolted fastener. Bushings are viable for bolted joints, but not acceptable for riveted joints. A study was conducted to evaluate different means of utilizing riveted fasteners without the enhancement of fatigue crack initiation. Conclusions from the study revealed that the use of adhesively bonded rivets significantly increased the joints life to failure as well as reduced the initiation of fatigue crack growth.

Some further conclusions are listed below [31]:

(a) the adhesive acts as a barrier to inhibit crack initiation which might otherwise have been accelerated by environmental interaction;

(b) the adhesive acts as a non-metallic interlayer, thus separating the rivets and hole surface and reducing the potentially deleterious effects of fretting;

(c) the adhesive provides improved load transfer characteristics at the section, both before and after crack initiation.

1.4 Previous Research

Prior to this dissertation, the repairability of impact-induced damage in Owens Corning SMC was explored. The material was made up of randomly oriented chopped glass (1" fibers) in a polyester matrix. The impact resistance and the notch sensitivity of the composite were characterized by tensile and flexural tests. An equivalent damage hole size evaluation was identified through the comparison of impact damage and notch sensitivity, and it was concluded that none of the damaged portion should be removed from the impacted composite during the repair procedure. The damaged material was then repaired with a technique combining resin injection and the application of reinforcing patch material. Resin injection was performed to seal the matrix cracks which would otherwise result in high stress concentrations from geometrical discontinuities. Reinforcing patches were employed to compensate for the strength reduction caused by fiber breakage. It was revealed, from various experiments, that the repair technique was very effective in restoring the tensile and flexural strengths of the composite after impact-induced damage [99-101].

1.5 Present Study

Based on the findings from previous research, the fundamental repair techniques for SMC composites are verified. In view of the variety of parameters associated with the repair of automotive components, such as, the material, its structural configuration, and loading type, the necessity of a broader study to gain overall knowledge concerning composite repair is essential. In this study, in addition to the Owens Corning SMC composite, two other composite materials manufactured by Excel Pattern Works are also investigated. The first material, Excel 8610, contains a continuous glass swirl mat in a vinylester matrix. The second material, Excel 2415, is made up of a cross-woven mat chemically bonded to randomly oriented chopped glass fibers in a vinylester matrix. Both of the Excel materials were produced by RTM (Resin Transfer Molding) processes. These three composite materials incorporate the three major types of fiber geometries and microstructures utilized in today's automotive industry.

In composite repair, both the damage mode and repair parameters are of primary concern since they have significant effects on the repair technique and the bonding efficiency. In order to cover as many types of composite damage as possible, perforation, bending fracture, tension, compression, torsion, and fatigue are investigated. Various repair parameters, such as the use of reinforcing patches, scarfing angles, and different bond line configurations are also examined. Based on these studies, it is also possible to present an optimal repair design for damaged composite structures. Furthermore, different adhesives are examined, and some special repair considerations are also discussed.

This dissertation outlines the following topics in chapters 2-7: the repairability of damaged composites, testing and repair facilities, materials and geometric parameters in composite repair, testing and results, associated parameters, and optimization of composite repair. Chapter 8 summarizes the aforementioned topics and lists some recommendations for further studies.

CHAPTER 2

COMPOSITE REPAIR

Composite materials are made of at least two constituents: the fiber and the matrix. Both of these constituents play an important role in the behavior of composite structures. Depending on the structural configuration, loading type, and boundary conditions, the damage modes of a composite structure can be very different. Therefore, the study of composite repair becomes overwhelming. However, in terms of damaged microstructures, the damage modes can be divided into the following categories: fiber breakage, matrix cracking, fiber-matrix debonding, and delamination. This categorization makes it possible to handle composite repair in a more systematic way. For example, fiber breakage can be restored with compensating fibers, such as the reinforcing patch material, while the matrix cracking can be repaired by introducing resin into the cracked, debonded, and delaminated areas.

2.1 Impact Damage

Various types of damage can take place in automotive structural composites. Among them, impact-induced damage is of major concern because of its high probability. Therefore, the repair for impact-induced damage in the form of indentation, perforation, and bending, must be addressed. However, since these damage types are dependent on the impact parameters such as impact velocity, loading direction, and contact area, the actual damage size can vary from one specimen to another. Hence, artificial damage is more suitable for a systematic and controllable study. In this study, an efficient standard repair technique is developed to address impact damage. This particular technique is discussed in detail in section 2.6 and is evaluated in Chapter 5.

2.2 Artificial Damage

As mentioned above, the composite materials used in the automotive industry are likely to experience impact damage. In view of the damage modes associated with impact, the investigation of artificial damage in the form of a line crack and circular perforation was performed. A straight cutting line was used to simulate bending fracture initiated from an impactor with a linear nose. However, if the impactor has a small pointed head, then perforation, in the form of a hole, may occur. A circular cut-out can be used to simulate this type of damage. See Figure 2.1.

2.3 Repair or Replace

Once the damage mode in a composite structure is identified, a repair strategy must be established. If a composite structure is severely damaged, then it is desirable to actually cut and replace the particular damaged section of the structure. However, this technique can become quite expensive in terms of capital investment, since it requires stocking a large variety of body components in each respective repair shop. However, if structural replacement is not pertinent, then a form of artistic repair should be employed. This technique is currently used to repair automotive bodies made of conventional metals. It is based on the individual technician's judgement and skill

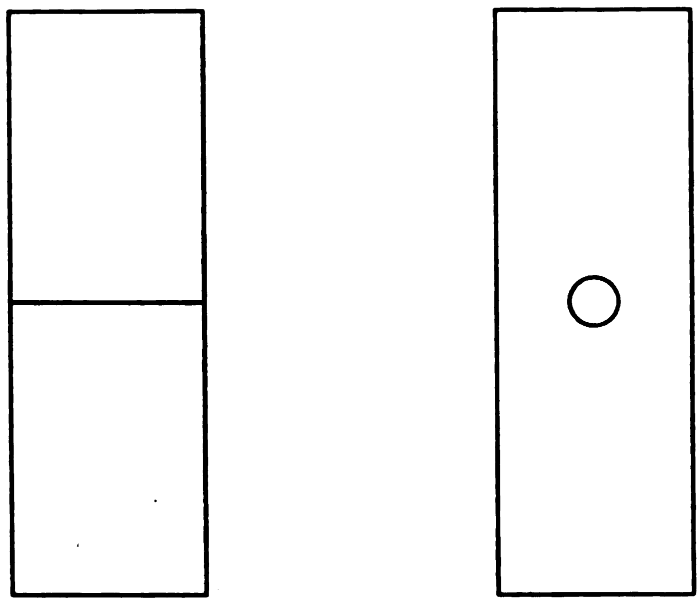

(a) Straight Line-crack

(b) Circular Cut-out

Figure 2.1 Artificial Damage

though some fundamental guidelines should be followed.

2.4 Repair Guidelines

When damage takes place in a composite structure, both the material property of the composite and the geometry of the structure can undergo change. The change in material property usually requires replacement or reinforcement, while repair can be applied to structures which have undergone only geometrical changes. If the structural strength is to be restored, then these two factors must be addressed. These are the fundamental requirements for composite repair.

In a damaged composite structure, both the geometric discontinuity and irregularity can create high stress concentrations; therefore, they must be eliminated from the damaged structure. However, removing the damaged portion of the structure may further degrade its strength. Consequently, it is important to take advantage of the damaged section of the composite by utilizing it as a filler during repair. For example, the damaged section can be mixed with resin to restore structural integrity. If this procedure is not sufficient, then reinforcing materials and adhesives can be added for further strength restoration. Hence, the stress concentrations due to geometrical discontinuity are reduced. However, stress concentrations due to material mismatch can also occur when introducing the reinforcing patch materials and adhesives to the repair zone. To reduce the stress concentrations to a minimum, it is advantageous to utilize repair materials which are compatible with the composite material being repaired.

2.5 Reinforcing Patch Material and Adhesives

Since the composite specimen panels investigated in this study are all made of glass fiber-reinforced thermosets, glass fabric or reinforcement should be used in the repair procedure. Therefore, the compatibility of the glass fabric with the fibers of the composite is satisfied. In addition, it is important to recognize the geometry of the fibers in the composite. Then, if possible, the reinforcing patch material should be aligned with the designated geometry and direction to achieve the highest restoration of strength. The reason that woven fabrics are selected as the reinforcing patch material in this study is because of their high strength (as opposed to a chopped fiber or swirled mat) and their ease in handling during repair.

For most automotive applications, a room-temperature curing adhesive can be used to produce effective mechanical and chemical bonding at the reinforcing patch/specimen interface. It is very important to maintain chemical compatibility with the matrix of the composite and the repair adhesive, since this will help to reduce the risk of debonding. In this study, an epoxy adhesive system manufactured by Marblot (trade name Maraset 658-resin, 558-curing agent) was selected as the adhesive for Owens Corning SMC repair, because of its low viscosity, short room temperature curing cycle, and good strength to failure. A comprehensive study on some other widely used adhesives was performed and the results are outlined in Chapter 6.

2.6 Standard Repair Technique

The standard procedure for repairing glass/epoxy specimens begins by following the proceeding steps described below [101]. This repair technique is performed on test specimen measuring 2" x 6" x 0.10" (50mm x 150mm x 2.5mm), primarily in light of the testing facilities and the materials available, as well as the types of composite damage to investigate.

(1) Abrade a 2" x 4" (50mm x 100mm) area, surrounding the artificially damaged (cut or drilled) area on the top and bottom surfaces of the specimens to improve the mechanical bonding.

(2) Clean each specimen from any debris created by the abrading process. This will insure a better chemical bond between repair materials and the composite.

(3) Mix the resin and curing agent thoroughly. Low viscosity of the epoxy is critical for proper wetting of the bonding region around the damage zone. In addition, low viscosity resin demonstrates superior permeability through the woven glass reinforcing patch material.

(4) Apply epoxy to each specimen. When the epoxy is ready, it is poured and spread evenly to fully wet the repair zone. For reinforcement purposes, glass fillers are sometimes added to the epoxy.

(5) Position two layers of glass reinforcing patch material over the repair zone and massage additional epoxy into the patches until they are evenly saturated. The patch material is a plane-woven mat with a thickness approximately 0.2mm. With one side repaired, each specimen must be flipped over and again epoxy and glass reinforcing patches are put into place.

(6) Add a single layer of release film to both sides of the wet, repaired specimens. Then

the repaired specimens are placed between two aluminum plates. Finally, the stacked aluminum plates containing the repaired specimens are placed in a press and are loaded, compressively, to approximately 100 psi (0.7 MPa). This load squeezes much of the excess epoxy and air voids away from the repaired area.

(7) Cure the epoxy at room temperature for minimum of one hour.

(8) Assess the repaired specimen. Once the repaired specimens are fully cured, they are removed from the press, trimmed, measured, and prepared for testing. The repaired specimens acquire a glossy smooth finish. However, their thickness is slightly greater (about 1.0mm greater) than that of the original specimens, because of the addition of the glass reinforcing patches and resin. The small change in thickness is acceptable in the repair procedure since the primary concern is the restoration of strength.

The aforementioned standard repair technique has been verified to be an efficient and effective procedure for structural composite material repair [101]. Consequently, it is the standard repair technique utilized throughout the current study.

2.7 Composite Joining Techniques

Composite repair is actually composite joining. Therefore, repair designs often focus on the bondable surface area surrounding the damaged zone. If this area is increased, then more contact surface area is created for the reinforcing patch to mechanically, and chemically bond to the specimen. The larger bonding area therefore reduces the risk of debonding between the reinforcement patch and the damaged composite. The technique being used to increase this bonding surface is called scarfing.

In addition to scarfing, the bond line geometry can also affect the joining efficiency. The following sections illustrate various geometries involved in composite joining. Furthermore, the type of filler used in the joining area is also discussed since this too plays a very important role in repair strength.

A. Geometric Configurations

The geometric configuration of the bond line is critical to the repair of (a) in-plane, (b) through-the-thickness, and (c) out-of-plane damage. The following sections give a brief overview of these three different forms of composite structure repair.

(a) In-Plane Bond Line Geometries

The bond line geometries were prepared by cutting each specimen to designated angles of 0°, 30°, 45°, 60° and 90° with respect to the in-plane direction of load. Each of the bond line geometry specimens were evaluated with respect to their depth of joint (in the plane of the specimens and their bond line angle to the direction of the loading force. This study was introduced to determine a correlation between the direction of applied force and the direction of the bond line. The different bond lines are illustrated in Figures 2.2-2.5.

Another bond line geometry consisted of cutting known shapes onto the 2" x 6" (50mm x 150mm) panels. Again, all of the bond line geometry specimens were separated joints and were repaired using the typical procedure listed in Section 2.6, utilizing two plies of reinforcing material per side. The shapes that were cut into the specimens were in the form of: V-, U-, W-, UU-, and WW-joints. All of these contours

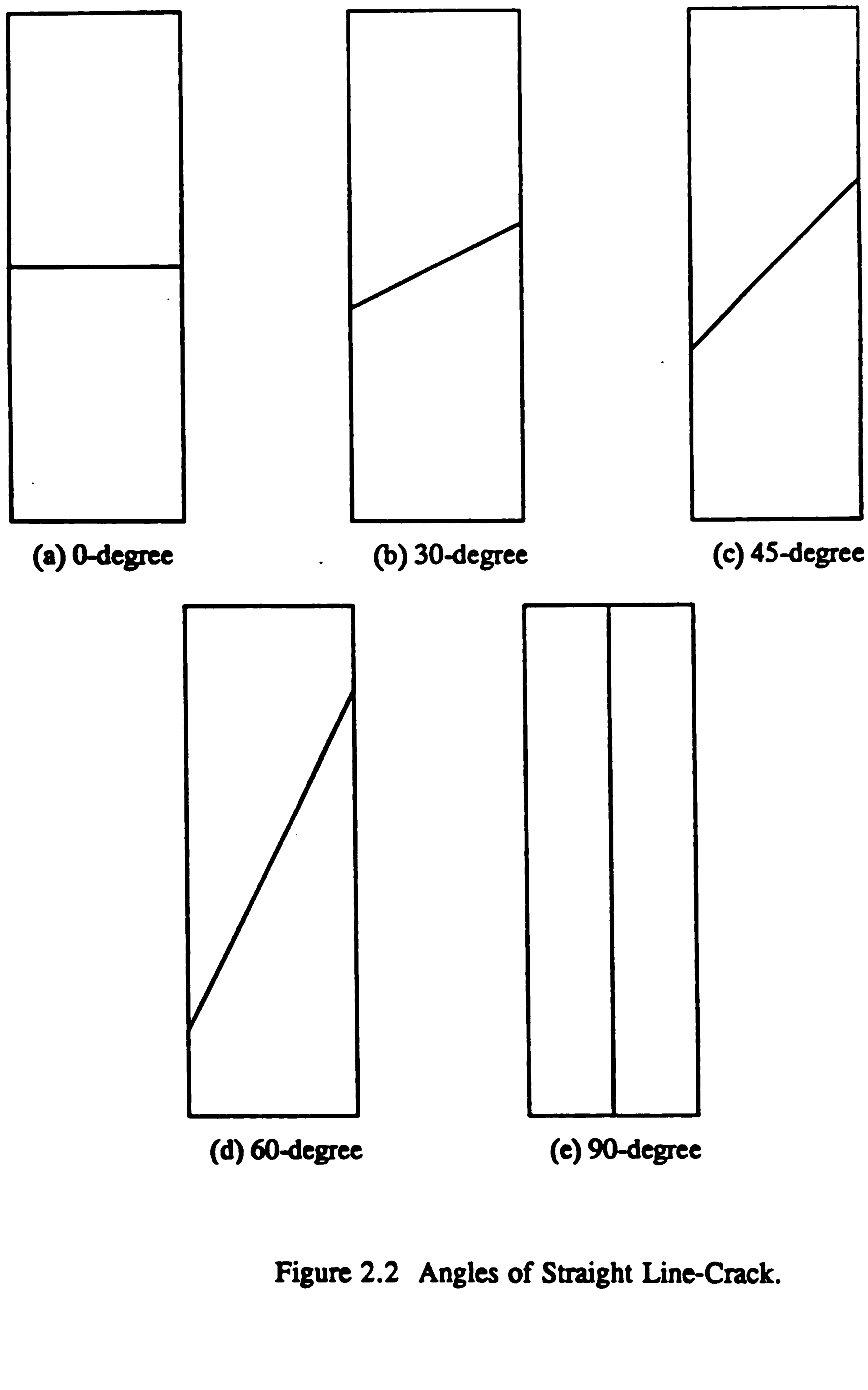

Figure 2.2 Angles of Straight Line-Crack.

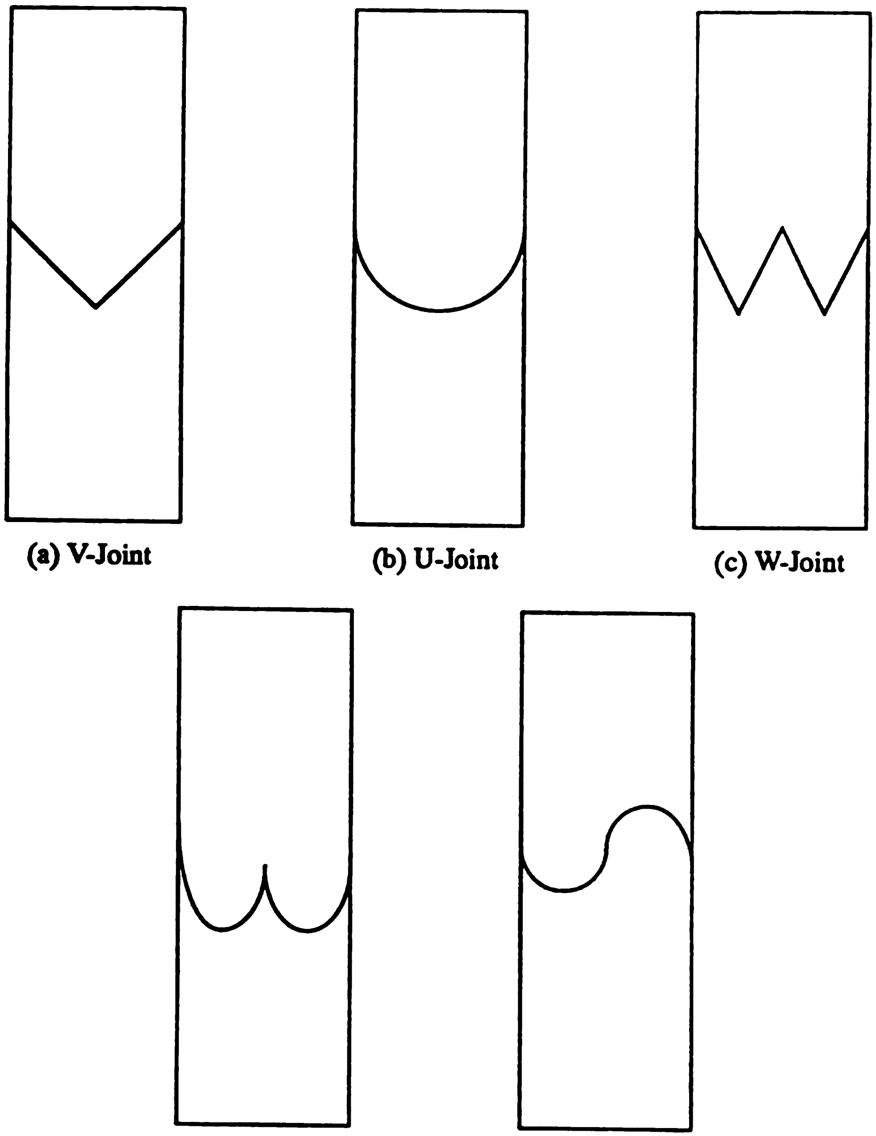

(a) V-Joint (b) U-Joint (c) W-Joint

(d) UU-Joint (e) S-Joint

Figure 2.3 Bond Line Configurations.

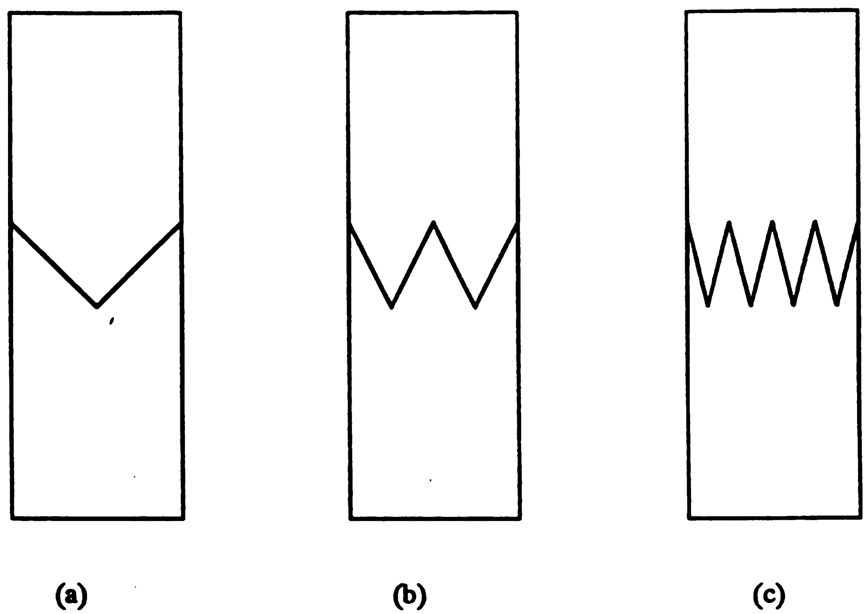

Figure 2.4 Bond Line Patterns.

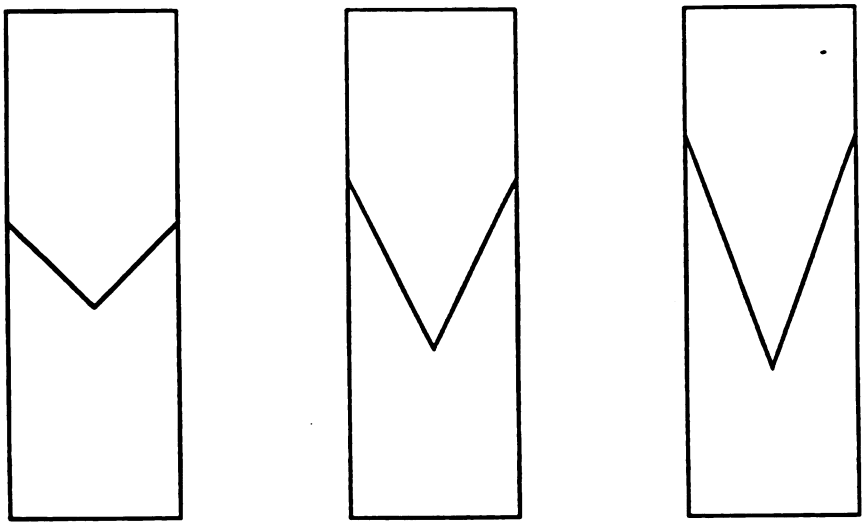

(a) (b) (c)

Figure 2.5 Bond Line Depths.

were performed in a 2" x 2" (50mm x 50mm) area in the center of the specimen panel.

(b) Through-The-Thickness Scarf Joining

In scarf joining, a bonding area is created that bevels away from the damaged zone and encompasses the area outward from the zone. Beveling or scarfing the surrounding area of the damaged zone also reduces some of the stress concentrations resulting from geometrical discontinuity in this area. The particular scarfing angles of interest in this study are 5°, 10°, 15°, and 90° with respect to the plane of the specimen surface. The 90° scarf or so-called butt-joint does not require scarfing. Illustrations of through-the-thickness scarfing are shown in Figure 2.6.

(c) Out-Of-Plane Curvatures

The aforementioned sections outlined in-the-plane and through-the-thickness repair. This information became the baseline reference for the testing of different repair techniques. Subsequently, the repair of composite structures with out-of-plane curvatures incorporated the same technique for repair as the two previously described geometries. See Figure 2.7. The only modification of the repair scheme was in the application of pressure at the bond line during the cure cycle of the epoxy. Further discussion regarding out-of-plane curvature repair is outlined in Chapter 5.

B. Associated Parameters

Once the geometrical bond line configuration has been selected, the next few repair parameters to evaluate are: (a) the reinforcing patch material, (b) the fillers, and (c) the adhesive selection. The following three sections review these parameters.

(a) Butt Joint

(b) Single Scarf Joint

(c) Double Scarf Joint

Figure 2.6 Through-The-Thickness Configuration.

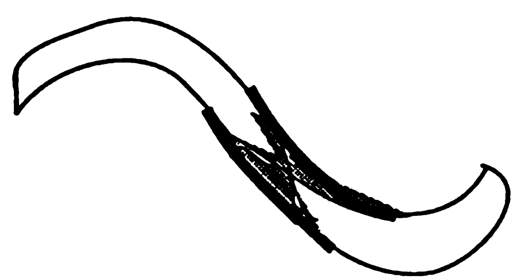

Figure 2.7 Repair of Curvatures.

(a) Reinforcing Patch Material

The reinforcing patch material selected for all repairs in this study was a plane-woven glass approximately 0.2mm in thickness. The primary reason for selecting this material was its ease of handling and its orthotropic properties. The orthotropic properties allowed for tailoring during repair for optimum efficiency of restored strength.

As addressed previously, two layers of reinforcing patch material per side give sufficient reinforcement to most of the repaired structure. In fact, the reinforcing patches simulate a double-lap joint repair on the composite structure. Figure 2.8 illustrates the details of the double-lap joint design. Some additional parameters associated with the reinforcing patch material are investigated further, for example, the reinforcing material, the number of patches, and the size of the patches.

(b) Fillers

For both the scarf and butt joints, different fillers for repair are also presented. If a scarf-joint is selected as the composite joining technique, then different fillers may be utilized in the scarfing zone. The effects of the different types of fillers on composite joining and repair is of major concern. In this study, four types of fillers were implemented, namely, pure resin, chopped fibers, rolled fabric, and a strap filler. The fillers are presented in Figure 2.9. The "strap-joint" filler was an innovative design implemented into the repair scheme for the repair of large voids. Results are discussed and illustrated in Chapter 7.

Further comments should also be made regarding the use of chopped glass fibers (CGF) and a rolled glass patch (RGP) as fillers at the joint. The application of these

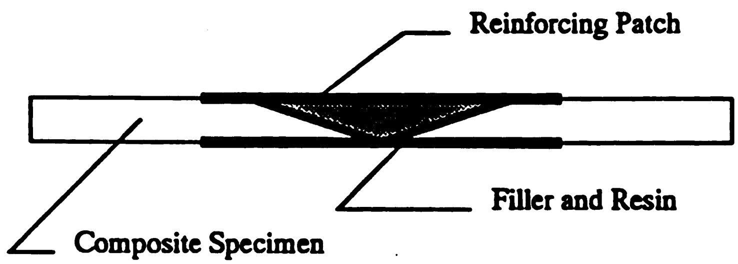

Figure 2.8 Overall Repair Configuration.

(a) Pure Resin

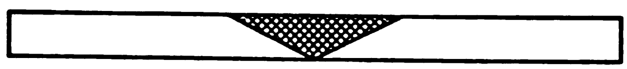

(b) Chopped Fibers

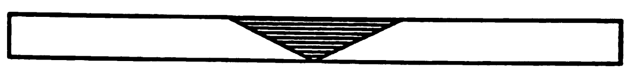

(c) Rolled Woven Fabrics

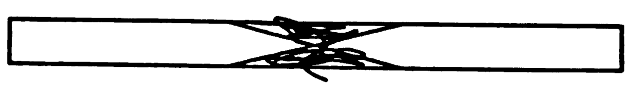

(d) Strap Joint

Figure 2.9 Types of Fillers.

materials tends to reduce the brittle resin content at the bond line, thereby creating a more flexible joint. This aspect should be noted and implemented during the repair design.

(c) Adhesives

The adhesive selected for this study was a two-part room temperature setting epoxy. The critical factors involved in choosing an optimum adhesive system are to (1) check its chemical compatibility with the matrix material in the composite, and (2) make sure its viscosity is low enough to sufficiently wet the woven-glass patch material. If the chemical and mechanical bonds between the reinforcing patch material and the composite adherend are sufficient, then delamination of the patch during testing will be alleviated. A survey to evaluate different adhesive systems is discussed in Chapter 6.

CHAPTER 3

TESTING AND REPAIR FACILITIES

Designing a repair facility to accommodate various aspects of composite repair became a very important and beneficial factor in this particular study. Previously, there were very limited machining facilities to prepare all of the desired repair configurations. To date, all of the specimen designs are more effectively and efficiently prepared in the laboratory. Both the quality and quantity of design specimen can then be achieved throughout the testing procedure.

3.1 Composite Cutting Saw

The critical component of the composite repair facility is the modified lapidary saw. The lapidary saw, which is contained in a thin-walled steel tub, was completely dismantled, and modified to become an exquisite wet/dry composite cutting saw. An advantageous feature of the saw is its blade orientation with respect to the traversing cutting table surface. The space and orientation allows for the implementation of different size saw blades. For this particular study, an 8" diameter diamond-edge blade is utilized. The speed of the diamond-edge saw blade can be modified by simply tensioning the drive pulley from the motor.

A precision saw table was designed to mount directly atop a traversing guide apparatus. The guide apparatus travels parallel back and forth past the diamond blade, and also has 5" of travel normal to the blade. Since the table was designed with two precision fence slots, a 180° mitre was implemented for cutting various angles into the test specimen. Figure 3.1 illustrates a schematic of the composite saw.

The composite saw can be used in both the wet and dry state. Since there is neither burning nor significant edge damage in the glass composite material during the cutting procedure, the dry mode of cutting is used with the application of a shop-vac nozzle at the location of the blade to draw the dust and debris. For thicker specimen panels and carbon fiber panels, because of excessive burning heat along the cutting line, a portable mister may be hooked into the system and mounted directly at the cutting edge of the blade.

3.2 Pneumatic Die Grinder

Another feature of the repair facility is the application of a pneumatically controlled die grinder. The mini-die grinder was designed to accommodate either a 2", 3", or 4" sanding disc. Three different grades of sand paper were purchased, but the coarsest grit (36) was used almost exclusively, due to its efficiency in providing a sufficiently rough or abraded surface.

The die grinder is very light weight and easy to maneuver. It is simply hooked, via a 1/2" diameter hose, into an air-fitting and is ready to use. The primary use of the apparatus is in the scarfing procedure of composite repair, as well as, during the surface abrading portion of the repair procedure. To alleviate excessive dust in the preparation area, a vacuum system (a shop-vac) is mounted, via a nozzle, on the work bench and all

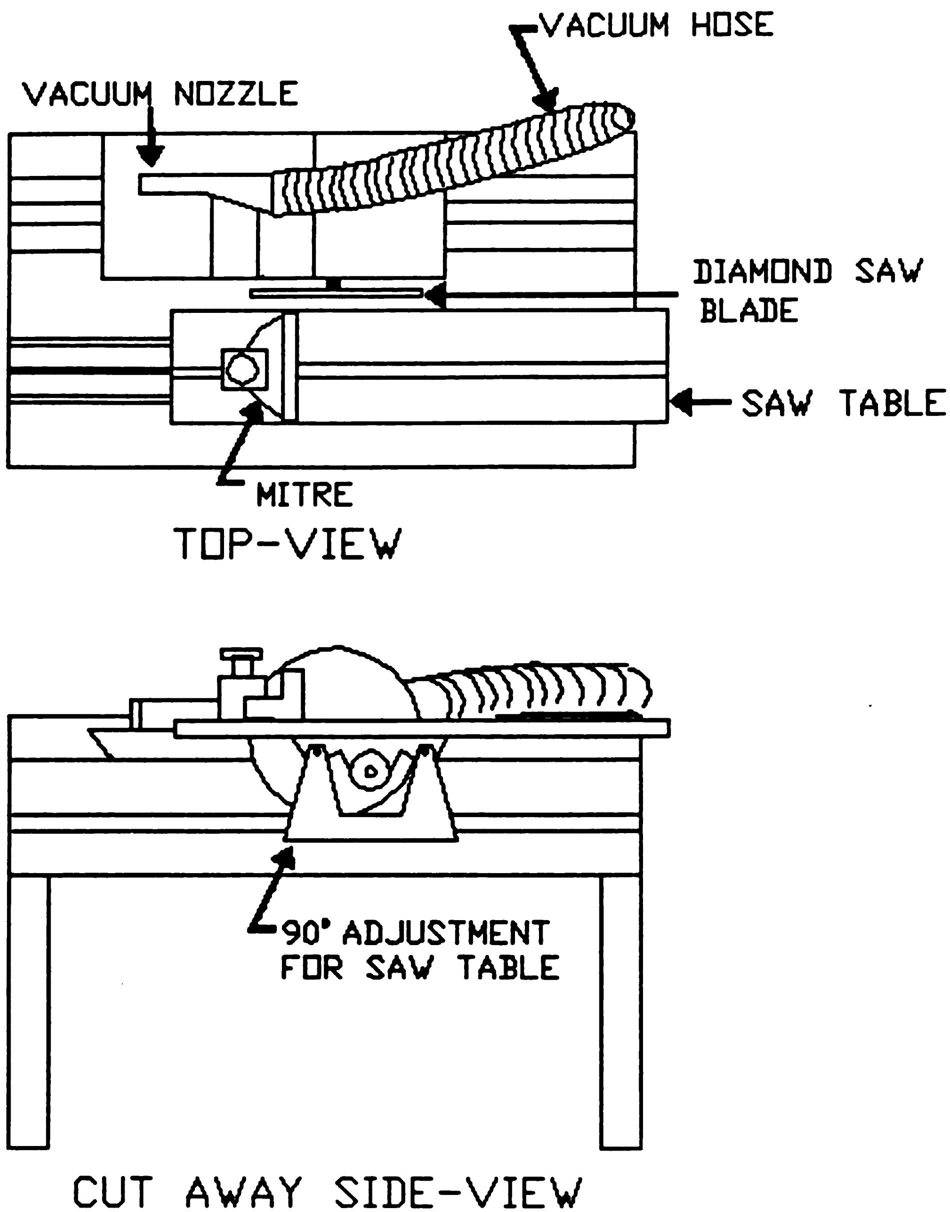

Figure 3.1 Schematic of Composite Cutting Saw.

of the grinding is demonstrated at the intake nozzle end.

3.3 Drill Press

A table-top drill press (1/2" chuck) was also utilized to further develop the repair facility. This apparatus was used almost exclusively for the circular cut-out portion of this study. In part of the circular cut-out study, a plug was press fit back into the drilled hole of the specimens. These plugs were created by using a core drill or hole saw in the drill press apparatus.

For the study on in-plane bond line contours, the drill press was used like a scroll saw by utilizing a tin coated end mill in the chuck. This technique worked remarkably well in the cutting of special in-plane curvatures on the specimens. However, a severe drawback incurred with hole and contour preparation in composite materials is the durability of the high speed steel and carbide tools. They aren't tough enough to withstand the hardness of the matrix supported glass fibers. A possible solution would be to utilize a diamond impregnated drill bit and end mill.

3.4 Three-Point Bending Fixture

The testing procedure used to evaluate the particular repair technique utilizes the three-point bending fixture on the Instron testing machine. Each 2"x 6" (50mm x 150mm) specimen is placed in the three-point bending apparatus and loaded until failure occurs. The span between supports on the apparatus is 4" (100mm) with the supporting pins located symmetrically at 2" (50mm) from the center and the loading pin located at the midspan. During testing, the loading pin is always symmetrically positioned atop the repair zone. The maximum strength is calculated using the flexural formula and is recorded, along with maximum load, flexure, and damage mode at failure for each particular specimen. Strength results are then compared to the various repair techniques, configurations, and the reference undamaged strengths of each material.

3.5 Servo-Hydraulic Tension-Torsion Instron Machine

Tests such as tension, compression, buckling, torsion, and cyclic fatigue utilized a servo-hydraulic tension-torsion Instron machine. Specimen preparation did not require the use of end-tabs, however, each specimen was abraded at the gripping area to alleviate slippage in the grips. Further discussions regarding the actual tension, compression, buckling, torsion, and fatigue analysis and results can be found in Chapter 6.

3.6 Dynatup Impactor

To evaluate the similarity between artificial damage and impact-induced damage, a series of tests were conducted by first impacting, to the point of perforation, glass/epoxy panels measuring 4" x 6" (100mm x 150mm). The Dynatup impactor utilized a tup which measured 1/2" (13mm) in diameter. After impact, the perforated specimens were trimmed to the dimension of 2" x 6" (50mm x 150mm) and tested under three-point bending to evaluate the residual flexural strength integrity. Results of this testing are outlined in Chapter 5.

CHAPTER 4

GEOMETRIC PARAMETERS IN COMPOSITE REPAIR

In the study of composite repair, both fiber geometry and matrix type are critical parameters. The following sections discuss the various fiber and joining geometries that were evaluated, as well as the effectiveness and efficiency of these geometries in the repair of damaged structural composites.

4.1 Fiber Geometry

Three different fiber geometries were investigated. They were: (1) a random chopped glass (1" fibers) in a polyester matrix, (2) a continuous glass fiber mat in a vinylester matrix, and (3) a mixture of cross-woven glass and random glass in a vinylester matrix. The random glass fiber was formed using SMC (sheet molding compound) while the other two configurations were formed using RTM (resin transfer molding). The fiber volume fractions for all of the materials were approximately 50%. These three fiber types represent the majority of composite materials used today in the automotive industry. The materials mentioned above are subsequently designated as, (1) Owens Corning SMC, (2) Excel 8610, and (3) Excel 2415, respectively. All of the specimen panels have an approximate thickness of 1/8" (3mm).

Because of their random fiber orientation, both Owens Corning SMC and Excel 8610 have isotropic properties. However, since Excel 2415 consists of an unbalanced cross-weave, it exhibits two dominant directions, namely the orthotropic principle axes.

The higher strength direction is called the warp direction. Normal to the warp direction is the fill direction. Hence, the warp and fill directions should be evaluated separately. In all of the subsequent investigations regarding Excel 2415, both the warp and fill directions are identified. Based on preliminary testing, the average flexural strengths of the undamaged specimens are as follows: 290MPa for Owens Corning SMC, 300MPa for Excel 8610, 478MPa for Excel 2415 in the warp direction, and 375MPa for Excel 2415 in the fill direction. These undamaged values are used as reference values for comparing all repair strengths.

4.2 Fiber Orientation Analysis (Excel 2415)

This study was conceptualized because of the extreme strength associated with the warp direction of the 2415 material. A survey was designed to prepare several 2" x 6" (50mm x 150mm) specimens from an Excel 2415 panel. Each set of three specimens were cut and referenced to the direction of warp. For example, specimens were cut with an angle of (0°, 30°, 45°, 60° and 90°) from the warp direction. All of the specimens were loaded to failure utilizing the three-point bending apparatus. After failure, each specimen was repaired utilizing two layers of reinforcing patch material per side and Resin Services resin. After repair, each specimen was again loaded to the point of fracture. Results are illustrated in Figure 4.1. The two lines at the top of the plot illustrate the average non-damaged strength of both the fill and warp directions after the application of two layers of glass reinforcing material per side. These two lines reveal the influence of the glass patch strength on the repair of non-separated specimens. It

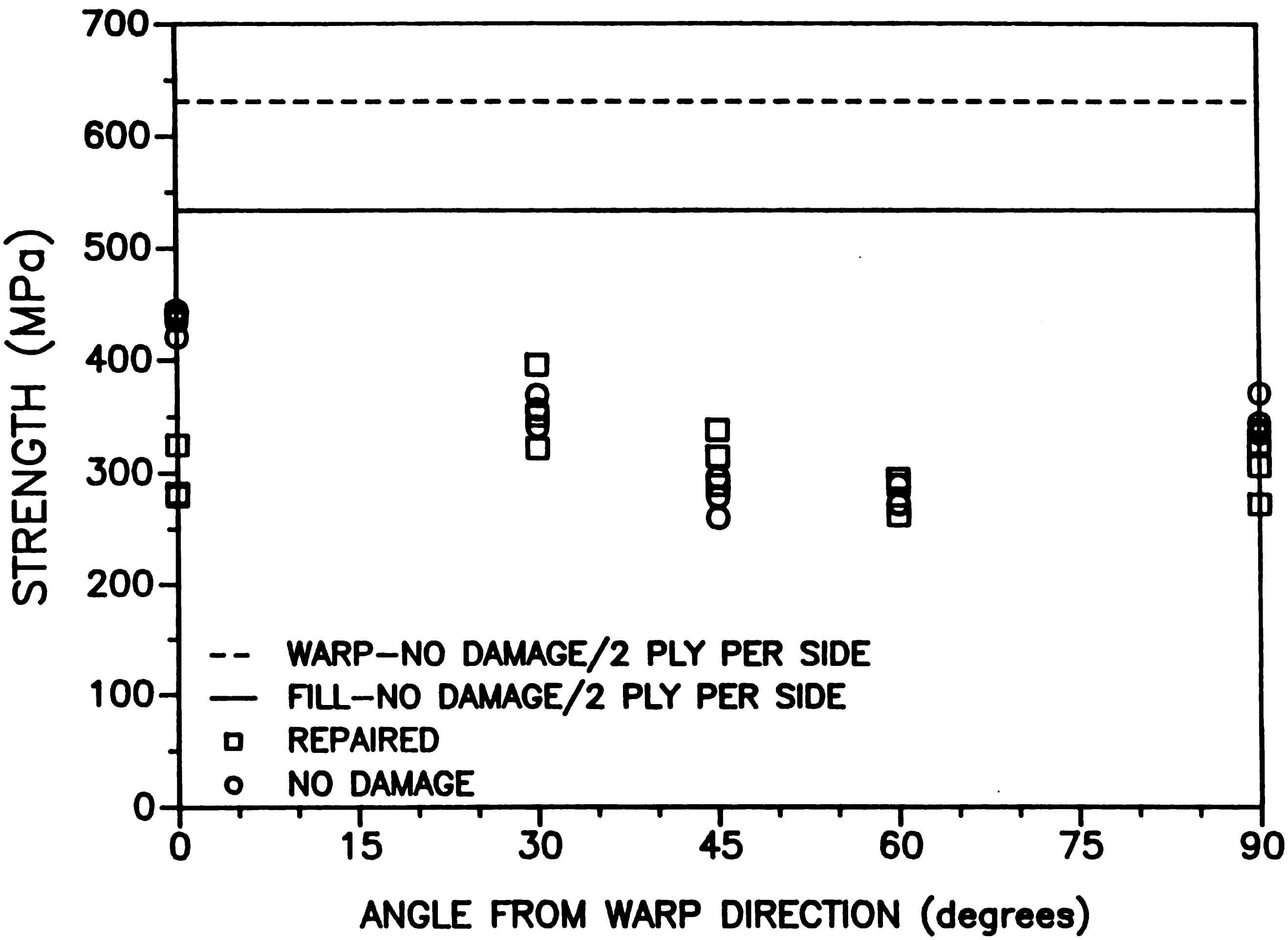

Figure 4.1 Excel 2415: Fiber Orientation Analysis to Illustrate the Dependence of the Fiber Orientation and and cutting angle on the Strength of the Joint. Standard Repair Was Utilized.

should be noted that the 45° orientation angle did not fail under the initial three-point bending loads. In fact, it seemed to twist in the fixture and demonstrated flexure values well above 1" (25mm) within the 4" (100mm) testing span. In addition, results showed that the 45° orientation maintained the highest repair efficiency. This is primarily due to the fact that the 45° fiber orientation creates the largest off-axis angle between the specimen's fiber orientation and the bending direction. Hence, its flexural property is more dominated by the matrix property instead of the fiber property and the repair efficiency for matrix is higher than that for fiber. Refer to Figure 4.2 for an illustration describing the patch and specimen fiber orientation.

The most important contribution of this survey was the information regarding the dependence that the fiber orientation has on the flexural strength of the specimen. Consequently, if any off-axis (off the specimen's warp direction) orientation is introduced into the repair design, then the strength is changed. This aspect was documented throughout subsequent testing of the Excel 2415 material.

4.3 In-Plane Bond Line Geometries

The geometrical parameters play very important roles in composite repair since they have significant effects on bonding efficiency and repair strength. Various geometrical parameters such as shape, size, and configuration were investigated in this study.

Depending on the loading situation, a damaged composite structure may exhibit a small portion of truncation or an unseparated damaged zone. Therefore, the

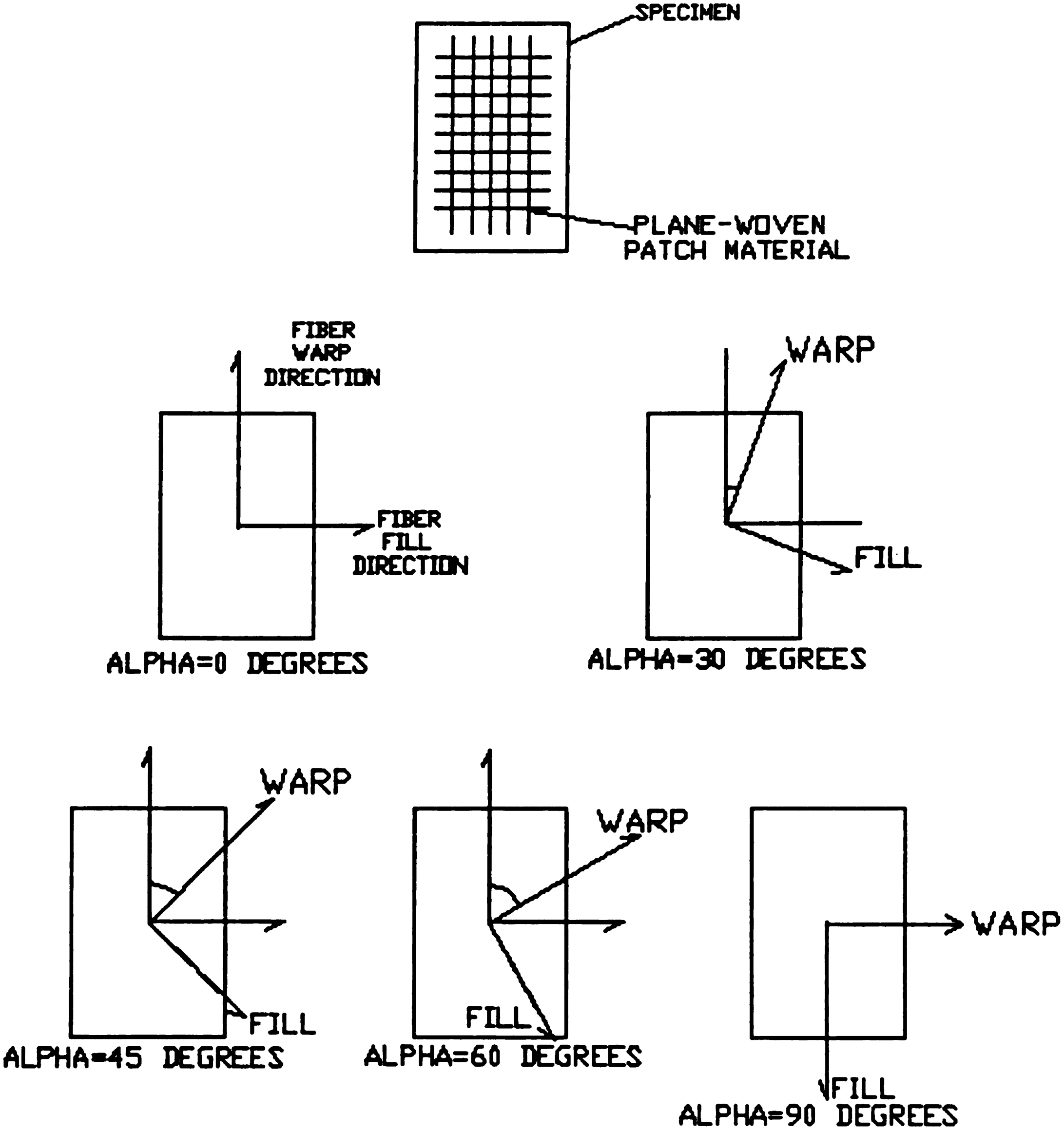

Figure 4.2 Patch and Specimen Fiber Orientation.

repairability of both the truncated and unseparated cases must be investigated. The specimens prepared with circular cut-outs fall into the truncated category while the line crack, due to failure, falls into the category of unseparation. These two scenarios illustrate that the joining technique must be tailored to meet the requirements of the individual damage modes.

A. Straight Line-Crack and Circular Cut-Out

The straight line-crack and circular cut-out were investigated because of their similarities to the damage modes involved in a composite material during an impact event, i.e., bending fracture and impact-induced perforation, respectively. Refer back to Figure 2.1, which illustrates these two types of artificial damage modes.

B. Angled Line-Crack Configurations

In Figure 2.2a, the crack line is oriented parallel to the direction of loading or the bending direction. However, this is a very idealized case, therefore the evaluation of line cracks at varying angles to the direction of loading must be evaluated. The evaluation revealed the influence of the bond line angle on the repair strength. Figures 2.2 b,c,d,and e, illustrates the angles of interest, i.e., 0°, 30°, 45°, 60°, and 90°, respectively. The results of this survey are discussed in Chapter 5.

C. Bond Line Configurations

In addition to a straight bond line, the boundary along the line of damage (the damaged boundary contour), may illustrate a more complex configuration. In order to simulate the different possibilities, various configurations of bond lines were investigated. For example, the V-joints and W-joints shown in Figures 2.3a and 2.3c, respectively, were developed utilizing the concepts from the previous straight line-crack study. The U-joint and UU-joint, depicted in Figures 2.3b and 2.3d respectively, were two modifications aimed at reducing the stress concentrations along the bond line edges of the V- and W-joints. In addition, an S-joint, as shown in Figure 2.3e, was also investigated. The S-joint was derived from a circular configuration which, theoretically, should result in uniform bonding efficiency and repair strength when subjected to loading from any direction. The S-joint is discussed further in Chapter 7.

D. Bond Line Patterns

With the same joining configuration as the V-joint, the joining efficiency and repair strength can be affected if the joining pattern is repeated within the same repair zone. The configurations shown in Figures 2.4a, 2.4b, and 2.4c, are all based on the V-joint and are designed with identical depths. However, by altering or repeating the number of V-configurations in the V-joints, the repair strength and efficiency is affected, which introduces another area of concern in composite repair. The results of this survey are discussed in Chapter 5.

E. Bond Line Depths

This study investigates the depth (in the plane of the specimen) of a particular joint. The V-joint was the reference configuration for this study, and the depth of the V-joint was modified. Figures 2.5a, 2.5b, and 2.5c illustrate the varieties of V-joint depths investigated and the results of the analysis are outlined in Chapter 5.

4.4 Through-The-Thickness Configurations

As mentioned before, the bonding configuration in the thickness direction also plays an important role in composite joining and repair. Figure 2.6a illustrates butt-joining, i.e. a 90° bond line, which is normal to the specimen surface. If the angle is less than 90°, then the type of joint is referred to as a scarf-joint. Figure 2.6b illustrates a typical scarf-joint with scarfing angle alpha (α). One of the important aspects of studying scarf-joining is to investigate the effects of the scarfing angle on the joining efficiency and repair strength. Since Figure 2.6b is designed with scarfing on only one side of the joint, it is considered a single-scarf-joint. The double-sided scarf, or double scarf-joint, as shown in Figure 2.6c, is another possible technique for composite joining and repair.

In addition, it is important to note that when utilizing the scarfing technique in the laboratory, the artificial damage modes of interest are both the straight line-crack and the circular cut-out. Both of these damage modes represent possible models to simulate impact damage. The straight line-crack, with scarfing, is prepared by cutting the 2" x 6" (50mm x 150mm) specimens in half and machining the designated 5°, 10°, and 15° scarf angles. Again, the scarfing procedure is demonstrated to determine if the increased surface area around the damaged zone will indeed increase the flexural strength of the repaired joint. Furthermore, a circular-scarf joint study was investigated. Each specimen was prepared by drilling a designated diameter hole through a 2" x 6" (50mm x 150mm) composite specimen. The hole was drilled to simulate a perforated zone in the composite material. The scarfing regions were then prepared radially outward from the hole.

4.4 Out-Of-Plane Curvatures

The material used for the of out-of-plane curvatures was an SMC made up of 28%, by volume, random chopped glass in a polyester matrix. The actual structure was a liftgate designed by Rockwell Plastics for Ford's Aerostar Minivan. Six different curvatures were evaluated throughout the structure. Each curvature was cut to the dimensions of 2" x 6" (50mm x 150mm) and loaded to failure under three-point bending. A detailed discussion regarding the repair and testing of curved panels can be found in Chapter 5. Figure 4.3 illustrates the variety of curvatures investigated in this study.

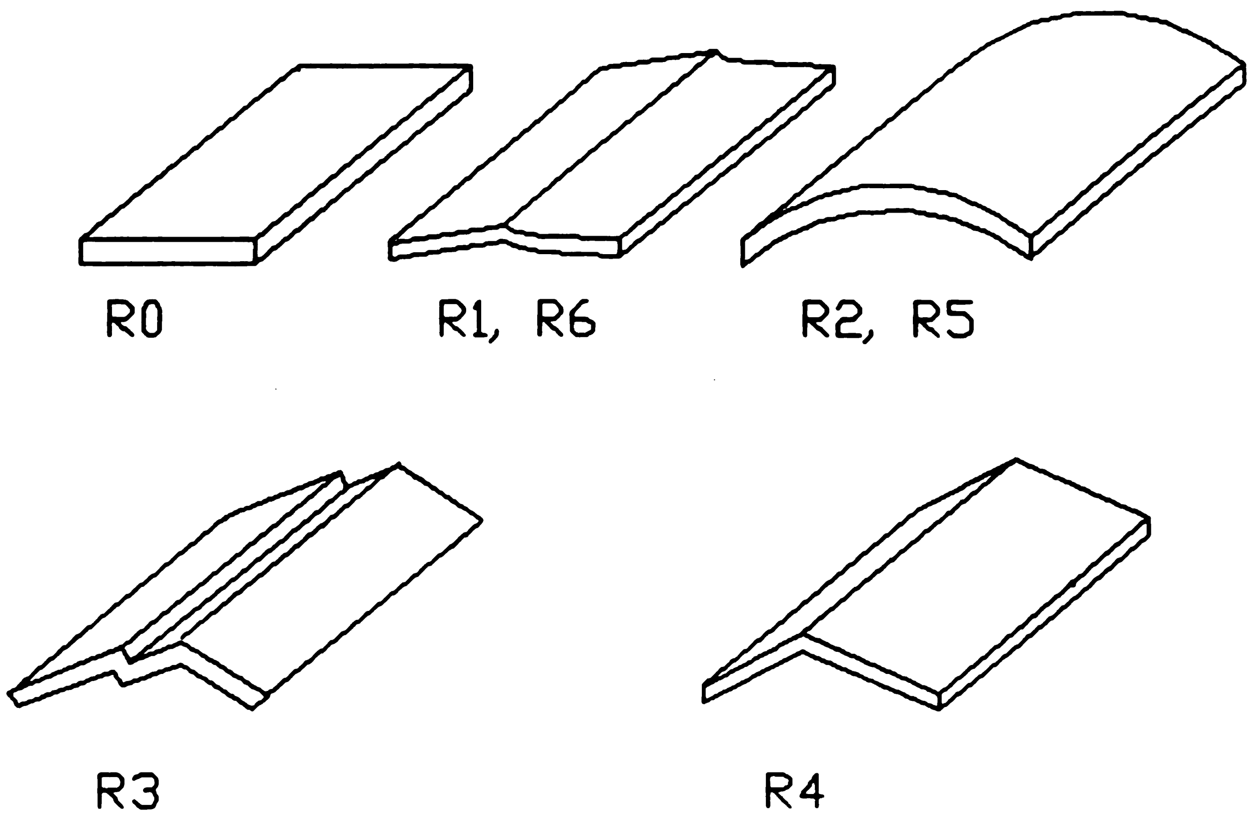

Figure 4.3 Illustration of the Different Out-Of-Plane Curvatures.

CHAPTER 5

TESTING RESULTS

Three-point bending was selected to asses the repairability of damaged composite structures because of its similarity to many real loading situations and its ease in specimen preparation (compared to uniaxial loading which requires the application of end tabs). The dimensions of the individual specimen were chosen to be 2" x 6" (50mm x 150mm), because of the availability of the testing apparatus and the versatility of possible repair design. However, the dimensions of the test specimens raises a question of its identity. Is it a beam-type or plate-type structure? To verify that the 2" x 6" (50mm x 150mm) specimens could be analyzed using beam theory, a scaling experiment was conducted. In this experiment the material Excel 8610 was utilized. Three samples of each of the following widths, 0.5" (12.6mm), 1"(25.4mm), 1.5"(38mm), and 2"(50mm), were cut, measured, and fractured under three-point bending. Refer to Figure 5.1. The results, illustrated in Figure 5.2, reveal a negligible effect due to the width dimension of the test specimen.

This discussion leads to the observance of another phenomenon which can occur in composite plates undergoing three-point bending. The phenomenon is referred to as "anti-clast". This phenomenon is illustrated in Figure 5.3, and can be described as a saddle type bending of the structure. If the dimensions of the specimen were more like a beam then this phenomenon could be neglected. This effect occurs, not only due to the geometry of the specimen, but it is predominant in woven-fiber composites which

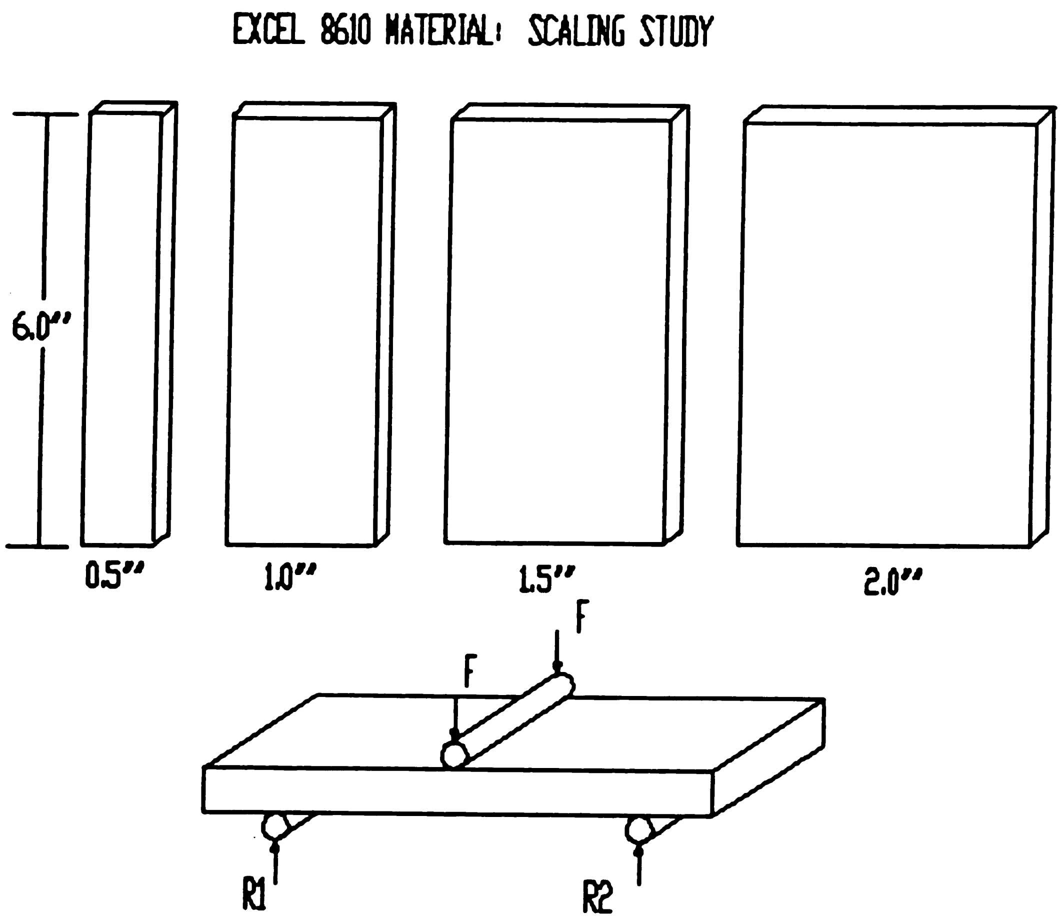

Figure 5.1 Excel 8610 Undergoing a Scaling Survey.

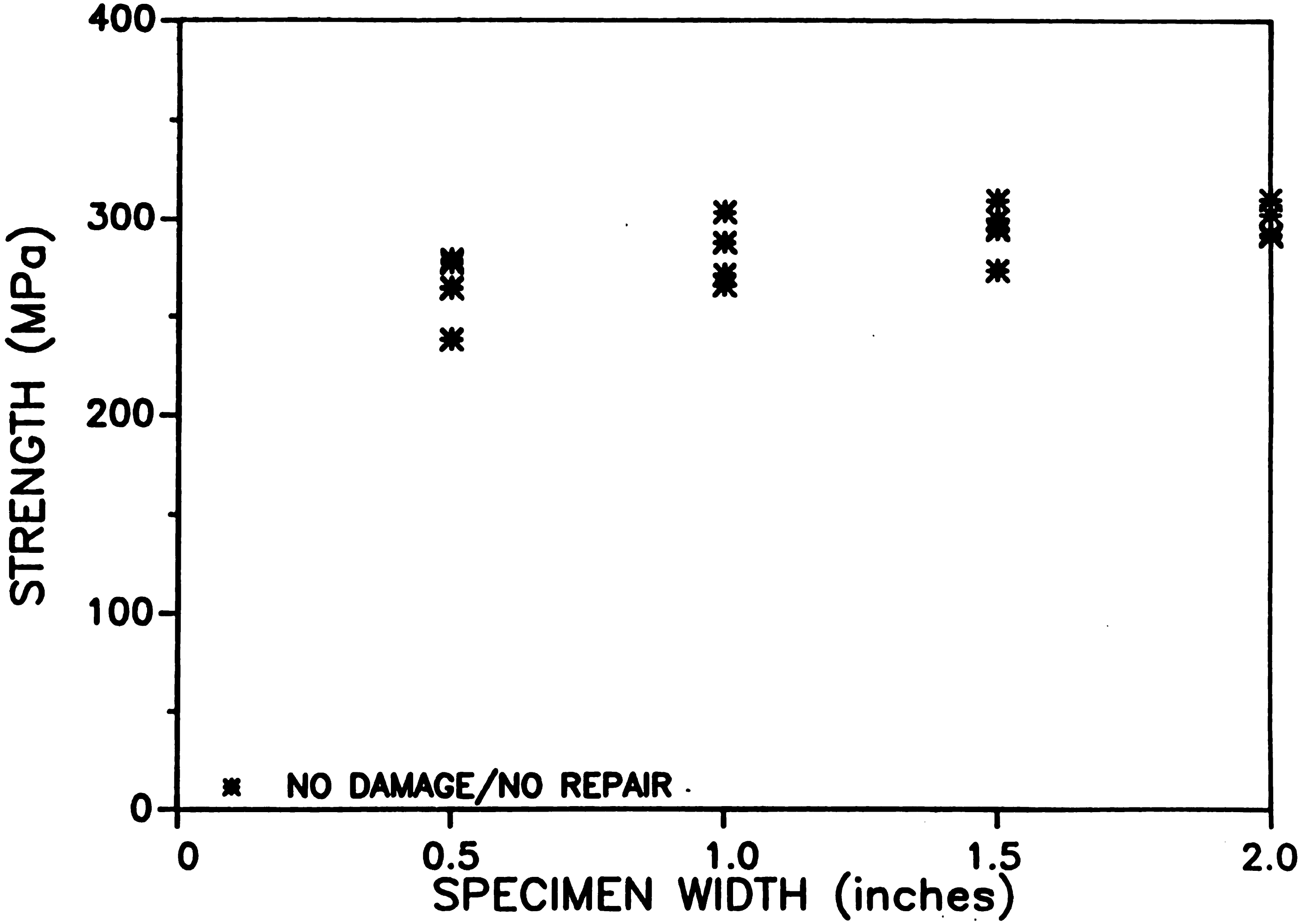

Figure 5.2 Excel 8610 Material Results For Scaling Study.

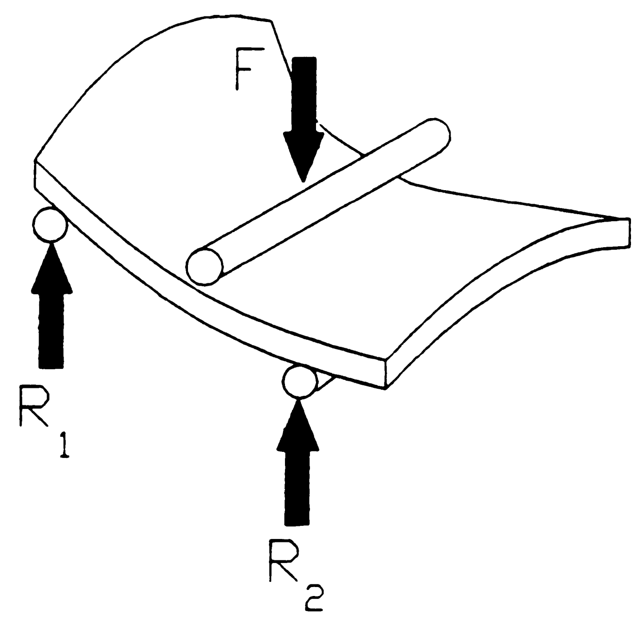

Figure 5.3 Schematic Illustrating the Anti-Clast Phenomena.

exhibit substantial amounts of anisotropy. In other words, it occurs in composites which contain two different, yet dominant fiber directions.

To evaluate this phenomenon, bi-directional strain gage rosettes were mounted to the surface of the Excel 8610 material. Figure 5.4 illustrates the placement and orientation of each of the rosettes. One rosette was mounted symmetrically at the center of the specimen and directly underneath the loading pin. The second rosette was mounted midway between the center of the specimen and the edge, and the third was located very near the specimen edge. The specimen was loaded under three-point bending, therefore all of the strain rosettes were mounted to the bottom (tensile) side of the specimen so as to not interfere with the loading pin. The results reveal that readings taken from the center-mounted rosette were purely axial, therefore verifying the negation of transverse strain. Also, the transverse strains increased in a direction outward toward the edge of the specimen and the results are illustrated in Figure 5.5. These results verify the possibility of an anti-clastic phenomenon being produced in the 2" (50mm) specimen during three-point bending. Therefore, this phenomenon is documented and during the calculation of stress, is negated by utilizing the flexural formula.

Calculating the stress at failure for repaired composite specimens is a very complicated, and nearly impossible, task. This is due to the variance in the thickness dimension caused by the application of reinforcing materials and resin. An accurate assessment of the fiber content in the damaged zone is impossible. Consequently, it was proposed that the original thickness of the specimens would be utilized in all subsequent stress calculations due to flexural loading. By setting this precedence, the comparison

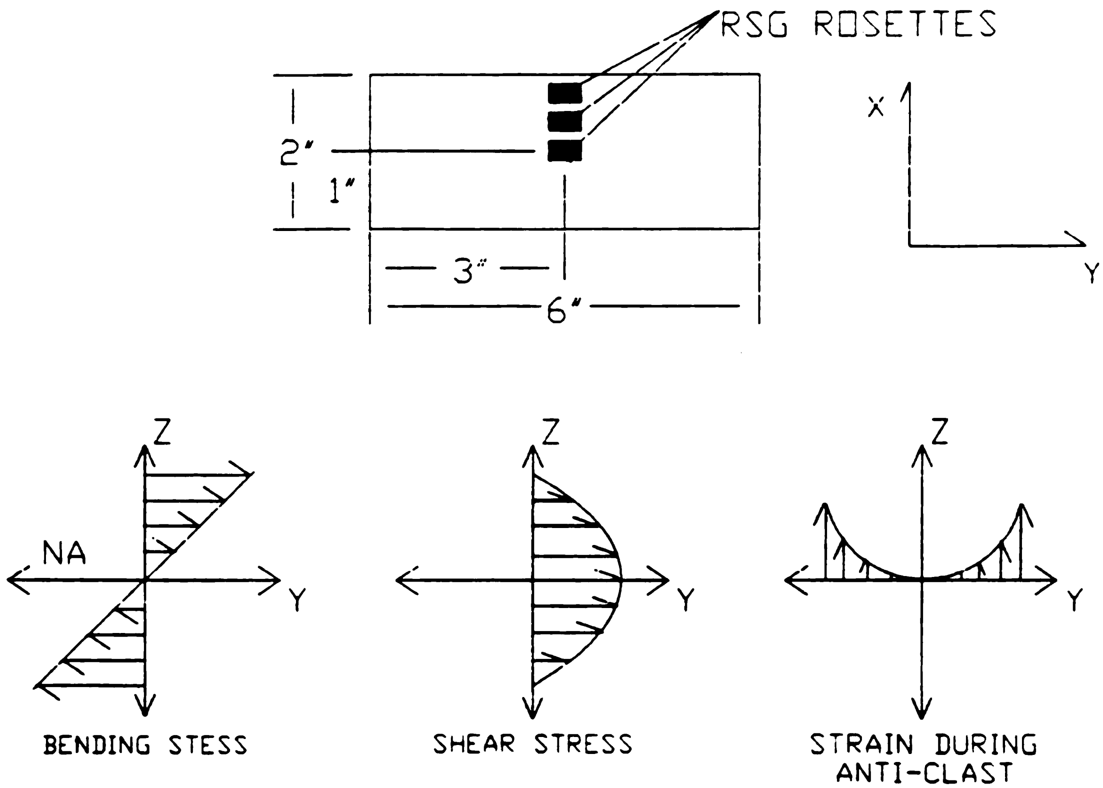

Figure 5.4 **Strain Gaging of Excel 8610 to Study the Poisson Effect During Three-Point Bending.**

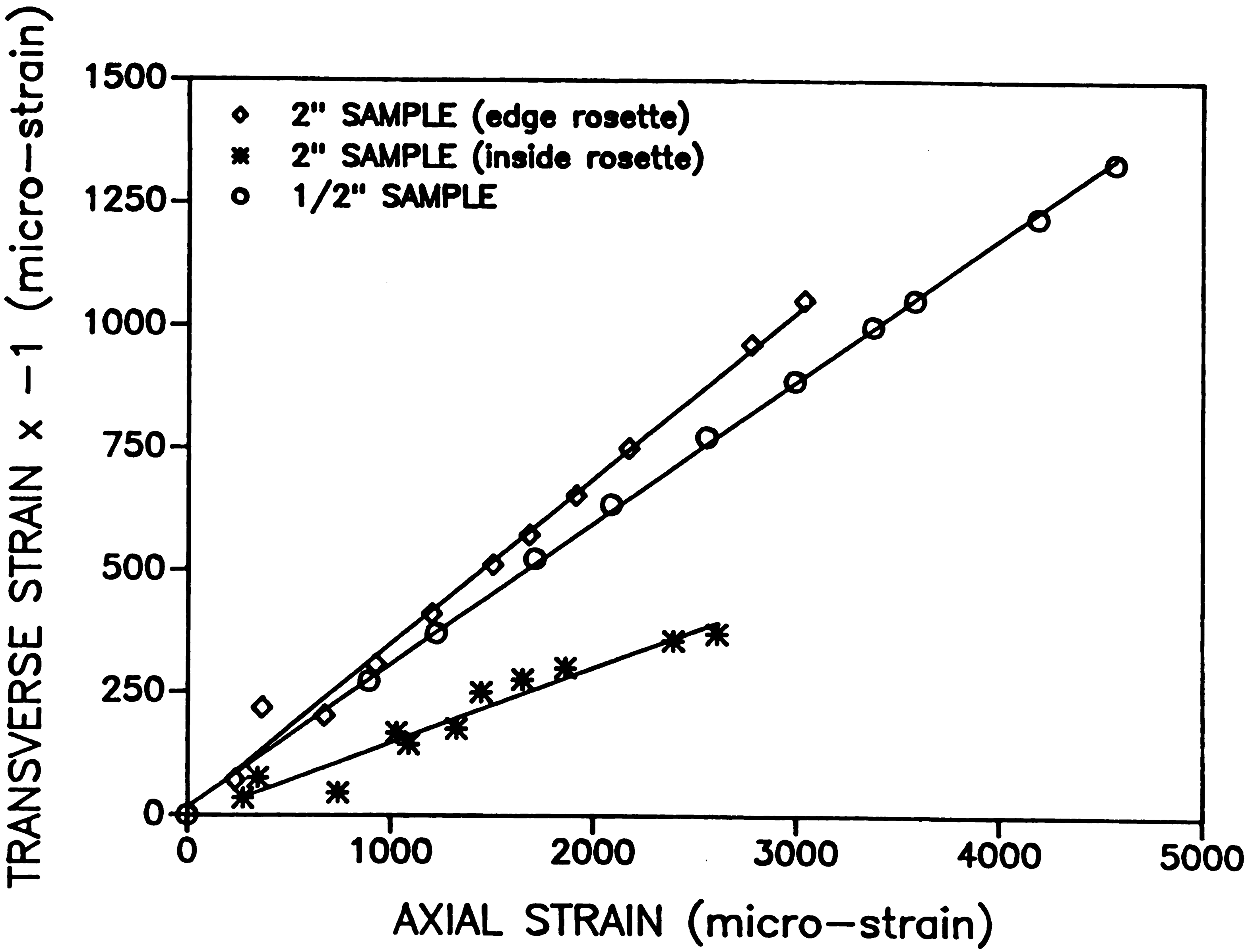

Figure 5.5 Excel 8610 Material Illustrating the Poisson Effect.

of original strength to recovered strength became the differential comparison during load to failure between the two situations. This differential mode of comparison was maintained throughout all testing procedures.

5.1 Impact-Induced Damage

A. Equivalent Damage Hole Size

An evaluation of the equivalent damage hole size began by utilizing the Dynatup impactor to create perforated impact damage in several 4" x 6" (100mm x 150mm) specimens. In this analysis, parameters such as impact velocity, impact energy, and total energy were documented. After impact perforation, each 4" x 6" (100mm x 150mm) specimen was trimmed to the dimensions of 2" x 6" (50mm x 150mm) and fractured under three-point bending. The residual flexural strength was then evaluated. The flexural strengths of the impacted specimens were compared to the drilled hole specimen to determine the equivalent damage hole size created by the impactor upon perforation of the specimens. In addition, the repairability of circular cut-out and impact-induced damage was also found. The motivation of this analysis was to determine a correlation between the void zone, damage zone, and repair zone, to evaluate composite damage. All three different fiber geometries were evaluated and the results are discussed in the following sections. Actual tables containing the raw data values can be found in the appendix of this document.

(a) Owens Corning SMC

The results for the Owens Corning material are illustrated in Figures 5.6-5.8. Figure

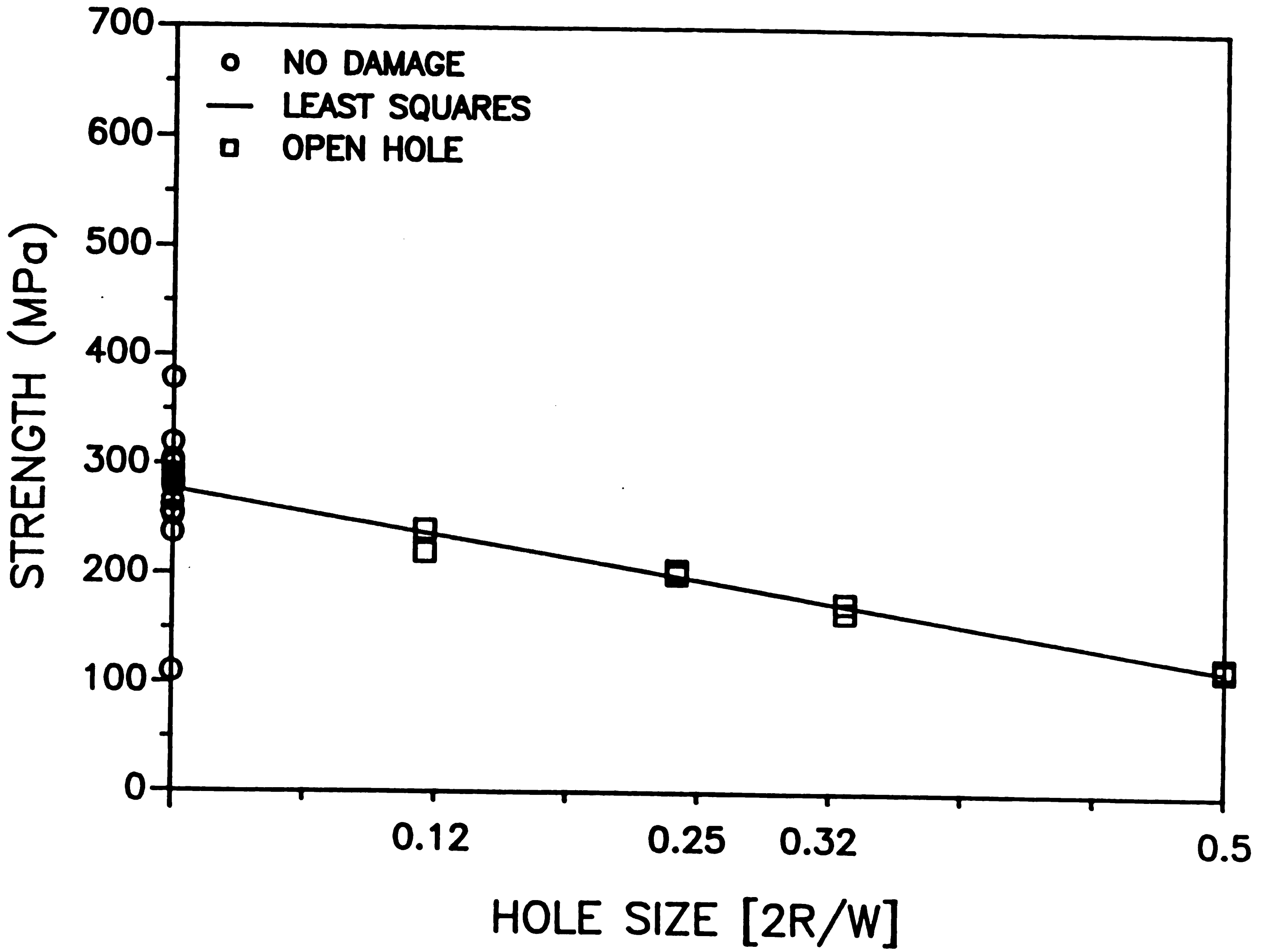

Figure 5.6 Owens Corning SMC: Drilled Hole Study to Illustrate the Loss of Strength After Creating Various Void Sizes.

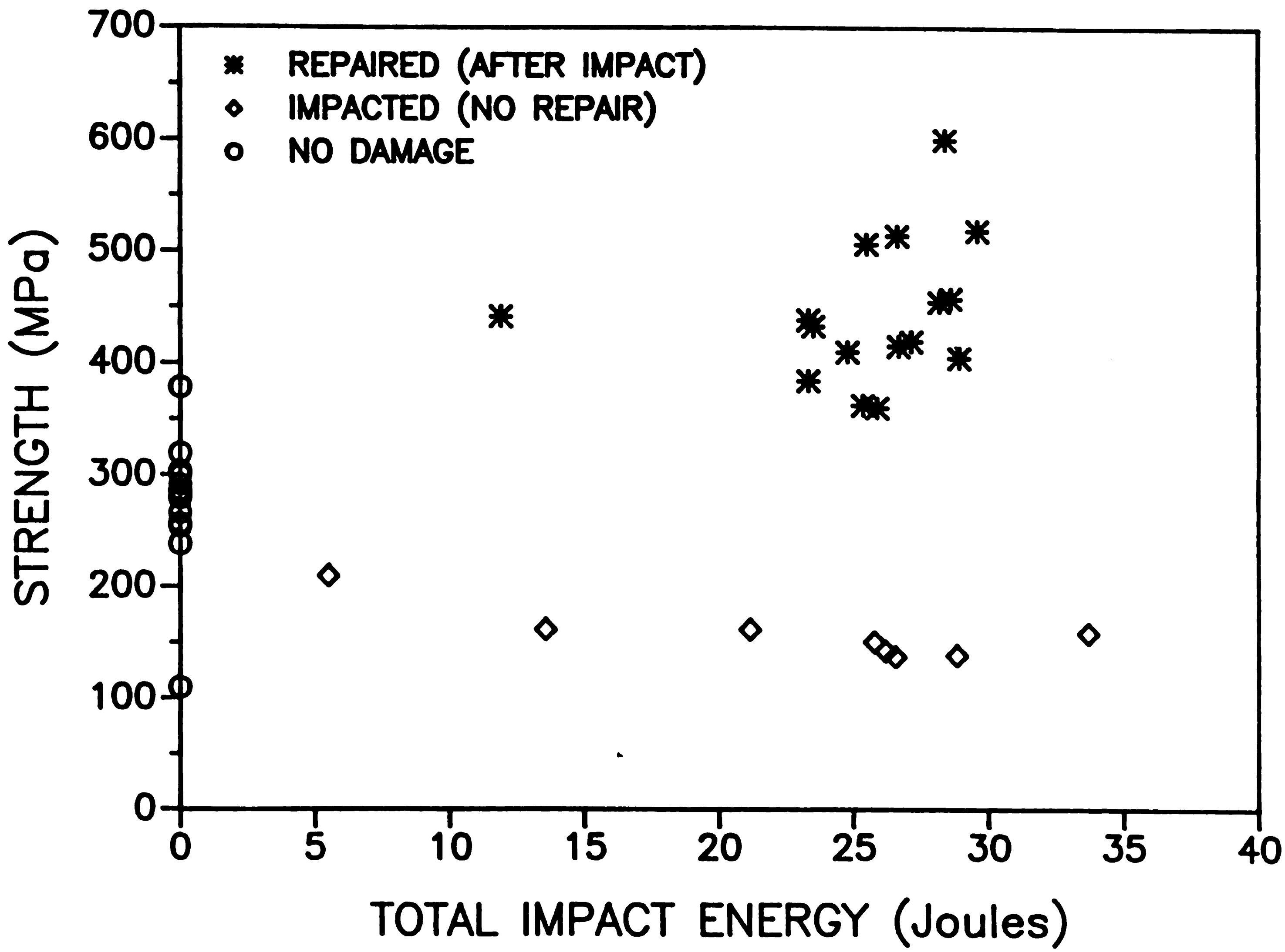

Figure 5.7 Owens Corning SMC: Impact-Energy Study. All Specimen were Impacted then Loaded to Failure Under Three-Point Bending. The Repaired Specimen Utilized the Standard Repair Technique.

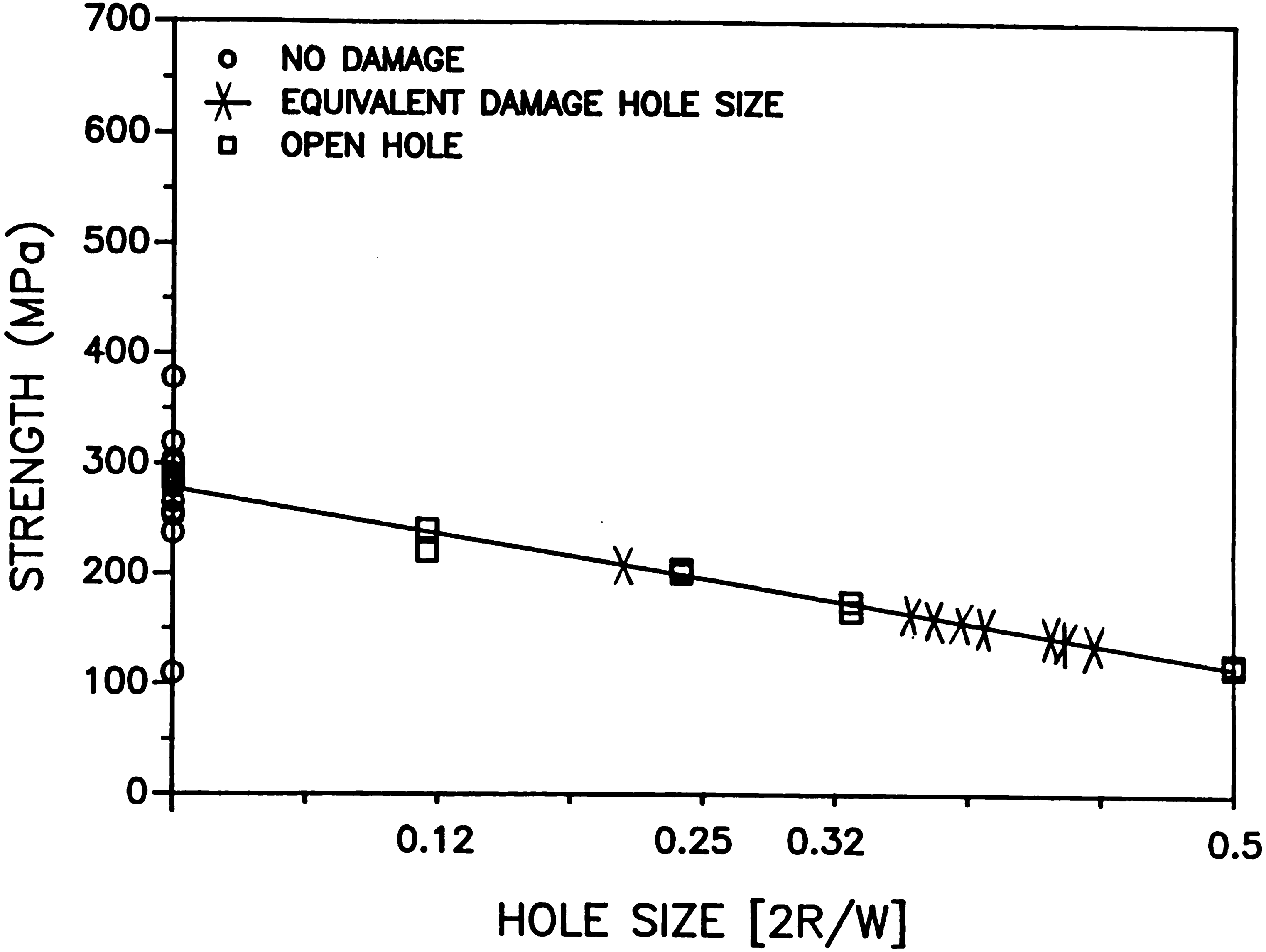

Figure 5.8 **Owens Corning SMC: Equivalent Damage Hole Size Evaluation to Correlate the Damage Zone Size with the Repair Zone Size.**

5.6 illustrates the amount of residual flexural strength in each specimen after drilling a known hole size into each of the specimen. A linear least-squares line is also depicted in the diagram. Figure 5.7 illustrates the residual flexural strength after perforated impact damage. The plot also depicts the flexural strength of particular specimen after the repair of perforated impact damage. Some of the impacted specimens were also repaired utilizing the repair scheme outlined in Chapter 2, and then fractured under three-point bending. In addition, it is advantageous to utilize the debris surrounding the perforated zone as the reinforcing material. Therefore, the superior flexural strength of the repair specimens, depicted in Figure 5.6, is primarily due to the strength of the glass reinforcing patch material.

To correlate the equivalent damage hole size, Figures 5.6 and 5.7 are superimposed and represented in Figure 5.8. Note that the resulting equivalent damage hole size in the SMC material is greater than the 1/2" (13mm) impactor. Having examined the damaged specimen further, it is verified that the damage zone is actually larger than the void zone. Therefore, the repair zone must encapsulate the larger damage zone area.

(b) Excel 8610

The results for the 8610 material are illustrated in Figures 5.9-5.11. The trend to notice in this evaluation is that the total energy absorbed into the panel is again quite high. Therefore, the equivalent damage hole size, illustrated in Figure 5.11, reveals a hole size slightly larger than 1/2" (13mm), though smaller in size than the SMC material.

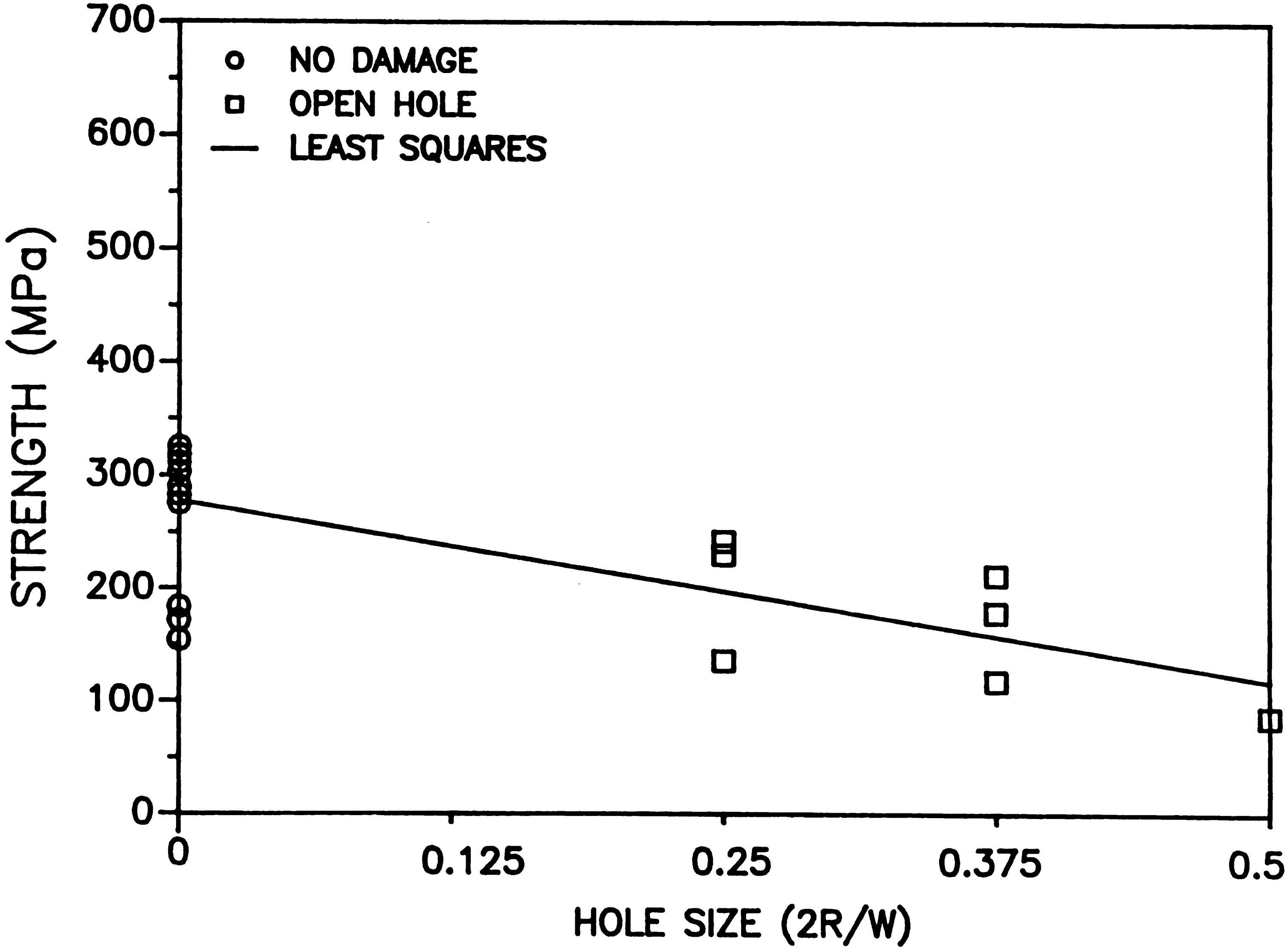

Figure 5.9 Excel 8610: Drilled Hole Study to Illustrate the Loss of Strength After Creating Various Void Sizes.

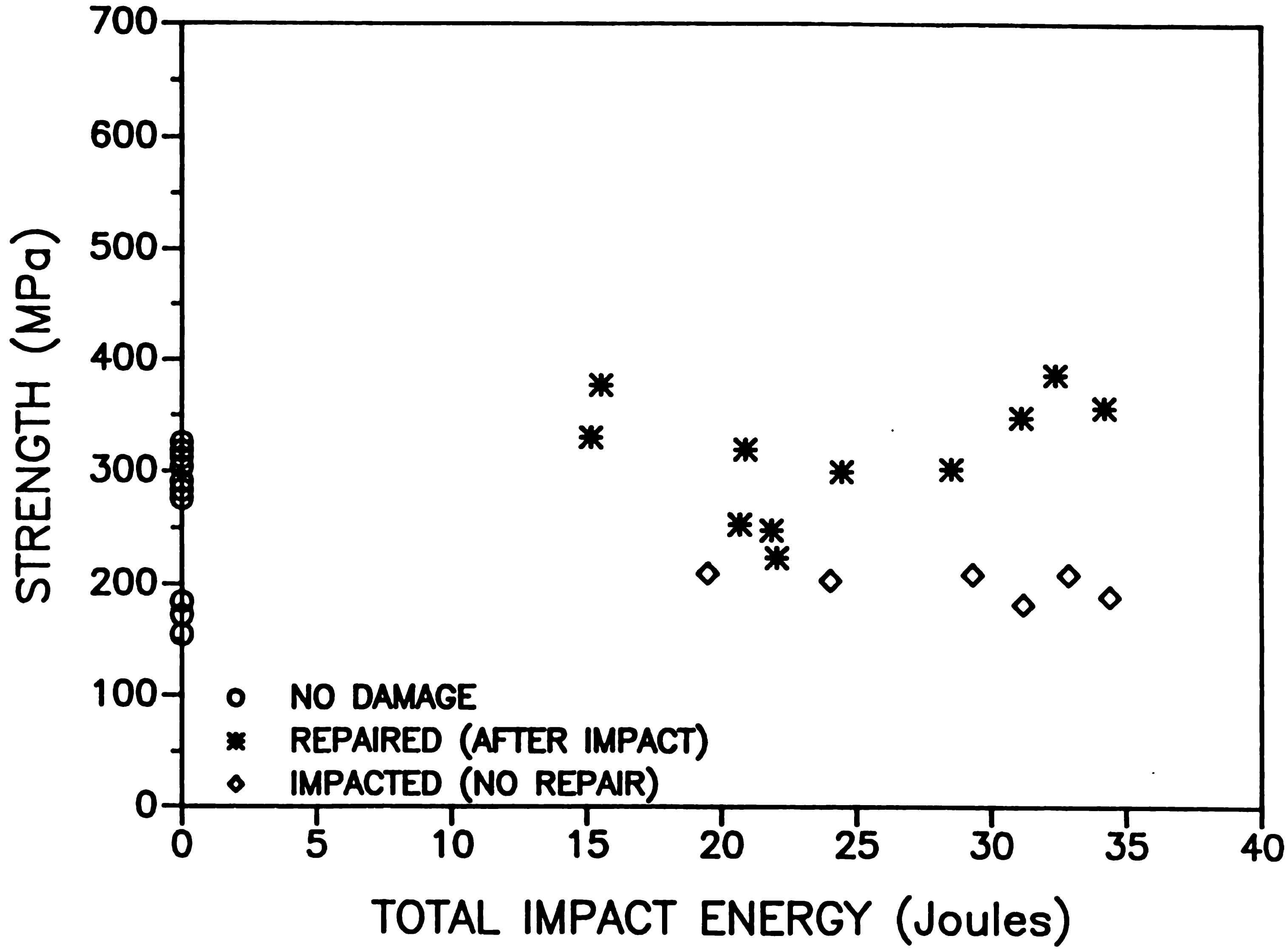

Figure 5.10 Excel 8610: Impact-Energy Study. All Specimen Were Impacted then Loaded to Failure Under Three-Point Bending. The Repaired Specimen Utilized the Standard Repair Technique.

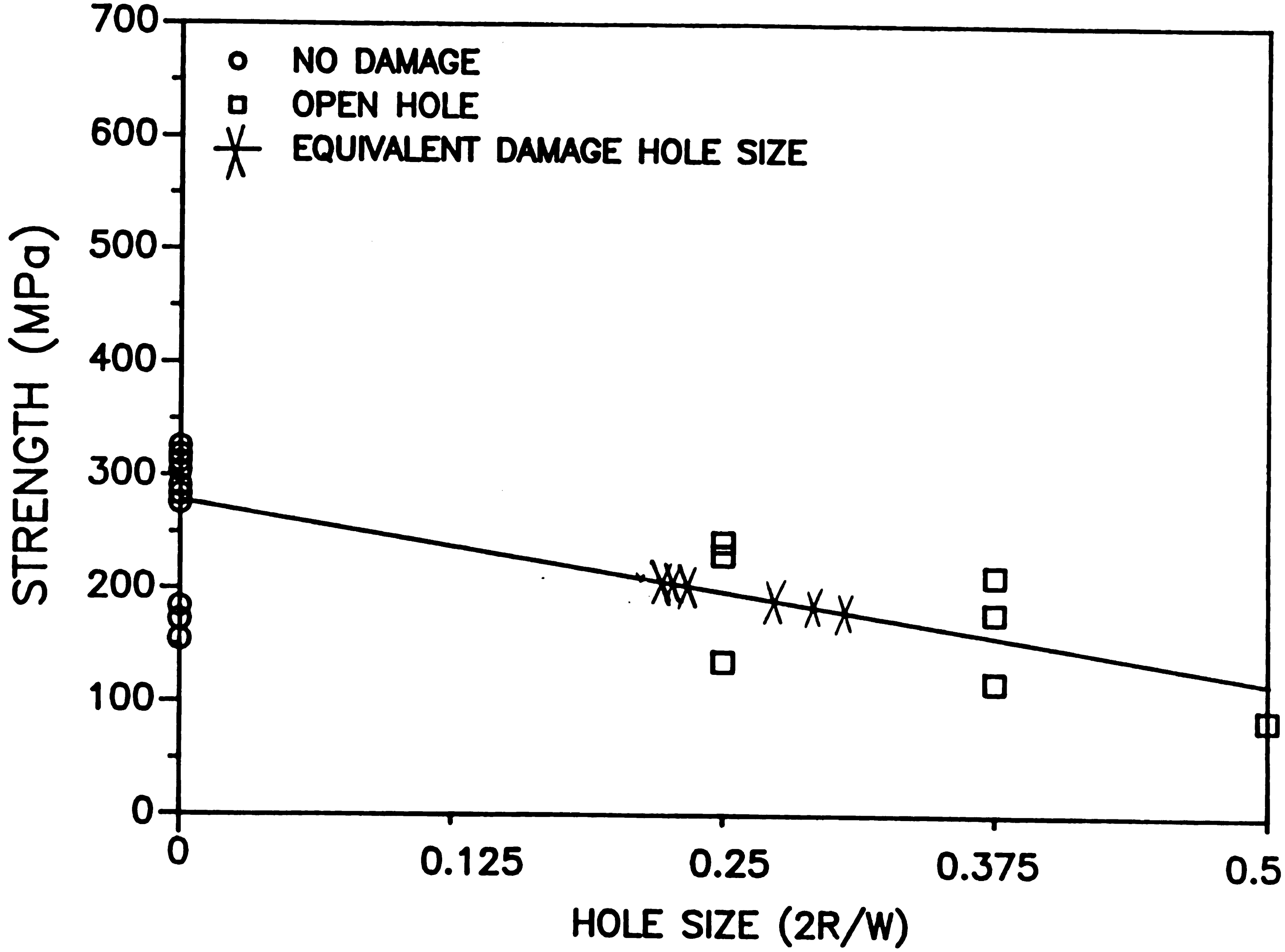

Figure 5.11 Excel 8610: Equivalent Damage Hole Size Evaluation to Correlate the Damage Zone Size with the Repair Zone Size.

The difference in equivalent damage hole size between the SMC material and the RTM is primarily a result of the fiber geometries of both materials, i.e., the SMC is random, chopped glass and the RTM is continuous swirl glass. The fiber continuity of the RTM material tends to be a bit stiffer under the same loading conditions. Note that the actual void region in the 8610 material is visually larger than the void region formed in the SMC material. However, the equivalent damage size data reveals a zone that is smaller than the SMC. Again, this difference in equivalent damage hole size is primarily due to the difference in fiber geometries.

(c) Excel 2415-Warp

The results for Excel 2415 are illustrated in Figures 5.12-5.14. The results illustrate equivalent hole sizes between 1/4" (6.35mm) and 1/2" (12.6mm). This would imply that the SMC and 8610 panels are absorbing more energy than the 2415 panels. Note that the fiber geometry of 2415 is a rigid cross-woven mat with the addition of random chopped glass chemically bonded into it. The rigid structure of the 2415 material displays very little deflection upon impact. The results show that it also absorbs a larger amount of energy. Furthermore, there is also a direct correlation between the total amount of energy absorbed in the panel and the size of the damage zone. If the panel absorbs a high amount of energy upon impact, then the damage zone envelopes a much greater area than the void zone or perforated hole zone. This conclusion is verified by comparing Figures 5.7, 5.10, and 5.13. Note also that the fiber orientation throughout the drilled hole survey and the equivalent damage hole size study is in the warp direction.

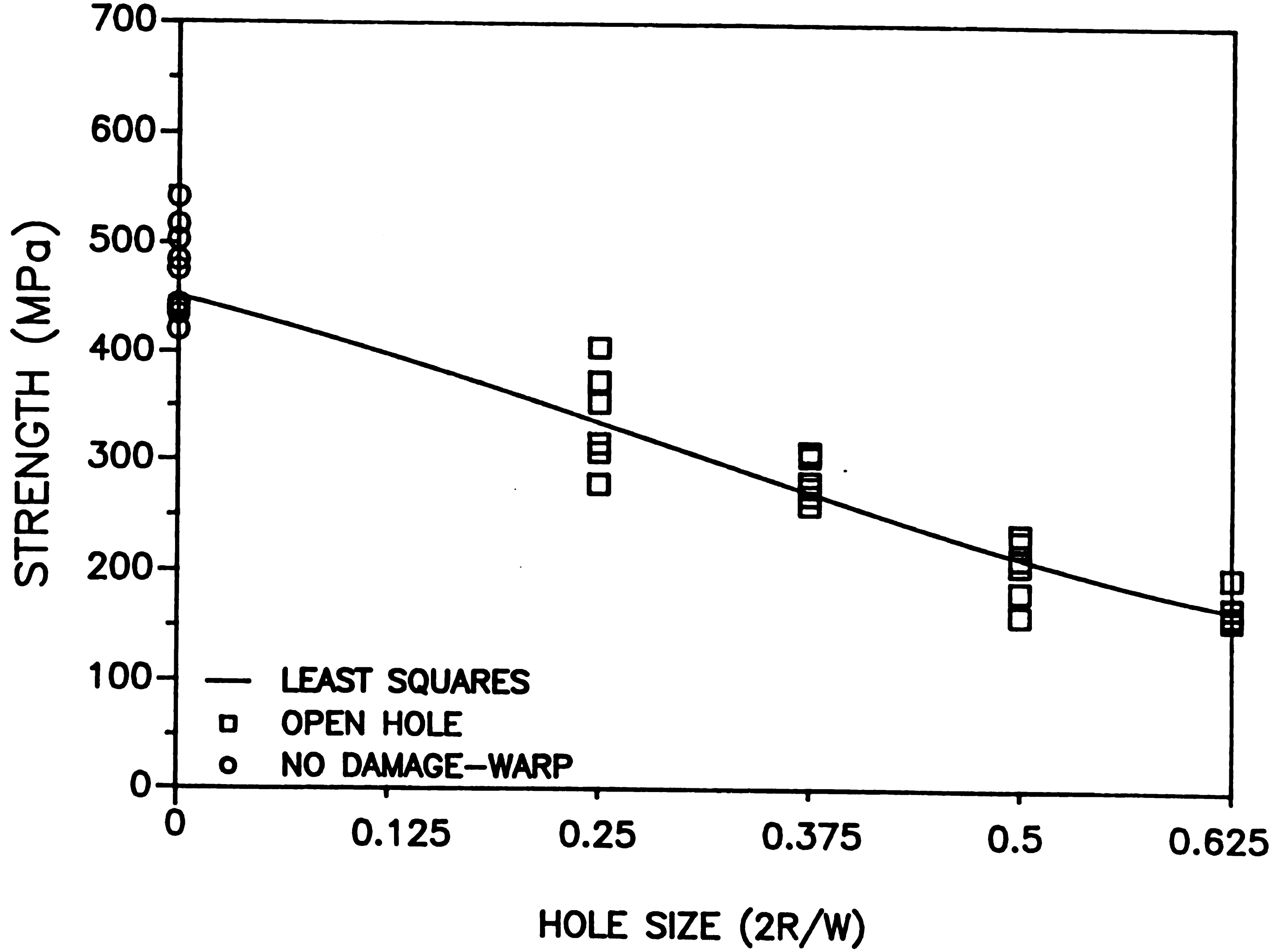

Figure 5.12 Excel 2415: Drilled Hole Study to Illustrate the Loss of Strength After Creating Various Void Sizes.

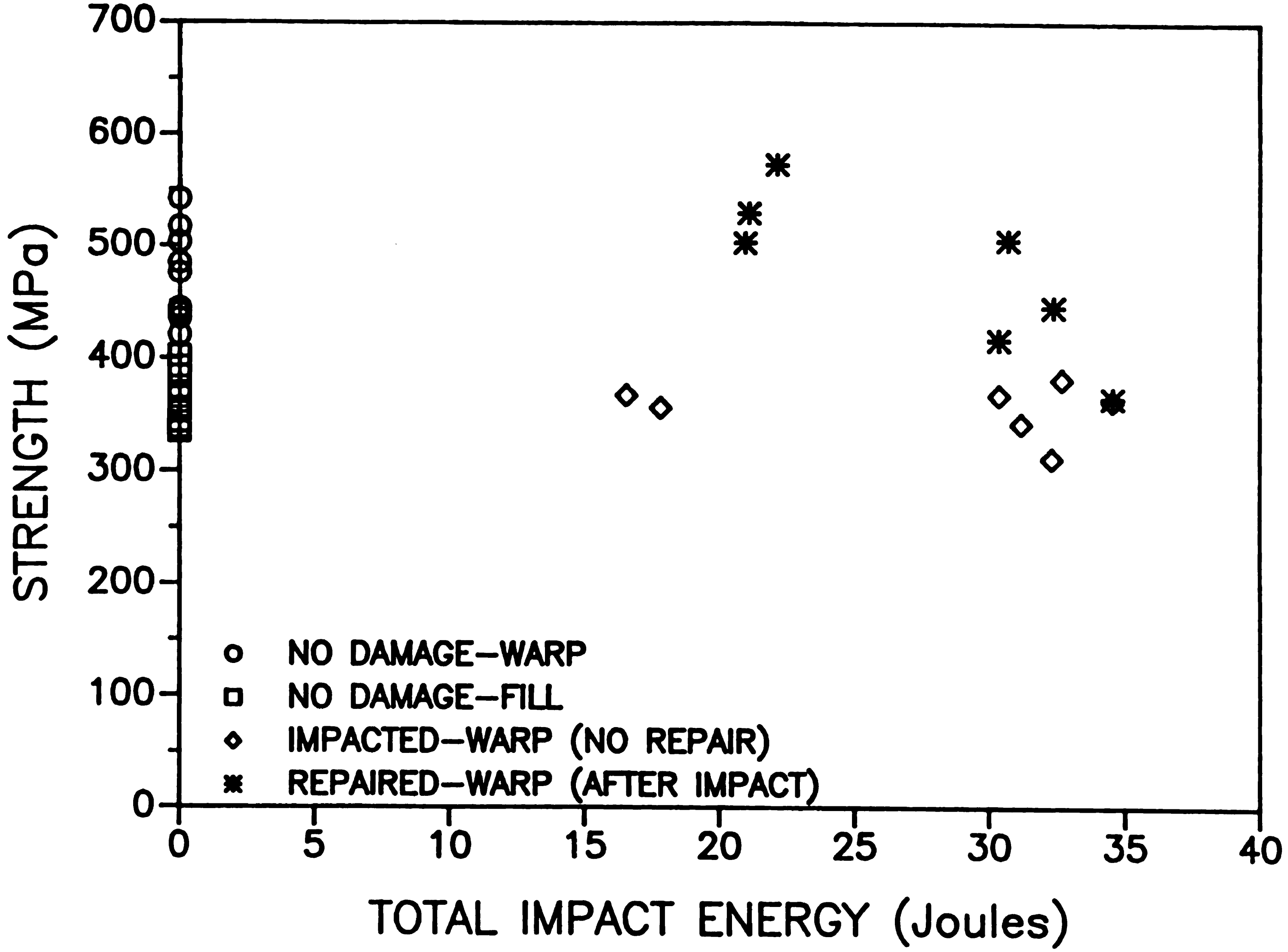

Figure 5.13 Excel 2415: Impact-Energy Study. All Specimen were Impacted then Loaded to Failure Under Three-Point Bending. The Repaired Specimen Utilized the Standard Repair Technique.

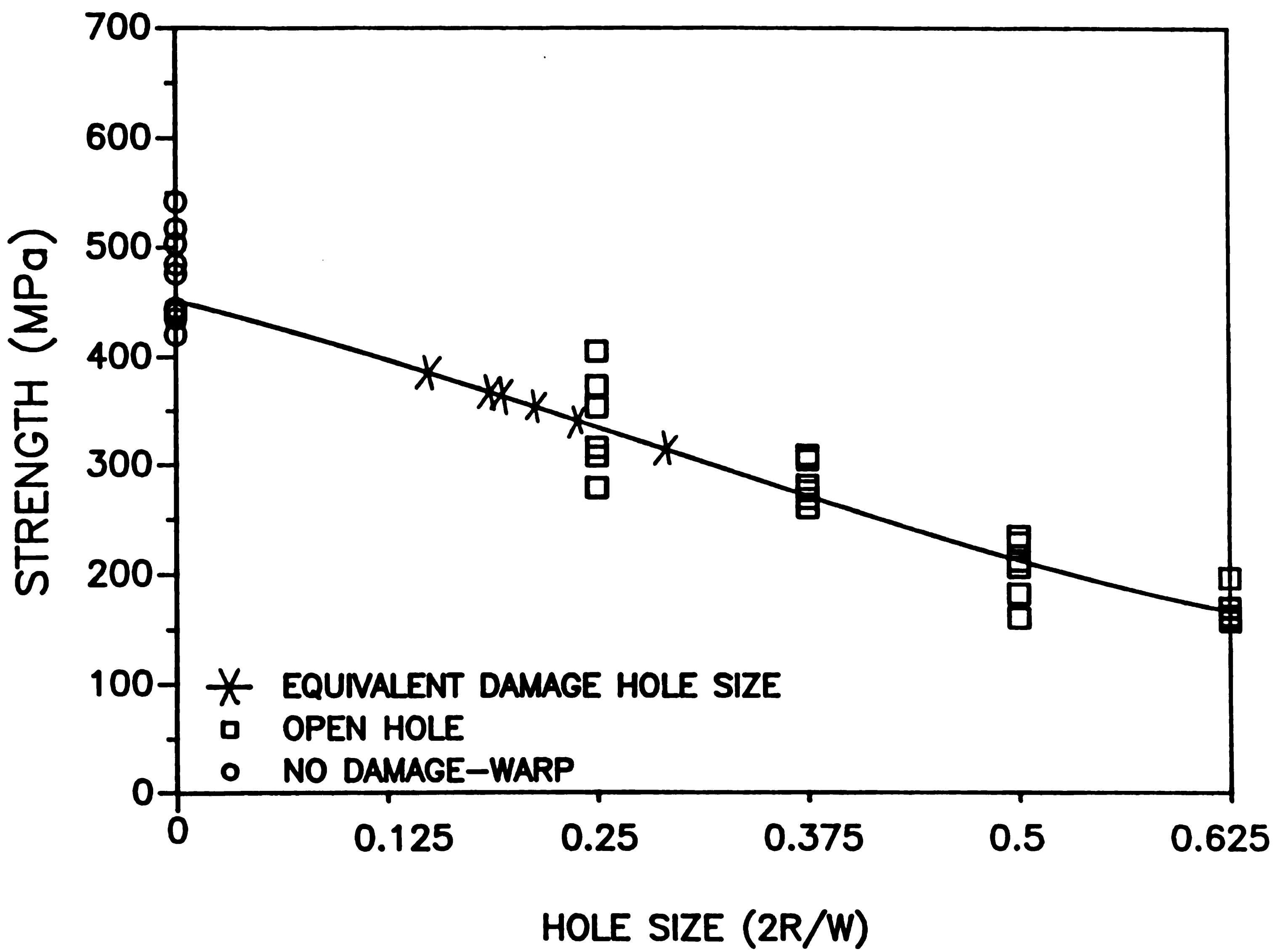

Figure 5.14 Excel 2415: Equivalent Damage Hole Size Evaluation to Correlate the Damage Zone Size with the Repair Zone Size.

Additional tests on both the warp and fill directions are discussed in the following sections.

B. Effects of Fillers in Circular Cut-Outs

The effect of the circular cut-out and the influence of using fillers in the damage zone is illustrated in Figure 5.15 for the Owens Corning SMC material. It can be seen that by increasing the hole size, the integrity or strength of the specimen is reduced significantly. Note that a non-dimensionalized hole size of 2R/W is used in the diagram. During the repair procedure various fillers, such as, resin, chopped glass, a plug and a strap were implemented into the void zone. The results conclude that regardless of the damage size, a filler/patch combination can be added to restore the original flexural strength of each specimen. This trend stayed consistent for the Excel materials as well.

5.2 Through-The-Thickness Scarf Joining (Owens Corning SMC)

A. Single-Scarf Joining (Owens Corning SMC)

In this particular study, each 2" x 6" (50mm x 150mm) specimen was cut into two halves and a single-scarfing angle was created along both edges of the cutting line. The standard repair technique was performed and the results are illustrated in Figure 5.16.

The results show that both the 5° and 10° single scarfs are superior to the 15° single scarf. This would verify that increasing the bondable surface area between the reinforcing patch and the repair zone increases the flexural strength of the repair.

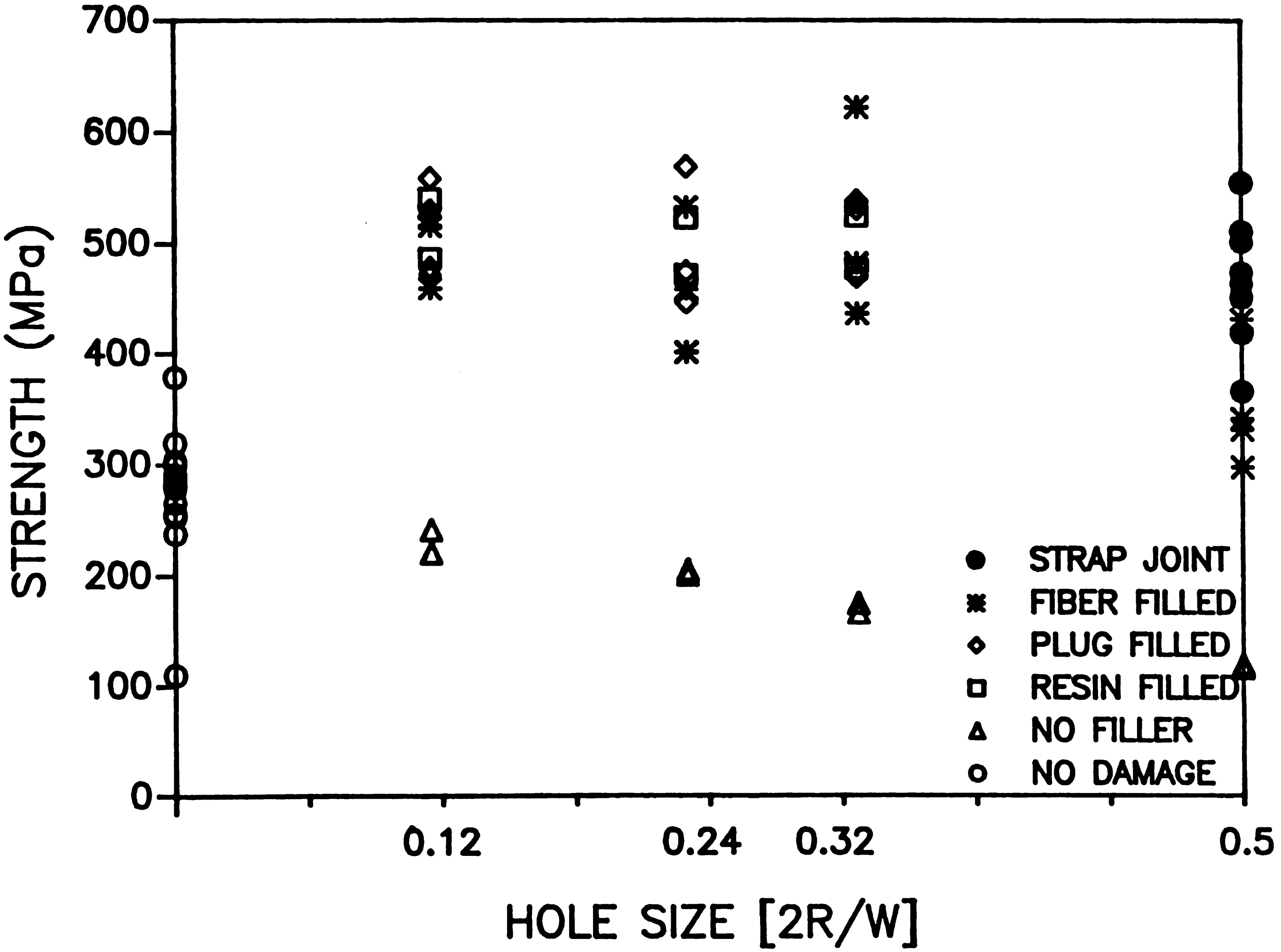

Figure 5.15 Owens Corning SMC: Drilled Hole Study Using Fillers in the Void Regions During Standard Repair.

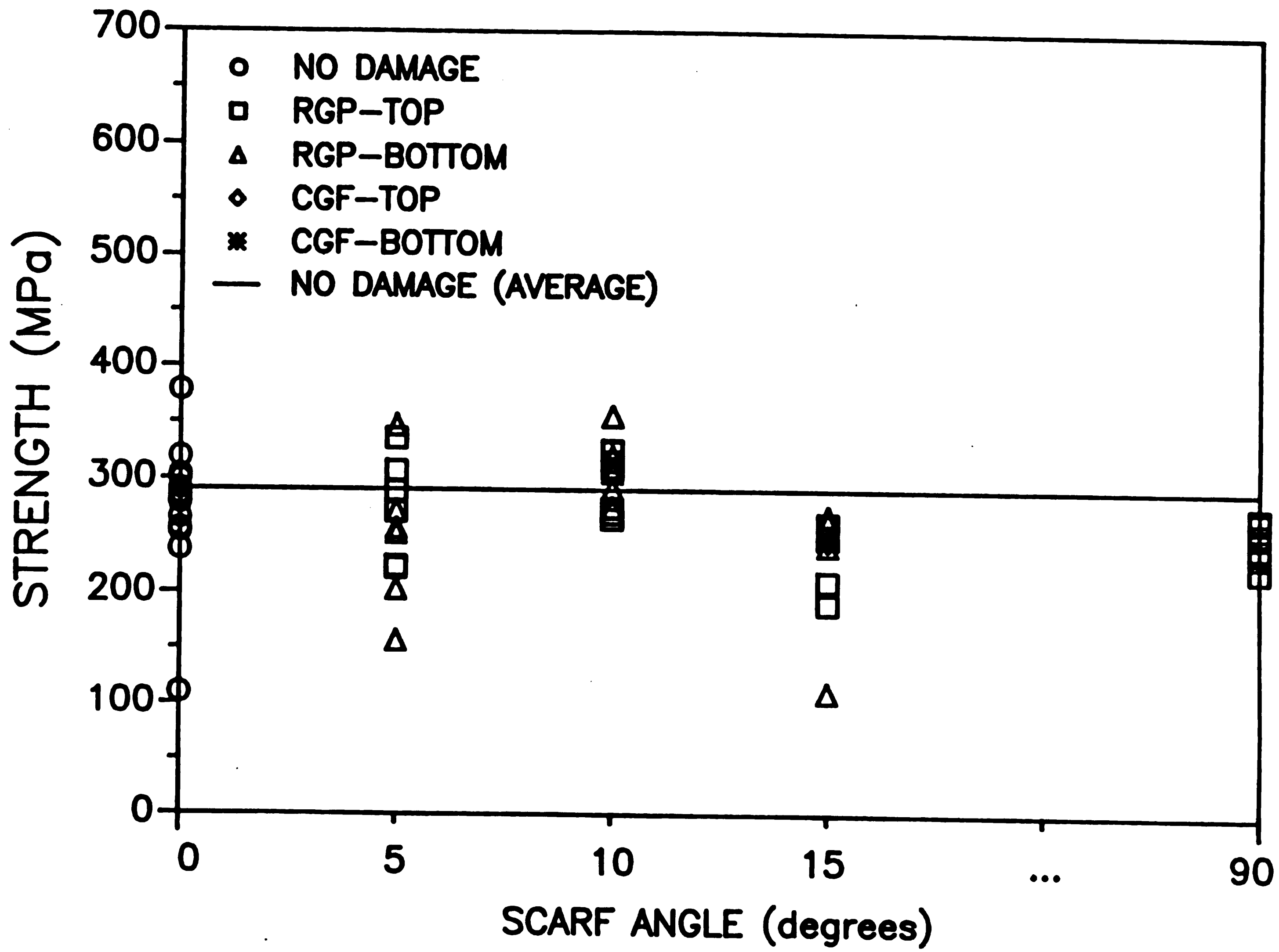

Figure 5.16 Owens Corning SMC: Illustrating the Influence of Single Scarf Joining, With and Without the use of Fillers During Standard Repair.

However, the 5° scarf is not superior to 10° scarf. A possible reason for this behavior is that the 5° scarf removes more material around the joining area than the 10° scarf, and the removal of more material creates a larger damaged zone. In addition, it should be noted that the variance in the repair strengths among the cases is not very significant. In view of the effort involved in specimen preparation, it was determined that the butt-joint proved more effective and efficient for thin composite panel repair.

During the analysis of the single scarf-joint, notations of loading either from the top or the bottom of the specimens are included in the diagram. The notations refer to failure loading exerted on the top (scarfed) side of the panel or bottom (non-scarfed) side of the panel. The top side of the joint experiences compression during loading while the bottom side experiences tension. The strengths from both types of loading do not reveal a significant difference, which implies that the scarf repair technique is valid for repair on panels which may experience both tension and compression. Again, note that regardless of the scarfing angle, 100% flexural strength can be restored in the specimens by simply utilizing a butt-joint with two layers of reinforcing patch material per side.

B. Scarf-Hole Study (Owens Corning SMC)

An analysis was also conducted on the Owens Corning SMC material to determine if scarfing the area around a 1/2" (13mm) drilled hole or circular void would increase the strength of the repaired joint. The scarfed region was created by grinding a 5° bevel radially outward from the void. This bevel encompassed a 2" (50mm) radial region outward from the center of the void. Initially, only one side of the damage was scarfed, and then both sides were scarfed. This simulated a single and double scarf-joint respectively. All scarfing was compared to both an undamaged 4" x 6" (100mm x 150mm) reference specimen group, and another set of 4" x 6" (100mm x50mm) reference specimen with a 1/2" (13mm) drilled hole in the center. The results are illustrated in Figure 5.17. They reveal that regardless of a single or double scarf joint repair technique, at least on this particular material, the flexural strength integrity can be restored by using the standard repair technique discussed initially in section 2.6. In fact, the repair strengths are much greater than the undamaged specimen strengths. Again this is primarily because of the high rigidity and strength of the glass reinforcing patch material. Note also the reference lines that are drawn from the left edge to the right edge of the plot. The lower line represents the average reference undamaged specimen strength, while the upper line represents the average reference undamaged specimen strength after two layers of glass reinforcing material have been added to both sides. This upper line illustrates the patch strength influence during non-separated specimen repair, and is discussed further in Chapter 6.

5.3 In-Plane Configuration Analysis

A. Bond Line Angle

A series of tests were conducted to evaluate the effects of altering the bond line of the separated joint repair specimens. By altering the bond line a correlation was developed to determine the effects of the direction of bending force with respect to the bond line configuration. In this study, all of the joints were separated and the two

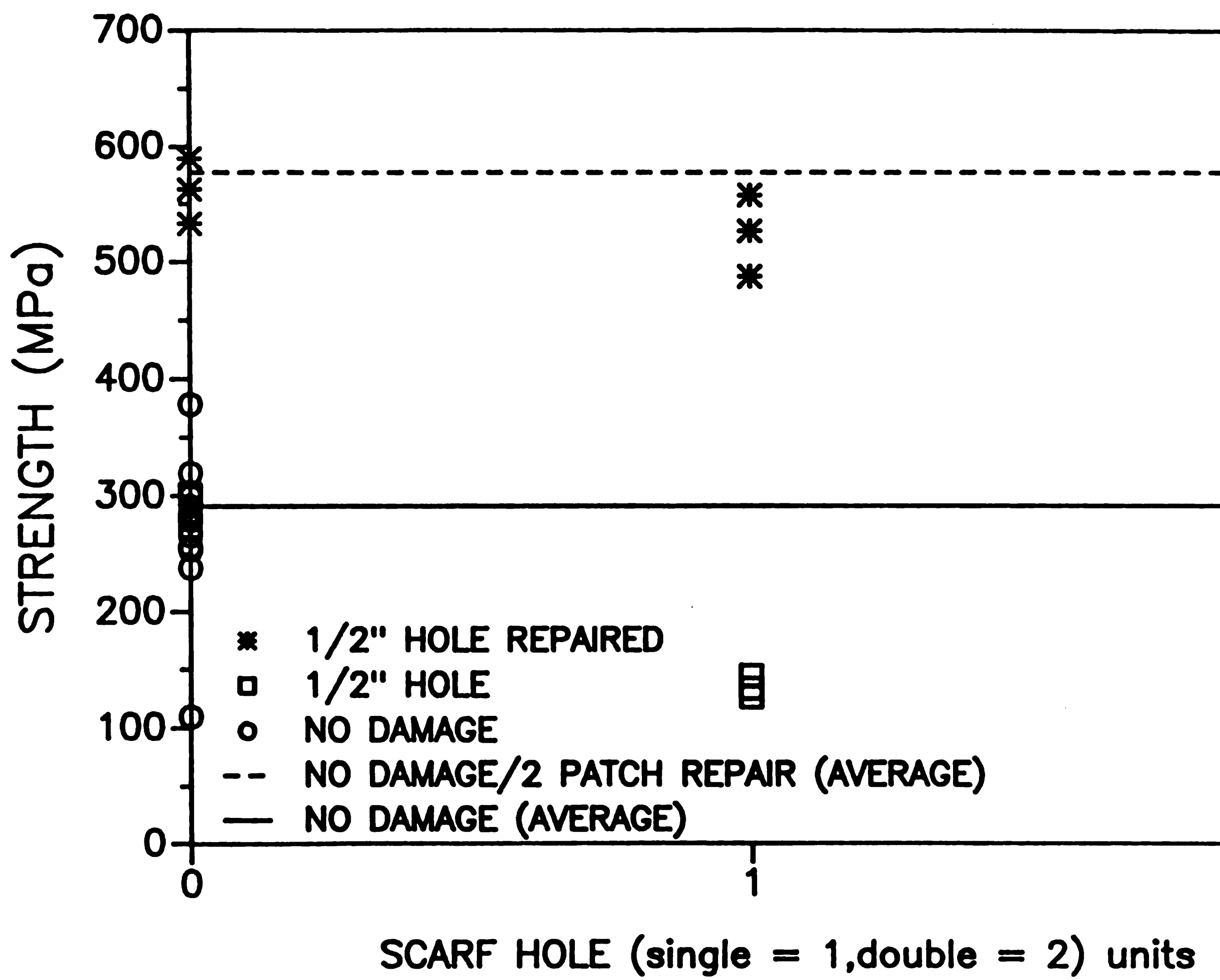

Figure 5.17 Owens Corning SMC: Scarf-Hole Study to Illustrate both Single and Double Scarfing a Thin Panel Joint, With Standard Repair.

mating parts of the specimens were joined in a butt-joint type configuration. The initial study consisted of an analysis of bond lines measuring 0°, 30°, 45°, 60°, and 90° to the direction of the loading pin.

(a) Owens Corning SMC

The results for Owens Corning are illustrated in Figure 5.18. The plots show that at an off-axis angle of 30° the strength of the repaired specimens is restored. In fact, an off-axis angle of about 15° would probably restore 100% of the flexural strength. Note the high repair strengths of the 60° and 90° bond lines. They are approximately the same, though ideally the 90° bond line should be superior since this bond line is complemented by the 6" (150mm) length of the specimen plus the double lap-joint repair. Again, the straight lines depicted in subsequent figures illustrate both the average undamaged strength (solid line) and the averaged undamaged strength (dashed line) with the application of two layers of reinforcing material per side.

(b) Excel 8610

The same testing outlined above was conducted for both of the Excel materials. The results for 8610 are illustrated in Figure 5.19. For the off-axis analysis the results followed a trend similar to that exhibited by the Owens Corning SMC. Again, 30° restored the strength of the specimens, as well it appears that 15° would again satisfy the strength requirement. A different trend is exhibited though for the 45° angle. There does not seem to be any increase in strength from the 30° angle. This change in trend may be a result of the different fiber geometry between Owens Corning SMC and Excel 8610. Another trend to highlight is the increase in flexural strength between 60° and 90°.

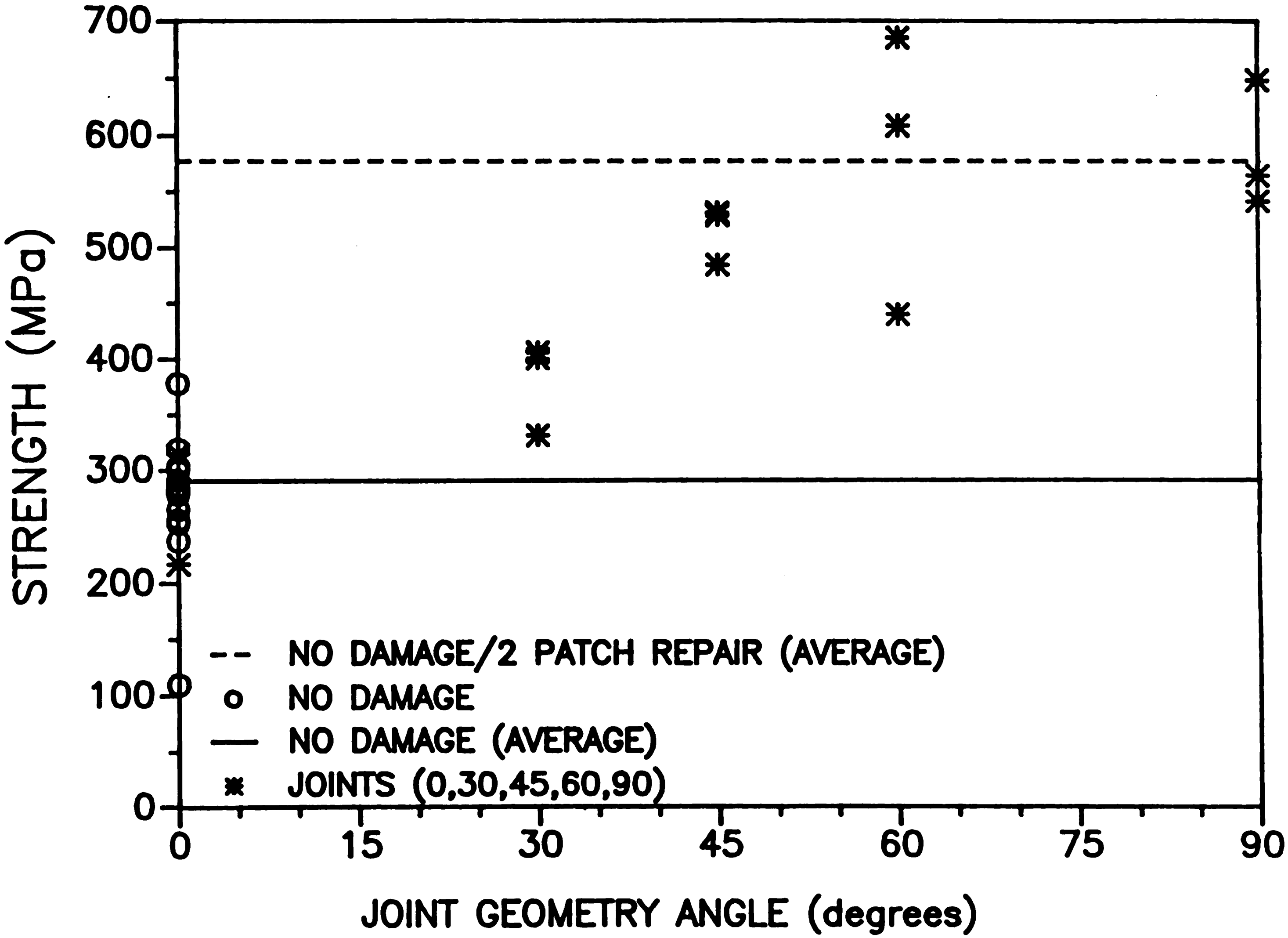

Figure 5.18 Owens Corning SMC: Off-Axis Joint Geometries to Illustrate the Effects of Modifying the Bond Line to the Direction of Load. Standard Repair Was Utilized.

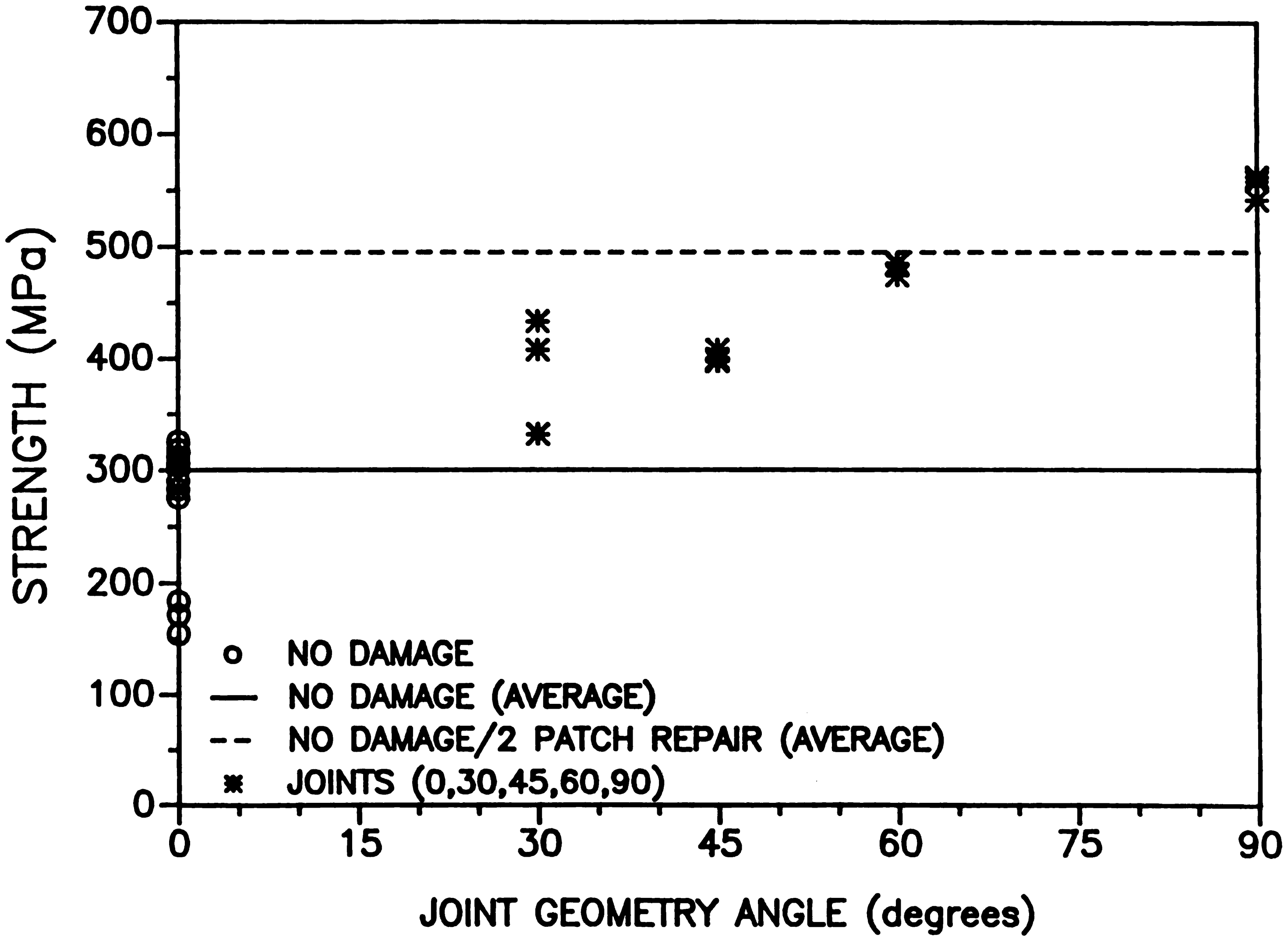

Figure 5.19 Excel 8610: Off-Axis Joint Geometries to Illustrate the Effects of Modifying the Bond Line to the Direction of Load. Standard Repair Was Utilized.

It is approximately 84%. This trend supports the idea that in repair, care must be exercised to not build in a repair strength that is too high since this can shift the damage into a different area.

The shifting of damage to another area is a topic of concern. Throughout all testing, remarks were documented regarding the failure modes, and the amount of flexure in each specimen at failure. The failure modes are listed as either catastrophic (brittle) or non-catastrophic (ductile). There seems to be a direct correlation between the amount of flexure in a specimen at failure and the failure mode. If the specimen fails in a non-catastrophic mode then the load being applied to fracture the specimen is being distributed further into the specimen, and its flexural value increases. However, it should be noted that this higher strength value could induce excessive loads elsewhere in the composite panel. Further comments regarding the failure modes are discussed in the appendix of this document.

(c) Excel 2415-Warp

Results for Excel 2415 reveal a couple of different trends. The results are illustrated in Figure 5.20. The bond line contour survey illustrates the same trends as shown by the other two materials, with the exception of the comparison of fiber warp direction to fiber fill direction. Figure 5.20 reveals that the strength of the fiber warp direction is restored at the 60° mark, as well, it indicates the incapability in restoring the strengths by using the reinforcing patch material in the cross-woven 2415 material. Consequently, the repair strength does not surpass the original undamaged reference strength of the composite until a bond line angle of approximately 50° is achieved. A

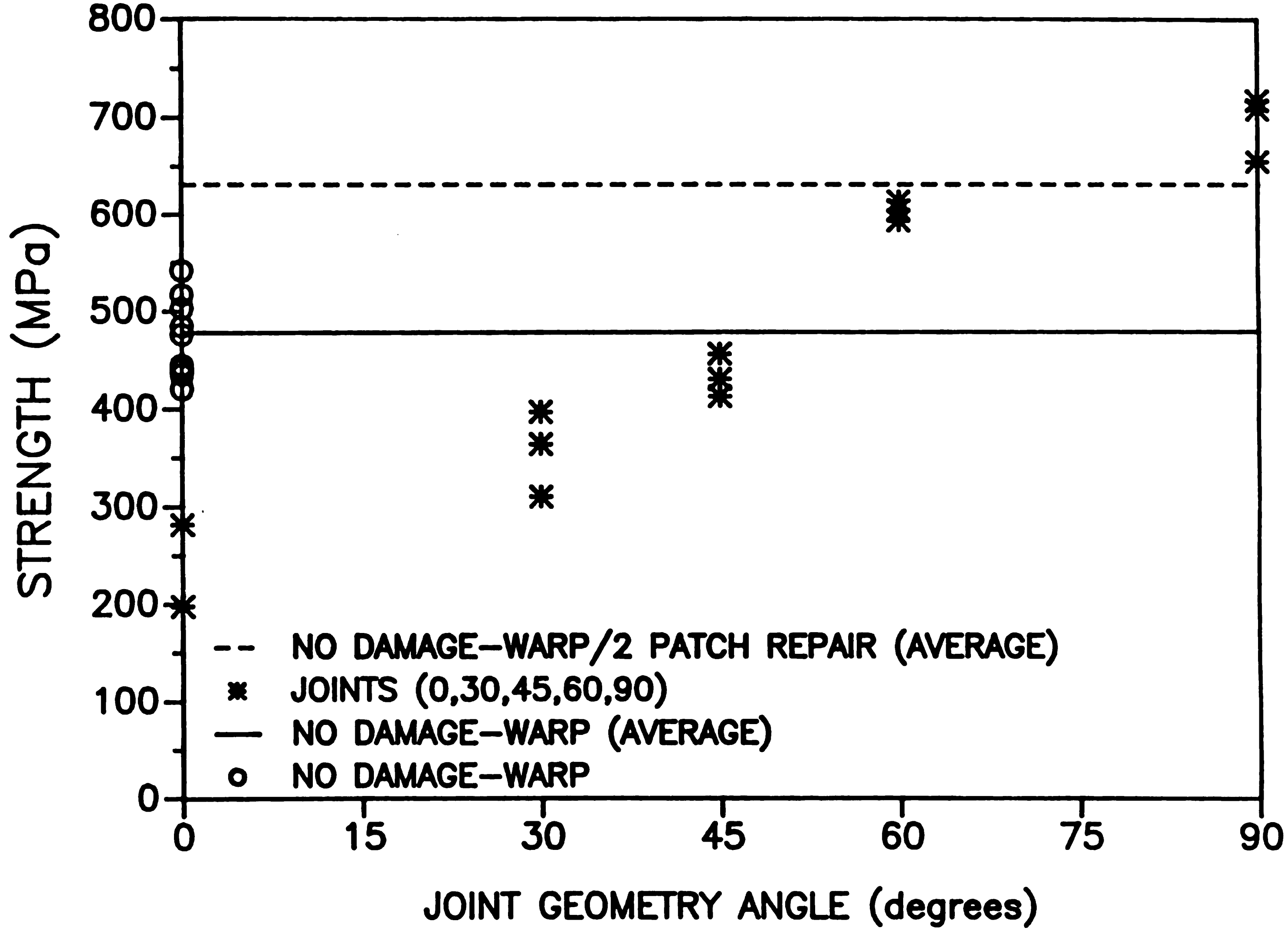

Figure 5.20 Excel 2415: Off-Axis Joint Geometries to Illustrate the Effects of Modifying the Bond Line to the Direction of Load. Standard Repair Was Utilized.

possible solution to this incapability is to repair the 2415 warp direction specimens with a sample of the Excel cross-woven mat. However, since the reinforcing material is very rigid, it will probably delaminate during failure rather than add more repair strength.

B. Bond Line Pattern

The secondary testing involved looking into the idea of cutting a known in-plane contour into each of the specimens. The contours were in the shape of a V-,U-,W-,UU-, WW- and S-joint. This investigation proved to be a very important.

The following sections present the results of the joint geometry study for all three different fiber geometries. All specimen were repaired following the standard procedures. The Owens Corning composite utilized Maraset as an adhesive, while the Excel materials used Resin Services resin.

(a) Owens Corning SMC

Since the 60° and 90° bond lines demonstrated such superior results (100% increased strength), it was determined that subsequent bond line contours would incorporate bond line angles from 60° to 90°. The resulting contours were symmetric and based on the form of the V-joint. The V-joint was cut into a 2" x 2" (50mm x 50mm) central area on the repair specimen. The slope of each side of the V was measured to be approximately 60°. The U-joint was designed to investigate if rounding off the corners of the V-joint, would reduce the stress concentrations at the bond line. The results show that indeed this was the case. The strength values, illustrated in Figure 5.21, were predominantly higher for both the U- and the UU- joints. Results also show

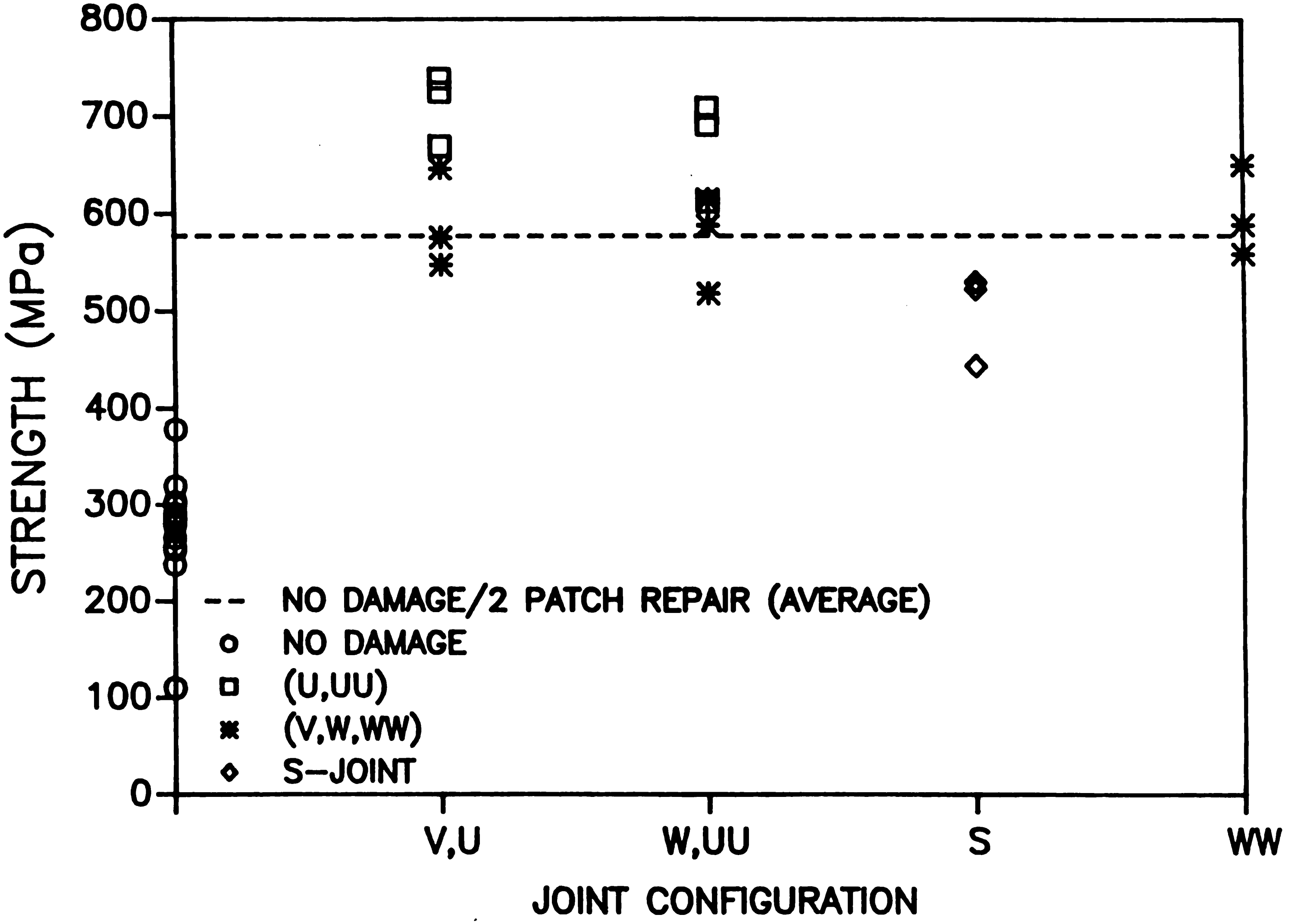

Figure 5.21 Owens Corning SMC: V- and W-Joint Analysis Which Incorporates the Results Found in Figure 5.17.

that regardless of a V-, W-, or WW-joint, at least over a 2" x 2" (50mm x 50mm) area, the strength values are approximately the same.

An additional contour was also evaluated under the title of S-Joint. This set of testing was designed to try to find an optimum bond line joining contour. Further discussion regarding the S-Joint is postponed until Chapter 7.

(b) Excel 8610

Results for the V-Joint analysis again utilize the optimum angle of 60° in the V-, U-, and W-joint design. Again the repair results, shown in Figure 5.22 are superior in restoring flexural integrity, though the results for the V- joint versus the U-joint are not consistent with those exhibited by the Owens Corning material. However, the UU-joint surpasses the W-joint like before.

(c) Excel 2415-Warp

The results of the V-joint contour study, shown in Figure 5.23, revealed that the V- and W- joints are superior to the U- and UU-joints. However, note that all joint configurations were successful in restoring the flexural strength of the specimens, even in the warp direction.

C. Bond Line Depth (Excel 2415-Warp)

The results of the joint geometry analysis provoked inquiry into a correlation between the in-plane depth (in the specimen's length direction) of the joint and its corresponding strength. The material used for this particular survey was Excel 2415 in the warp direction. This investigation was designed to determine an optimum depth of

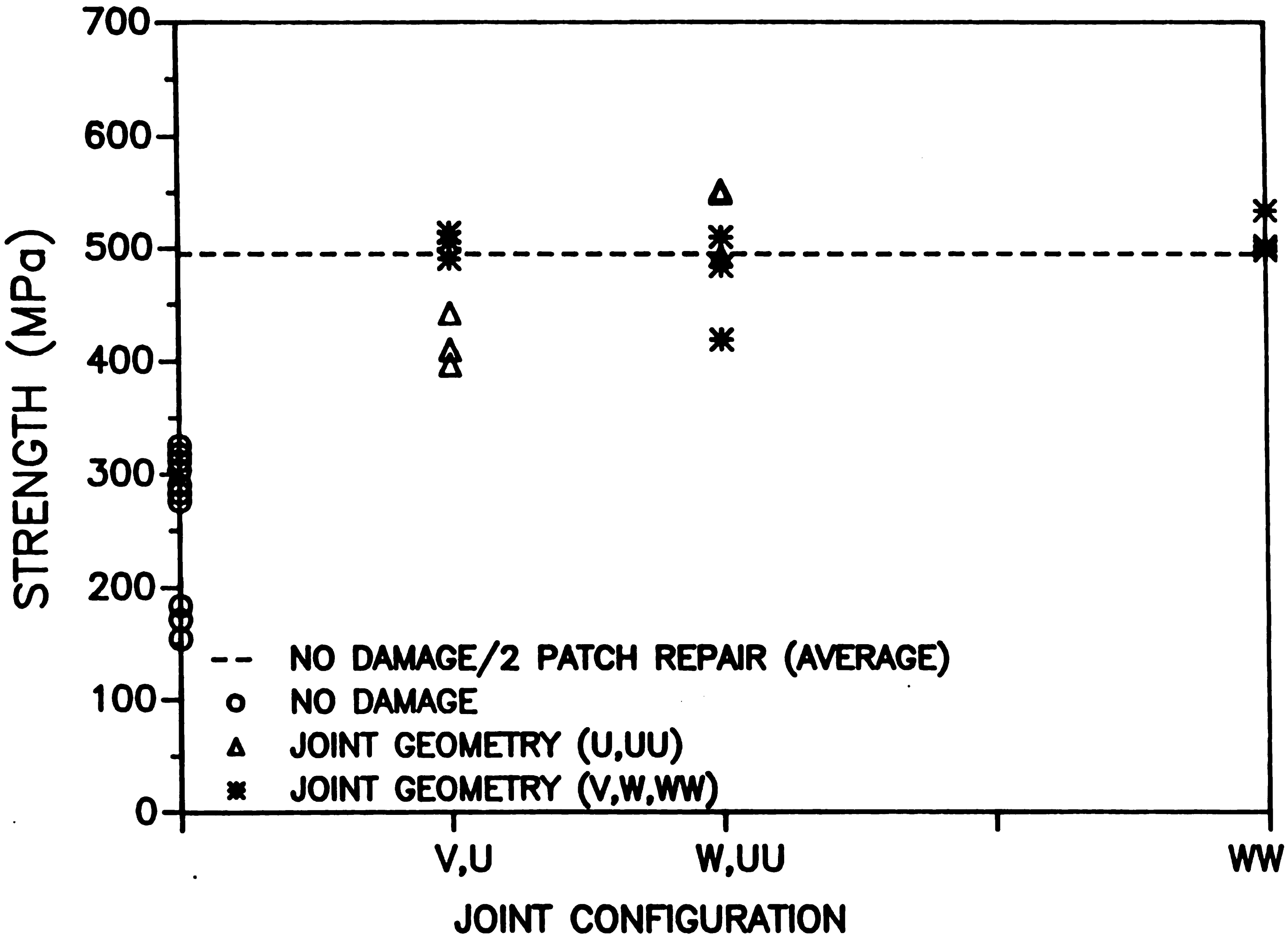

Figure 5.22 Excel 8610: V- and W-Joint Analysis Which Incorporates the Results Found in Figure 5.18.

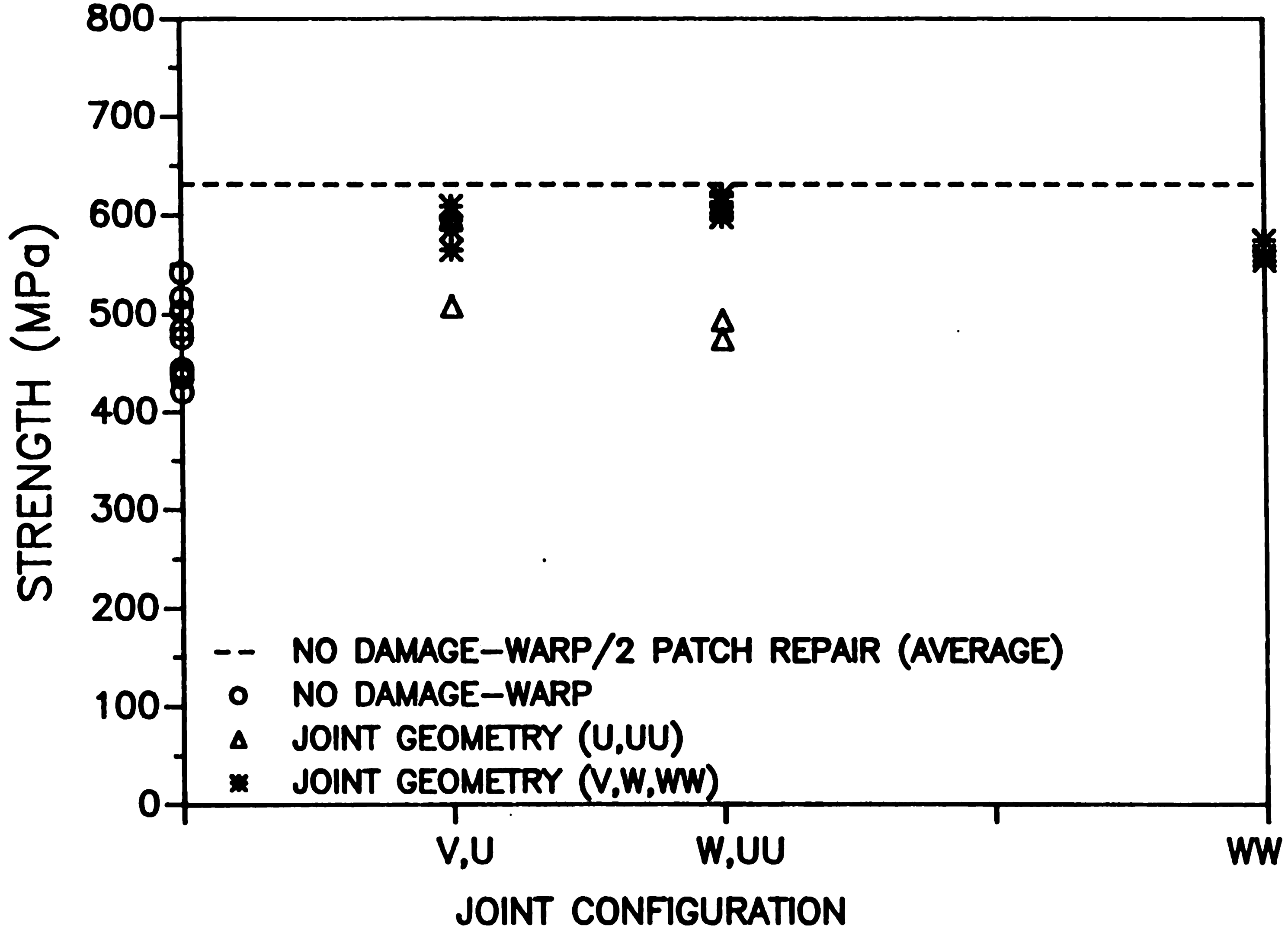

Figure 5.23 Excel 2415: V- and W-Joint Analysis Which Incorporates the Results Found in Figure 5.19.

joint, from correlating the results of the 60°-90° bond line investigation. The two different contours that were evaluated were the V- and W-joints. The V-joint was designed over the following specimen areas: (1) 4" x 2" (100mm x 50mm), (2) 3" x 2" (75mm x 50mm), (3) 2" x 2"(50mm x 50mm), and (4) 1" x 2" (12.6mm x 50mm). The depths of each joint are listed first, therefore depths of 4"(100mm), 3"(75mm), 2"(50mm), and 1" (25mm) were analyzed. The depth design of 4"(100mm) incorporated a 76° bond line, while the 3"(75mm), 2"(50mm) and 1" (25mm) depth designs incorporated a 72°, 63° and 45° bond line, respectively. Plots illustrating the results of this analysis are shown in Figures 5.24-5.25. In addition, an analysis was conducted on a set of V-joint specimen with a 1" (25mm) joint depth. In this study, the edges of the V-joint were slightly scarfed to check if scarfing would reduce the stress concentration along the bond line, and possibly shift the failure mode, or increase the strength of the joint. Figure 5.24 reveals the results of both the V-joint and the V(scarf)-joint. The results illustrate that the flexural strength of the joint was not substantially increased by utilizing the scarfing technique. Further results show that for the 4" (100mm) depth design the flexural strength was increased by approximately 50%. This strength result was similar to the 75° bond line result from the preliminary bond line orientation study on Excel 2415. The steep bond line allowed the reinforcing patch material to utilize a larger bondable zone as well as more of the parent material. In the shallower joints, e.g. 1" (25mm) depth, the parent material cannot help out as much under bending. Therefore, it was concluded from the results that, any bond line depth equal to or greater than 2" (50mm) is capable of restoring 100% flexural strength in the repaired specimen.

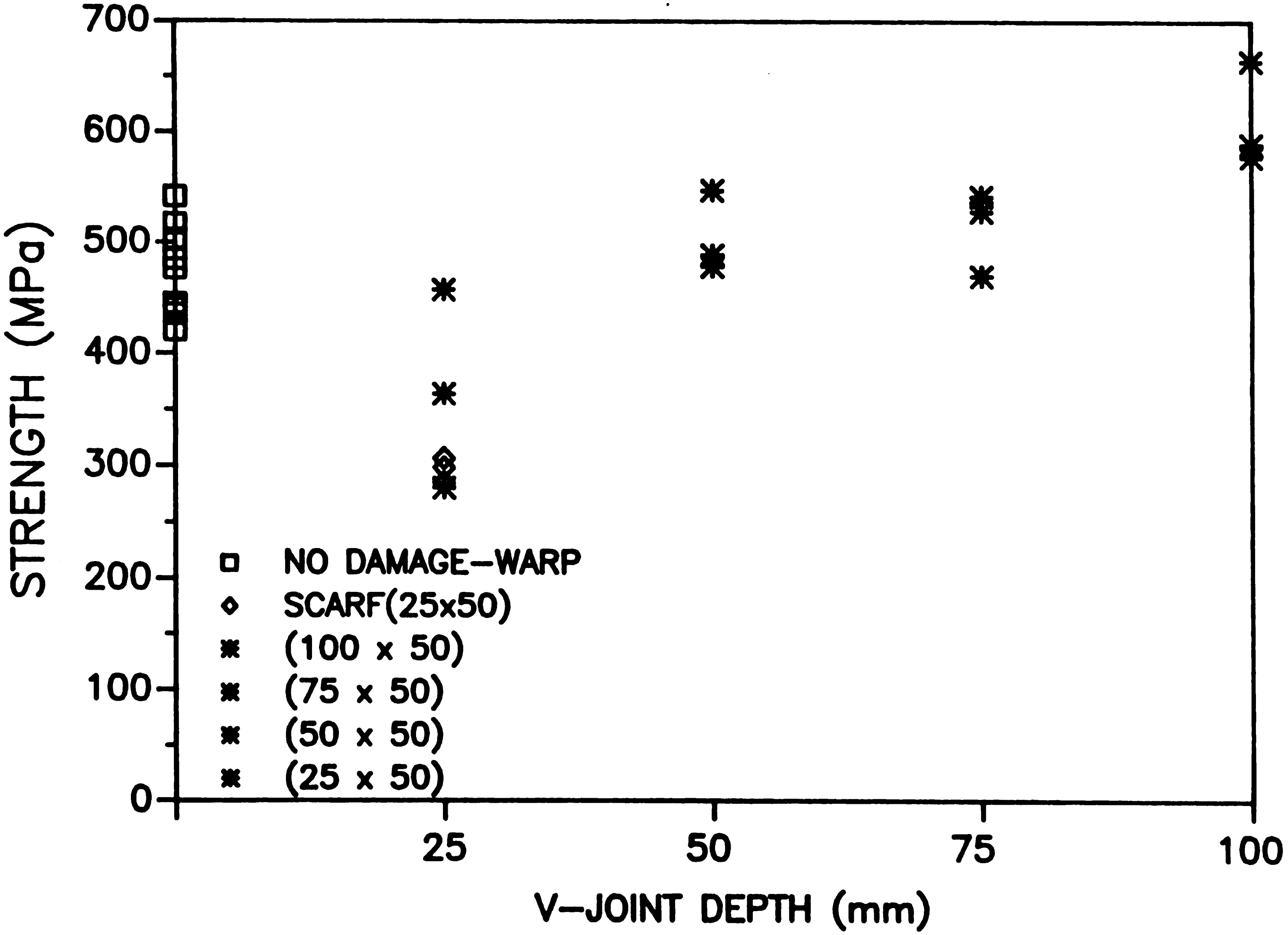

Figure 5.24 Excel 2415: Depth-Of-Joint Analysis to Illustrate the Strength Contribution From Utilizing Different Bond Line Depths and Angles. Standard Repair Was Utilized.

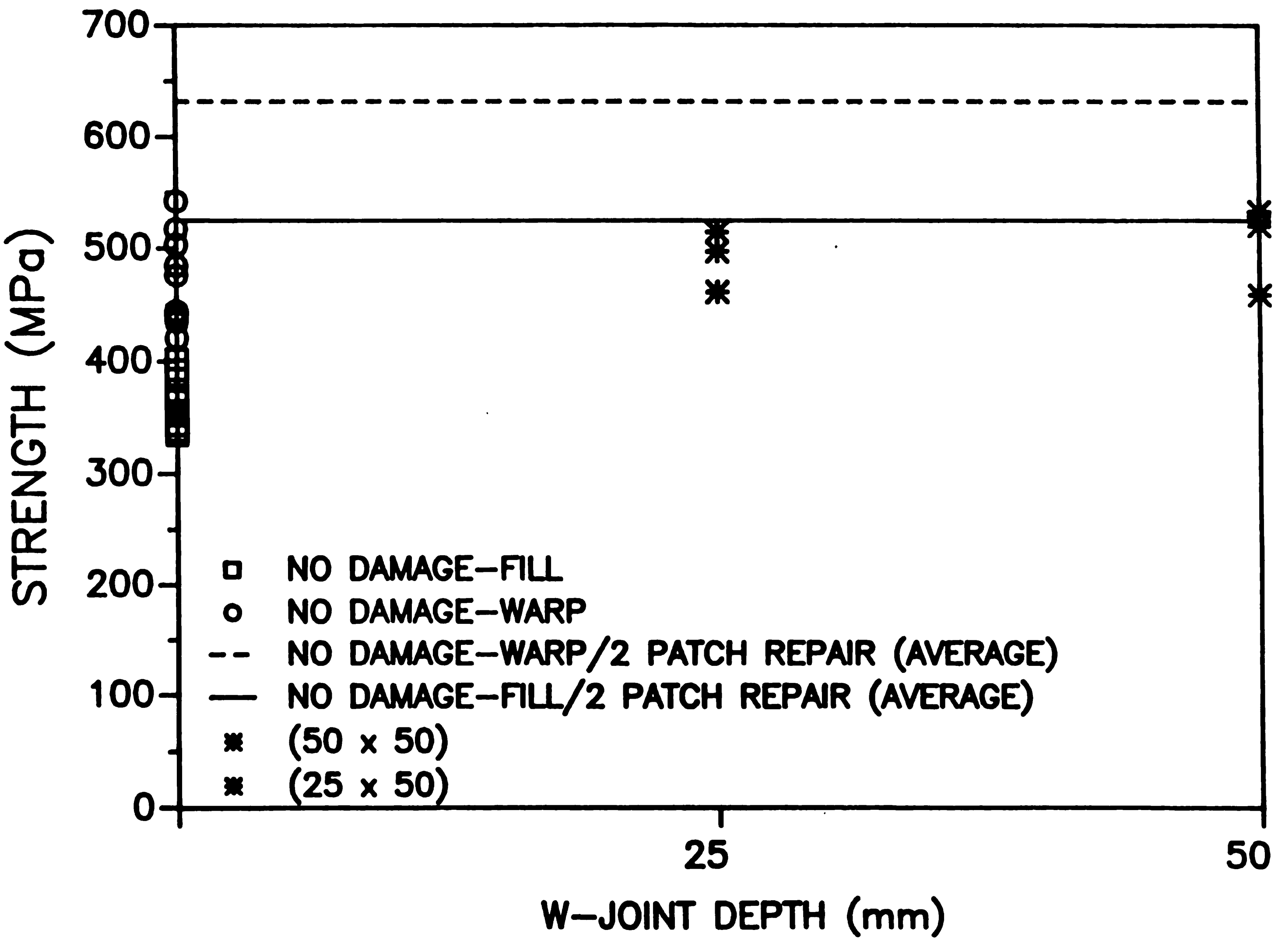

Figure 5.25 Excel 2415: Depth-Of-Joint Analysis to Illustrate the Strength Contribution From Utilizing Different Bond Line Depths and Angles. Standard Repair Was Utilized.

The W-joint design was developed for only two different depths; 2"(50mm) and 1" (25mm). The 2" (50mm) depth utilized a 76° bond line, while the 1" (25mm) depth utilized 72°. The results are plotted in Figure 5.25, and they reveal that regardless of a depth of 2"(50mm) or 1"(25mm), the flexural strength can be restored. It should be noted that the angle for both of the W-joints exceeded 70°. Consequently, it was determined that the bond line angle is the dominant factor in restoration of separated joint strength and also in bond line design [101].

5.4 Out-Of-Plane Curvatures

The material used for this evaluation was an SMC made up of 28% random chopped glass in a polyester matrix. Six different curvatures were evaluated throughout the structure. Each curvature was cut to the dimensions of 2" x 6" (50mm x 150mm) and loaded to failure under three-point bending. After damage, the specimen were repaired, using a technique similar to that outlined in section 2.6, and three-point loaded again to failure. Again, the parameter under differential comparison was the load to failure. The results illustrated in Figure 5.26 reveal that the standard repair technique utilized for flat panel repair is also superior for curved panel repair. It is worth noting that during the repair process there was no pressure exerted along the bond line during the curing cycle of the epoxy. This did not seem to complicate matters. To make sure there was no problem with increased voids, an additional test was conducted to repair a flat panel of the same material without the application of bond line pressure during the resin cure cycle. This value is illustrated in Figure 5.26 as the reference repaired

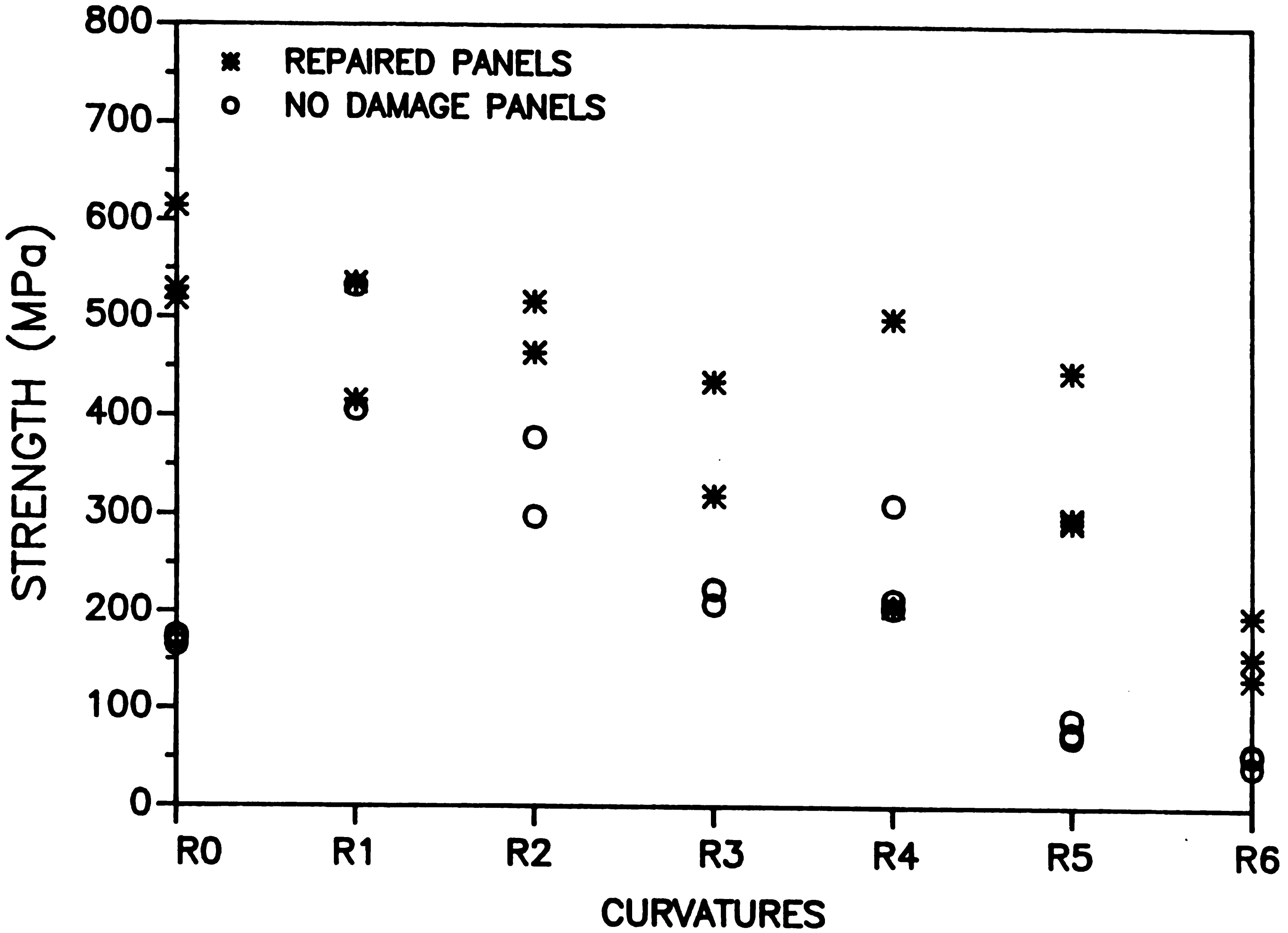

Figure 5.26 Results of Curved Panel Repair After Three-Point Bending Fracture. Rockwell SMC Material.

specimen and demonstrates the same repair strength value as the specimens with applied bond line pressure. There are actually six marks revealed on the plot, three for pressurized, and three for non-pressurized.

CHAPTER 6

ASSOCIATED PARAMETERS

The purpose of this particular chapter is to completely address some of the associated parameters regarding composite repair, for example, selection of adhesives, the determination of the number of reinforcing patch layers, and the evaluation of different types of loading.

6.1 Adhesive Study (Owens Corning SMC)

The first parameter to evaluate was the choice of adhesive to be used, and the effects of the adhesive on the joining strength. The material that was used exclusively for this investigation was the Owens Corning SMC. The reason for using the SMC material was its random fiber geometry, which is not influenced as much by loading direction. Also, the SMC material had displayed superior repair results from utilizing the Maraset epoxy. However, the Maraset epoxy was abandoned for subsequent testing on the Excel material due to compatibility problems.

A. Evaluation of Adhesives

The results of this study are illustrated in Figure 6.1. All joints were 90° butt-joints utilizing two layers of reinforcing glass material per side. In this study, six different resin systems were investigated. All were two-part, room-temperature curing systems. The different adhesive systems are outlined as follows.

(1) Fusor - This is manufactured by Lord Industries and is designated as a structural

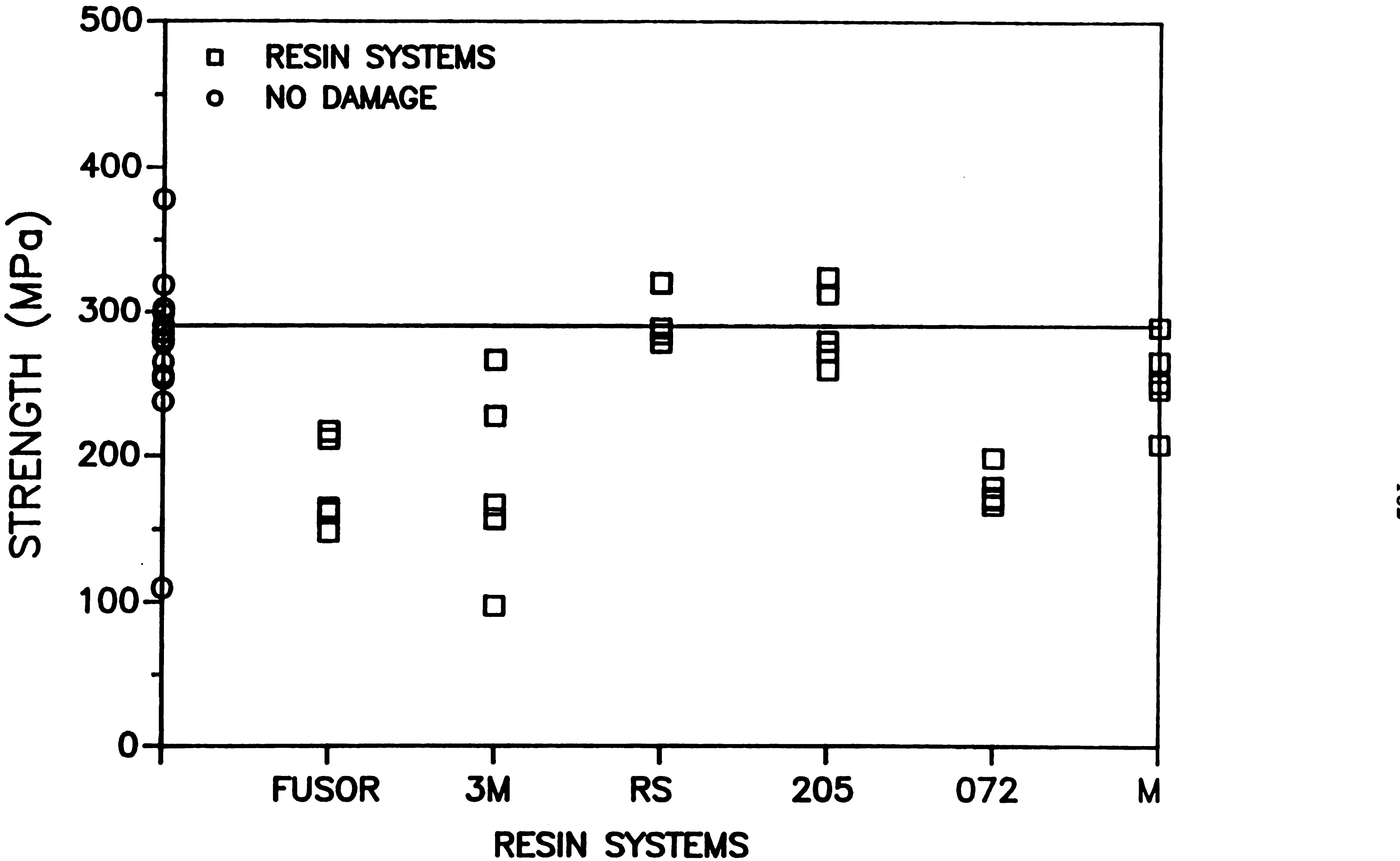

Figure 6.1 Owens Corning SMC: Adhesive Study to Evaluate the Influence of the Adhesive System on the Standard Repair of Damaged Composites.

adhesive. It is very viscous (thixsotropic) and does not saturate the patch material uniformly.

(2) 3M - This is another structural adhesive and responded quite similarly to the Fusor material. The high viscosity system did not permeate the patch material completely, consequently creating an adhesive pocket at the bond line.

(3) Resin Services - This particular epoxy resin system showed superior bonding strength and did not demonstrate any delamination between the patch material and the adherend. The viscosity of this system was very low and seemed to fully saturate the patch material during repair. Therefore, this particular resin system became the adhesive of choice.

(4) TCC205 - This is another low viscosity epoxy resin system that turned in superior results during the study. There was no delamination of the patch material from the adherend and the bonding strength was very close to that of the Resin Services adhesive.

(5) TCC076 - This particular material is a low-viscosity polyester. It saturated the patch material well but displayed some delamination during testing. The results were consequently very poor.

(6) Maraset - Since Maraset was used exclusively for the Owens Corning material, a comparison to the Resin Services epoxy became pertinent. The results indicated that indeed, the Maraset and Resin Services resin are complementary to the repair of the Owens Corning SMC material.

The adhesive study was conducted to verify the present resin systems being used. During the preparation of this particular study, ten different adhesive coupons were developed. Each coupon was cut into three specimens and characterized for their flexural strengths. The results, illustrated in Figure 6.2, verify once again that the Resin Services system displays superior flexural integrity and rigidity. The modes of failure were also reviewed and both the vinylester and polyester samples proved to be much more flexible than the rigid epoxy. The amount of adhesive rigidity is a very critical parameter in composite repair. In general, Figure 6.2 illustrates that the more rigid the adhesive, the higher the strength of the joint will be. However, there will be a high stress concentration along the bond line. Therefore, it is advantageous to utilize an adhesive system that responds very similarly to the original matrix of the composite in order to mimic the flexural response and lower the stress concentrations along the bond line.

B. High-Viscosity Adhesives

The aforementioned results imply that the high viscosity of the Fusor and 3M material may be superior for perforation damage repair and cosmetic type repair. It is the objective of this particular study to further evaluate their applications. Several 4" x 6" (100mm x 150mm) panels were impacted to the point of perforation. Then each specimen was trimmed to the standard testing dimensions of 2" x 6" (50mm x 150mm). After trimming, much of the damaged zone material was pushed back into the void region and utilized as filler while the rest was sanded off using the die grinder. The repair procedure was a bit different for this survey. Instead of repairing with epoxy and two layers of reinforcing patch material, just resin was placed into the damaged zone of each sample. Figure 6.3 illustrates the results. Fusor, not the 3M material, displayed

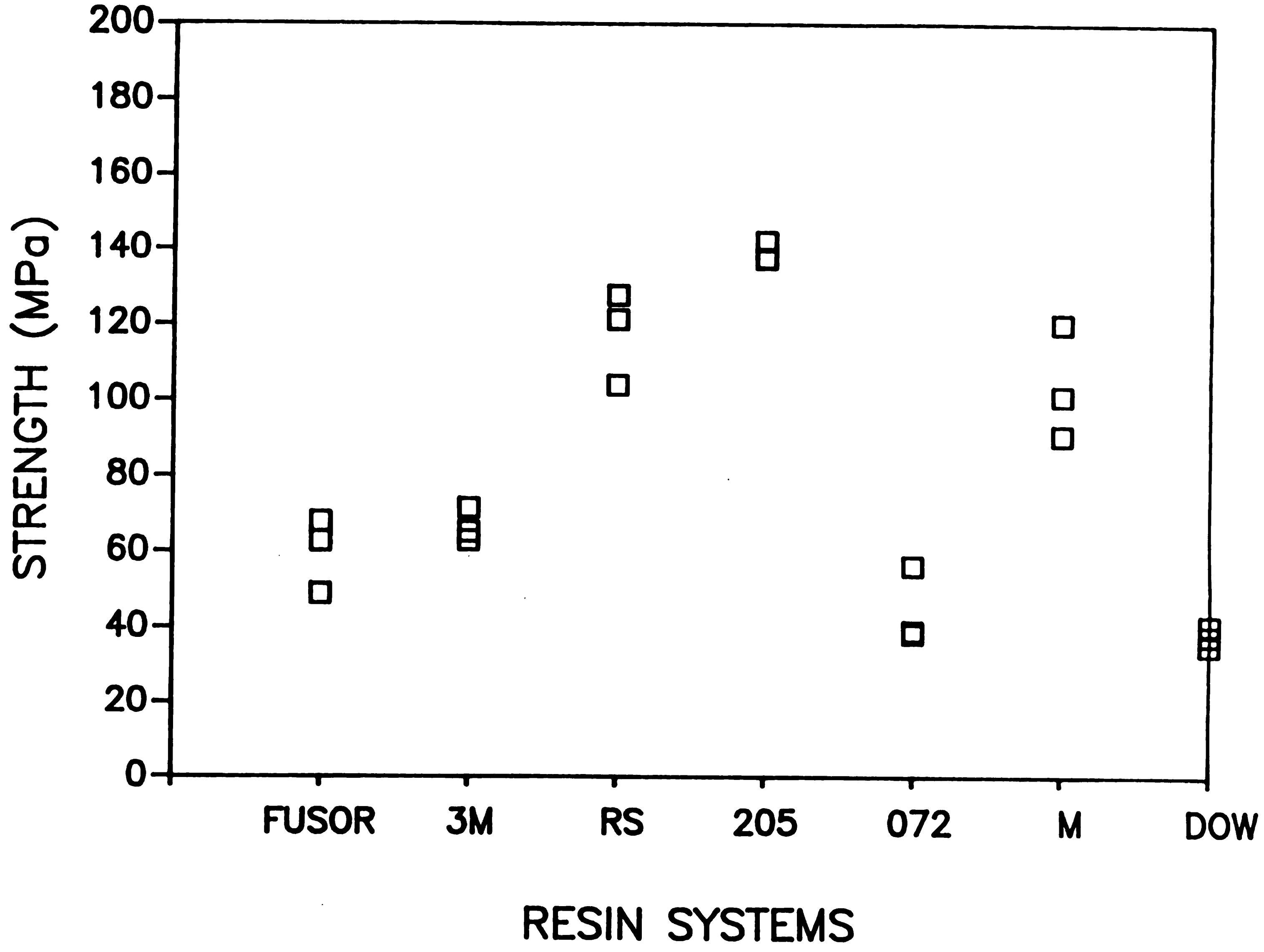

Figure 6.2 Three-Point Bending Results for Adhesive Coupons.

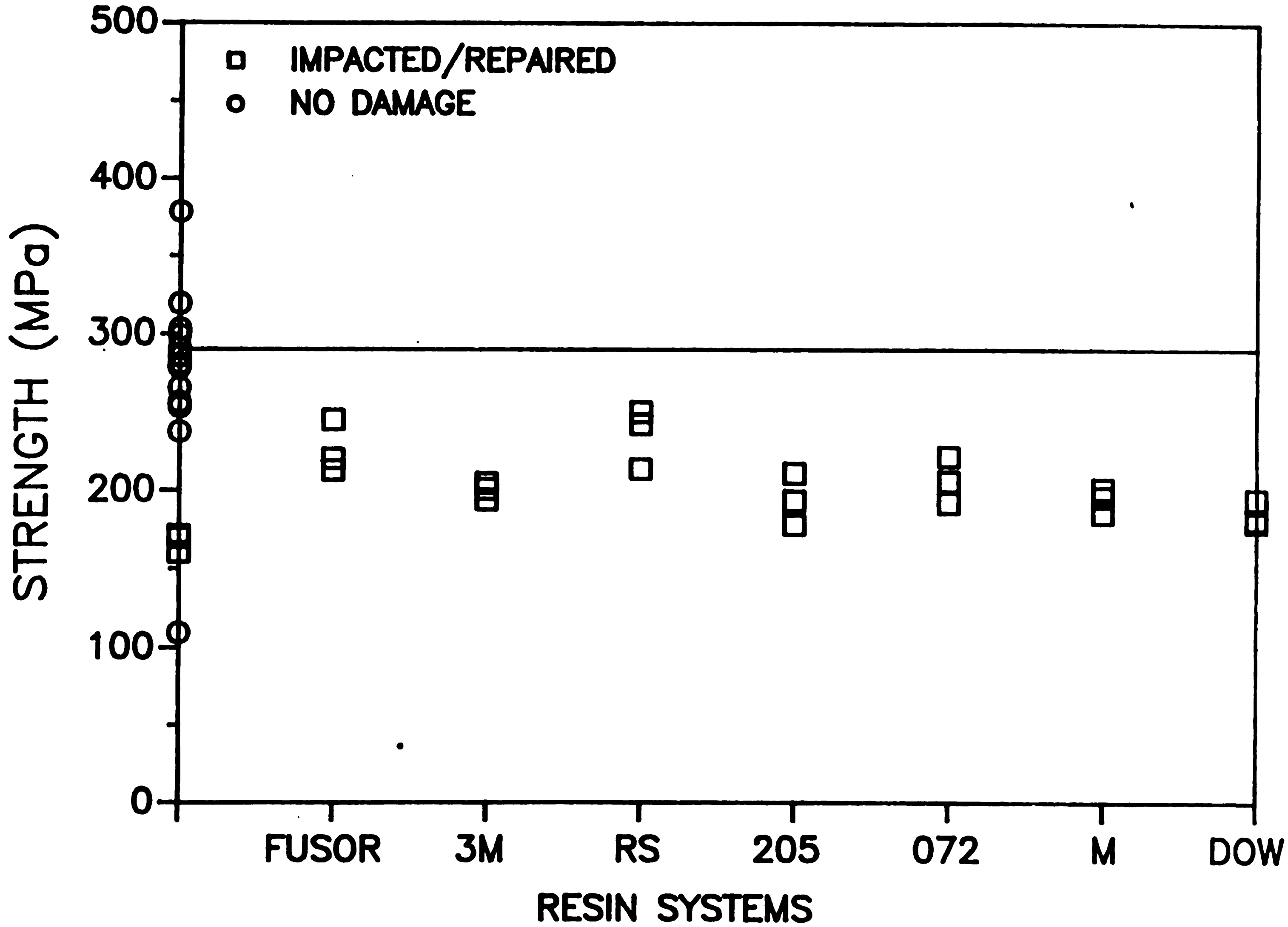

Figure 6.3 Owens Corning SMC: Impact-Adhesive Study to Illustrate the Effects of Utilizing only an Adhesive System During Repair of Perforated Impact Damage.

superior results. However, an interesting observation revealed that the Resin Services system also displayed complementary results. This again is primarily due to the superior bondability of the Resin Services system. The line of failure cut through the center of the void, while the more thixsotropic adhesives debonded from the edge of the void. The major findings of this study were that the strengths of the repaired panels were not disturbed regardless of voids in the repair region. Similar results took place in Fusor, that is, the Fusor material enhanced the aesthetic repair of the small holes or indented regions at least up to 80% of the composite's original strength.

6.2 Reinforcing Patch Study

A. Number of Reinforcing Layers for Butt-Joint

The main reasons for utilizing a plane-woven glass patch for reinforcement was because of its ease in handling and effective repair strength for all of the different fiber geometries. In addition, compatibility of material and consistency of fiber direction are two factors which must not be forgotten during the development of an optimal patch design.

The influence of each glass reinforcing patch on the ultimate strength of butt-joint repair in Owens Corning SMC is illustrated in Figures 6.4-6.5. In each case there are two layers of glass patch material on the top (compressive) side and one to four layers of patch on the bottom (tension) side of the butt-joint specimen. Note that the average undamaged specimen strength is 290Mpa. Also note that two and three layers of glass patch restore approximately 100% of the undamaged specimen strength, and four layers

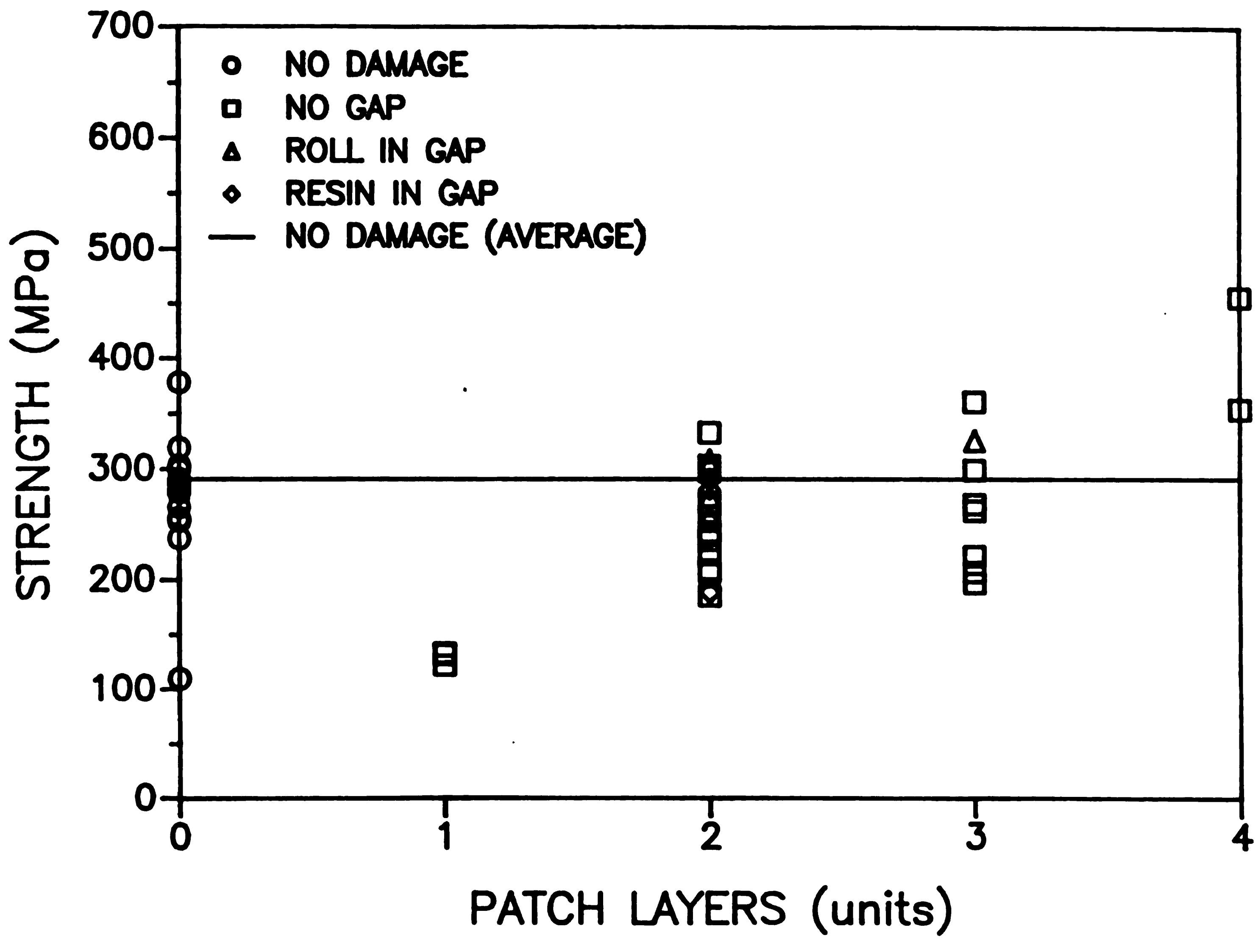

Figure 6.4 Owens Corning SMC: Evaluation of the Strength of the Glass Patch Reinforcement.

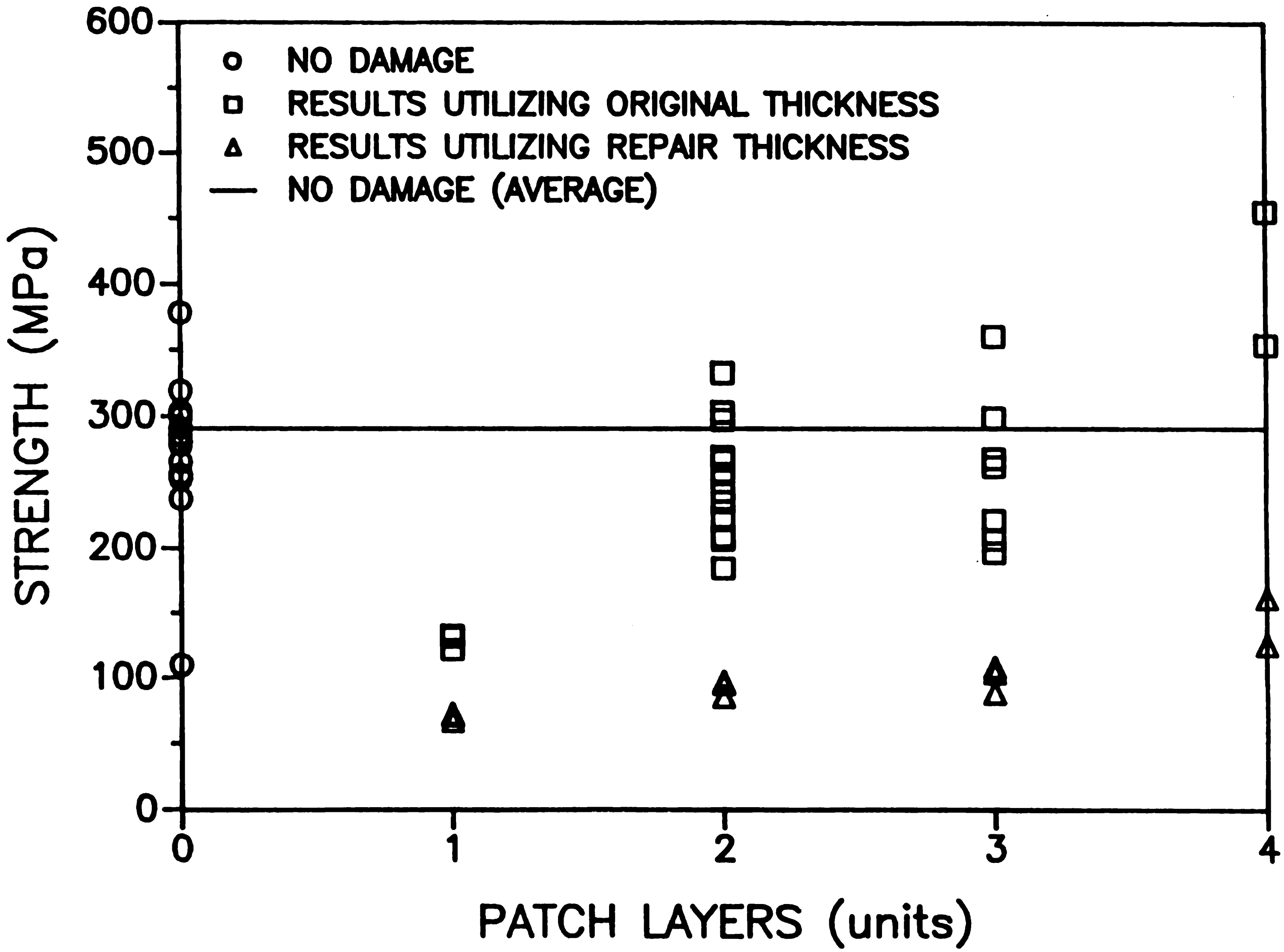

Figure 6.5 Owens Corning SMC: Butt-Joint Patch Repair Utilizing the Original and the Repair Thickness Dimensions.

far exceeds the 100% restored strength and could therefore cause failure in an undamaged portion of the specimen. These superior repair strengths verify that the plane-woven geometry of the glass reinforcing patch material maintains a higher flexural strength than the random chopped glass composite itself. An additional comment should be made regarding the results in Figure 6.5. Note the repair strength of the butt-joints that utilized the repair thickness dimension rather than the original thickness dimension during the calculation of stress. It was determined that the repair thickness dimension did not demonstrate the significance of the relationship between increased load to failure due to increased patch layers. Therefore, the repair thickness dimension was not used for all subsequent calculations of repair strength.

Additional testing was conducted on the Excel materials. The results for Excel 8610, shown in Figure 6.6, reveal again that only two layers of reinforcing patch material are necessary for complete restoration of flexural strength. Again, the Excel 8610 material is a continuous swirl mat, which is not as flexurally stiff as the plane-woven glass repair patches.

The results for Excel 2415, illustrated in Figure 6.7, reveal the need for three (fill direction) to four (warp direction) patch layers for complete repair. The increase in patch layers for the 2415 material is primarily a result of the fiber geometry of the specimen. The 2415 consists of a cross-woven fiber geometry, with a weave thickness of approximately 1mm, while the reinforcing patch material is a plane weave with a weave thickness on the order of 0.2mm. This difference in thickness implies that the strength of the 2415 fibers is much greater than the patch material. Consequently, more

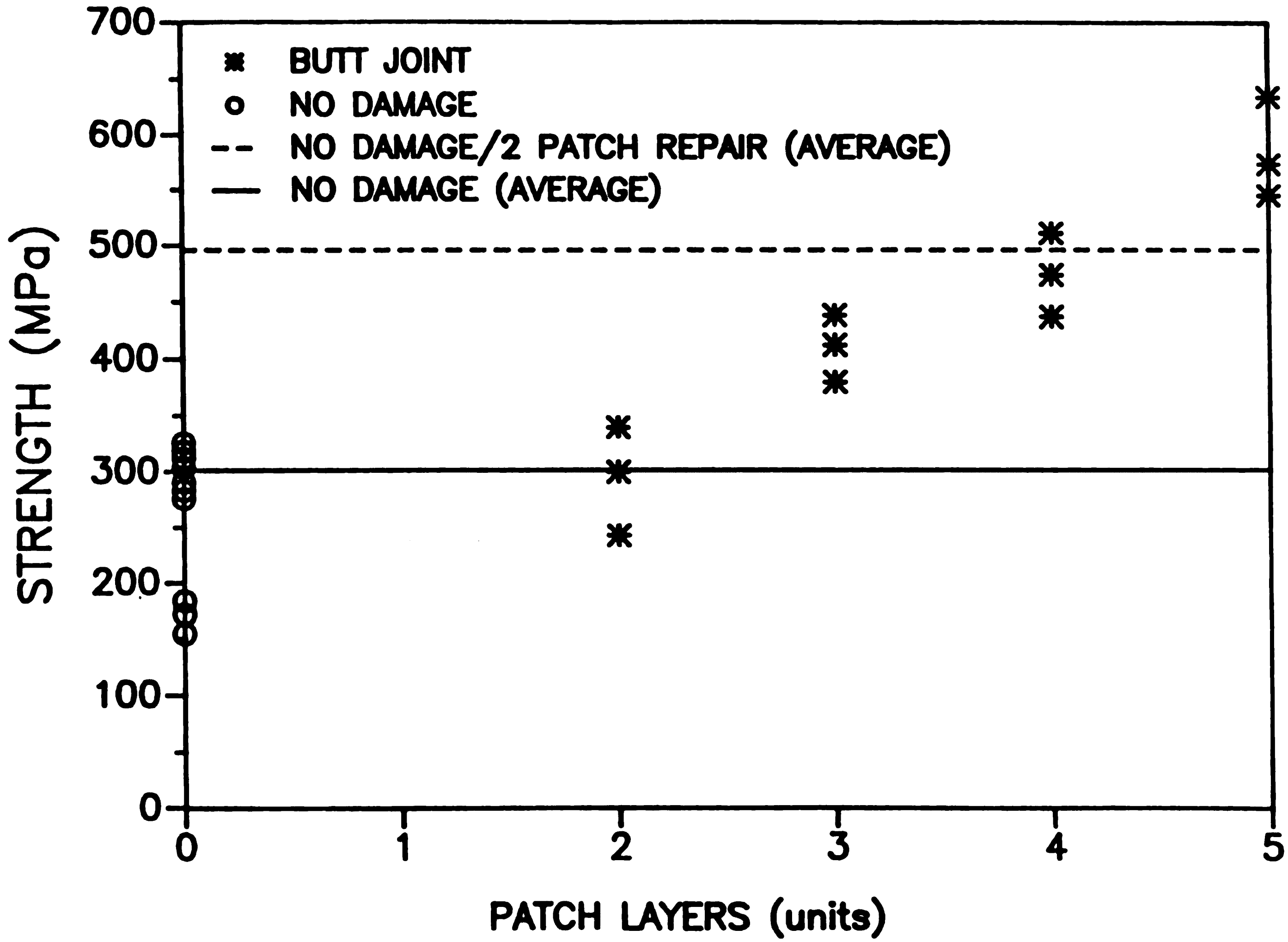

Figure 6.6 Excel 8610: Evaluation of the Strength of the Glass Patch Reinforcement.

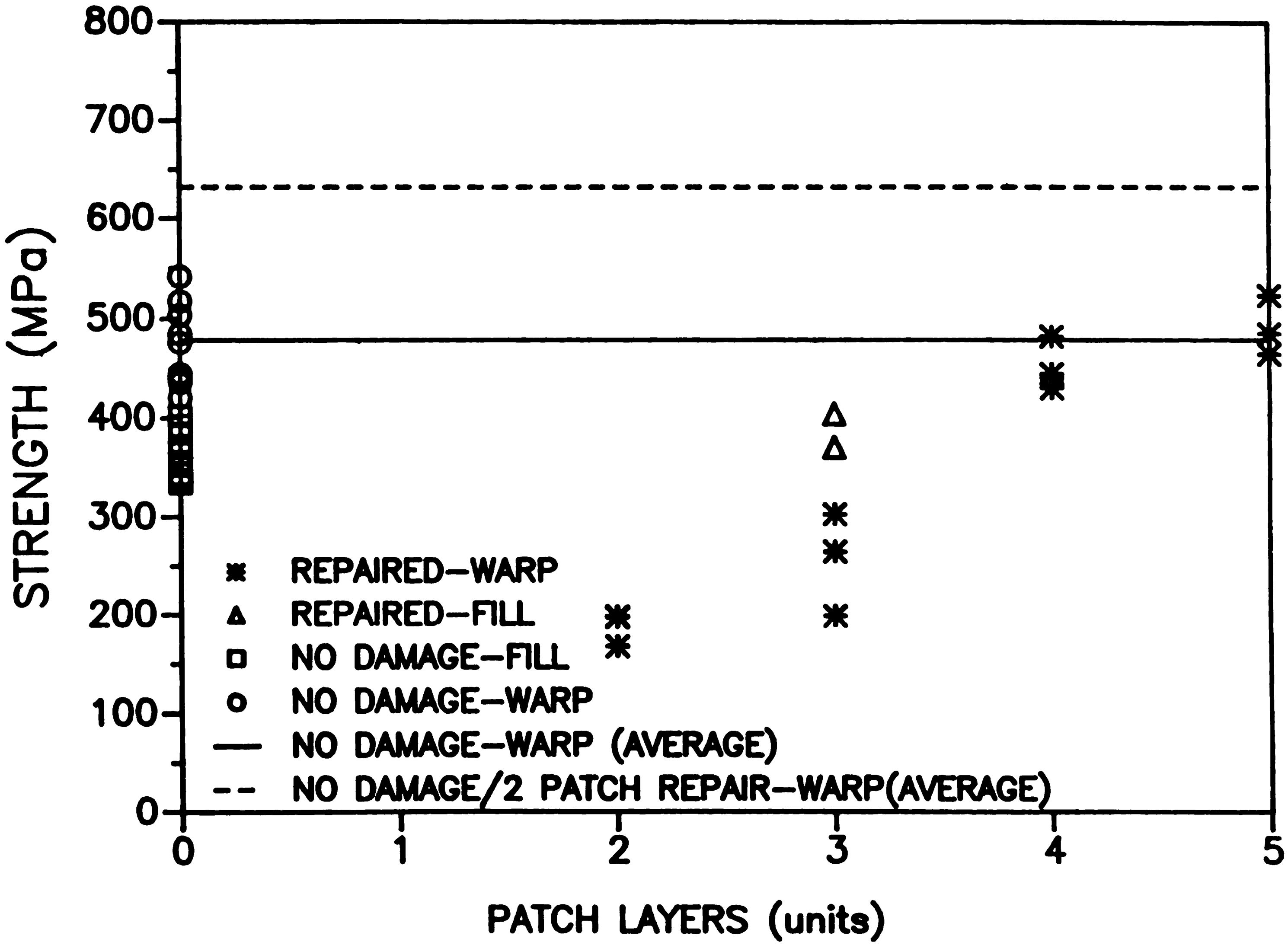

Figure 6.7 Excel 2415: Evaluation of the Strength of the Glass Patch Reinforcement.

patch layers are needed to restore the desired strength. Figure 6.7 verifies this conclusion.

B. Number of Reinforcing Layers for Bending Fracture

This particular study was introduced to evaluate the strength contribution of the glass patch layers in non-separated specimen repair. Specimens were loaded to the point of three-point bending fracture and then repaired with two, three, four, and five reinforcing patch layers on the bottom (tension) side of the joint. Two layers of patch were used on the top side of the joint, since two patches seemed to be able to sustain the top (compressive) load induced on the specimens. The results are illustrated in Figures 6.8 and 6.9. Results revealed that two patch layers restored the flexural strength for the fill direction, while three layers were necessary to restore the strength in the warp direction. The results were also compared to the butt-joint layer survey in Figures 6.4-6.7. The conclusions were virtually the same, i.e., in general, a separated joint requires more layers of reinforcing patch material than a non-separated joint.

Comparative results for this survey are illustrated in Figures 6.4-6.7, and are highlighted as follows. For non-separated repair, the increase in strength values compared to the original undamaged strengths are: (1) Owens Corning (64%), (2) Excel 8610 (52%), (3) Excel 2415 - warp (41%), and (4) Excel 2415 - fill (40%). These results again verify that the random fiber and continuous mat swirl fibers can be repaired quite efficiently with the plane-woven glass reinforcing patches, while the Excel 2415 material requires a bit more strength in the patch material to complement its own fiber geometry.

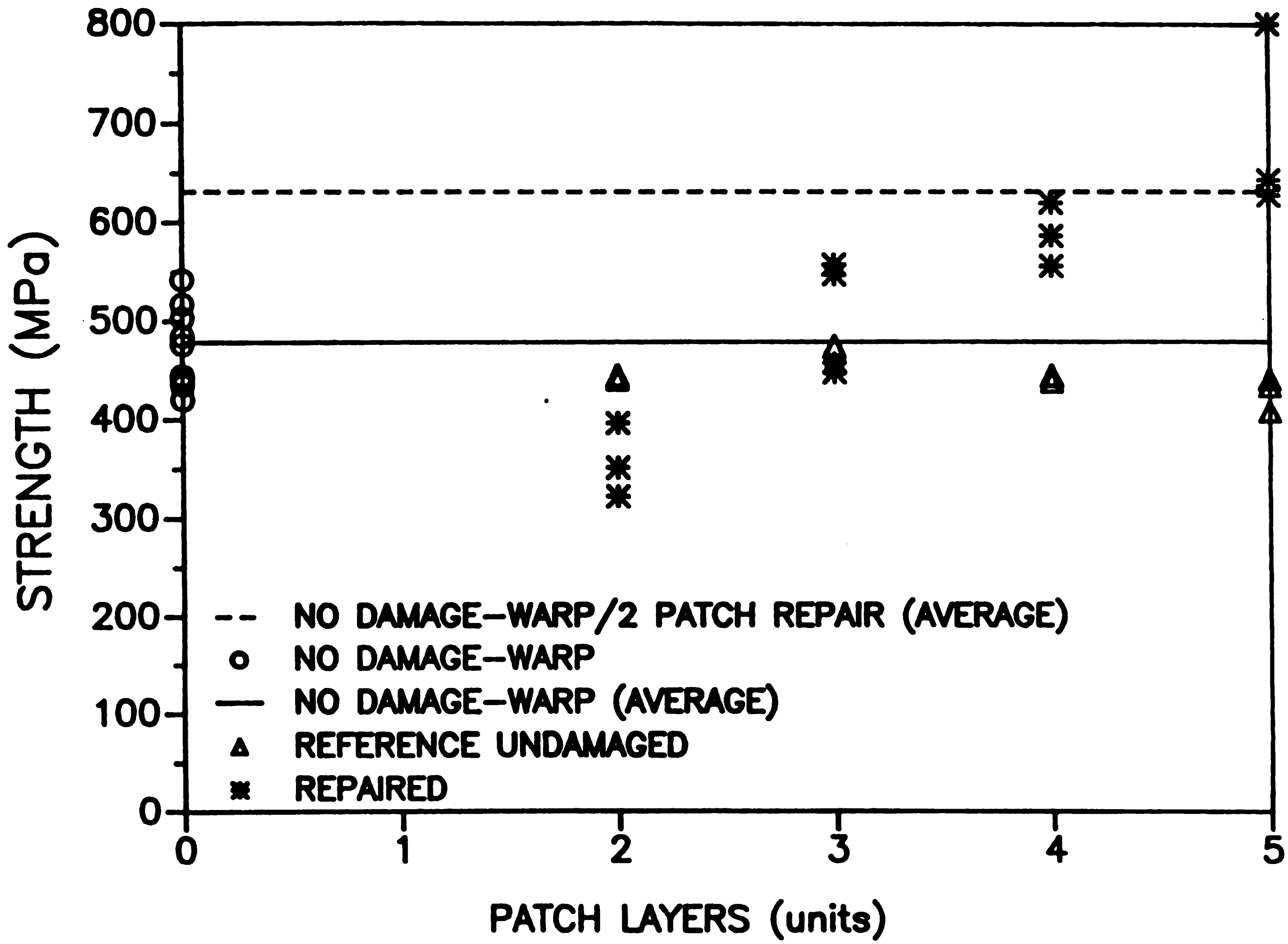

Figure 6.8 Excel 2415: Bending Fracture Layer Study to Evaluate the Restoration of Strength to a Non-Separated Joint After Standard Repair.

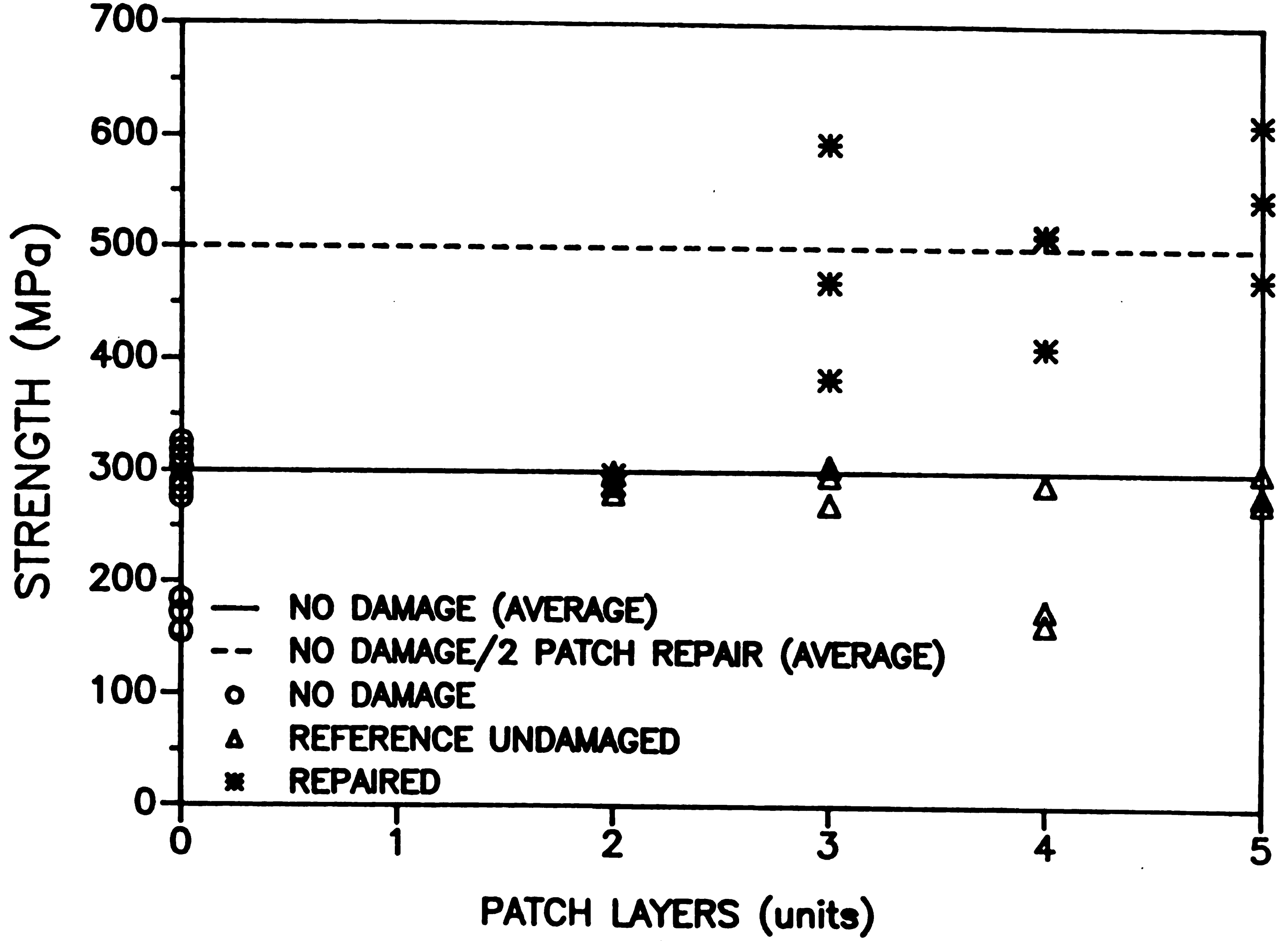

Figure 6.9 Excel 8610: Bending Fracture Layer Study to Evaluate the Restoration of Strength to a Non-Separated Joint After Standard Repair.

C. Woven-Patch Orientation Study (Excel 8610)

A plane-woven glass fabric was utilized during repair to supplement the loss of fibers during failure of the specimen, as well as to add flexural rigidity. However, it should be noted that the plane-woven patch material has two dominant strength orientations namely the 0° and 90° directions. As stated in Chapter 2, it is very important to identify the fiber direction in the material that is under repair and supplement the strength of that direction with the strength from the reinforcing patch material. However, the misalignment of the woven patch with respect to the fiber orientation of the damaged material is also a concern. The results of this investigation are in Figure 6.10.

The patch orientation study was conducted utilizing the Excel 8610 material. The repair procedure was consistent with that which was described previously. The only repair modification was the patch orientation angle. Two layers of glass patch were incorporated per side. The first patch orientation angle was (0°,90°). This was considered the reference angle. The second orientation was (+45°-45°). Note the reduction of flexural strength. The third case exhibited an orientation on the first layer of (0°,90°), while the second layer was (+45°/-45°). Subsequent orientations were, (30°,-60°) and (15°,-75°). The results were very interesting since they revealed that only for the orientation angle of 45° was there any appreciable reduction in flexural strength. It was therefore determined that the orthotropic behavior of the glass reinforcing material is not a critical factor if its orientation angles stays within 45° of the damaged material's fiber direction. In fact, if an isotropic orientation is required, then a combination

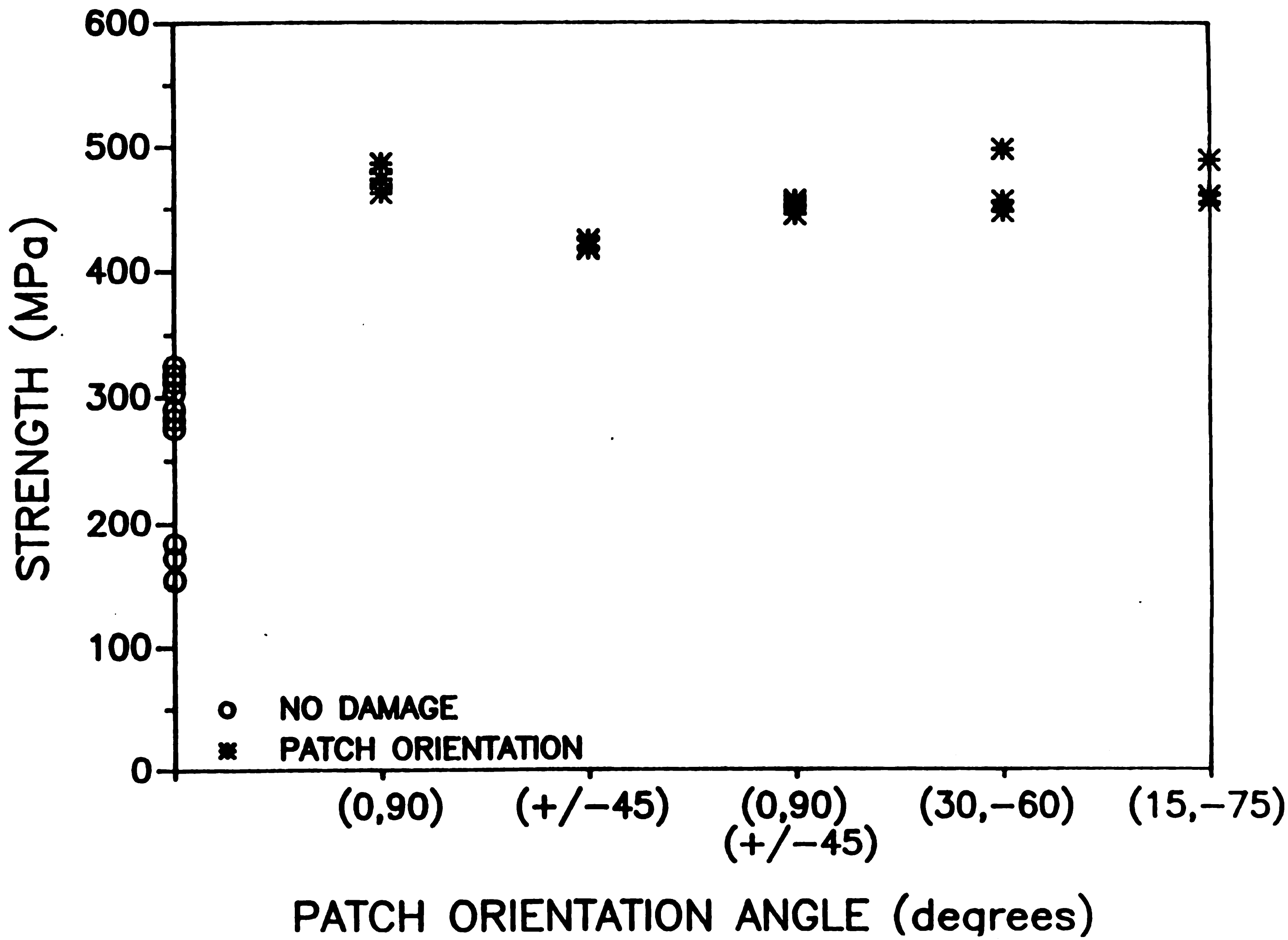

Figure 6.10 Excel 8610: Plane-woven Patch Orientation Study.

utilizing (0°,90°) and (+45°/-45°) layers can be installed.

6.3 Aesthetic Repair

Aesthetic repair was discussed briefly in Chapter 1. To reiterate, aesthetic repair is a form of non-structural repair and lends itself to a lot of artistic freedom. The study outlined in section 6.1B describes the aesthetic repair scheme utilized to restore strength in impacted panels. Again, Figure 6.3 revealed that a thixsotropic structural epoxy system should be the adhesive of choice for aesthetic repair. As a note, the thixsotropic adhesive resembles the material referred to as "bondo". To date, bondo containing random chopped glass fibers can be purchased at any auto-body repair shop. The study outlined in section 6.1B supports the use of a product such as this.

6.4 Types of Loading

The major types of loading that were discussed and evaluated throughout Chapter 5 were three-point bending. This section is focused on discussing the additional loading types, i.e., tension, compression, torsion, and cyclic fatigue, that were used to completely characterize each fiber geometry. Throughout a majority of the testing, the specimen dimensions of 2" x 6" (50mm x 150mm) were adhered to in order to alleviate the complication of any other testing parameters. This also helped with keeping in a differential and comparative mode between testing techniques.

A. Tension and Compression

The evaluation of tension and compression utilized the servo-hydraulic Instron machine and was conducted under stroke control. Readings of stress and load were monitored simultaneously during compressive displacement. The specimen dimensions for tensile testing were 2" x 6" (50mm x 150mm) (gage length = 2.75", 70mm) while the compression specimen were cut to 2" x 3" (50mm x 75mm) (gage length = 1.5", 40mm), this dimension was also utilized to instigate compressive failure while preventing buckling.

The determination of Young's modulus and Poisson's ratio were evaluated via tensile testing of each material with the application of bi-directional strain rosettes. Large strain gage areas were utilized to create more of an averaging effect of axial and transverse strain. This helped to alleviate the possibility of an extraneous strain readings due to the placement of the gage on either a resin rich or fiber rich zone. Table 6.1 contains all of the characteristic material properties, such as tensile and compressive moduli, tensile and compressive strengths, and Poisson's ratio, for all three composite fiber geometries.

B. Critical Buckling

The evaluation of buckling was also conducted on the Instron machine and was monitored under strain control. This required the use of an extensometer. The extensometer was modified to incorporate a 50mm gage length and was fitted with 50mm knife edges on both ends. This special modification is of particular interest when analyzing strains in composite materials. The larger gage length and knife edges produce

Table 6.1 Listing of the Composite Material's Characteristic Properties

E = YOUNG'S MODULUS, E^c = COMPRESSIVE MODULUS,
σ_t= TENSILE STRENGTH, σ_c= COMPRESSIVE STRENGTH
ϑ = POISSON'S RATIO
σ = REFERENCE UNDAMAGED STRENGTH
σ_p= REFERENCE UNDAMAGED STRENGTH W/2 LAYERS OF GLASS REINFORCING MATERIAL (with resin) PER SIDE
P = PATCH STRENGTH INFLUENCE

OWENS CORNING:
E = 1.8Mpsi, E_c= 2.0Mpsi
σ_t= 19 ksi, σ_c= 24.2 ksi
ϑ = 0.3
σ = 42 ksi
σ_p= 69 ksi, P = 27 ksi

EXCEL 8610:
E = 1.56Mpsi, E_c= 1.63 Mpsi
σ_t= 23 ksi, σ_c= 26 ksi
ϑ = 0.24
σ = 44 ksi
σ_p= 66 ksi, P = 23 ksi

EXCE 2415-WARP:
E = 2.71Mpsi, E_c= 2.15Mpsi
σ_t= 26 ksi, σ_c= 29 ksi
ϑ = 0.25
σ = 69 ksi
σ_p= 98 ksi, P = 29 ksi

EXCEL 2415-FILL:
E = 2.26Mpsi, E_c= 1.64Mpsi
σ_t= 35 ksi, σ_c= 34.2 ksi
ϑ = 0.15
σ = 54 ksi
σ_p= 76 ksi, P = 22 ksi

an averaging effect of the strain over the surface of the specimen. This is very critical for composite materials for the simple reason that it allows for more of a "whole-field" approach to strain mapping rather than "point-by-point". The whole field approach for composite material evaluation helps to prevent the positioning of the extensometer directly atop a fiber, or resin rich zone. The averaging of strains gives a much more accurate strain mapping of the surface of the composite undergoing deformation. Although this testing was conducted under strain control, stress versus strain was monitored and recorded simultaneously.

Critical buckling analysis was conducted for all three of the different fiber geometries. The theoretical analysis for buckling utilized Euler's buckling formula in the form:

$$P_{cr} = \frac{4(\pi)^2 EI}{l_e^2}$$

where: E = Young's modulus

I = second moment of area

l_e = specimen's effective length

Even though Euler's formula is designed for isotropic, homogeneous material analysis, the theoretical calculations were within 20% of the experimental values. Figures 6.11-6.12 illustrate the buckling phenomena during loading while Tables 6.2 and 6.3 list the theoretical versus experimental values for P_{cr}.

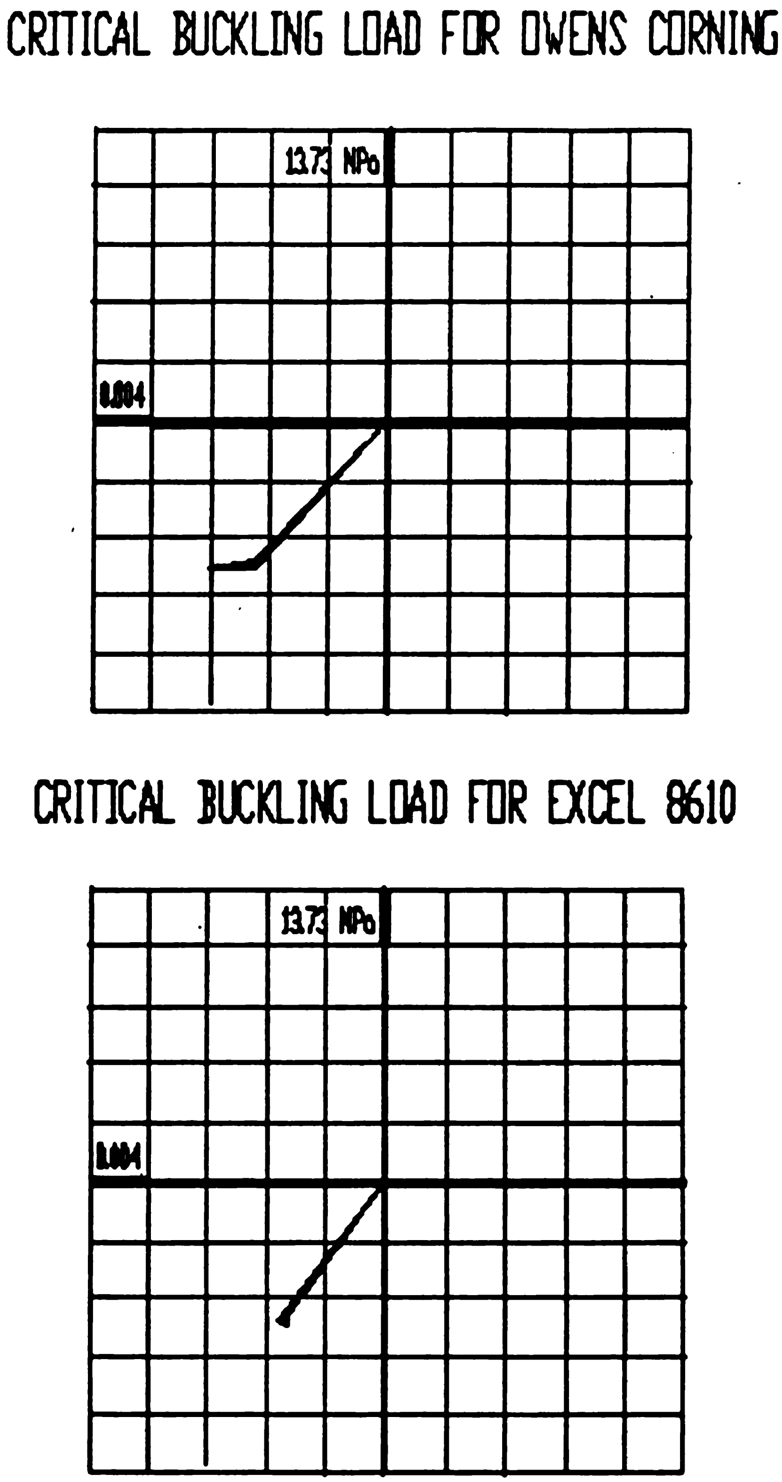

Figure 6.11 Buckling Phenomenon for Owens Corning and Excel 8610.

CRITICAL BUCKLING LOAD FOR EXCEL 2415 FILL

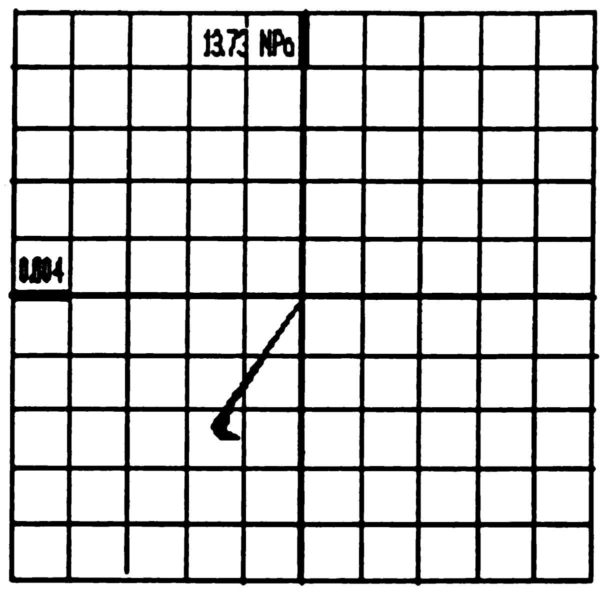

CRITICAL BUCKLING LOAD FOR EXCEL 2415 WARP

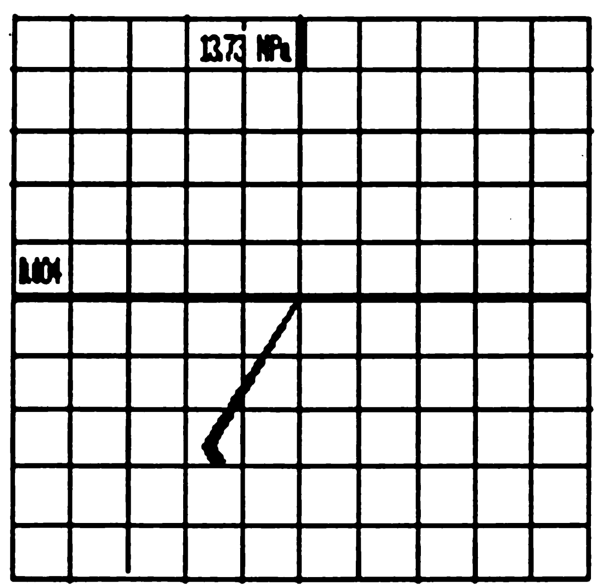

Figure 6.12 Buckling Phenomenon for Excel 2415.

Table 6.2 Theoretical vs Experimental Load Values for Critical Buckling.

MATERIAL	LENGTH L_e (in)	WIDTH (in)	THICK (in)	MODULUS (Mpsi)	CRITICAL LOAD $P_{cr\text{-}theory}$ (lbs)	CRITICAL LOAD $P_{cr\text{-}exp}$ (lbs)
OWENS CORNING	1.30	1.931	0.104	1.80	2120	2114
EXCEL 8610	1.40	1.965	0.123	1.56	2040	2501
EXCEL 2415 WARP	1.38	1.923	0.113	2.71	2280	2597
EXCEL 2415 FILL	1.3	1.918	0.114	2.26	2024	2264

<u>% DIFFERENCES IN P_{cr} ARE:</u>

OWENS CORNING:	**0.3%**
EXCEL 8610:	**18%**
EXCEL 2415W:	**12%**
EXCEL 2415F:	**11%**

Table 6.3 Experimental Critical Buckling Load Data for the S-, and Butt-Joints.

SPECIMEN ID	AREA (sq.in)	MODULUS (Mpsi)	CRITICAL STRESS (kpsi)	CRITICAL LOAD (lbs)	COMMENTS
OCND-15	.228	1.80	7.79	1760	NO REPAIR
OCBJ-6	.237	1.80	12.52	2980	BUTT-JOINT
OCSJ-6	.242	1.80	19.28	4600	S-JOINT
86ND-15	.244	1.56	7.80	1752	NO REPAIR
86BJ-9	.250	1.56	17.39	4200	BUTT-JOINT
86SJ-14	.229	1.56	15.53	3480	S-JOINT
24FND-15	.223	2.26	7.44	1664	NO REPAIR
24FBJ-12	.213	2.26	14.08	2908	BUTT-JOINT
24FSJ-14	.216	2.26	15.46	3368	S-JOINT
24WND-15	.220	2.71	9.90	2110	NO REPAIR
24WBJ-9	.209	2.71	14.17	2780	BUTT-JOINT
24WSJ-11	.212	2.71	18.65	3990	S-JOINT

C. Cyclic Fatigue

The evaluation of fatigue began by utilizing the results from the buckling analysis. Specimen containing the same 2" x 6" (50mm x 150mm) dimensions were utilized. It was decided that the cyclic fatigue testing would be run in a fully reversed (R=-1) tension-compression mode, since this mode simulates a worst case scenario for the loading of structures. The critical buckling load data was used to establish the fatigue load limits. The tensile and compressive loads were established to be 50% of the critical buckling load. This particular load value corresponded to a strain value of approximately 0.0002 or .02% strain.

The series of specimens were analyzed under strain control, therefore an extensometer was implemented. Again, this extensometer was modified to evaluate average strains over the surface of the composite. Two strips of double stick tape were utilized under both of the knife edges to prevent any slipping of the extensometer during the cycling process.

The idea behind the fatigue testing was to cycle both the undamaged or reference panels, and the repaired panels for 100, 1000, and 10,000 cyclic intervals. It was originally planned to run specimens to 100,000 cycles but the facilities and time did not permit this series of tests to be run. After cycling, the panels were fractured under three-point bending to see if there was any degradation of flexural strength due to cyclic fatigue. The results are illustrated in Figures 6.13-6.16. Note that all four fiber geometries were evaluated and the parameters being compared were the reference strength, butt-joint and the S-joint. The butt-joint and S-joint were the chosen repair

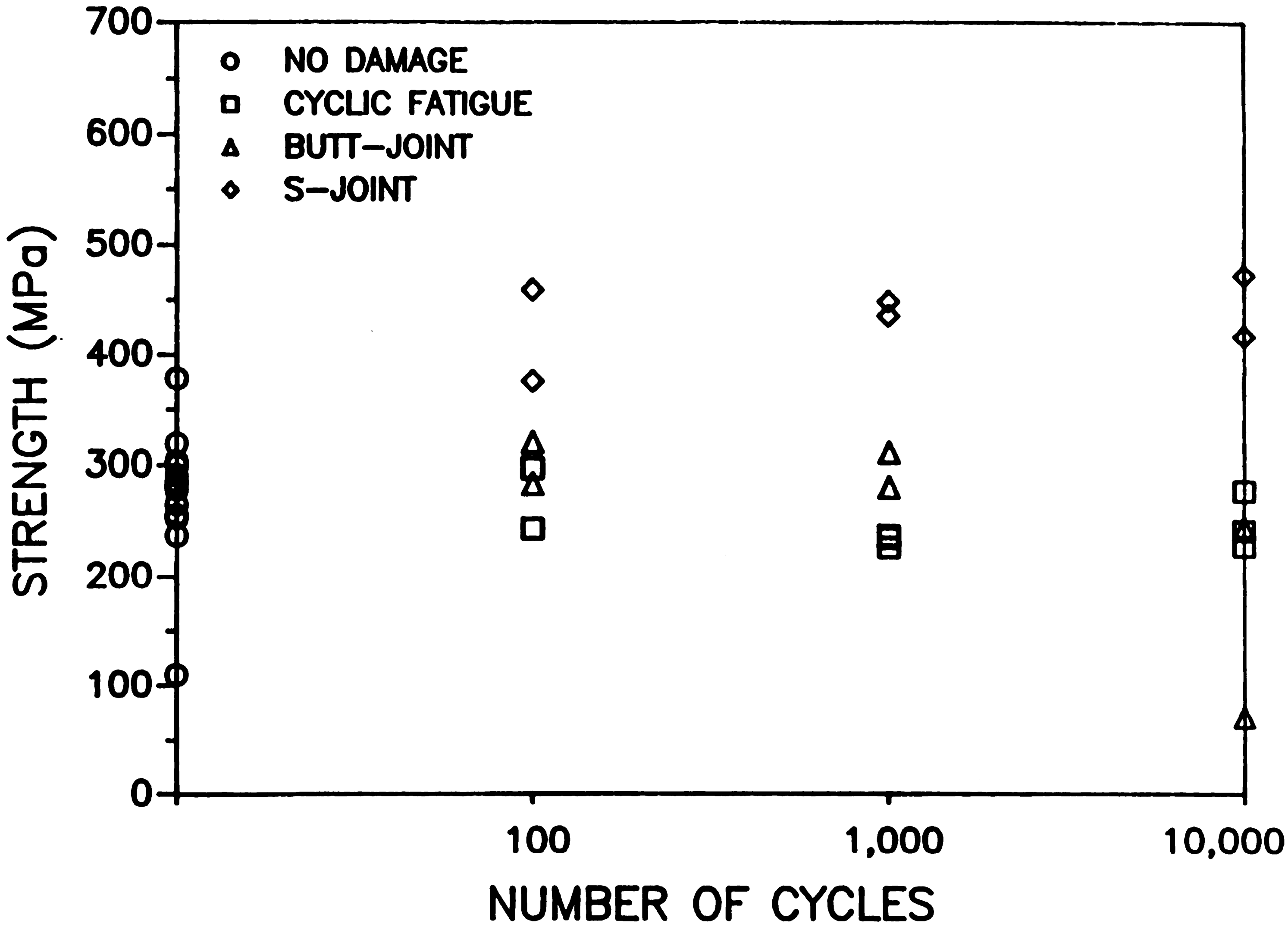

Figure 6.13 Fatigue Results for Owens Corning Reference and Repair Panels.

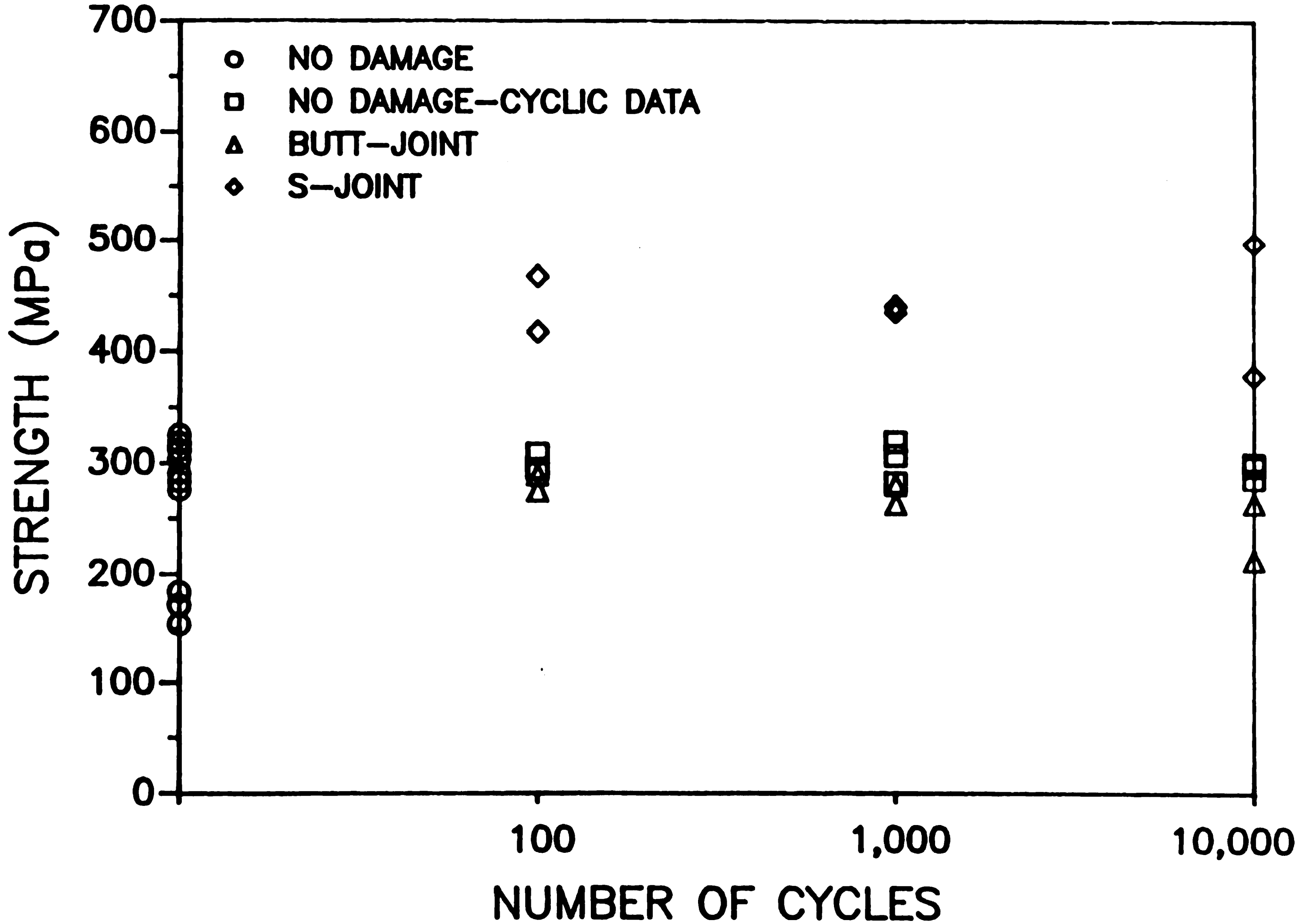

Figure 6.14 Fatigue Results for Excel 8610 Reference and Repair Panels.

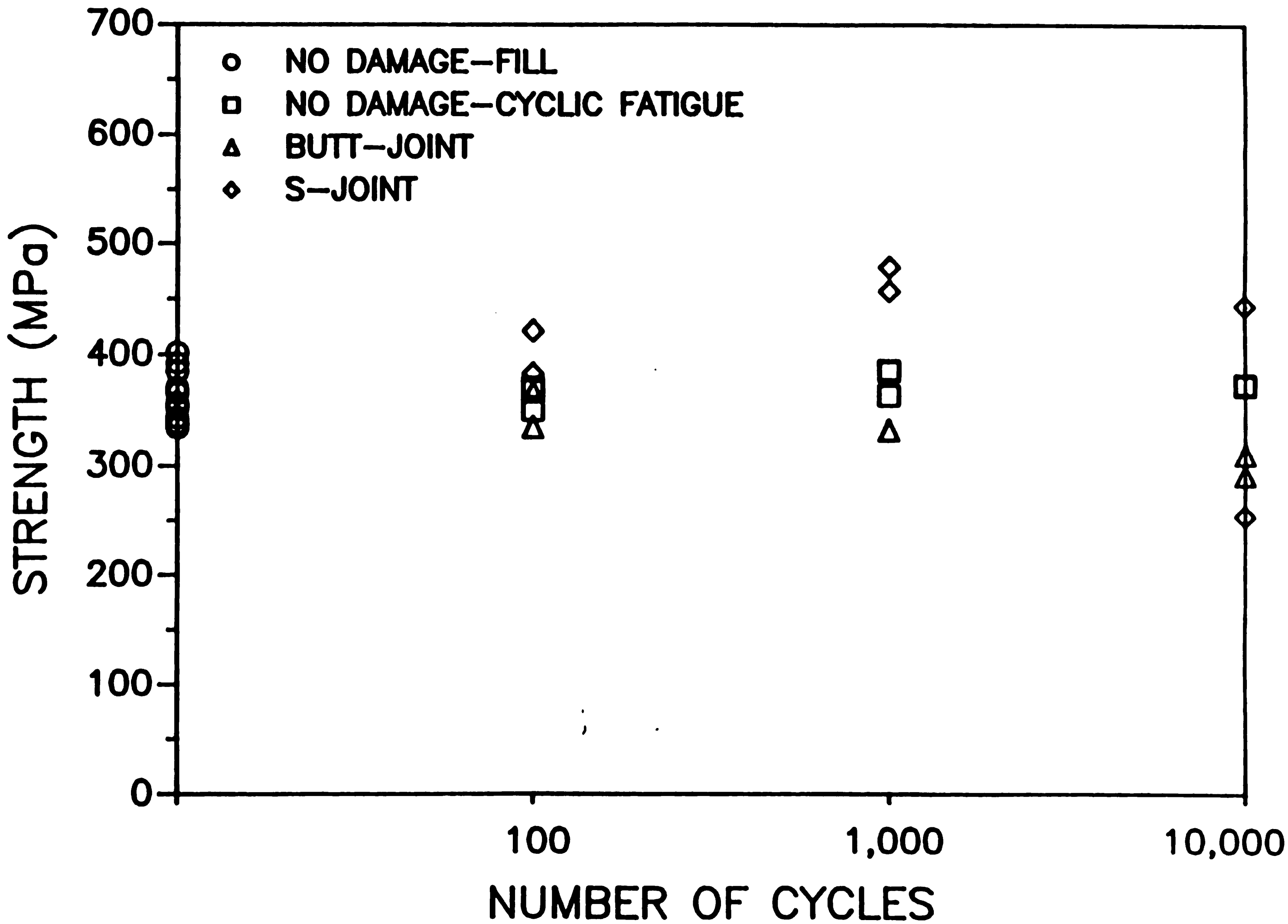

Figure 6.15 Fatigue Results for Excel 2415(Fill) Reference and Repair Panels.

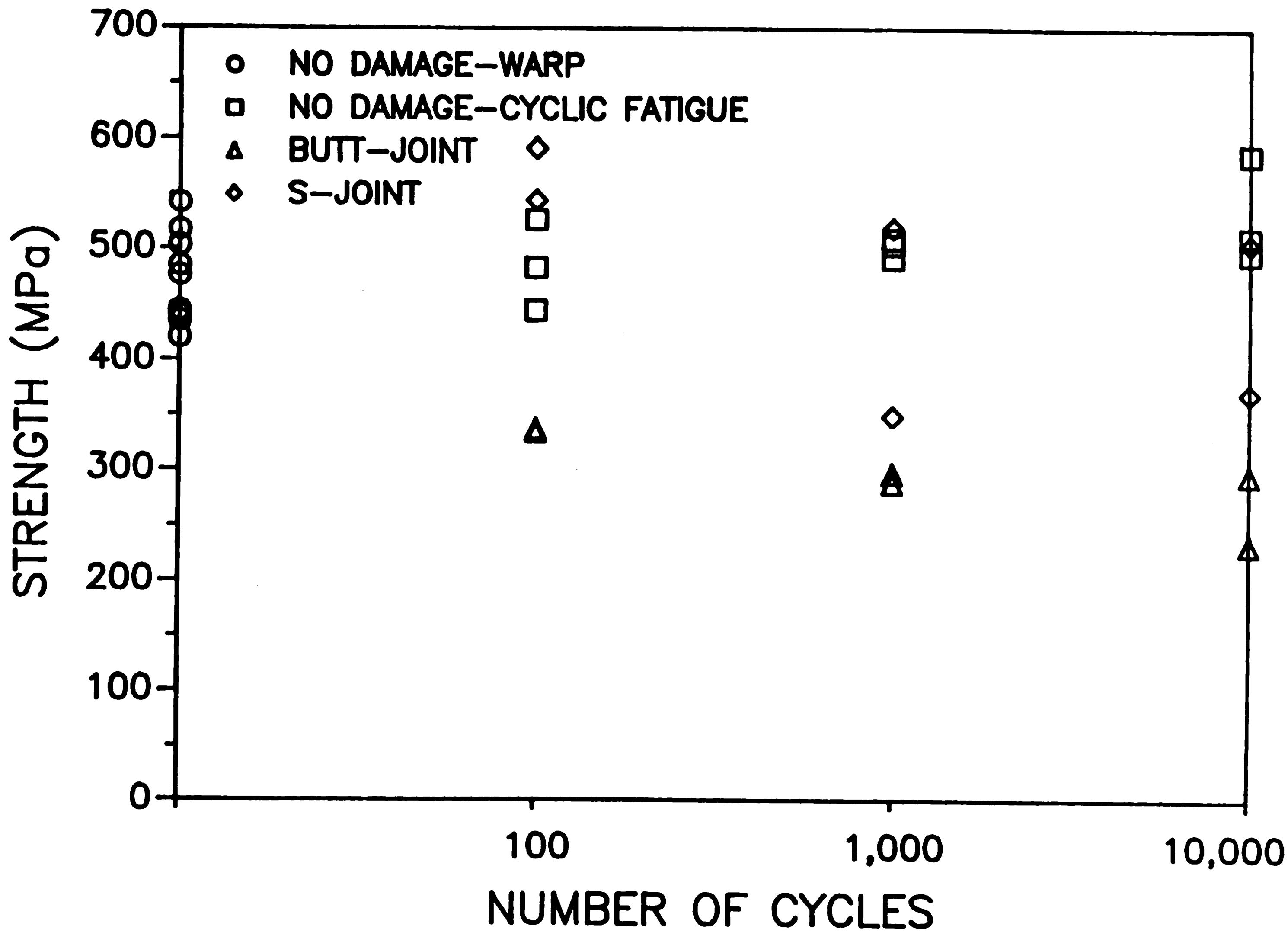

Figure 6.16 Fatigue Results for Excel 2415(Warp) Reference and Repair Panels.

configurations from the standpoint that they demonstrate two opposing forms of in-plane repair. The S-joint is described in complete detail in Chapter 7.

D. Torsion

The torsion analysis was conducted by also utilizing the servo-hydraulic Instron machine. This testing was conducted in stroke or rotation control. Each specimen was machined from the dimensions of 2" x 3.5" (50mm x 90mm) into a dogbone configuration of 1.5" x 2" (40mm x 50mm). This evolved through preliminary testing. Preliminary observations revealed that the 4" (100mm) gage length of the typical 2" x 6" (50mm x 150mm) repair specimen could not be used since it did not exhibit failure in the gage length after a torsional rotation of 50°, which was the rotational limit on the Instron. During testing,rotation angles in 5° increments were utilized to better reveal the maximum torsional load to failure. Results for the torsional testing are postponed until Chapter 7 as well as a further discussion regarding some intriguing developments for torsional damage repair.

CHAPTER 7

OPTIMIZATION OF COMPOSITE REPAIR

This research and development of composite repair evolved into a comprehensive study to evaluate optimum repair designs for various types of composite panel failure. The following sections outline three special approaches for thin panel composite repair. The final section discusses the, "optimization of design," computer model that was utilized in conjunction with the experimentation.

7.1 The Strap-Joint

The idea of implementing a strap-joint to repair small circular voids was a novel approach focused primarily at reducing the degree of catastrophic failure during bending fracture. The strap-joint procedure consisted of cutting two glass patches approximately 2" x 8" (50mm x 200mm) and knotting one to the other separately which eventually created two knots at both of their centers. This double knot was then placed into the void region of the damaged specimen and the tails of the knot were drawn outward along the top and bottom surfaces of the specimen. The knot stabilized the position of the filler as well as reduced the stress concentrations in the repair zone. The design demonstrated a continuous patch from the top of one surface of the joint, through the center of the joint to the opposing surface, as shown in Figure 2.9e. The results illustrated in Figure 5.14 verify not only the restoration of flexural strength, but also the reduction of the degree of catastrophic failure in the repair zone.

7.2 The S-Joint Design

In-the-plane repair of thin panel composites was primarily the focus of this study. In evaluating many creative joining designs, it became apparent that there should be an optimal "isotropic" design for joining two separated composite panels. The S-Joint design attempts to optimize all of the advantageous repair results determined in the results section (Chapter 5) of this study.

Looking back to the study of in-plane bond line geometries, or specifically the "In-Plane Bond Line Geometries," the results concluded that a bond line angle of 90° to direction of load was indeed the optimum design. When the bond line angle study was taken one step further it revealed that a V-joint configuration, which utilized a bond line angle of 76°-86°, depending on the particular design, exhibited superior results. It was proven in the study titled, "Depth of Joint", that the superior strength results encountered were primarily due to the bond line angle rather than the depth of the joint.

All of the preliminary bond line analysis supported the fact that if the bond line could be maintained at an angle of 90° to the direction of force, then it would be the ideal bond line configuration. This is where the idea of the S-Joint came from. Figure 7.1 illustrates the S-Joint bond-line configuration. Note that the design is based on the adjacency of two circles, offset on a 45° axis. The repair zone was established to be 2" x 2" (50mm x 50mm) to maintain symmetry. Also, it was proven in the "Depth-Of-Joint Study" that a 2" (50mm) bond line depth was sufficient for the restoration of flexural strength. Note also that the centers of both circles are offset along the 45° line, to allow for the radii to be greater than 0.5" (13mm). The idea of

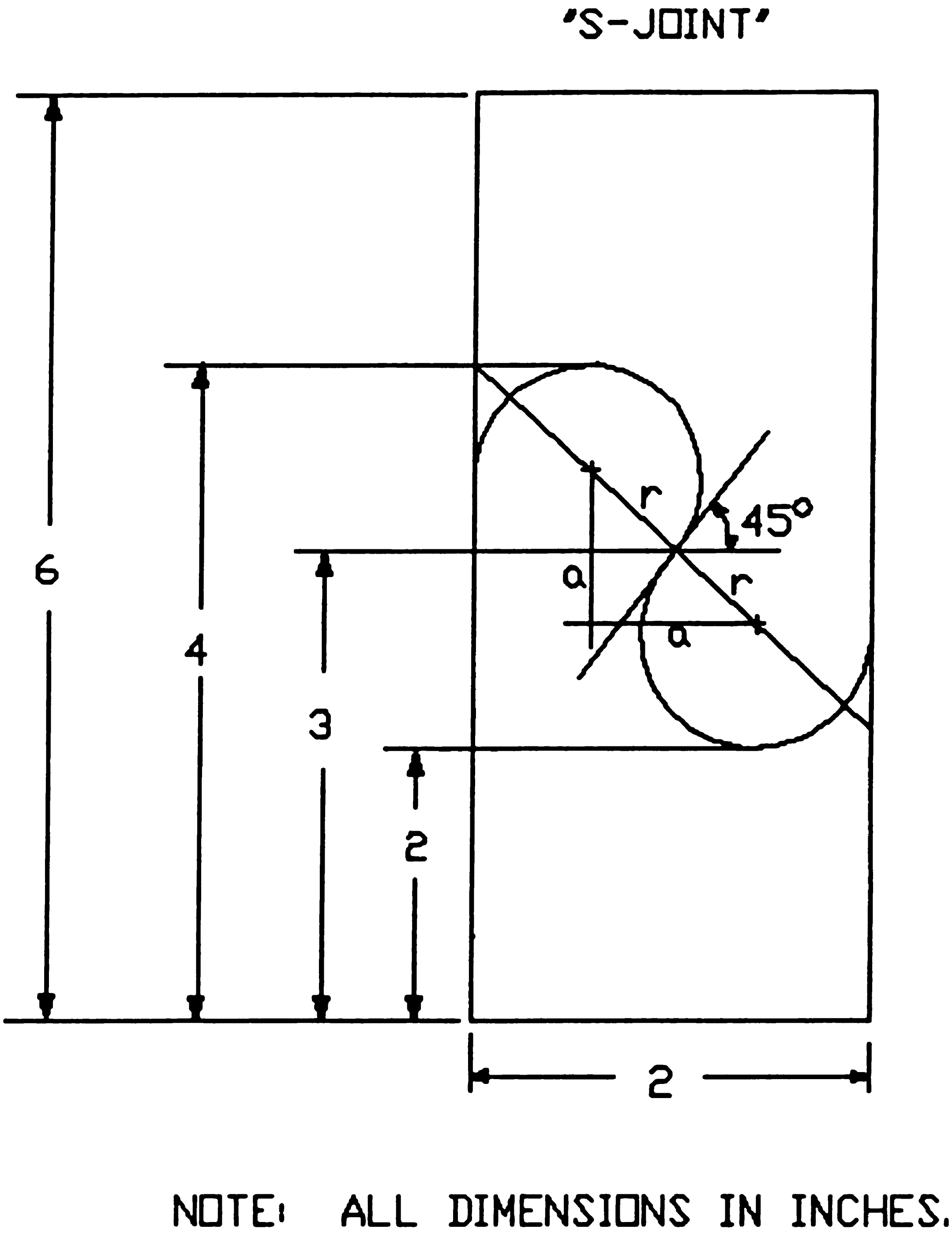

Figure 7.1 The "S-Joint" Bond Line Configuration.

utilizing a modified circle as a bond line supports the isotropic bond line model which attempts to keep the direction of force always at 90° to the bond line.

A calculation for the diameter of the S-joint circle must be determined before repair takes place, and the circle diameter is dependent on the size of the area needing repair. A sample calculation for a 2"x 2" (50mm x 50mm) repair zone is as follows.

Using the pythagorean theorem,

$$a^2 + a^2 = (2r)^2$$

$$a = (2)^{1/2}\, r$$

Since the repair zone is 2"x 2" (50mm x 50mm), (r) results in,

$$2'' = 2r + a = 2r + (2)^{1/2}\, r$$

$$= 3.414\, r$$

$$r = 2''/3.414 = 0.5858''$$

A. Three-Point Bending

The first series of tests designed to evaluate the S-Joint was the three-point bending analysis. It was decided that the analysis of the S-Joint would primarily be compared to the butt-joint, which is the least desirable bond line configuration. Results for this series of tests are illustrated in Figure 7.2. They reveal that indeed the S-Joint

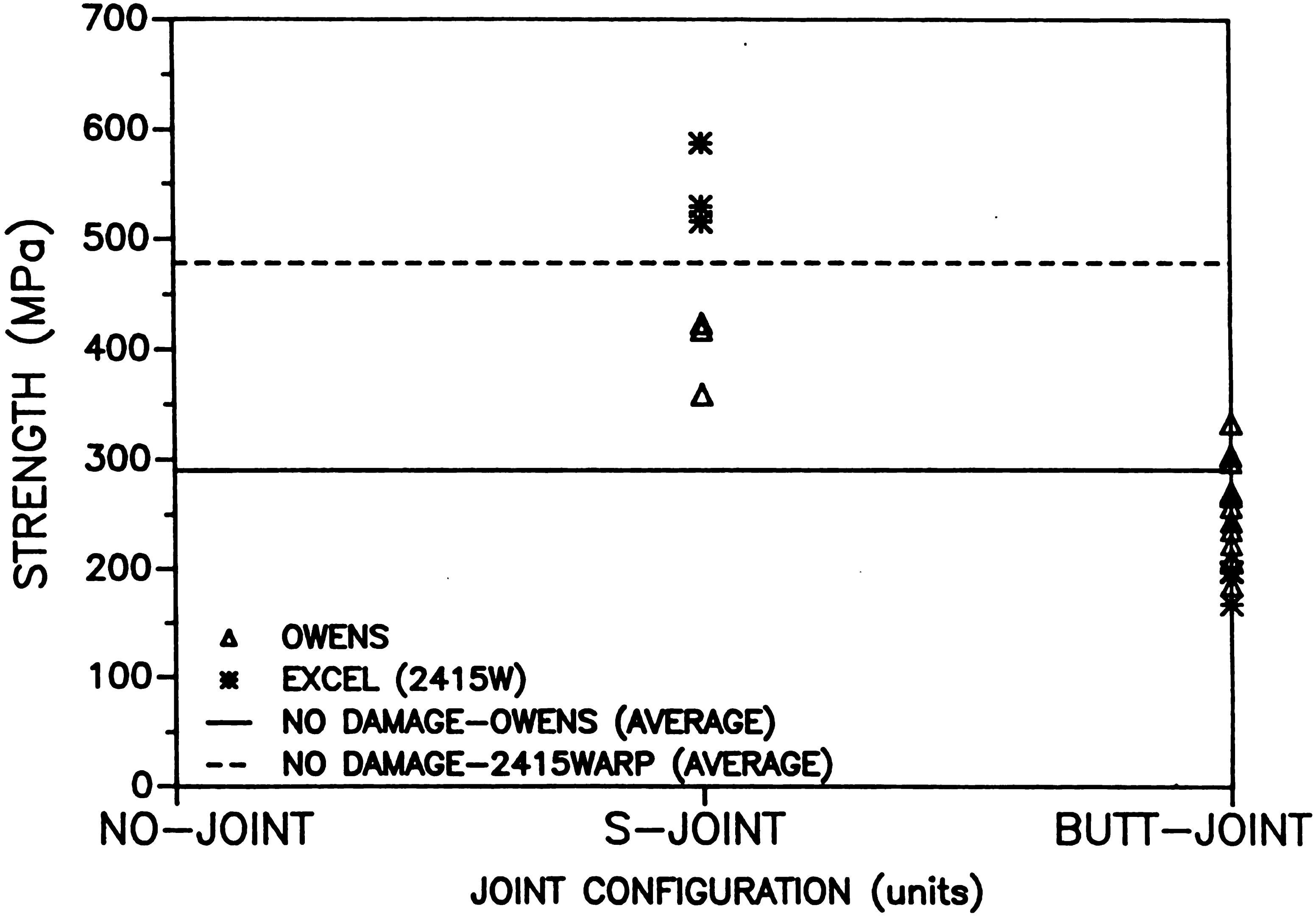

Figure 7.2 Comparative Results for the S-Joint, After Standard Repair and Three-Point Bending Analysis.

is superior in flexural strength to the butt-joint by a margin of 45%, for the 0° joint orientation. The testing was conducted utilizing the standard repair procedure outlined in section 2.6, which implemented two layers of glass reinforcing patch material per side (a double-lap joint).

An additional set of evaluations were setup to also vary the orientation of the S-Joint within the 2" x 2" (50mm x 50mm) repair area. The different orientation angles were 45° and 90°. The results are illustrated in Figure 7.3. The results are slightly lower than the 0° orientation. Consequently, it appears that the repair area is actually too small to achieve valid symmetric testing of flexural strength for the S-Joint design.

B. Critical Buckling

The next series of tests were conducted to establish, not only the S-Joint's critical buckling load, but also the compressive limit load to be utilized during fatigue testing. As a note, the S-Joint was not evaluated for compressive strength since its minimal gage length of 2" (50mm) allowed buckling to occur. The S-Joint specimen were abraded at both ends to alleviate slippage in the grips on the Instron machine. Again, the theoretical calculations were evaluated using Euler's theory, and the results of this survey are listed in Table 6.3. The results revealed that the S-Joint, at an orientation of 0°, was again superior to the butt-joint with regards to its critical buckling load.

C. Fatigue

With the critical buckling load information in hand, the next survey was to

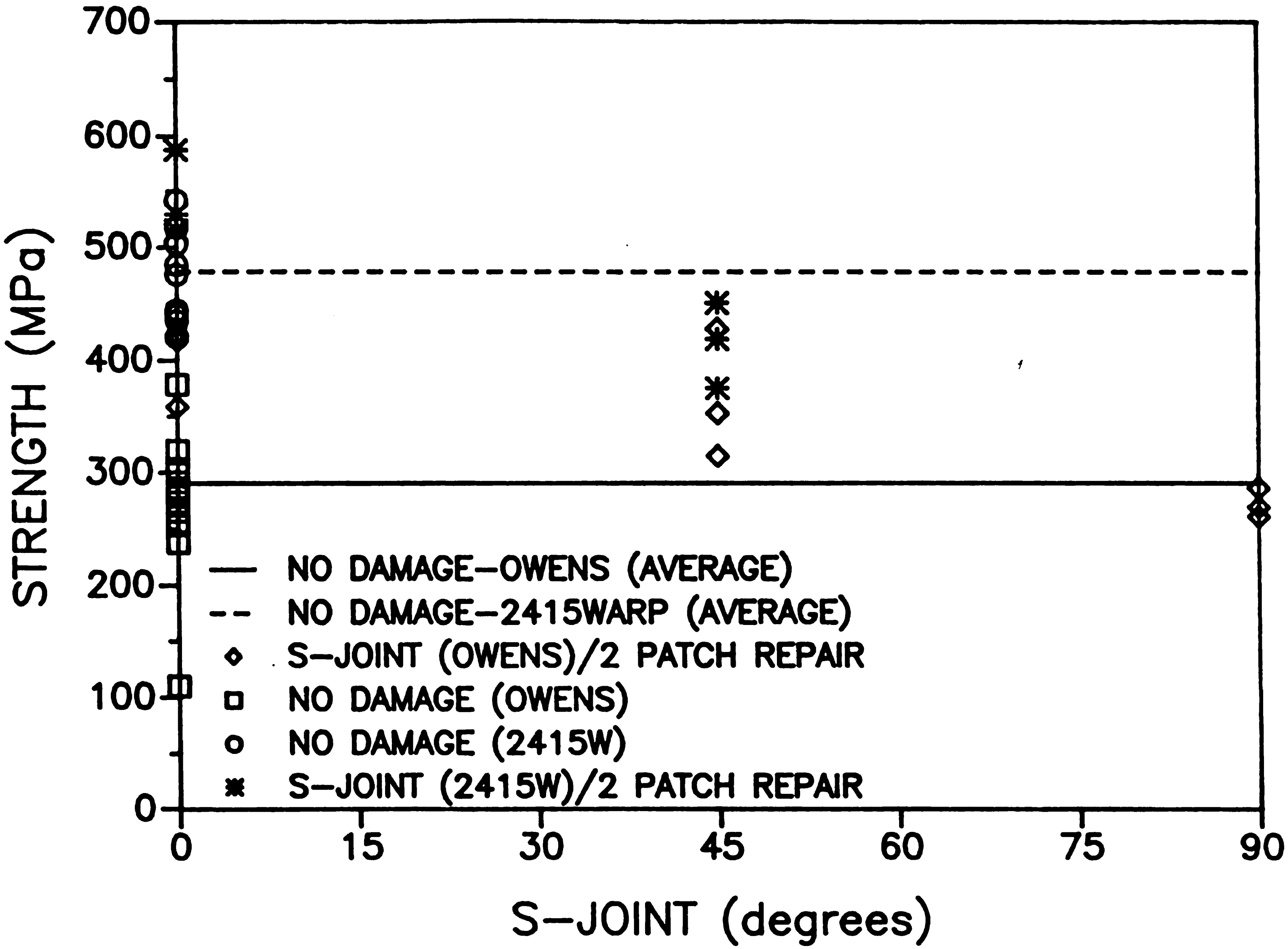

Figure 7.3 Results for Different Orientations of the S-Joint, After Standard Repair and Three-Point Bending Analysis.

cyclically fatigue both the S-Joints and the butt-joints at 100, 1,000, and 10,000 and cyclic intervals. This was investigated to evaluate if there was any loss in flexural strength after cycling. The results are shown in Figures 6.12-6.15. The most prevalent observation was that during cycling, if there was any gap along the bond line, then the glass patch material tended to locally delaminate atop of the gap. In some cases, this initiated bending failure at a lower load, however, the patch material still distributed the load very well, and failure of both joints was primarily due to patch failure rather than patch delamination.

D. Torsion

The servo-hydraulic Instron was again instituted to conduct torsion studies on the S-Joint and butt-joint. Again, both ends of the specimen were abraded to alleviate slippage in the Instron grips. Rotations of 5° were applied to each specimen, while a simultaneous reading of torque was recorded. This procedure was carried out until the maximum Instron rotation of 50° was achieved. The results for torsional rigidity are illustrated in Figures 7.4-7.7. The 0° S-Joint again revealed superior strength to the butt-joint.

E. Tension

A comparison of tensile strengths was undertaken to verify if the 0° S-Joint was superior to the W-Joint and the Straight-Line joint. Results for the three joints undergoing tensile failure are illustrated in Figure 7.8. However, the results reveal that

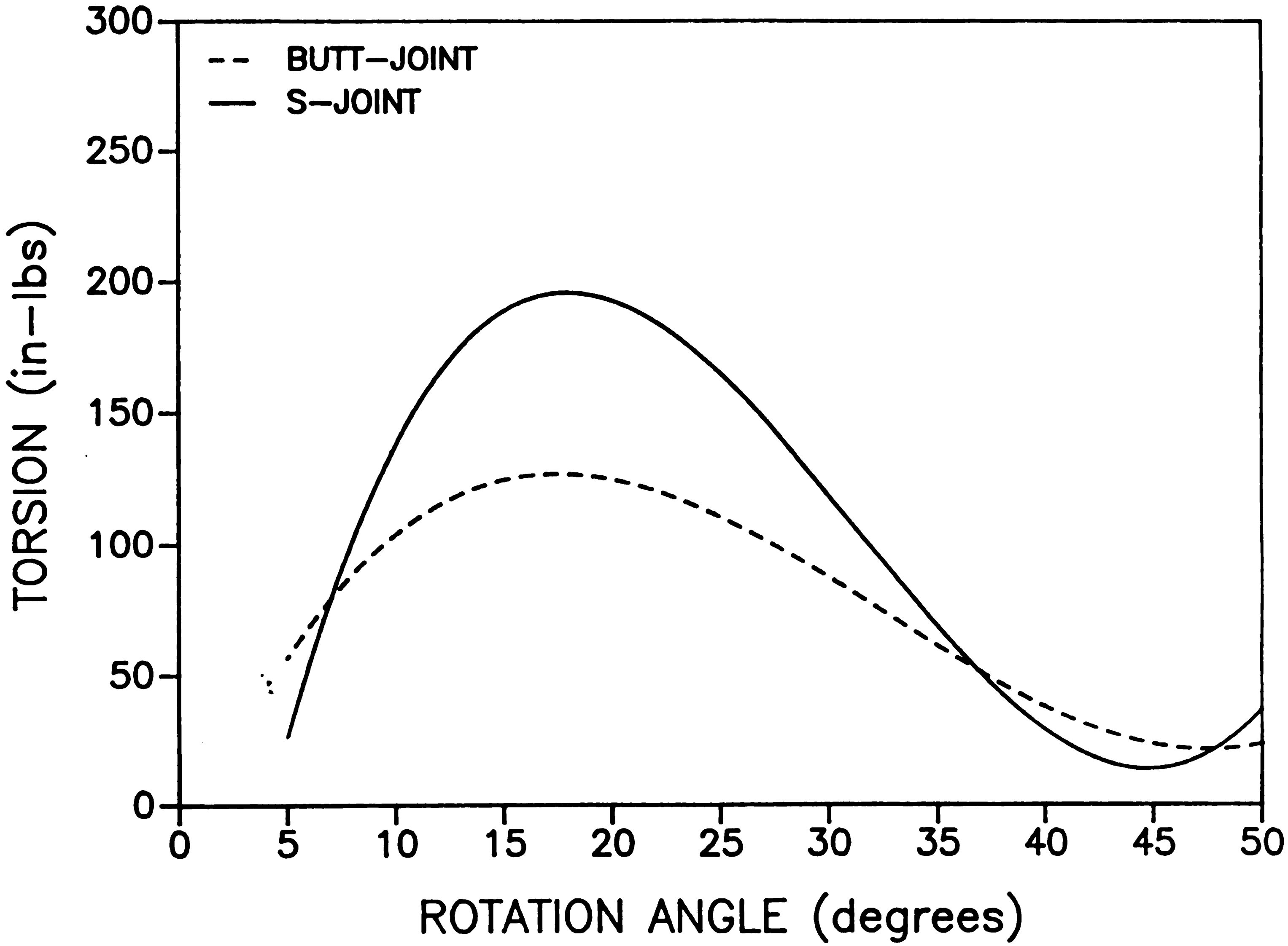

Figure 7.4 Owens Corning SMC. Torsional Rigidity for the S-Joint vs the Butt-Joint. Standard Repair Was Utilized.

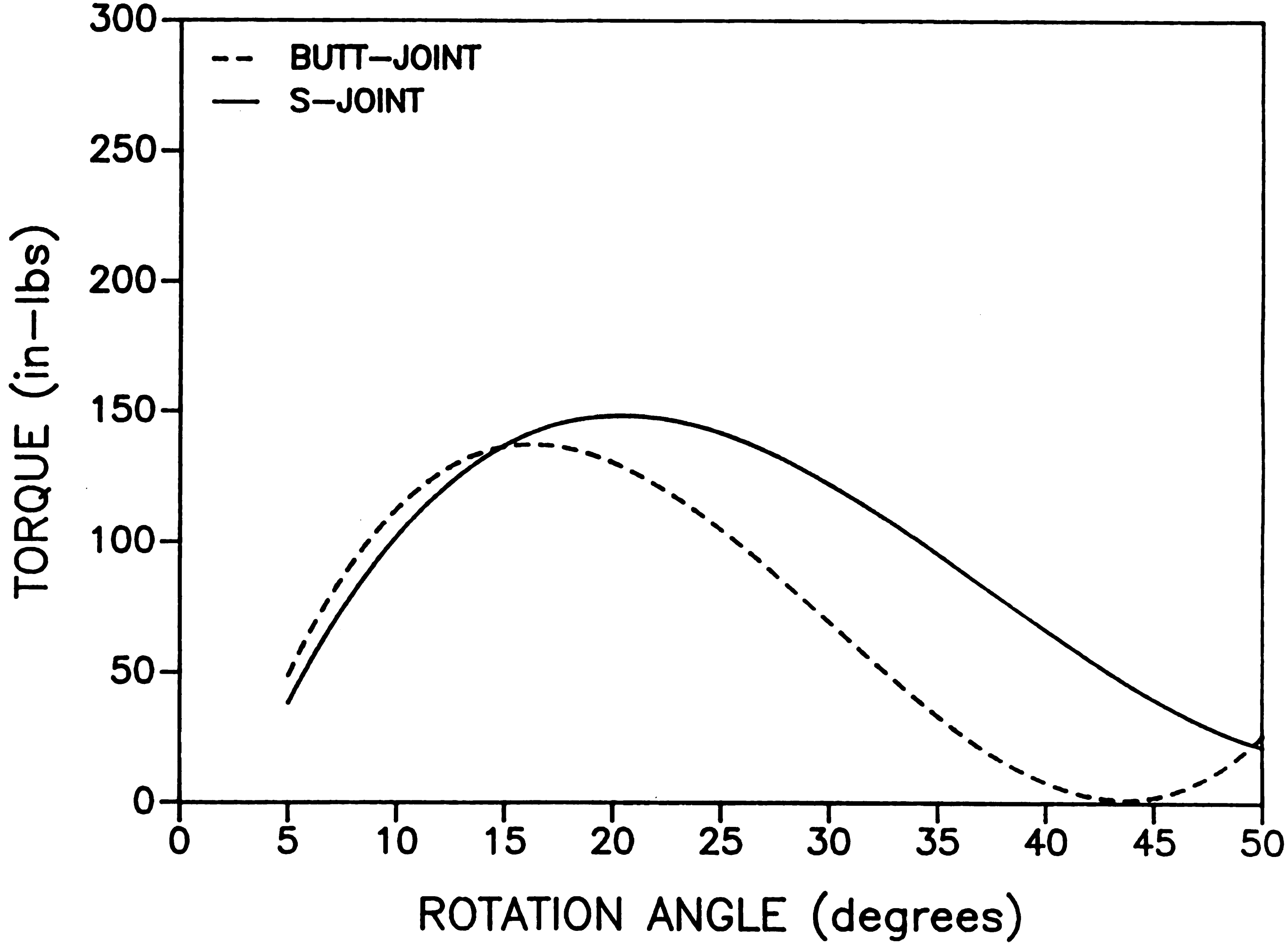

Figure 7.5 Excel 8610. Torsional Rigidity for the S-Joint vs the Butt-Joint. Standard Repair Was Utilized.

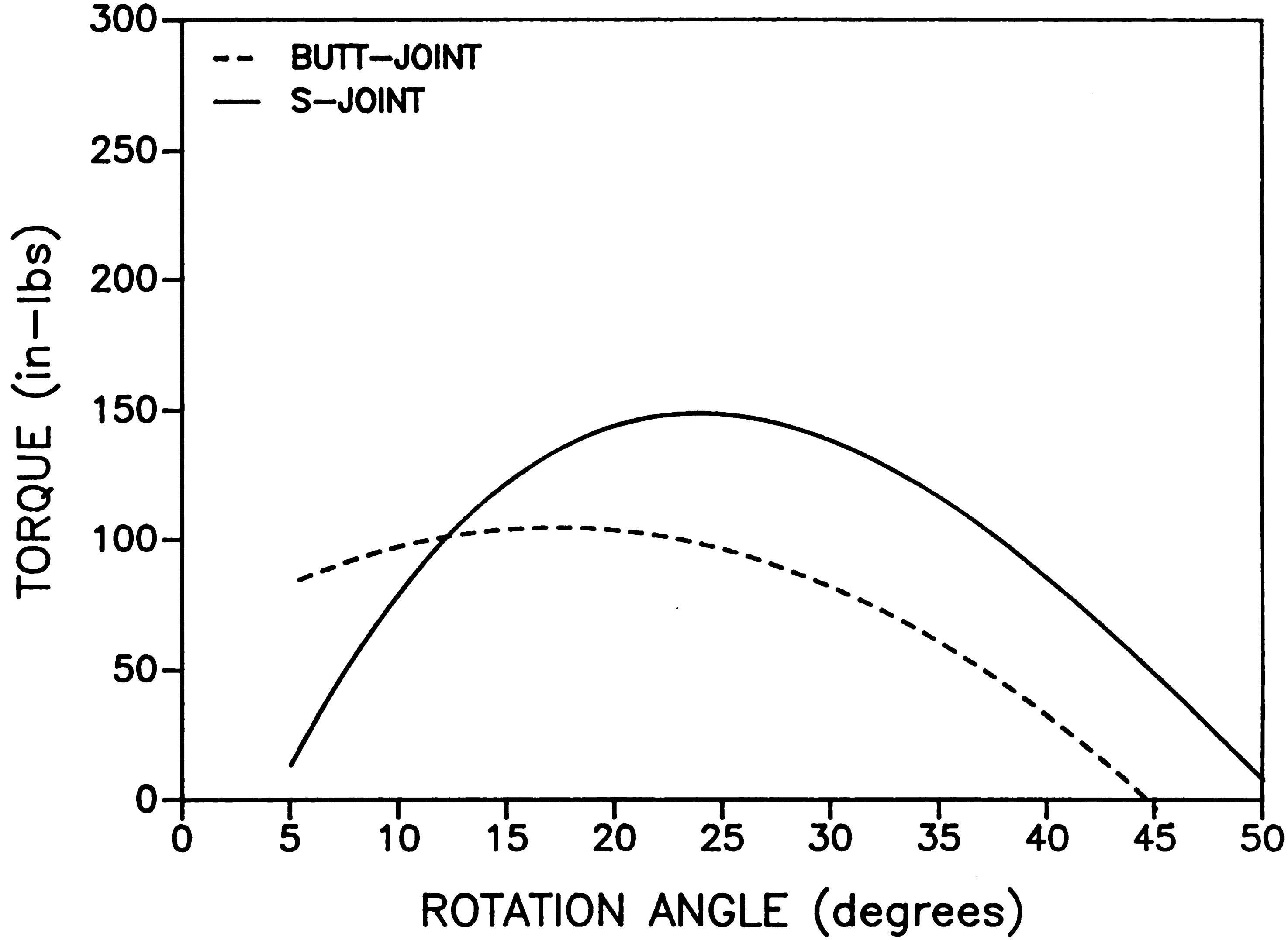

Figure 7.6 Excel 2415-Fill. Torsional Rigidity for the S-Joint vs the Butt-Joint. Standard Repair Was Utilized.

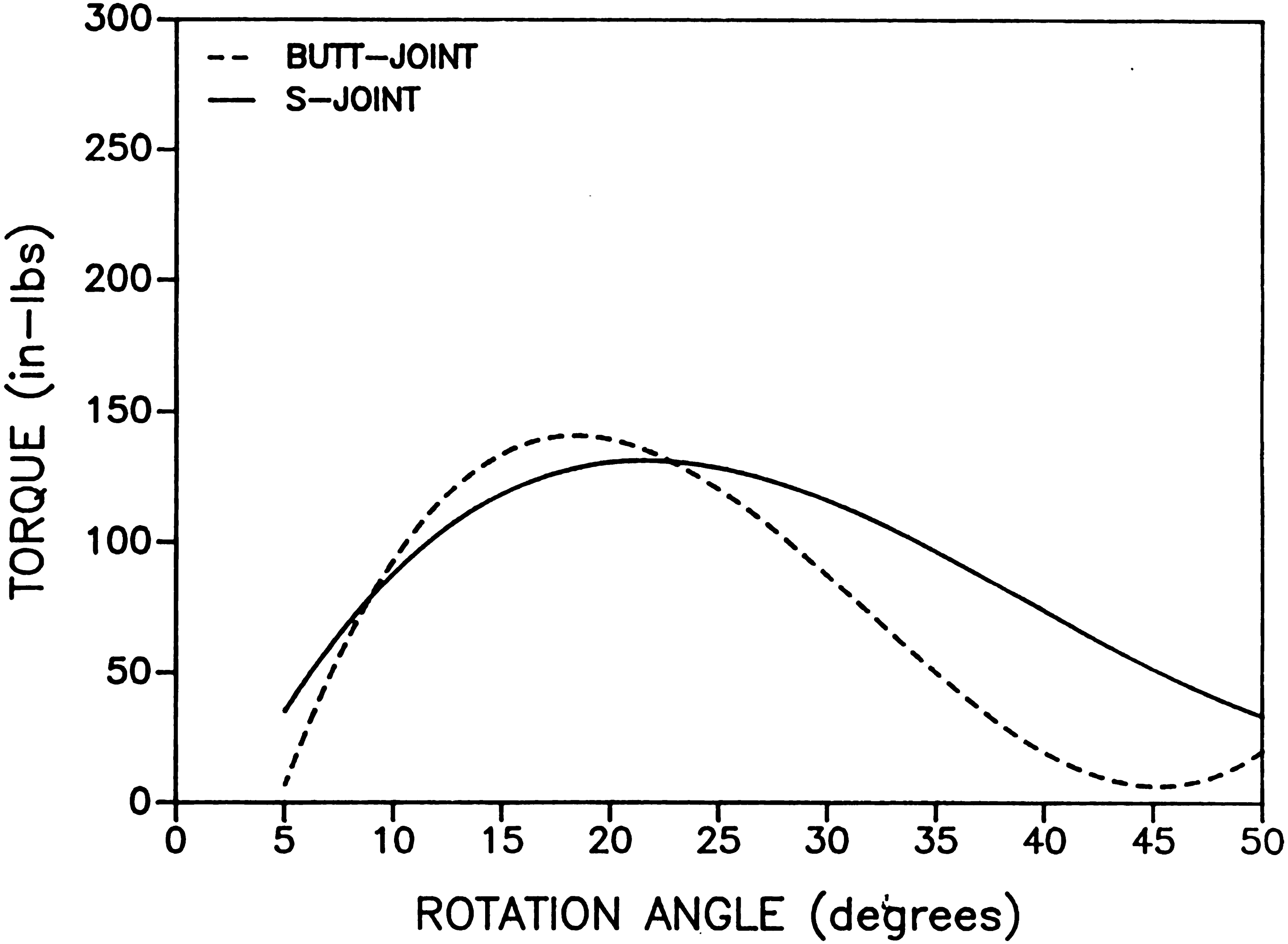

Figure 7.7 Excel 2415-Warp. Torsional Rigidity for the S-Joint vs the Butt-Joint. Standard Repair Was Utilized.

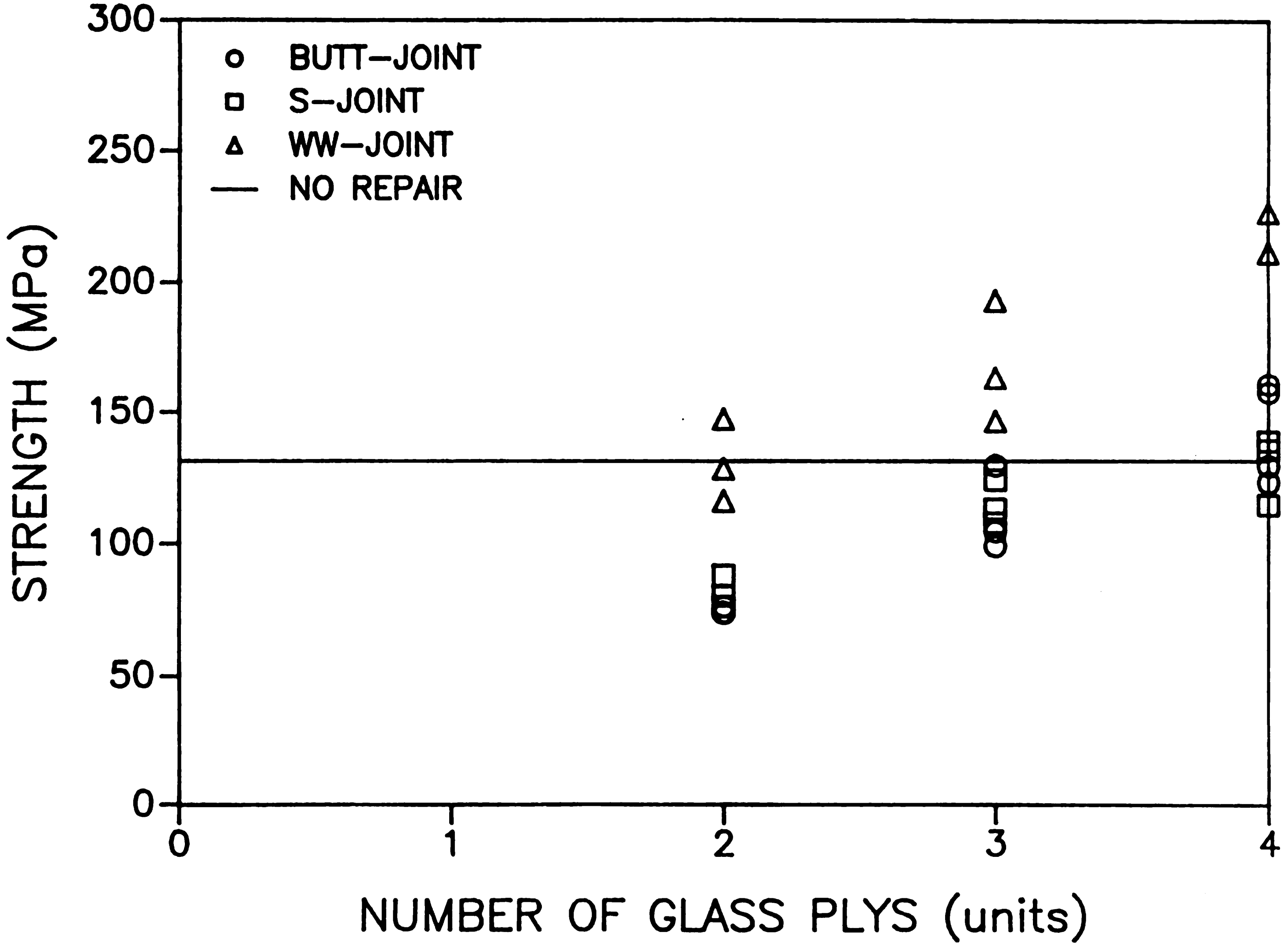

Figure 7.8 Comparison of S-, W-, and Butt-Joints Undergoing Tensile Failure. Standard Repair Was Utilized.

the W-Joint is superior to the S-Joint. The reason for this phenomenon may best be interpreted by observing Figure 7.9 and the particular bondline loading configurations. The three-point bending bondline for the W-Joint follows a consistant 83°, while the S-Joint bond line traverses though both 0° and 90°. It has been shown that the optimum bond line angle for bending should be close to 90° while remaining invariant the direction of loading. The S-Joint is the optimum configuration to satisfy this criteria. Therefore, the W-Joint exhibited superior results in this particular loading configuration because the bond line was not allowed to shift. However, if the bond line was shifted to a parallel position to the W-Joint's 83° then an insufficient butt-joint type bond line would be created. Additional comments should also be made regarding the tension bond line configurations. Again the W-Joint retains a consistant 7° while the S-Joint again traverses through 0°, 45°, and 90°. Therefore, the results show that the optimum bond line configuration for tensile loading should be close to 0° to the direction of loading. Since the W-Joint maintains this set of criteria, it remains the optimum joint for pure tensile loading.

Ultimately, the results shown in Figures 5.20 and 7.2 reveal that the W-Joint is superior in three-point bending and in tension. However, note again the bond line differences between the S-Joint and the W-Joint. If the W-Joint were loaded along the edge of its "W-Shape", then it would simulate a butt-joint configuration which is much less superior, in strength, to the more "isotropic" configuration of the S-Joint.

7.3 Stitching Repair for Torsional Damage

	'WW-JOINT'	'S-JOINT'
TENSION BOND LINE	(7,7,7,7,7,7,7,7,7)	(0,90,0,45,0,90,0)
THREE-POINT BENDING BOND LINE	(83,83,83,83,83,83,83,83)	(90,0,90,45,90,0,90)

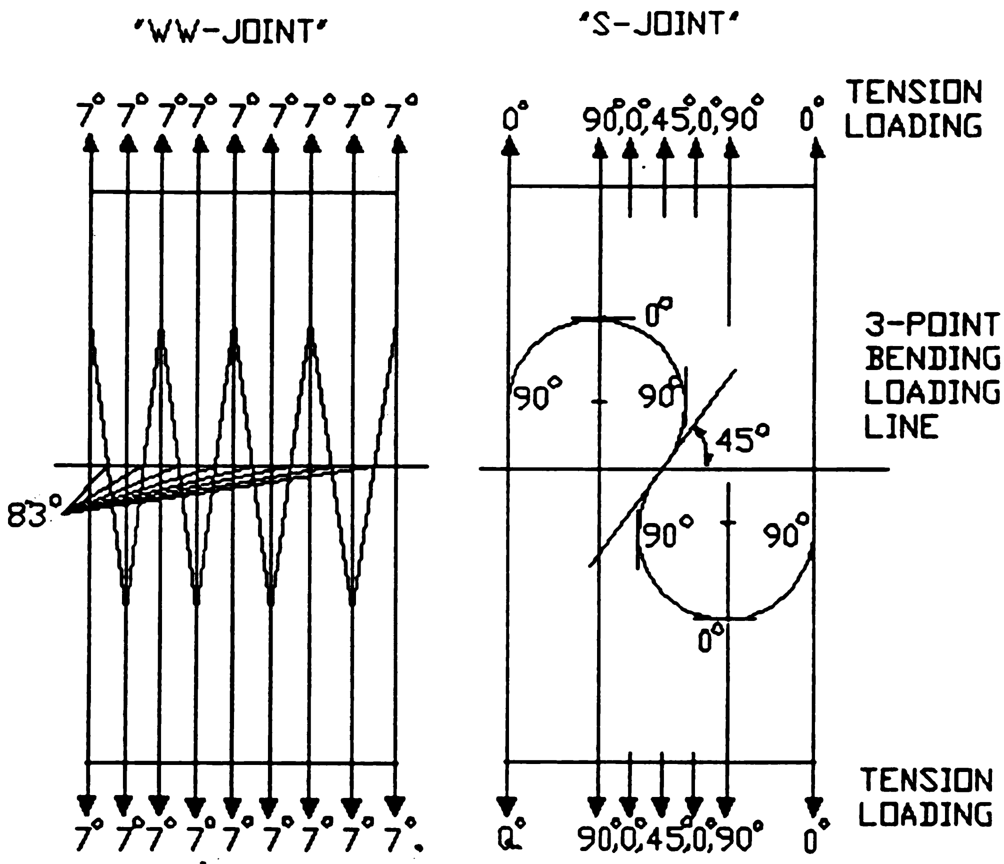

Figure 7.9 Schematic of the S- and WW-Joints under both Tensile and Three-point Bending Loading.

The effects of torsional damage are quite different from the damage modes created through impact, bending, tension, compression, and fatigue failure. None of these damage modes experience any appreciable delamination of the matrix material in the composite during failure. This aspect is what separates torsional damage repair from the rest. Therefore, a different technique must be implemented to restore the torsional rigidity of the specimen after failure.

Preliminary tests revealed that to create failure, the torsional coupons would have to be trimmed into dogbone specimens with a gage area of 1.5" x 2" (37mm x 50mm). This again was necessary to create failure at a rotation angle of 50°. The failure mode that occurred is illustrated in Figure 7.10. The first mode of failure started on the edge of the specimen in the form of matrix cracking. The crack soon propagated across the top and bottom of the gage length and met, through delamination, at the middle.

The first screening of repair followed the conventional form used for the bending specimen. The results are listed in Figures 7.11-7.14, and reveal that the original torsional rigidity could not be restored utilizing this repair technique. Therefore, it was decided to try a combination of mechanical and adhesive bonding in the form of stitching [102]. Consequently, this repair mode shifted into a through-the thickness mode rather than in-the-plane repair.

Two different thread types, nylon and steel, were used during this repair procedure. The parameter under differential comparison was the thread density in the repair zone. Some typical patterns of stitch design are illustrated in Figure 7.15. The holes were drilled with a 3/32" drill bit. The nylon thread was approximately 1/32"

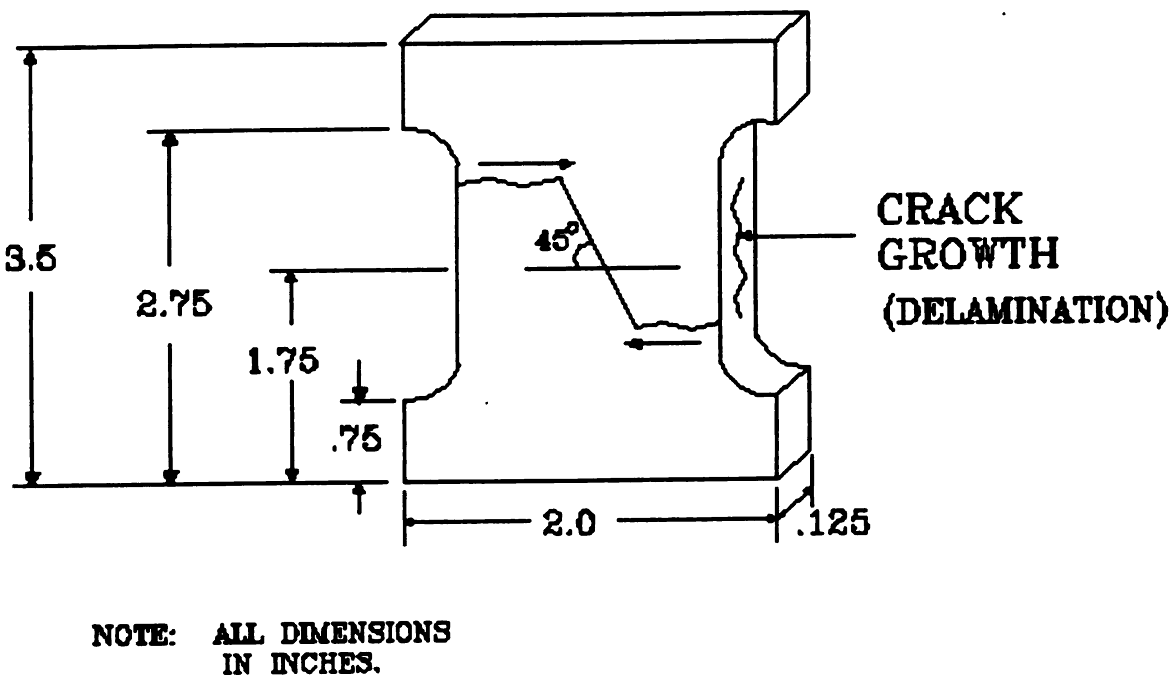

Figure 7.10 Torsional Failure Mode for Owens Corning SMC.

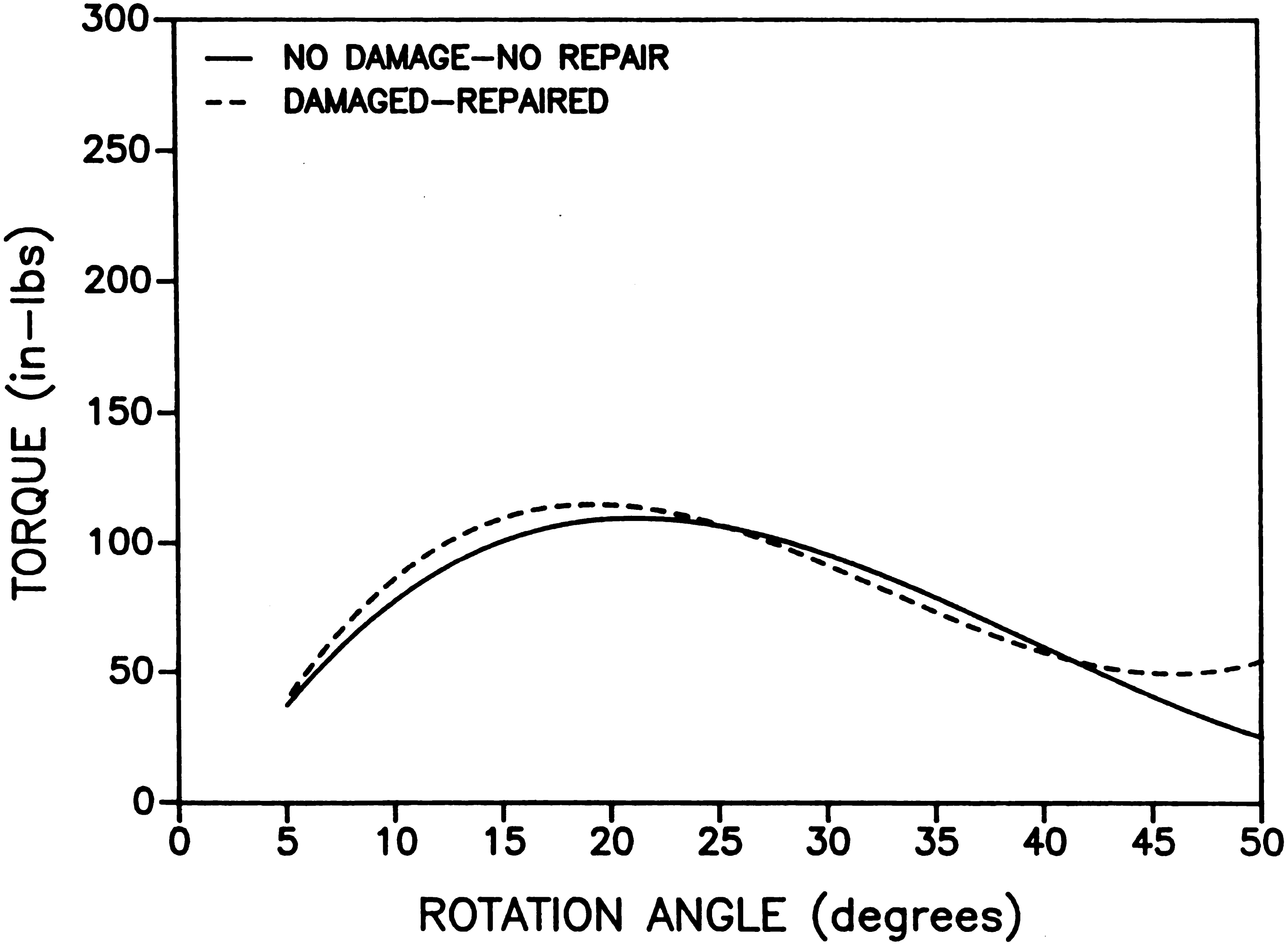

Figure 7.11 Torsional Rigidity of Owens Corning Material Before Damage and After Standard Repair.

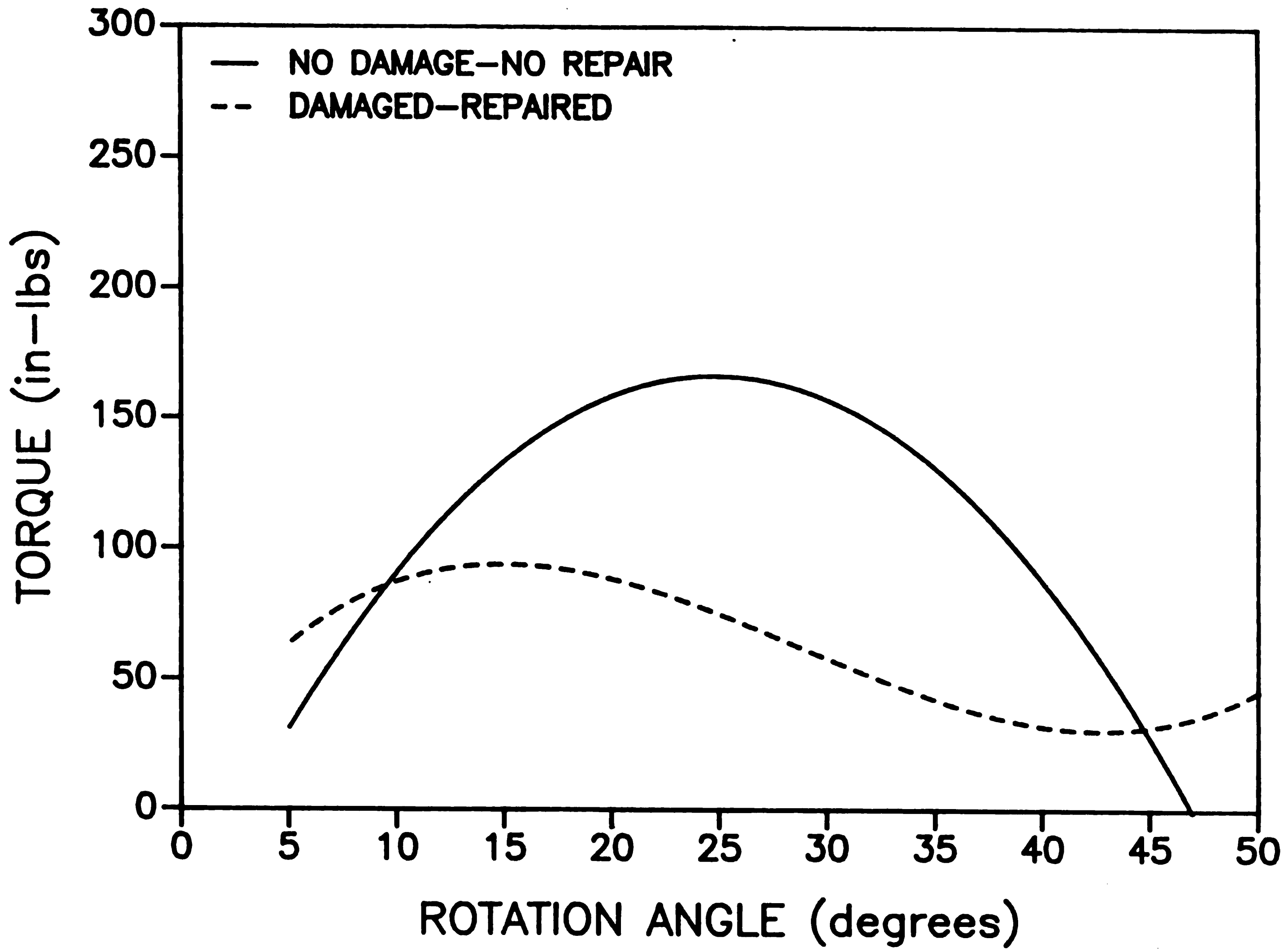

Figure 7.12 Torsional Rigidity of Excel 8610 Material Before Damage and After Standard Repair.

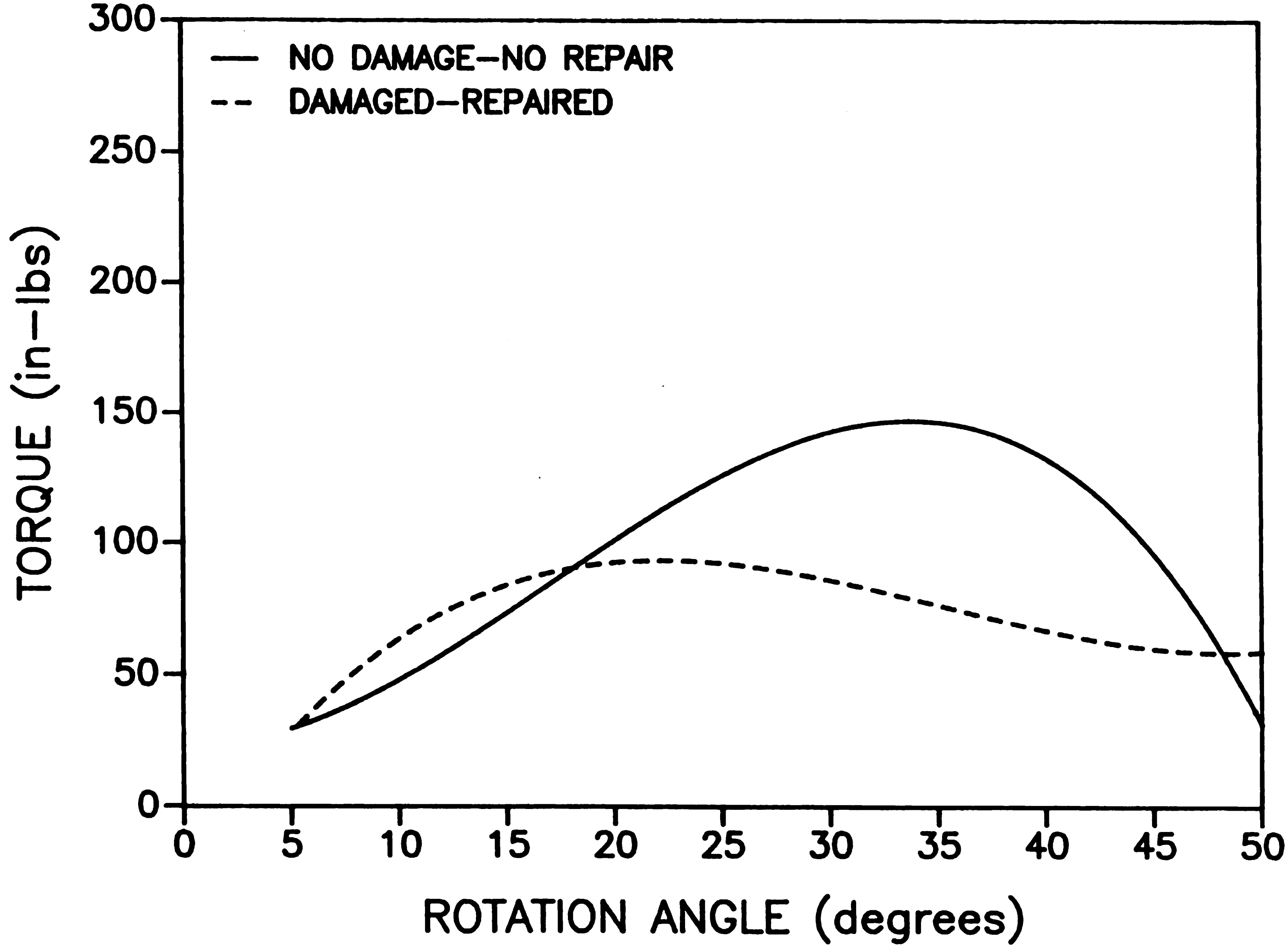

Figure 7.13 Torsional Rigidity of Excel 2415 (Fill) Material Before Damage and After Standard Repair.

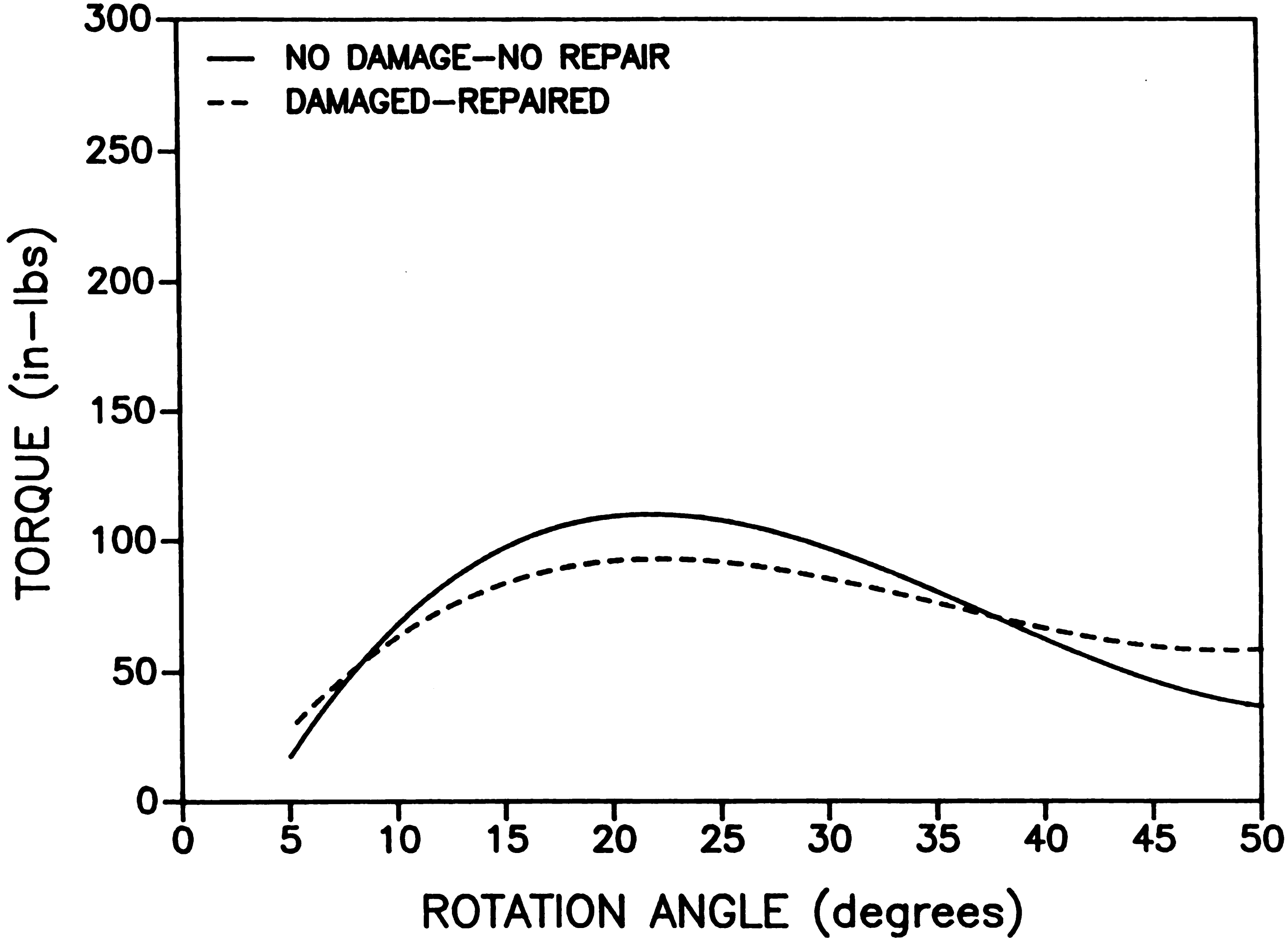

Figure 7.14 Torsional Rigidity of Excel 2415 (Warp) Material Before Damage and After Standard Repair.

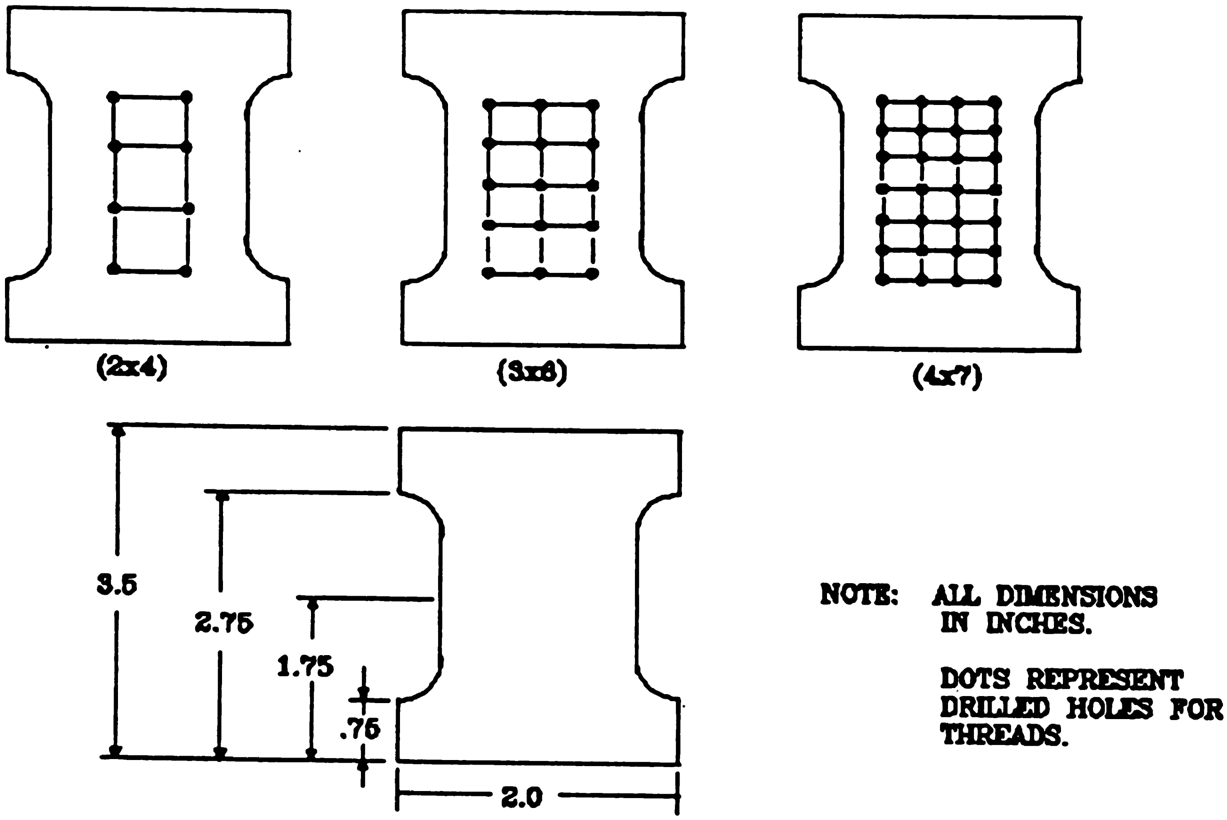

Figure 7.15 Sketch of Drilled Hole Patterns for Stitching During Torsional Repair.

while the steel thread was approximately 2/32". Motivation behind this particular hole and thread size was to (1) not create holes too large since this would create large voids, and (2) choose a thread diameter that fits well through the hole without too much of a gap. Any gap that was created between the thread and the drilled hole was filled by the application of epoxy on the specimen surface. Since the steel thread was less flexible than the nylon, it could only be drawn through the hole once. In some cases the nylon thread was drawn through the holes twice, therefore doubling the density at that spot.

In this repair scheme, no glass patch material was utilized, only thread (mechanical) and epoxy (adhesive). The results of this new form of repair are illustrated in Figures 7.16-7.18. The conclusions from the nylon thread revealed that the nylon thread was not rigid enough to enhance the through-the-thickness rigidity. Also, it was an interesting observation that the failure propagated from the same zones as it had before in the reference undamaged specimen, which revealed that the edge density of the stitching pattern is very important, while repair of the central region adds less structural rigidity.

The results for the steel thread are illustrated in Figures 7.19-7.21. Note the increase in strength over the nylon thread as well as the increase due to thread density. By achieving a stitching pattern of 3 x 6, the torsional rigidity was restored. At the thread density of 4 x 7, the torsional rigidity was 33% higher than the original undamaged specimen rigidity.

These conclusions were very encouraging, but there was still a question as to what parameter was contributing the most to the repair rigidity. Was it the portion of thread

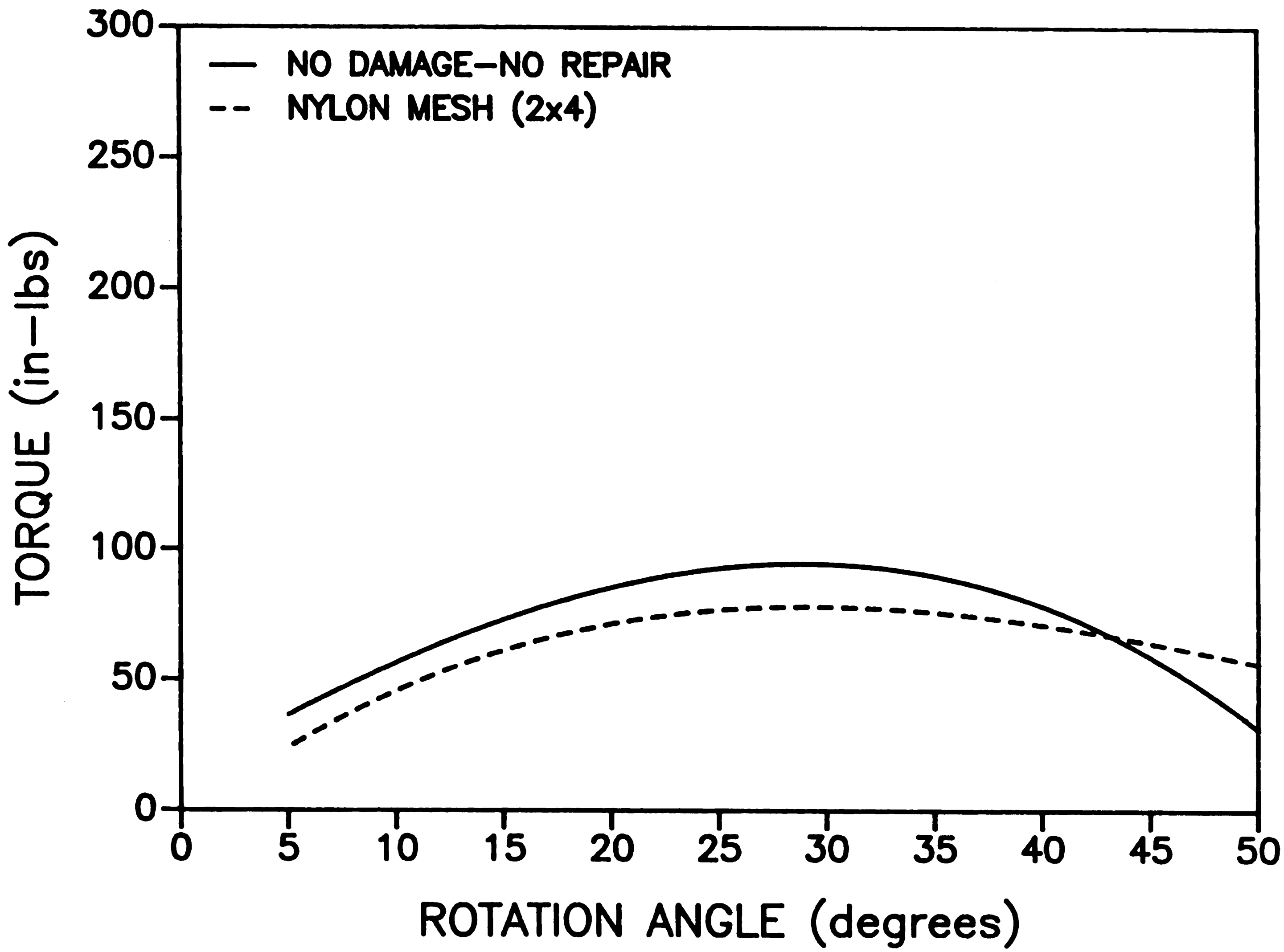

Figure 7.16 Torsional Rigidity of Owens Corning Material Before Damage and after Stitching Repair. The Thread is Nylon, and No Glass Reinforcing Layers are Utilized. Mesh Density = (2x4).

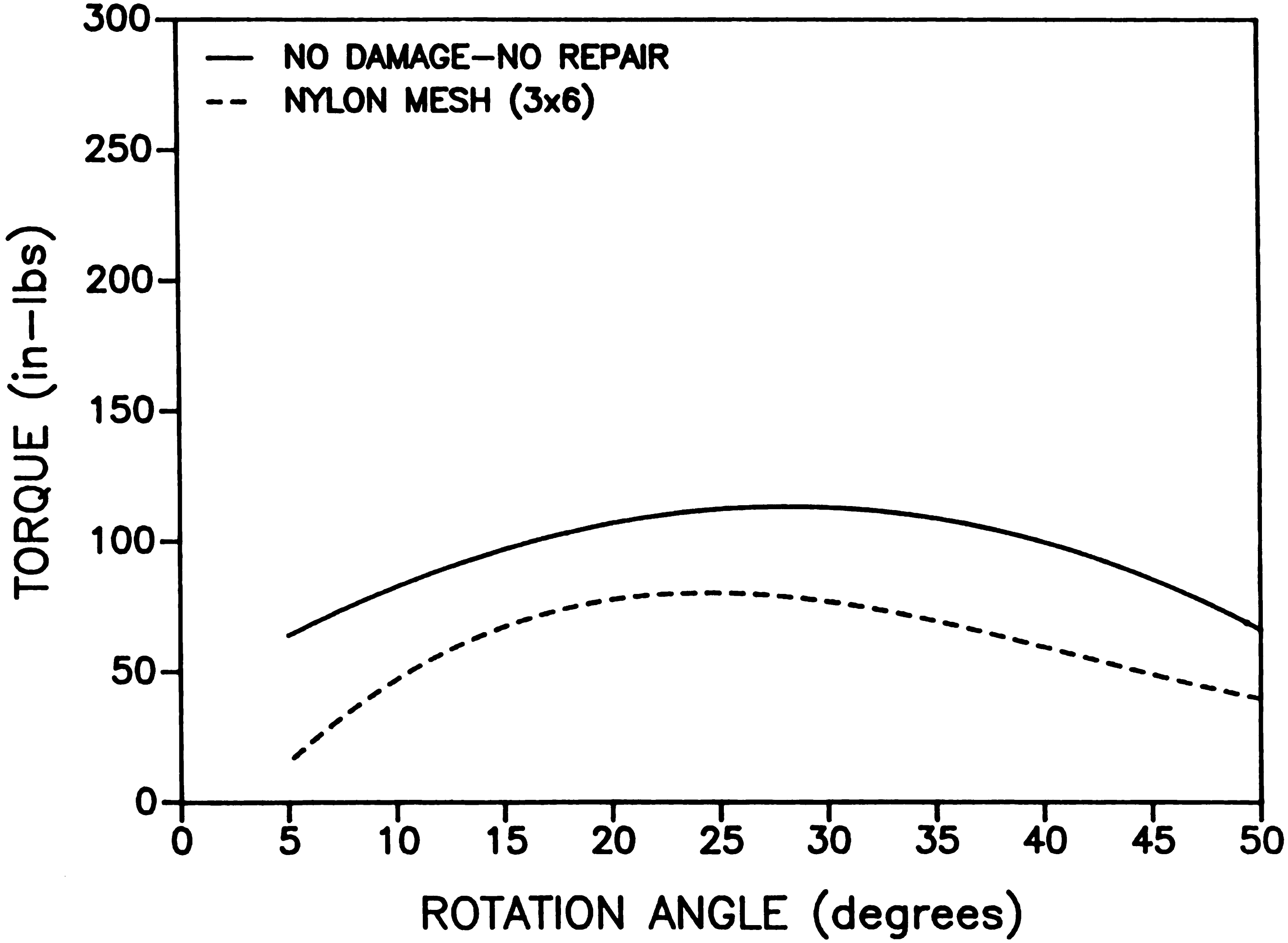

Figure 7.17 Torsional Rigidity of Owens Corning Material Before Damage and after Stitching Repair. The Thread is Nylon, and No Glass Reinforcing Layers are Utilized. Mesh Density = (3x6).

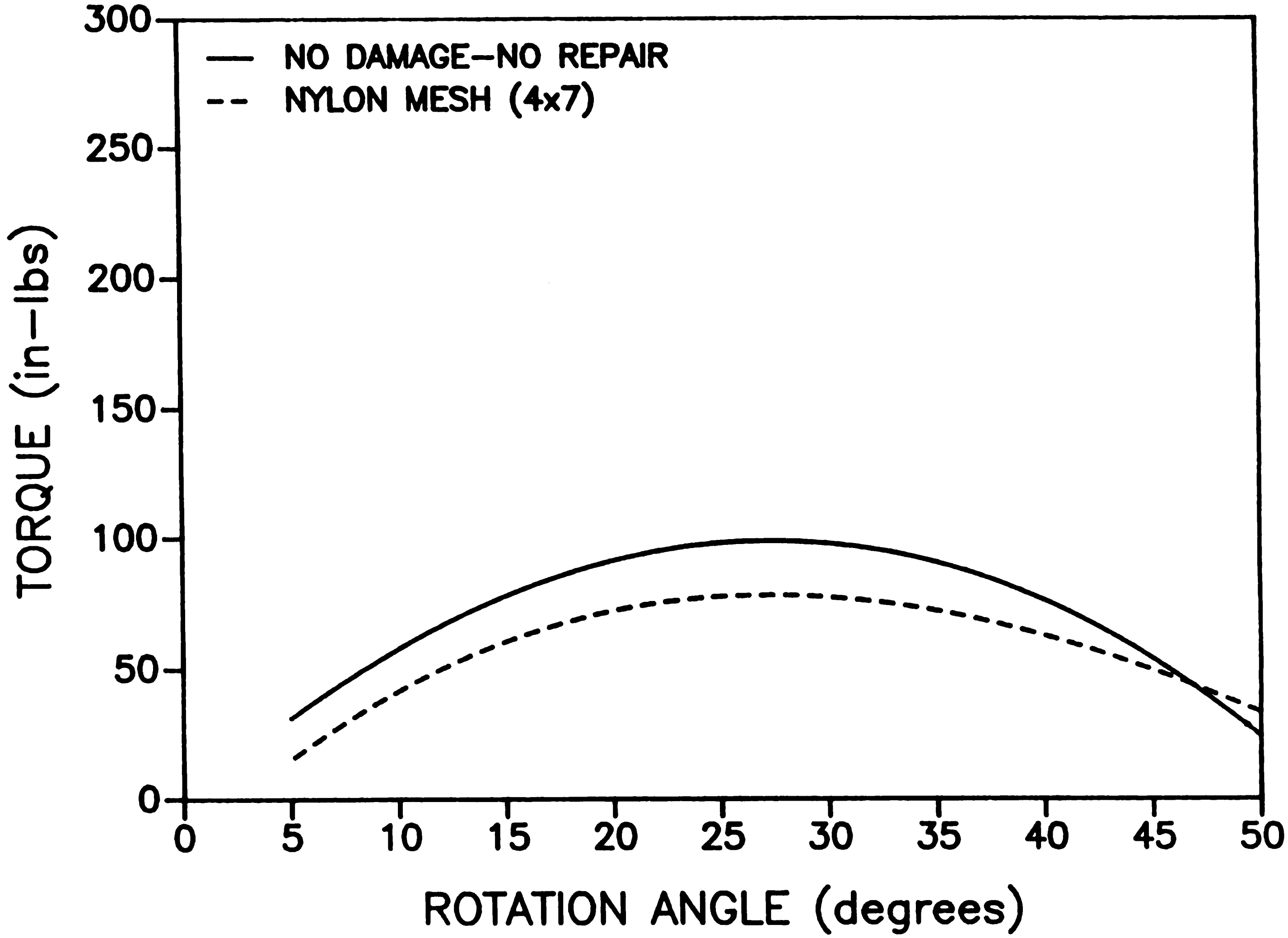

Figure 7.18 Torsional Rigidity of Owens Corning Material Before Damage and after Stitching Repair. The Thread is Nylon, and No Glass Reinforcing Layers are Utilized. Mesh Density = (4x7).

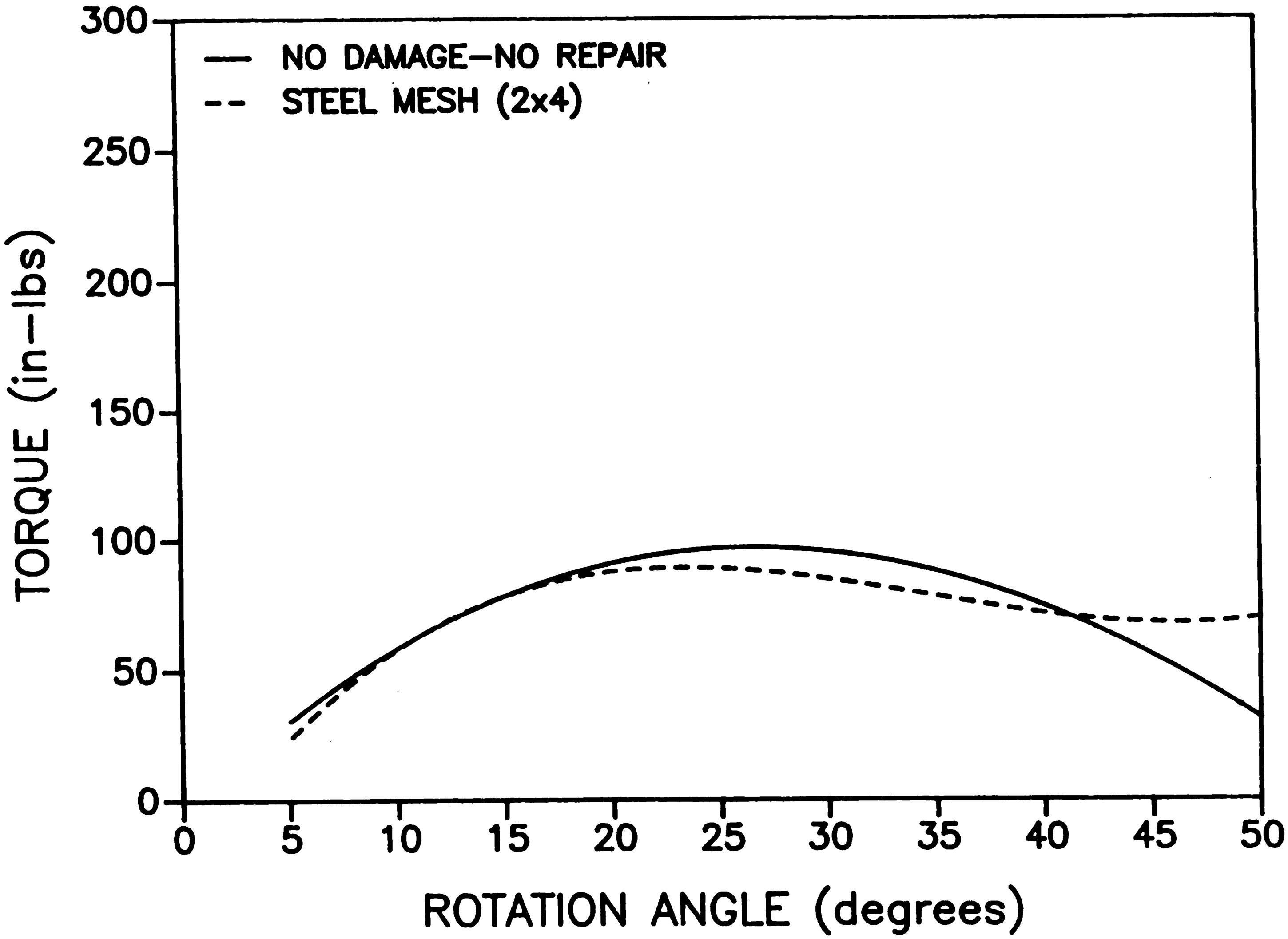

Figure 7.19 Torsional Rigidity of Owens Corning Material Before Damage and after Stitching Repair. The Thread is Steel, and No Glass Reinforcing Layers are Utilized. Mesh Density = (2x4).

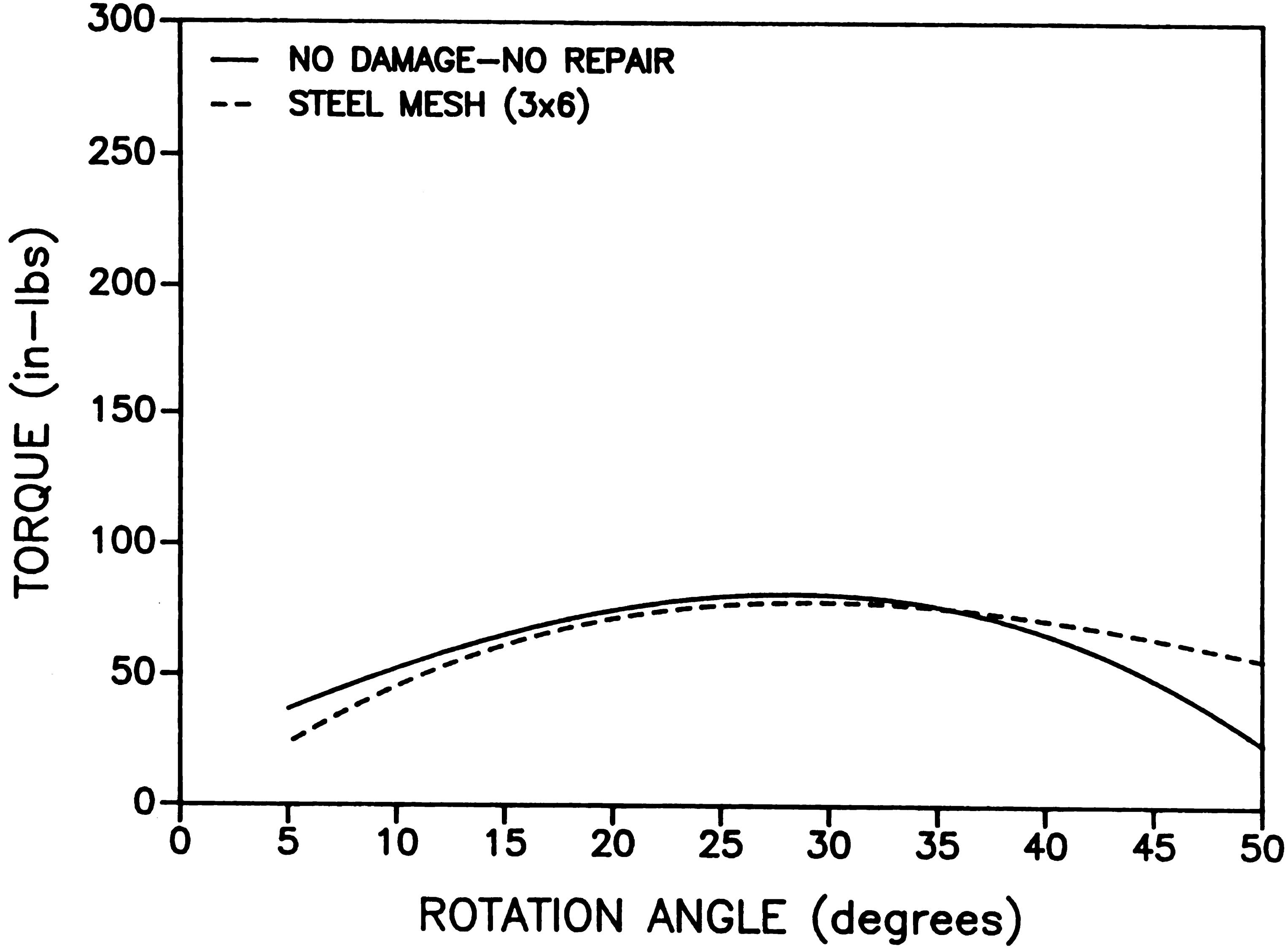

Figure 7.20 Torsional Rigidity of Owens Corning Material Before Damage and after Stitching Repair. The Thread is Steel, and No Glass Reinforcing Layers are Utilized. Mesh Density = (3x6).

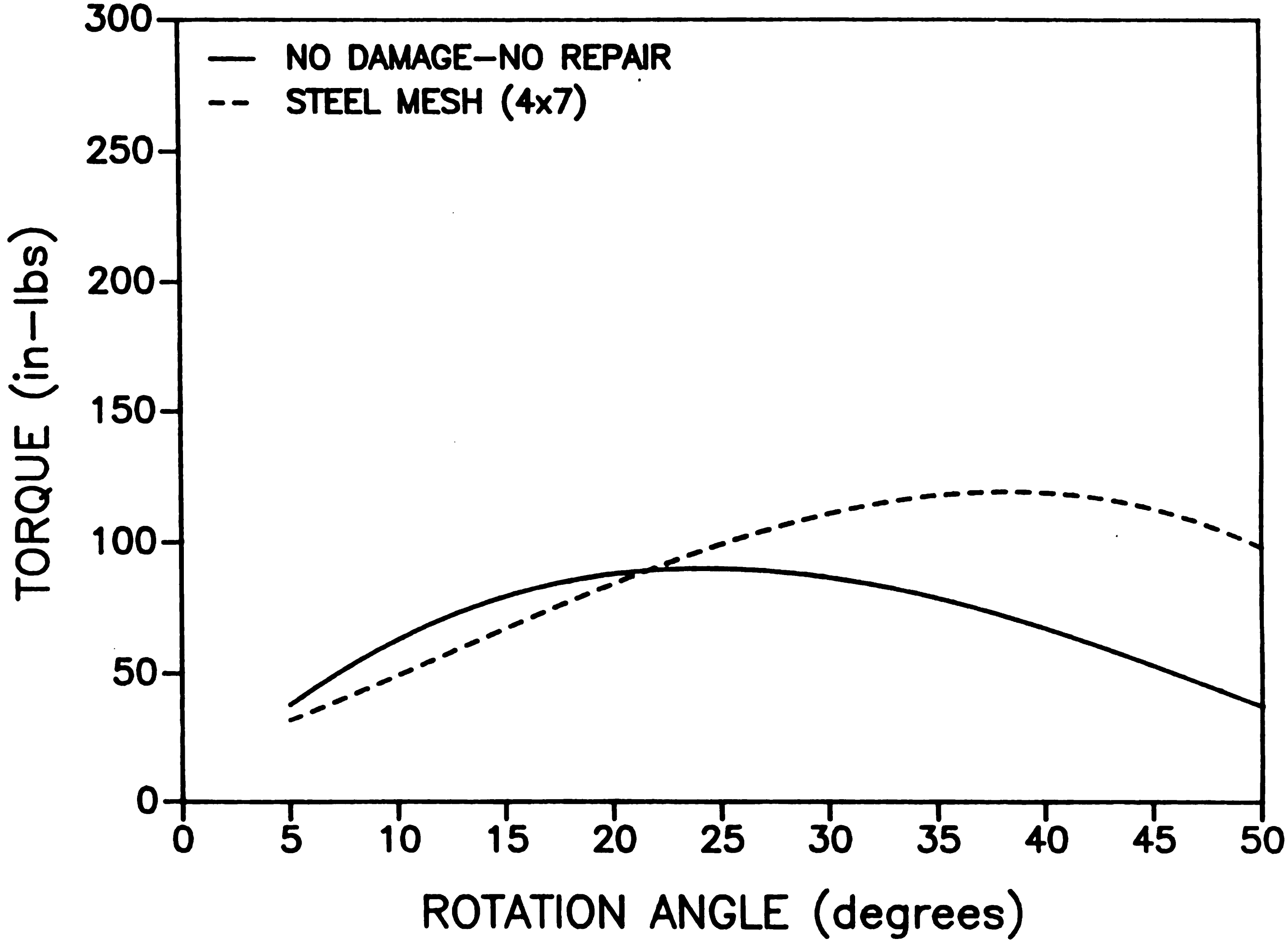

Figure 7.21 Torsional Rigidity of Excel 2415(Fill) Material Before Damage and after Stitching Repair. The Thread is Steel, and No Glass Reinforcing Layers are Utilized. Mesh Density = (4x7).

that was through-the-thickness of the specimen or the portion that was in-the-plane? One more test was conducted to evaluate this question. A torsionally damaged specimen was repaired by laying four steel wire strips along the gage length on both sides of the specimen. See Figure 7.22. The wire strands were set in place and coated with epoxy. The wire ends were left long enough so that during the testing procedure the ends could also be anchored in the Instron grips. This simulated in-the-plane repair with added supports in the gage length by the addition of two anchor supports at both ends of the specimen. The results are illustrated in Figure 7.23, and they reveal that about 50% of the restored torsional rigidity is contributed by the in-plane stiffeners while the remaining 50% comes from through-the-thickness stiffeners.

The application of such a repair design focuses primarily on those endurable goods that simply must be repaired rather than replaced. With the absence of glass reinforcing material, the thickness direction of the repaired specimen is negligibly enhanced, only about 0.02". This aspect is very desirable when and if the torsional repair specimen is a spinning shaft, since it would reduce the effects of any complicating factors due to rotational eccentricities and surface roughness.

7.4 Optimization of Design - A Computer Model

After the designs for the S-joint were complete, a computer model [103] was implemented to evaluate an in-plane repair geometry resembling a butt-joint. The finite element model is based on interlaminar stress continuity theory which utilizes a multiple layer approach. Therefore, the analysis of through-the-thickness repair can take place.

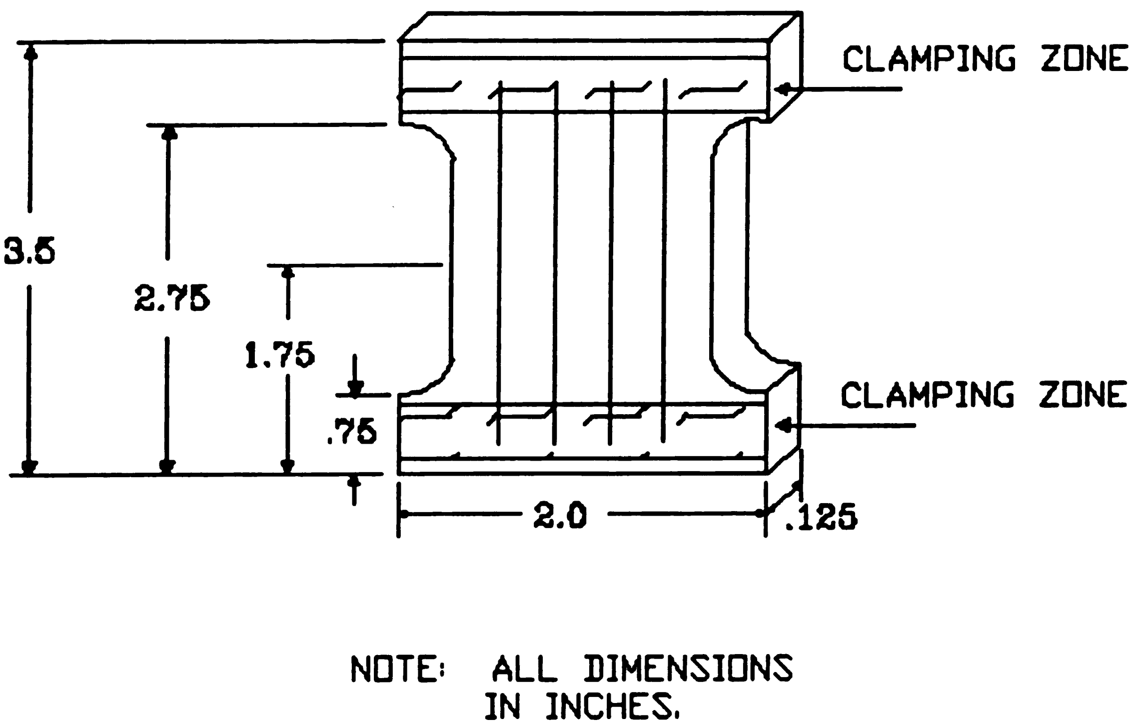

Figure 7.22 Schematic Showing the "4-Wire-Strand" Configuration.

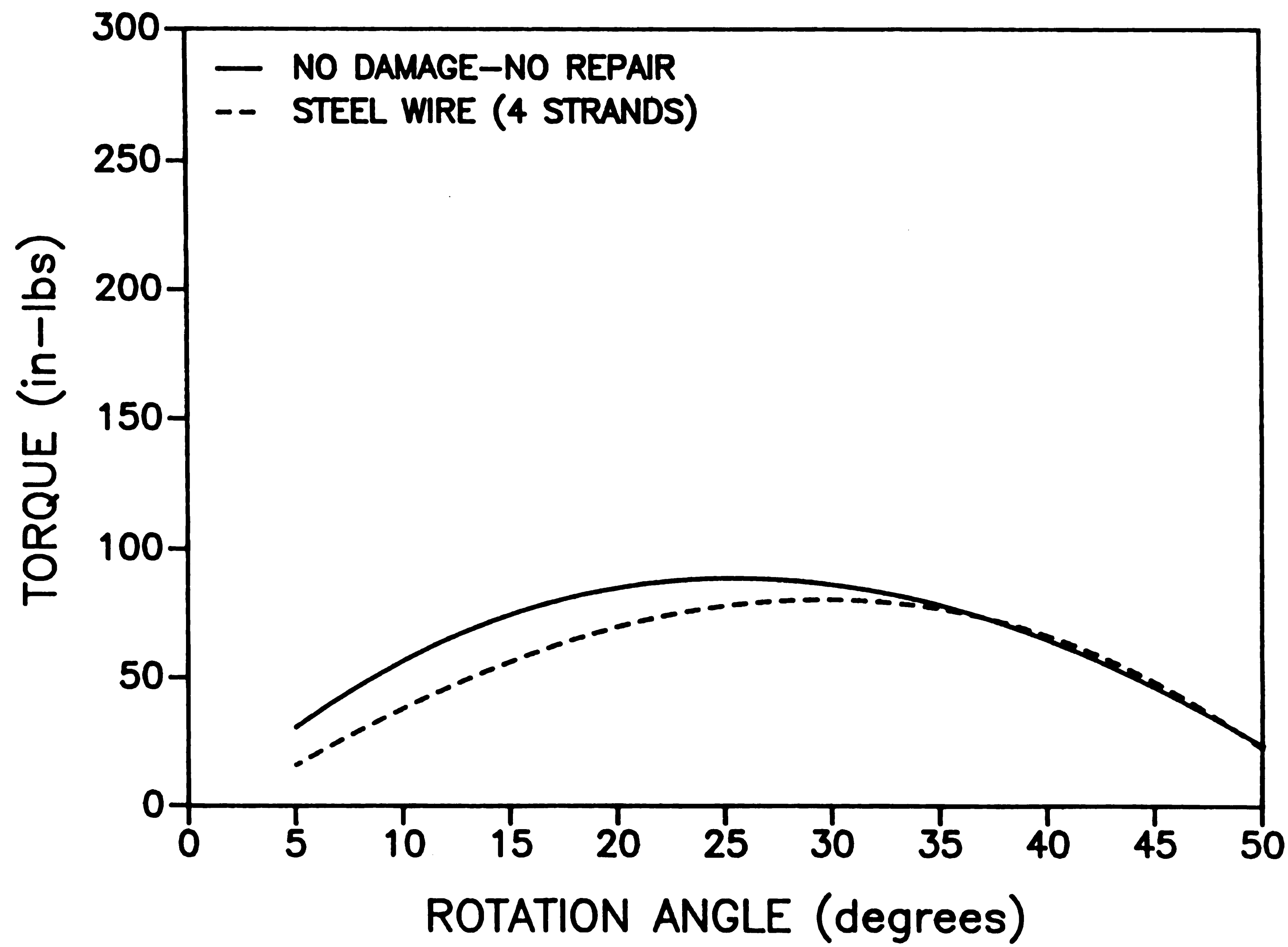

Figure 7.23 Results for Owens Corning SMC With a Four-Strand Wire Grid for the Torsion Repair Study.

The model incorporates a Hermite cubic shape function to analyze the composite layer assembly in the thickness direction. By using the high-order shape function, the transverse shear deformation can be considered in the analysis. The high-order shape function enables the evaluation of interlaminar shear stress and interlaminar normal stress at the laminate interfaces directly from the constitutive equations, rather than recovering them from the equilibrium equations. Consequently, since the theory and technique are two-dimensional, it is valid for both thin and thick composite laminates. Numerical results show that there is excellent agreement with the elasticity solution.

The finite element mesh that was developed using the aforementioned model consisted of six layers and ten elements. The model was subjected to three-point bending throughout the analysis. Figure 7.24 is a schematic of the finite element mesh. The six evaluation layers consisted of: (1) patch material plus resin on the top two layers, (2) the composite material on the middle four layers, and (3) patch material plus resin on the bottom two layers. The freedom of the six different layers allowed modification of not only the composite material, but also the patch thickness, and moduli. Because of this freedom, three different surveys were undertaken. The first analysis evaluated variances in patch thickness. The different thicknesses were based on two layers of patch on the top side of the composite measuring 0.4mm, and the addition of one, two, three, four, and five patch layers with thicknesses measuring 0.2mm, 0.4mm, 0.6mm, 0.8mm, 1mm respectively to the bottom side. Results of this survey are illustrated in Figure 7.25, along with a correlation of the experimental data. Note that the values of stress have been normalized in order to correctly correlate the experimental value with the computer

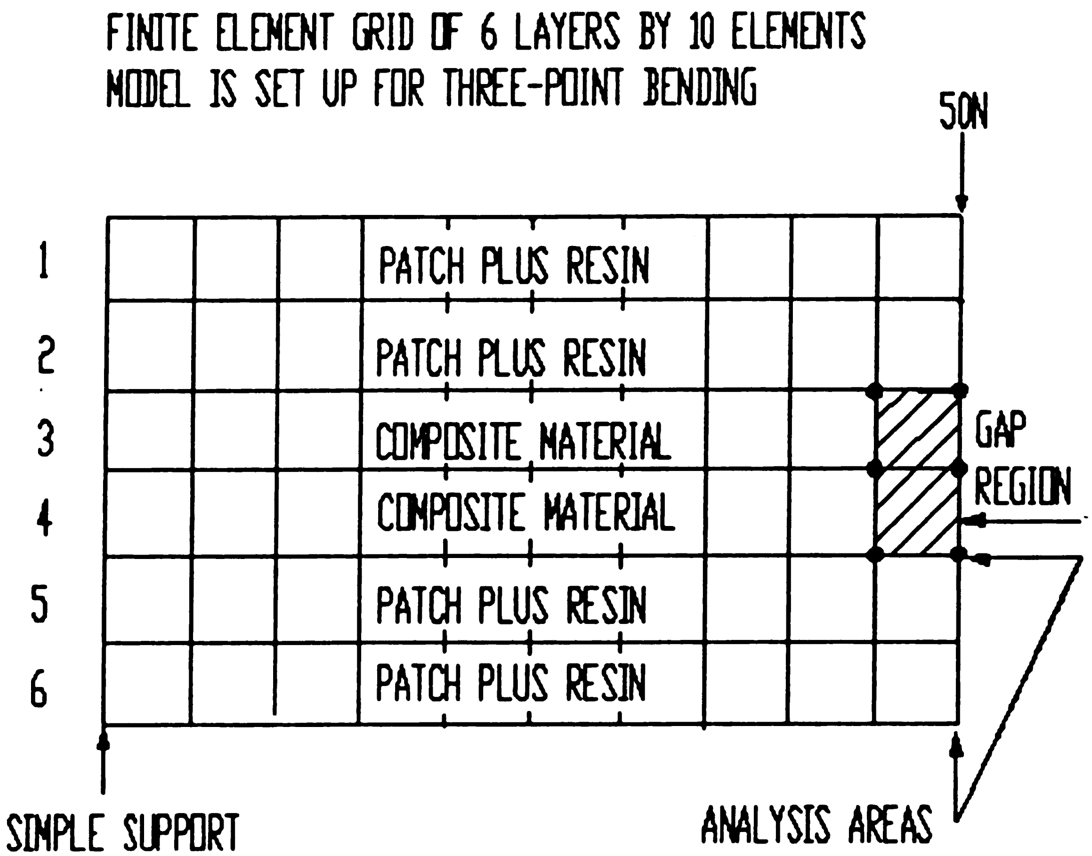

Figure 7.24 Schematic of the Finite Element Mesh.

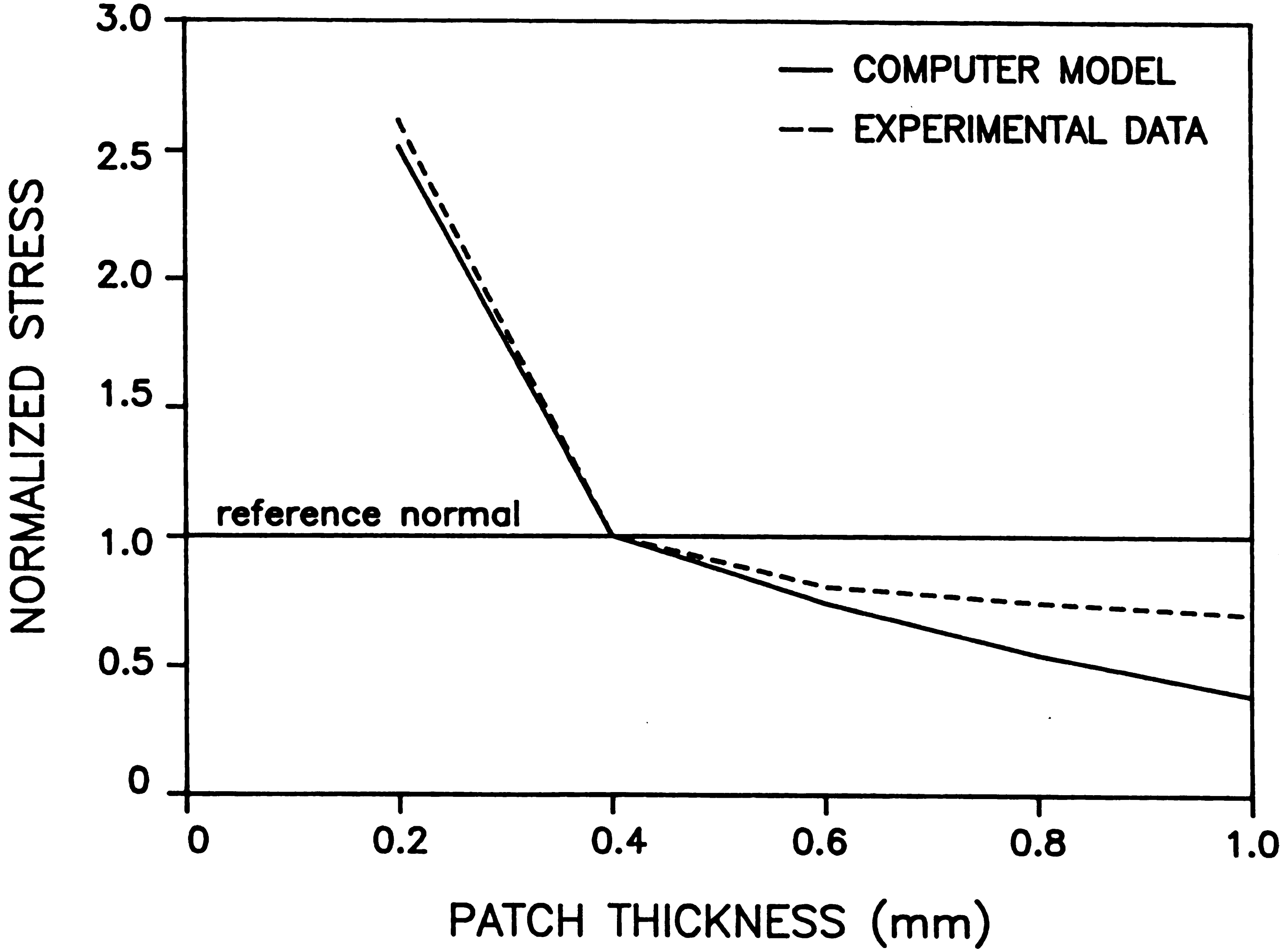

Figure 7.25 Computer Modeling of Patch Thicknesses. Normalized Stress.

model. The second survey dealt with varying a gap or void size on the composite layers of the model. Gap sizes that were evaluated were based on a half gap length due to the fact that the finite element model is symmetric with respect to the composites in-plane centerline. The half-gap lengths that were evaluated were 0mm, 1mm, 2mm, 3mm, 4mm, and 5mm. These gaps were created assuming pure epoxy resin was to take their place. The normalized stress results are listed in Figure 7.26 and 7.27. Figure 7.27 correlates the shear stress occurring at the bottom of the composite layer two and inward from the centerline of 5mm. The third survey, kept the half gap length at 5mm and modified the fillers used in the gap or void zone. The results for both normalized stress and normalized shear stress are illustrated in Figures 7.28 and 7.29. The experimental results correlate very well to the computer model with respect to displaying the same trends during loading.

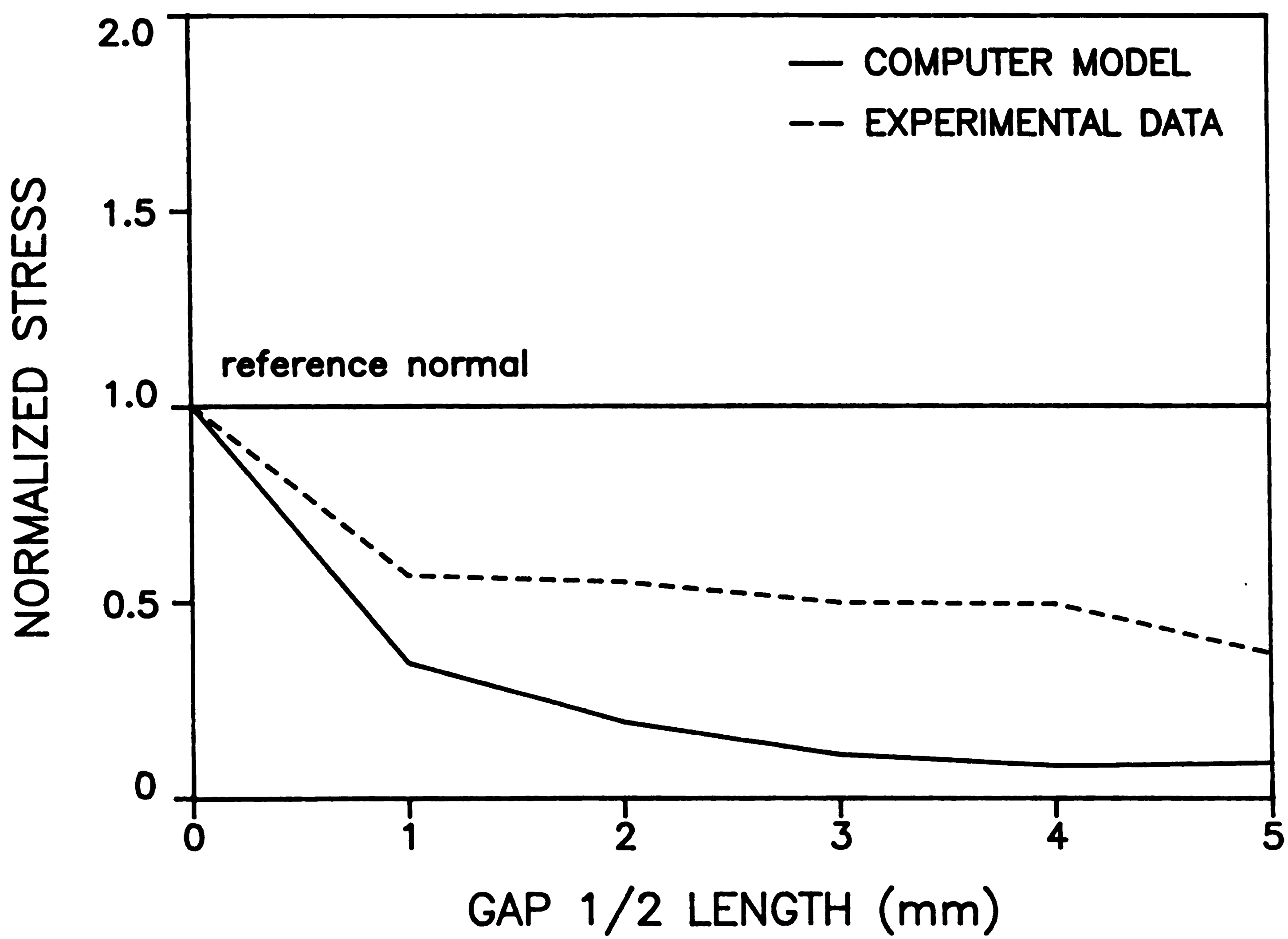

Figure 7.26 Computer Modeling of Butt-Joint Gap Lengths. Normalized Stress.

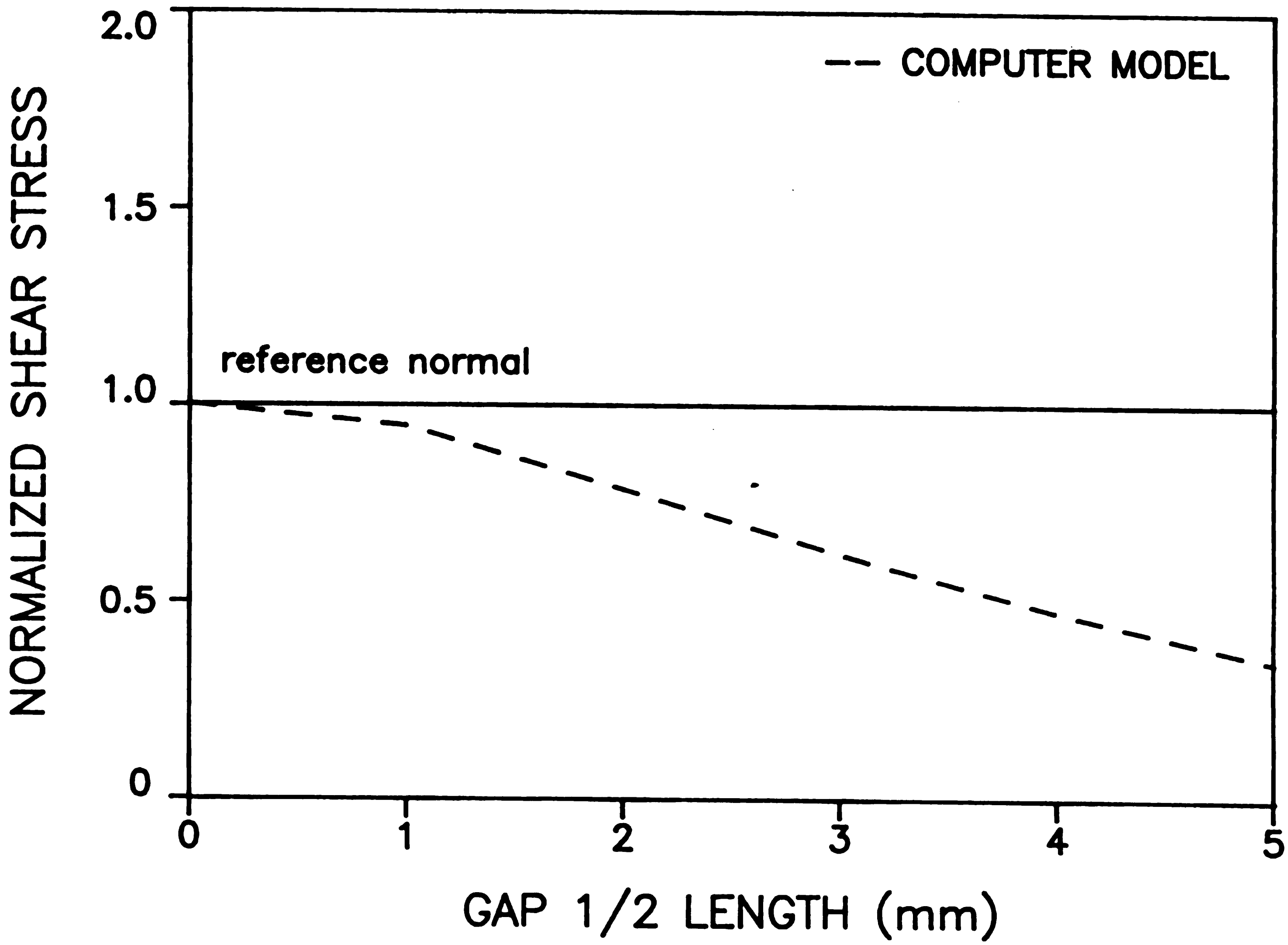

Figure 7.27 Computer Modeling of Butt-Joint Gap Lengths. Normalized Shear Stress.

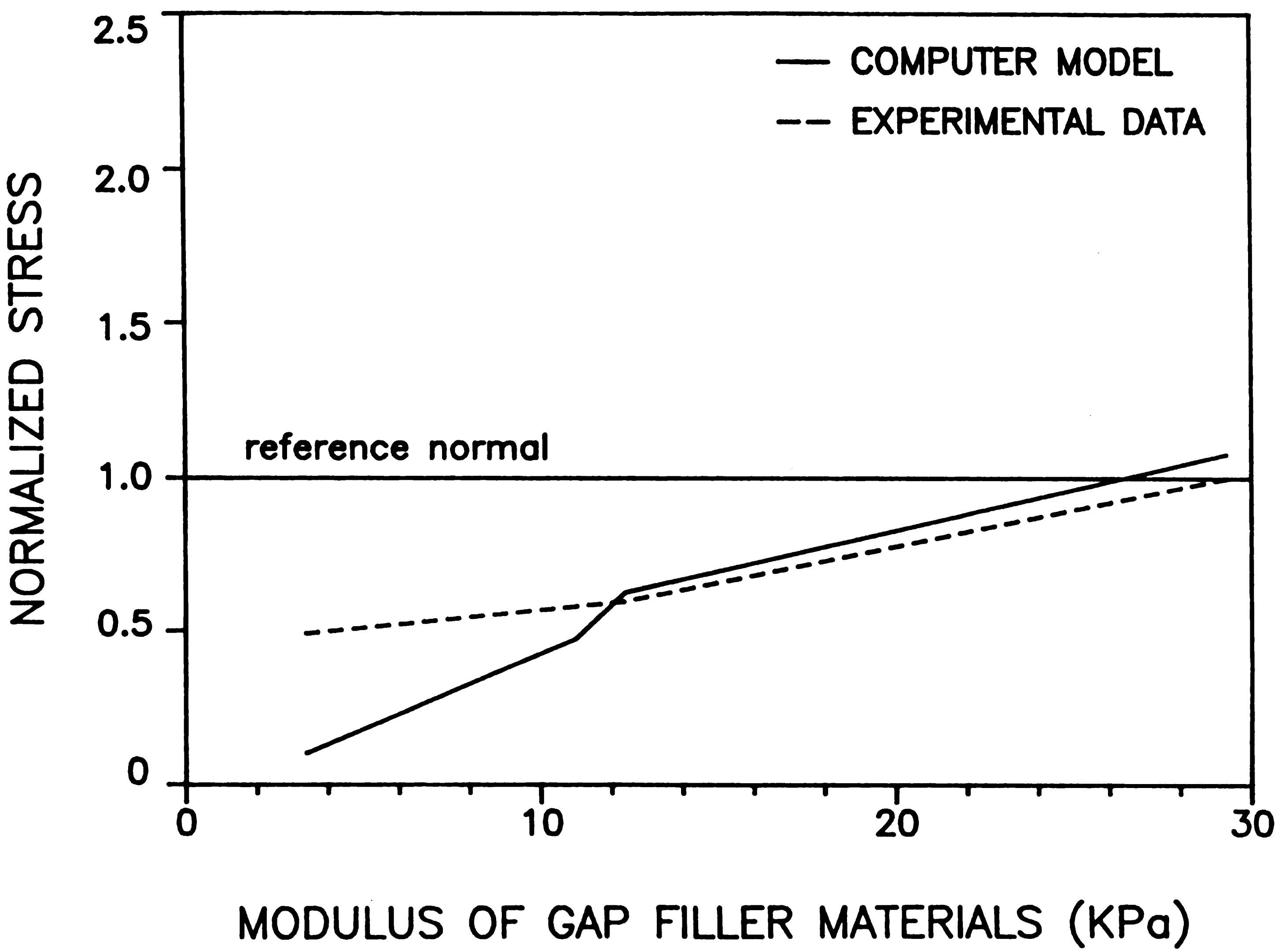

Figure 7.28 Computer Modeling of Butt-Joint Gap Fillers. Normalized Stress.

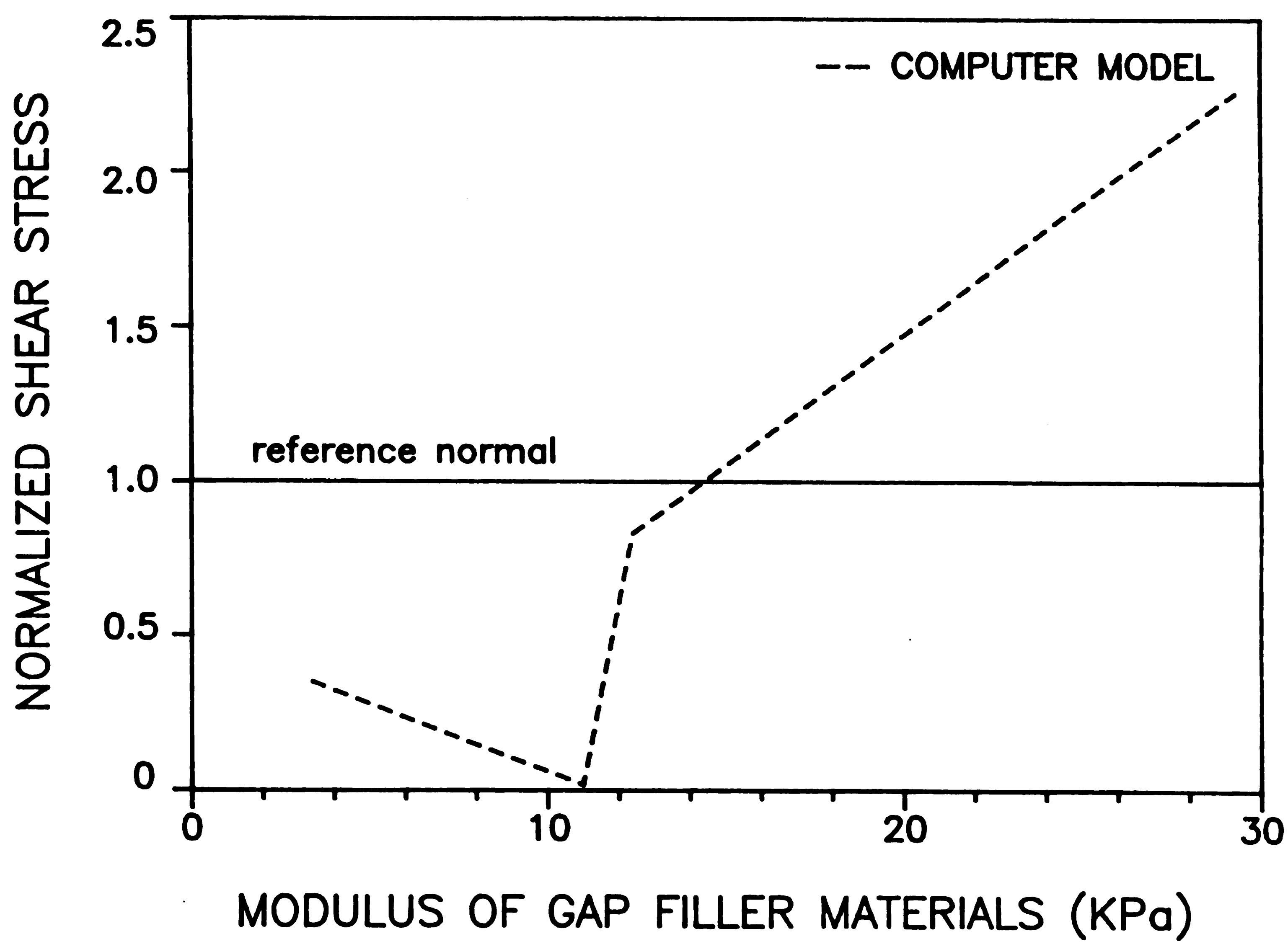

Figure 7.29 Computer Modeling of Butt-Joint Gap Fillers. Normalized Shear Stress.

CHAPTER 8

SUMMARY

Based on the experimental results, some important conclusions and recommendations can be summarized as follows.

1. A standard repair technique based on reinforcing patch and bonding adhesive has been verified to be a feasible technique for repairing composites with line cracks and circular cutouts. Since these two types of artificial damage modes and their combinations can closely simulate various types of impact-induced damage, the standard technique can be used for repairing real damage.

2. In order to have good bonding efficiency, the mechanical properties of the reinforcing patch and adhesive should be compatible with those of the fiber and matrix, respectively, of the composite under repair. In addition, a low viscosity adhesive and a woven type of reinforcing patch material can help to improve the repair efficiency.

3. The fiber geometry plays a very important role in composite repair. Composites consisting of chopped fibers and continuous swirl mats have randomly oriented fibers. Therefore their properties are more matrix dominated. The woven fabric composite is more fiber-dominated. Hence, the matrix-dominated composite can be more efficiently repaired than can the fiber-dominated composite since the latter requires a higher strength reinforcing patch to achieve the required repair strength.

4. In addition to the type of adhesive and reinforcing patch material, the geometrical parameters are the most important elements for efficient composite repair and

joining. The geometrical parameters can be divided into three categories: in-plane configurations, through-the-thickness scarfing, and out-of-plane curvatures.

5. Many in-plane configurations have been examined. It has been found that an angle between 60° and 90° with respect to the loading direction results in the greatest repair efficiency. This result can be used in designing an optimal bond line configuration. A complex bond line geometry gives both higher repair strength and sufficient bonding area.

6. Bonding configurations associated with the thickness direction are scarf joints. A smaller scarf angle has been verified to be more effective than a larger angle, though the difference is not very significant. Therefore, a butt-joint is recommended for thin-layer composite repair, because of their efficiency in preparation.

7. The effects of out-of-plane curvatures on the joining and repair efficiencies are also important factors, and should be incorporated into the repair design.

8. Through-the-thickness stitching has been verified to be very effective and efficient for repairing failure due to delamination in torsion.

With the complete information from the geometrical analysis, the adhesive study, the filler examination, and the reinforcing patch investigation, it is believed that the optimization of repair design for damaged composite structures can be achieved.

APPENDIX

TABLES

Table 5.1a Owens Corning Panels: Drilled Hole Survey with Fillers.

SPECIMEN ID	WIDTH (mm)	THICK (mm)	STRENGTH (MPa)	FLEX (mm)	FILLERS
1/4H-1	50.00	2.7	219.9	-	1/4" HOLE
1/4H-2	50.00		240.9	-	-
1/4R-1	50.69		485.89	13.88	RESIN IN HOLE
1/4R-2	49.89		540.29	16.18	-
1/4P-1	51.21		477.74	10.38	PLUG IN HOLE
1/4P-2	50.35		523.50	10.94	-
1/4P-3	51.81		471.41	11.14	-
1/4P-4	50.43		558.57	11.88	-
1/4P-5	51.40		529.62	12.62	-
1/4F-1	51.02		458.95	14.14	CHOPPED GLASS
1/4F-2	50.29		522.90	14.68	IN HOLE
1/4F-3	50.54		515.83	10.56	-
1/2H-1	50.00		204.40	-	1/2" HOLE
1/2H-2	50.00		200.0	-	-
1/2R-1	51.63		470.67	11.83	RESIN IN HOLE
1/2R-2	51.13		522.76	10.39	-
1/2P-1	51.19		568.77	11.19	PLUG IN HOLE
1/2P-2	51.30		473.69	9.97	-
1/2P-3	51.99		445.24	11.98	-
1/2F-1	51.19		400.35	10.76	CHOPPED GLASS
1/2F-2	51.75		458.04	11.22	IN HOLE
1/2F-3	51.81		532.18	11.08	-

Table 5.1b Owens Corning Panels: Drilled Hole Survey with Fillers.

SPECIMEN ID	WIDTH (mm)	THICK (mm)	STRENGTH (MPa)	FLEX (mm)	FILLERS
5/8H-1	50.00		174.6	-	5/8" HOLE
5/8H-2	50.00		165.8	-	-
5/8R-1	51.82		476.48	10.01	RESIN IN HOLE
5/8R-2	51.28		524.44	10.42	-
5/8P-1	50.92		538.25	9.57	PLUG IN HOLE
5/8P-2	51.32		468.30	11.67	-
5/8P-3	51.51		471.76	10.66	-
5/8P-4	50.73		536.61	11.32	-
5/8P-5	50.73		530.12	10.62	-
5/8F-1	51.63		481.43	10.57	CHOPPED GLASS
5/8F-2	51.81		435.34	10.13	IN HOLE
5/8F-3	51.14		622.22	9.53	-

Table 5.1c Owens Corning Panels: Drilled Hole Survey with Fillers.

SPECIMEN ID	WIDTH (mm)	THICK (mm)	STRENGTH (MPa)	FLEX (mm)	FILLERS
OCH1-1	49.74	3.11	116.40	13.5	1" HOLE
OCH1-2	50.17	2.99	114.90	13.0	NO FILLER
OCH1-3	49.53	3.06	119.00	13.1	
OCCP-1	51.39		472.28	16	STRAP JOINT
OCCP-2	50.05		364.21	16	IN 1" HOLE
OCCP-3	49.88		417.46	16	1-3= 1 PATCH
OCCP-4	51.52		462.18	17	2 PATCHES
OCCP-5	50.58		500.37	18	2 PATCHES
OCS-1	50.03	3.08	554.00	15	2 PATCHES
OCS-2	49.92	3.09	509.60	10	2 PATCHES
OCS-3	51.00	3.09	449.80	10	2 PATCHES
OCF-1-3	51,50	3.09	340,296	10.8	CHOPPED GLASS
OCCF-1	51.15		429.80	-	CHOPPED GLASS

Table 5.2 Owens Corning Panels: Impact Study-Specimen Repaired with Two Glass Patches Per Side.

SPECIMEN ID	WIDTH (mm)	THICK (mm)	STRENGTH (MPa)	ENERGY (Joules)	FLEX (mm)	HEIGHT (inches)	R
OCI-1	49.56	2.70	512.9	26.59	10.8	38.5	Y
OCI-2	51.43		414.6	26.65	10.8	38.5	Y
OCI-3	48.27		404.0	28.91	11.2	35	Y
OCI-4	48.39		456.8	28.58	11.6	35	Y
OCI-5	49.80		599.3	28.35	10.9	35	Y
OCI-6	51.68		517.3	29.59	10.7	37	Y
OCI-7	50.55		453.6	28.16	11.5	37	Y
OCI-8	52.28		418.5	27.12	10.6	37	Y
OCI-9	49.60		432.4	23.50	11.6	40	Y
OCI-10	49.17		505.6	25.46	10.7	40	Y
OCI-11	49.53		409.4	24.77	11.1	30	Y
OCI-12	48.22		362.1	25.34	11.3	30	Y
OCI-13	51.29		359.8	25.86	10.8	25	Y
OCI-14	48.98		437.8	23.32	11.3	20	Y
OCI-15	49.22		383.9	23.32	10.7	20	Y
OCI-16	48.75		440.8	11.90	9.9	12	Y
OC1R	52.18	2.78	208.8	5.49	15.1	8.25	N
OC2R	49.84	2.98	161.1	13.57	13.4	14.5	N
OC3R	49.66	2.95	161.2	21.15	12.2	21.25	N
OC4R	51.29	2.98	142.4	26.17	11.2	25	N
OC5R	51.00	2.95	150.6	25.77	12.3	27.5	N
OC6R	49.36	3.08	138.5	28.82	10.8	27.5	N
OC7R	50.40	3.06	137.4	26.53	11.0	27.5	N
OC25R	49.18	2.74	158.2	33.70	12.7	30.0	N

NOTE: R = REPAIRED EITHER YES (Y) OR NO (N).

Table 5.3 Excel 8610: Drilled Hole Survey.

SPECIMEN ID	WIDTH (mm)	THICK (mm)	STRENGTH (MPa)	HOLE SIZE (inches)	FILLERS
8610N-1	49.28	3.04	175.06	0	NONE
8610N-2	49.40		292.85	0	NONE
8610N-3	50.06		181.05	0	NONE
8610ND-1	50.40		320.75	0	NONE
8610ND-2	51.18		307.34	0	NONE
8610ND-3	49.99		309.42	0	NONE
8610ND-4	50.03		345.89	0	NONE
8610H1-1	50.64		86.06	1	CHOPPED GLASS
8610H4-1	49.25		178.72	3/4	FIBERS
8610H4-2	49.30		117.57	3/4	-
8610H4-3	49.73		212.05	3/4	-
8610H2-1	49.17		230.41	1/2	-
8610H2-2	50.17		242.32	1/2	-
8610H2-3	50.11		135.65	1/2	-

Table 5.4 Excel 8610: Impact Study For Equivalent Damage Hole Size.

SPECIMEN ID	WIDTH (mm)	THICK (mm)	STRENGTH (MPa)	HEIGHT (inches)	ENERGY (Joules)	REPAIR vs NO REPAIR	FLEX (mm)
8610-A	51.33	3.03	-	22.5	24.46	NR	
8610-B	51.20	3.00	-	20	21.86	NR	
8610-C	50.49	2.95	-	19	22.05	NR	
8610-D	51.89	3.08	-	18	20.88	NR	
8610-E	49.41	3.00	-	18	20.68	NR	
8610-F	50.73	3.82	347.78	28.5	31.12	R	13
8610-G	51.68	3.16	208.26	28.5	29.32	NR	
8610-H	52.47	3.22	209.27	25	19.49	NR	
8610-I	50.24	3.09	202.95	27	24.04	NR	
8610-J	53.75	3.64	330.05	22.5	15.17	R	14.5
8610-K	51.98	3.49	301.76	28.5	28.52	R	13.3
8610-L	52.18	3.64	356.47	34.5	34.20	R	13
8610-M	53.37	3.23	208.20	34.5	32.86	NR	
8610-N	53.08	3.84	385.90	28.5	32.38	R	13.5
8610-O	48.69	3.92	376.69	22.5	15.54	R	13.4
8610-P	50.86	3.12	188.48	30	34.39	NR	
8610-Q	51.39	2.96	181.54	29	31.20	NR	

Table 5.5 Excel 2415: Drilled Hole Survey with Fillers.

SPECIMEN ID	WIDTH (mm)	THICK (mm)	STRENGTH (MPa)	COMMENTS	FIBER DIRECTION
2415-EXCEL	50.0	2.70	384.3	NO DAMAGE	FILL
2415-31	48.93	2.88	353.3	NO REPAIR	FILL
2415-32	49.11	2.85	391.9	FLEX =24	FILL
2415-33	49.06	2.93	355.8		FILL
2415-34	48.99	2.70	401.5		FILL
2415-35	49.08	2.95	351.6		FILL
2415-36	48.98	2.95	364.7		FILL
2415-7	49.03	2.87	278.3	1/2" HOLE	WARP
2415-8	49.02	2.84	307.6	NO REPAIR	WARP
2415-9	49.04	2.80	373.0	FLEX=18mm	WARP
2415-10	48.69	2.79	405.0		WARP
2415-11	49.02	2.85	315.5		WARP
2415-12	48.84	2.92	353.1		WARP
2415-13	49.02	2.92	280.4	3/4" HOLE	WARP
2415-14	49.06	2.87	268.1	NO REPAIR	WARP
2415-15	49.04	2.78	275.3	FLEX=15mm	WARP
2415-16	48.97	2.94	259.8		WARP
2415-17	49.03	2.81	307.9		WARP
2415-18	49.00	2.92	303.7		WARP
2415-19	49.08	2.90	205.9	1" HOLE	WARP
2415-20	48.97	2.87	227.7	NO REPAIR	WARP
2415-21	49.04	2.92	159.9	FLEX=13mm	FILL
2415-22	48.99	2.70	181.6		FILL
2415-23	48.97	2.87	233.7		WARP
2415-24	49.12	2.88	211.6		WARP
2415-25	48.98	2.81	195.8	1 1/4" HOLE	WARP
2415-26	49.02	2.83	168.3	NO REPAIR	WARP
2415-27	48.92	2.87	161.9	FLEX=13	WARP
2415-28	48.99	2.84	157.0		WARP
2415-29	49.07	2.73	158.6		FILL
2415-30	48.93	2.84	169.4		WARP

Table 5.6 Excel 2415: Impact Study-Warp Direction.

SPECIMEN ID	HEIGHT (inches)	TOTAL ENERGY Ft-lbs,Joules	WIDTH (mm)	THICK (mm)	STRENGTH (MPa)	REPAIR/ NO REPAIR
2415-E	40.5	25.49,34.56	51.62		364.55	R
2415-F	40.5	25.49,34.56	51.77	2.79	361.82	NR
2415-G	34.5	22.65,30.71	52.12		504.89	R
2415-H	28.5	23.81,32.29	51.91	2.79	311.01	NR
2415-I	22.5	15.55,21.09	53.94		529.44	R
2415-J	34.5	24.1,32.68	51.89	2.62	381.08	NR
2415-K	28.5	23.87,32.37	53.87		444.93	R
2415-L	22.5	13.15,17.83	52.73	2.74	356.11	NR
2415-M	25	16.32,22.13	53.92		573.14	R
2415-N	26	15.45,20.95	53.06		502.66	R
2415-O	27	22.99,31.17	52.79	2.71	341.81	NR
2415-P	27	22.39,30.36	54.55		416.01	R
2415-S	22.5	12.21,16.56	51.86	2.79	367.18	NR

Table 5.7a Owens Corning Panels: Butt-Joint Study.

SPECIMEN ID	WIDTH (mm)	THICK (mm)	STRENGTH (MPa)	GAP (mm)	GAP FILL	LAYERS TOP, BOTTOM
B-10-NG	51.84	2.70	332.5	0	-	2,2
B-11-ROL	50.90		307.2	9.66	ROLL	2,2
B-12-RES	51.66		289.8	8.50	RESIN	2,2
B-13-NG	50.90		302.9	0	-	2,2
B-14-ROL	51.14		304.7	9.02	ROLL	2,2
B-15-RES	51.10		281.1	8.00	RESIN	2,2
B-16-NG	52.46		297.0	0	-	2,2
B-17-ROL	52.22		286.7	9.12	ROLL	2,2
B-18-RES	51.46		187.9	6.08	RESIN	2,2
B-19-NG	51.24		360.1	0	-	2,3
B-20-ROL	51.66		274.9	9.00	ROLL	2,2
B-21-RES	51.24		252.3	4.94	RESIN	2,2
B-22-NG	51.06		280.0	0	-	2,2
B-23-ROL	51.30		325.2	9.20	ROLL	2,3
B-24-RES	52.86		254.0	3.20	RESIN	2,2
B-25-NG	50.70		298.6	0	-	2,3
B-1	48.95		266.3	0	-	2,2
B-2	50.45		222.1	0	-	2,2
B-3	49.22		235.4	0	-	2,2
B-4	50.44		243.1	0	-	2,2
B-5	50.30		269.6	0	-	2,2
B-6	49.18		256.4	0	-	2,2

GAP MATERIAL: ROL = ROLLED GLASS PATCH IN GAP, RES = PURE RESIN IN GAP
NG = NO GAP

Table 5.7b Owens Corning Panels: Butt-Joint Study.

SPECIMEN ID	WIDTH (mm)	THICK (mm)	STRENGTH (MPa)	GAP (mm)	GAP FILL	LAYERS TOP, BOTTOM
B-1-B	49.62		121.2	0	-	2,1
B-2-B	48.92		131.0	0	-	2,1
B-3-B	49.26		132.4	0	-	2,1
B-4-B	49.26		208.6	0	-	2,2
B-5-B	49.44		184.4	0	-	2,2
B-6-B	49.26		206.4	0	-	2,2
B-7-B	49.52		220.9	0	-	2,3
B-8-B	49.14		262.0	0	-	2,3
B-9-B	49.92		267.9	0	-	2,3
B-1-T	48.95		196.4	0	-	2,3
B-2-T	50.43		206.5	0	-	2,3
B-3-T	49.25		455.3	0	-	2,4
B-4-T	50.40		353.6	0	-	2,4

GAP MATERIAL: ROL = ROLLED GLASS PATCH IN GAP, RES = PURE RESIN IN GAP
NG = NO GAP

Table 5.8 Excel 8610: Butt-Joint Layer Study.

SPECIMEN ID	WIDTH (mm)	THICK (mm)	YIELD STRENGTH (KN)	ULTIMATE STRENGTH (MPa)	FLEX (mm)	PATCH LAYERS TOP,BOTTOM
86B-21	46.67	3.13	738.3	242.3	6.3	2,2
86B-22	47.16	2.90	896.6	339.2	7.2	2,2
86B-23	47.15	3.13	920.8	299.1	6.3	2,2
86B-31	46.68	3.11	1141	379.2	7.8	2,3
86B-32	48.27	2.99	1184	411.7	8.5	2,3
86B-33	47.07	2.98	1219	437.6	8.1	2,3
86B-41	47.72	3.16	1621	510.4	9.6	2,4
86B-42	47.82	3.07	1310	436.1	8.8	2,4
86B-43	50.60	2.98	1417	473.1	11.1	2,4
86B-51	51.29	2.95	1621	544.9	12.3	2,5
86B-52	50.63	2.95	1863	634.4	13.3	2,5
86B-53	50.20	3.06	1796	573.3	9.1	2,5

NOTE: ALL FAILURE MODES WERE CATASTROPHIC

Table 5.9 Excel 2415: Butt-Joint Layer Study.

SPECIMEN ID	WIDTH (mm)	THICK (mm)	STRENGTH (MPa)	FLEX (mm)	COMMENTS	PATCHES
24B2-1	52.64	2.81	197.65	8.4	WARP	2
24B2-2	51.99		166.76	8.6	DIRECTION	2
24B2-3	53.45		196.54	7.7	RS-RESIN	2
24B3-1	52.05		197.92	11.8	WARP	3
24B3-2	52.31		264.20	10.3	DIRECTION	3
24B3-3	52.15		302.16	9.1	RS-RESIN	3
24B4-1	53.58		481.48	9.9	WARP	4
24B4-2	53.49		429.02	10.6	DIRECTION	4
24B4-3	51.37		443.76	8.5	RS-RESIN	4
24B5-1	51.04		463.75	9.1	WARP	5
24B5-2	49.18		522.62	9.9	DIRECTION	5
24B5-3	51.81		484.29	8.9	RS-RESIN	5
24BF3-1	49.0		369.47	10.0	FILL	3
24BF3-2	48.31		369.47	9.2	DIRECTION	3
24BF3-3	48.83		403.12	10.0	RS-RESIN	3

Table 5.10a Owens Corning Panels: Scarf-Joint Survey, Two Reinforcing Patches Per Side.

SPECIMEN ID	SCARF (degree)	FILLERS IN GAP	LOADING TOP,BOT	STRENGTH (MPa)	FLEX (mm)	WIDTH (mm)
S5-1	5	ROLLED	T	307.2	10.2	49.55
S5-2	5	GLASS	T	335.9	12.3	49.68
S5-3	5	PATCH	T	289.0	11.6	49.50
S5-4	5		B	347.0	16.9	48.70
S5-5	5		B	272.0	12.4	48.29
S5-6	5		B	202.2	7.5	49.41
S5-7	5		T	289.5	10.3	50.82
S5-8	5		T	270.7	11.3	50.44
S5-9	5		T	221.0	12	49.94
S5-10	5		T	223.0	12	50.08
S5-11	5		B	155.7	6.88	50.59
S5-12	5		B	256.4	10	50.12
S5-13	5		B	271.8	9.7	49.79
S5-14	5		B	252.0	10.4	51.84
S10-1	10		B	355.8	11	49.27
S10-2	10		B	320.5	10.9	49.47
S10-3	10		B	309.4	10.7	50.95
S10-4	10		T	324.9	11.3	50.59
S10-5	10		T	326.0	11.6	49.17
S10-6	10		T	310.5	10	50.07
S10-7	10		T	316.0	9.8	51.56
S10-8	10		T	265.2	11	50.19
S10-9	10		T	275.0	11.5	50.29
S10-10	10		T	270.0	-	49.83
S10-11	10		B	306.1	10.3	50.52
S10-12	10		B	320.5	9.3	50.41
S10-13	10		B	275.2	9.9	49.59
S10-14	10		B	291.7	10	53.22

Table 5.10b Owens Corning Panels: Scarf-Joint Survey, Two Reinforcing Patches Per Side.

SPECIMEN ID	SCARF (degree)	FILLERS IN GAP	LOADING TOP,BOT	STRENGTH (MPa)	FLEX (mm)	WIDTH (mm)
S15-1	15		T	190.0	5.6	48.12
S15-2	15		B	242.0	8	49.77
S15-3	15		T	249.7	8	49.28
S15-4	15		B	268.5	9	48.84
S15-5	15		T	261.9	8.3	50.07
S15-6	15		B	110.5	7.5	49.07
SS15-8	15		B	263.3	-	51.47
SS15-7	15		T	209.9	-	51.82
SS15-6	15		B	150.1	-	51.89
SS15-5	15		T	209.8	-	51.09
SS15-4	15	CHOPPED	B	246.3	-	51.20
SS15-3	15	GLASS	T	248.6	-	50.85
SS15-2	15	FIBERS	B	175.9	-	51.62
SS15-1	15	IN GAP	T	198.8	-	51.95

FOR SPECIMEN SS15-1,2,5,6...ONLY 1 LAYER OF PATCH IS USED ON THE BOTTOM SIDE.
THE SPECIMEN THICKNESS USED FOR THIS IS 2.70 mm.

Table 5.11a Owens Corning Panels: Scarf-Hole Survey.

SPECIMEN ID	WIDTH (mm)	THICK (mm)	STRENGTH (MPa)	FLEX (mm)	SCARF (degree)	REPAIR
OCSJ0-1	101.13	2.70	273.44	20	0	NO
OCSJ0-2	98.32		301.05	18	0	NO
OCSJ0-3	98.06		300.49	17	0	NO
OCSJR-1	98.94		589.56	13	0	YES
OCSJR-2	98.43		562.31	13	0	YES
OCSJR-3	102.84		532.29	14	0	YES
OCSSJ-1	100.54		144.18	19	5	NO
OCSSJ-2	100.39		133.13	27	5	NO
OCSSJ-3	101.42		125.95	21	5	NO
OCSSJR-1	98.00		525.89	14	5	YES
OCSSJR-2	101.54		486.83	14	5	YES
OCSSJR-3	99.75		557.07	13	5	YES

Table 5.11b Owens Corning Panels: Scarf-Hole Survey.

SPECIMEN ID	WIDTH (mm)	THICK (mm)	STRENGTH (MPa)	FLEX (mm)	SCARF (degree)	REPAIR
OCDSJ-1	101.42		140.31	20	5	NO
OCDSJ-2	101.89		143.07	17	5	NO
OCDSJ-3	101.23		160.74	18	5	NO
OCDSJR-1	101.39		441.30	13	5	YES
OCDSJR-2	99.93		527.88	13	5	YES
OCDSJR-3	99.60		569.56	14	5	YES
OCREF-1	100.99		311.54	20.2	0	NO
OCREF-2	100.83		329.77	21.5	0	NO
OCREF-3	100.71		333.64	19.8	0	NO

Table 5.12a Owens Corning Panels: Joint Geometry Study.

SPECIMEN ID	WIDTH (mm)	THICK (mm)	STRENGTH (MPa)	COMMENTS
JG0-1	52.37	2.70	314.39	
JG0-2	52.19		217.02	
JG0-3	51.77		292.42	
JG30-1	51.86		405.89	
JG30-2	50.57		330.79	
JG30-3	52.07		399.91	
JG45-1	52.62		528.16	
JG45-2	50.77		484.28	
JG45-3	53.09		530.77	
JG60-1	52.74		685.14	
JG60-2	51.43		608.06	
JG60-3	51.58		439.18	
JG90-1	51.66		541.17	
JG90-2	51.61		648.75	
JG90-3	50.24		564.17	
JGV-1	51.37		575.43	
JGV-2	50.83		645.93	
JGV-3	50.68		547.28	
JGU-1	52.81		725.04	
JGU-2	50.64		738.64	
JGU-3	51.53		669.07	
JGW-1	51.28		614.14	
JGW-2	52.20		587.44	
JGW-3	52.01		517.35	
JGUU-1	49.68		611.69	
JGUU-2	52.46		690.91	
JGUU-3	51.76		708.75	
JGWW-1	51.94		558.47	
JGWW-2	52.78		588.31	
JGWW-3	49.64		650.01	

STUDY INCLUDES: V,U JOINT CONFIGURATIONS CUT OVER A 2"x 2" AREA.

Table 5.12b Owens Corning Panels: Joint Geometry Study.

SPECIMEN ID	WIDTH (mm)	THICK (mm)	STRENGTH (MPa)	COMMENTS
OCS-1	51.44	3.00	358.40	S-JOINT
OCS-2	51.68	3.02	417.00	0-DEGREES
OCS-3	51.14	3.02	423.00	
OCS-4	50.62	2.89	427.60	S-JOINT
OCS-5	50.46	3.10	352.10	45-DEGREES
0CS-6	51.25	3.06	313.90	
OCS-7	98.62	3.06	285.30	S-JOINT
OCS-8	99.18	3.06	268.50	90-DEGREES
OCS-9	99.26	3.06	260.10	

STUDY INCLUDES: V,U JOINT CONFIGURATIONS CUT OVER A 2"x 2" AREA.

Table 5.13a Excel 8610: Joint Geometry Study.

SPECIMEN ID	WIDTH (mm)	THICK (mm)	STRENGTH (MPa)	FLEX (mm)	FAILURE MODE
86JG0-1	51.52	3.04	307.0	5.9	CATASTROPHIC
86JG0-2	51.57		283.0	-	-
86JG0-3	50.68		314.7	-	-
86JG30-1	51.38		331.7	6.6	-
86JG30-2	51.72		407.7	6.6	-
86JG30-3	52.76		433.5	8.2	-
86JG45-1	52.92		396.9	9	-
86JG45-2	51.33		407.6	8.8	-
86JG45-3	52.79		399.5	8.5	-
86JG60-1	53.20		484.8	11	NON-CATASTROPHIC
86JG60-2	52.05		483.9	10	-
86JG60-3	51.40		474.0	14	-
86JG90-1	52.79		541.4	13.3	-
86JG90-2	49.64		558.3	13.5	-
86JG90-3	51.15		562.2	13	-

Table 5.13b Excel 8610: Joint Geometry Study.

SPECIMEN ID	WIDTH (mm)	THICK (mm)	STRENGTH (MPa)	FLEX (mm)	FAILURE MODE
86JGV-1	52.08		513.6	10	CATASTROPHIC
86JGV-2	50.58		505.7	10.7	-
86JGV-3	52.38		490.0	10.9	-
86JGU-1	53.91		441.4	10.2	NON-CATASTROPHIC
86JGU-2	51.63		409.3	11.5	-
86JGU-3	52.24		396.1	11	-
86JGW-1	51.95		418.5	10.5	-
86JGW-2	52.23		509.7	11	-
86JGW-3	52.97		483.7	10.8	-
86JGUU-1	53.93		548.7	11	-
86JGUU-2	52.59		551.0	11.5	-
86JGUU-3	52.81		491.8	12	-
86JGWW-1	51.73		497.8	10.5	-
86JGWW-2	50.96		533.5	11	-
86JGWW-3	51.35		501.5	10.3	-

Table 5.14a Excel 2415: Joint Geometry Study-Warp Direction.

SPECIMEN ID	WIDTH (mm)	THICK (mm)	STRENGTH (MPa)	FLEX (mm)	COMMENTS
24JG90-1	50.95	2.81	716.96	13	
24JG90-2	48.12		707.96	16	
24JG90-3	48.39		654.61	13	PLOT
24JG60-1	51.66		613.00	12	CRACK STARTS
24JG60-2	51.58		604.12	15	ALONG SEAM AND
24JG60-3	51.54		592.68	15	THEN TO PATCH
24JG45-1	51.63		411.72	8.1	
24JG45-2	52.4		429.20	8.5	
24JG45-3	51.86		455.28	9.2	PLOT
24JG30-1	53.31		363.51	5.6	
24JG30-2	51.86		309.75	5.6	
24JG30-3	49.02		396.37	6.6	
24JG0-1	52.64		197.65		
24JG0-2	49.09		281.53		
24JG0-3	53.45		196.54		
24JGV-1	49.73		609.13	10.5	
24JGV-2	52.62		585.39	13	
24JGV-3	50.67		564.62	12.3	
24JGU-1	51.98		597.49	12.4	NOT AS
24JGU-2	51.96		594.84	12.8	CATASTROPHIC
24JGU-3	51.57		507.24	13	FAILED ON EDGE
24JGW-1	51.89		619.07	10.4	CATASTROPHIC
24JGW-2	52.65		612.15	16.8	
24JGW-3	52.13		597.63	12	PLOT

Table 5.14b Excel 2415: Joint Geometry Study-Warp Direction.

SPECIMEN ID	WIDTH (mm)	THICK (mm)	STRENGTH (MPa)	FLEX (mm)	COMMENTS
24JGUU-1	51.05		473.52	14.3	FAILED ON EDGE
24JGUU-2	51.30		493.25	12.5	FAILED ON EDGE
24JGUU-3	52.78		605.03	13	NO EDGE FAILURE
24JGWW-1	51.07		574.18	16	
24JGWW-2	51.23		553.47	13.2	
24JGWW-3	50.64		558.95	14.6	PLOT
24WS-1	48.92	2.70	587.30	13.3	S-JOINT
24WS-2	48.38		515.20	11.8	0-DEGREES
24WS-3	48.23		529.10	12.5	
24WS-4	48.36		450.30	11.0	S-JOINT
24WS-5	49.55		418.30	13.0	45-DEGREES
24WS-6	49.41		374.60	15.6	

Table 5.15a Excel 2415: Depth-Of-Joint Survey.

SPECIMEN ID	WIDTH (mm)	THICK (mm)	STRENGTH (MPa)	V-AREA (mm)	V-ANGLE (degree)
24JGV4-1	51.80	2.81	577.97	100 x 50	76
24JGV4-2	50.83		664.19	-	-
24JGV4-3	50.68		589.66	-	-
24JGV3-1	51.26		528.28	75 x 50	71.6
24JGV3-2	52.71		469.24	-	-
24JGV3-3	51.58		541.80	-	-
24JGV2-1	50.22		547.36	50 x 50	63
24JGV2-2	49.31		477.83	-	-
24JGV2-3	49.14		488.80	-	-
24JGV1-1 24V1-1	51.16 51.11		456.54 306.34	25 x 50 SCARFED	45 EDGE
24JGV1-2 24V1-2	51.58 51.82		363.84 284.40	- SCARFED	- EDGE
24JGV1-3 24J1-3	51.89 52.19		280.10 298.04	- SCARFED	- EDGE

Table 5.15b Excel 2415: Depth-Of-Joint Survey.

SPECIMEN ID	WIDTH (mm)	THICK (mm)	STRENGTH (MPa)	V-AREA (mm)	V-ANGLE (degree)
24JGW2-1	49.48		532.85	50 x 50	76
24JGW2-2	49.08		458.24	-	-
24JGW2-3	48.95		519.88	-	-
24JGW1-1	52.00		460.93	25 x 50	71.6
24JGW1-2	51.96		514.29	-	-
24JGW1-3	51.75		496.67	-	-

Table 5.16a Excel 2415: Fiber Orientation Study.

SPECIMEN ID	WIDTH (mm)	THICK (mm)	STRENGTH (MPa)	FLEX (mm)	REPAIRED STRENGTH (MPa)
2490-1 2490R-1	49.11 51.16	2.76	343.5	19 9.5	 325.47
2490-2 2490R-2	49.18 49.25	2.81	334.0	19 8.7	 305.45
2490-3 2490R-3	49.06 49.64	2.95	337.8	17 7.5	 271.25
2460-1 2460R-1	49.54 50.72	2.75	272	26.8 18	 293.96
2460-2 2460R-2	49.47 50.33	2.74	288.5	27 12	 288.80
2460-3 2460R-3	50.97 51.62	2.78	271.0	28.7 12	 261.43
2445-1 2445R-1	47.58 49.78	2.90	294.9	33 10.5	 288.57
2445-2 2445R-2	51.24 51.16	2.85	259.4	33 12	 313.97
2445-3 2445R-3	46.68 48.00	2.85	278.3	33 27.6	 337.76
2430-1 2430R-1	47.72 48.88	2.85	340.8	23.8 23	 395.56
2430-2 2430R-2	50.31 51.65	2.90	356.0	24 25.4	 350.43
2430-3 2430R-3	49.56 51.10	2.84	368.8	26 18	 321.43

Table 5.16b Excel 2415: Fiber Orientation Study.

SPECIMEN ID	WIDTH (mm)	THICK (mm)	STRENGTH (MPa)	FLEX (mm)	REPAIRED STRENGTH (MPa)
240-1 240R-1	49.08 50.93	2.73	442.7	19 8.5	 324.64
240-2 240R-2	49.06 50.66	2.87	439.6	19.4 8.6	 281.79
240-3 240R-3	49.06 51.16	2.81	444.0	18 8.0	 279.12
24REF0-1	50.96	2.67	434.6	17.3	
24REF0-2	51.11	2.75	420.0	16.5	
24RF90-1	49.11	2.75	370.0	20	
24RF90-2	49.07	2.80	369.6	21	

Table 5.17 Excel 2415: Bending Fracture Layer Study.

SPECIMEN ID	WIDTH (mm)	THICK (mm)	STRENGTH (MPa)	FLEX (mm)	COMMENTS
24WRP3- 24WRP3-1	49.12 49.21	2.69	471.5 546.5	18.5 8.2	- CATASTROPHIC FAILURE
24WRP3-2 24WP3-2	49.06 49.22	2.73	473.5 556.7	18.9 9.4	- CATASTROPHIC FAILURE
24WRP3-3 24WP3-3	48.99 49.11	2.75	455.6 446.8	19.0 8.0	- CATASTROPHIC FAILURE
24WRP4-1 24WP4-1	51.58 51.60	2.87	442.8 555.3	18.6 8.1	- CATASTROPHIC FAILURE
24WRP4-2 24WP4-2	51.35 51.49	2.80	437.2 585.8	18.4 9.5	- CATASTROPHIC FAILURE
24WRP4-3 24WP4-3	51.20 51.43	2.80	443.7 619.2	19.7 10.3	- CATASTROPHIC FAILURE
24WRP5-1 24WP5-1	49.40 49.61	2.78	432.7 800.7	18.1 12.5	- CATASTROPHIC FAILURE
24WRP5-2 24WP5-2	51.40 51.14	2.78	406.8 626.8	17.4 8.9	- CATASTROPHIC FAILURE
24WRP5-3 24WP5-3	49.39 50.33	2.73	439.8 693.2	18.3 7.7	- CATASTROPHIC FAILURE

Table 5.18 Excel 8610: Bending Fracture Layer Study.

SPECIMEN ID	WIDTH (mm)	THICK (mm)	YIELD STRENGTH (KN)	ULTIMATE STRENGTH (MPa)	FLEX (mm)	PATCH LAYERS TOP,BOTTOM
86-21 86-21R	50.92 50.99	3.16	974.5 977.2	287.6 288.0	18.9 -	2,2
86-22 86-22R	51.18 51.28	3.06	894.0 950.3	279.9 296.9	19.1 -	2,2
86-23 86-23R	51.3551. 67	3.04	945.0 920.8	298.8 289.3	19.3 8.2	2,2
86-31 86-31R	49.25 49.27	3.18	1012 1272	304.9 383.0	18.2 9.4	2,3
86-32 86-32R	49.59 49.86	3.14	966.4 1538	296.6 469.4	17.5 8.2	2,3
86-33 86-33R	50.06 50.01	3.06	845.6 1855	270.7 594.4	16.8 10.3	2,3
86-41 86-41R	48.79 49.83	3.03	485.9 1557	162.8 510.6	17.5 9.5	2,4
86-42 86-42R	49.22 49.16	3.08	547.7 1592	176.0 512.2	17.6 9.8	2.4
86-43 86-43R	49.28 49.55	3.21	979.9 1399	289.5 411.1	17.3 8.3	2,4
86-51 86-51R	49.12 49.98	3.00	808.1 1635	274.3 545.4	20.0 10.6	2,5
86-52 86-52R	49.22 49.50	3.18	1001 2046	301.7 613.3	18.9 9.2	2,5
86-53 86-53R	49.22 50.11	3.13	902.0 1546	280.7 472.5	17.6 7.7	2,5

Table 5.19 No Damage/Two Patch Layers Per Side Evaluation to Determine the Influence of the Glass Patches on Non-Separated Specimen.

SPECIMEN ID	WIDTH (mm)	THICK (mm)	YIELD STRENGTH (KN)	ULTIMATE STRENGTH (MPa)	FLEX (mm)	AVERAGE STRENGTH (MPa)	% FROM NO DAMAGE
OCL-1	51.13	2.98	1560	515.5	11.9	476.12	64
OCL-2	50.95	2.99	1393	458.9	11.6		INCREASE
OCL-3	51.34	2.97	1278	423.4	13.1		OWENS
OCL-4	50.53	2.94	1369	470.3	12.6		CORNING
OCL-5	51.96	2.98	1576	512.5	12.5		
24W-1	49.04	2.7	1777	745.8	14.5	675.04	41
24W-2	50.39	2.69	1541	634.1	14.1		INCREASE
24W-3	49.22	2.7	1388	580.4	14.6		EXCEL
24W-4	48.94	2.73	1592	654.9	13.9		2415-WARP
24W-5	49.11	2.76	1895	760.0	15.2		
24F-1	49.19	2.79	1385	542.7	14.8	523.98	40
24F-2	49.51	2.84	1230	462.1	14.2		INCREASE
24F-3	50.66	2.76	1243	483.3	14.8		EXCEL
24F-4	49.44	2.89	1442	524.0	13.8		2415-FILL
24F-5	49.18	2.89	1664	607.8	14.3		
86-1	49.14	3.14	1530	473.8	14.0	457.10	52
86-2	49.30	3.17	1546	468.2	15.2		INCREASE
86-3	49.59	3.22	1474	430.1	14.1		EXCEL
86-4	50.07	3.12	1458	448.8	15.6		8610
86-5	49.88	3.17	1552	464.6	13.8		

Table 6.1 Three-Point Bending of Adhesive Coupons

SPECIMEN ID	WIDTH (mm)	THICK (mm)	MAX. STRESS (MPa)	MAX. LOAD (MPa)	FLEX (mm)	COMMENTS
3M-1	14.54	8.48	62.79	.8752	3	3M-EPOXY
3M-2	11.78	8.55	71.33	.8188	-	
3M-3	11.91	8.39	65.10	.7275	3.3	
RS-1	12.40	6.33	127.7	.8456	2.3	RESIN SERVICES
RS-2	11.95	6.36	121.2	.7812	2	EPOXY
RS-3	13.23	6.51	103.8	.7758	-	
205-1	12.96	8.06	137.6	1.544	3.5	TCC-205-EPOXY
205-2	11.95	7.96	137.5	1.388	3.3	
205-3	14.66	7.60	142.2	1.605	3.8	
F-1	12.78	9.58	48.76	.7624	2.3	FUSOR-EPOXY
F-2	12.96	9.51	62.54	.9772	2.2	
F-3	13.97	8.85	67.73	.9879	2.1	
M-1	12.80	6.84	120.1	.9584	3	MARASET-EPOXY
M-2	12.87	6.92	90.51	.7436	2.3	
M-3	13.93	6.78	101.0	.8617	4.2	
DOW-1	12.14	6.03	40.60	.2389	1.2	DOW-VINYLESTER
DOW-2	12.19	5.90	35.13	.1987	.95	
DOW-3	14.07	6.03	37.79	.2577	.97	
072-1	12.77	6.00	38.98	.2389	1.04	TCC-072-EPOXY
072-2	12.09	5.90	38.28	.2148	.75	
072-3	14.18	5.95	56.16	.3758	1.07	

Table 6.2 Owens Corning Panels: Adhesive Study.

SPECIMEN ID	WIDTH (mm)	THICK (mm)	STRENGTH (MPa)	FLEX (mm)	COMMENTS
FUSOR-1	50.57	2.70	163.85	7.0	HIGH
FUSOR-2	50.76		148.00	8.8	VISCOSITY
FUSOR-3	49.36		161.16	6.4	STRUCTURAL
FUSOR-4	50.69		211.40	5.2	ADHESIVE
FUSOR-5	52.26		216.67	6.0	WITH GAPS
3M-1	52.92		165.99	8.4	HIGH
3M-2	51.13		97.23	7.5	VISCOSITY
3M-3	51.54		227.20	7.8	STRUCTURAL
3M-4	53.89		266.51	7.4	ADHESIVE
3M-5	56.00		156.86	8.0	WITH GAPS
RS-1	49.63		320.56	7.2	LOW
RS-2	52.65		284.32	5.5	VISCOSITY
RS-3	50.34		288.57	6.5	EPOXY
RS-4	49.58		278.51	5.6	
RS-5	49.87		320.09	7.6	
TCC205-1	51.89		272.50	4.9	LOW
TCC205-2	50.80		324.03	5.0	VISCOSITY
TCC205-3	51.75		312.76	6.3	EPOXY
TCC205-4	50.82		279.33	5.9	
TCC205-5	51.71		259.60	4.8	
TCC076-1	50.46		198.14	4.5	LOW
TCC076-2	50.06		171.03	5.0	VISCOSITY
TCC076-3	49.37		177.92	7.2	POLYESTER
TCC076-4	49.17		169.65	6.3	
TCC076-5	49.58		166.00	4.8	
MARASET-1	49.16		207.85	10.1	MEDIUM
MARASET-2	49.89		289.03	7.4	VISCOSITY
MARASET-3	49.74		265.41	7.2	EPOXY
MARASET-4	48.52		250.56	7.2	
MARASET-5	50.15		245.65	6.2	

NOTE: FUSOR AND 3M ARE THICKSOTROPIC AND CREATE A NON-UNIFORM BONDLINE DURING THE REPAIR PROCEDURE. VOIDS AT THE BONDLINE REDUCED THE OVERALL STRENGTH OF THE REPAIR BY A NEGLIGABLE AMOUNT.

Table 6.3 Owens Corning Panels: Impact Adhesive Study.

SPECIMEN ID	WIDTH (mm)	THICK (mm)	STRENGTH (MPa)	FLEX (mm)	ENERGY (Joules)
OC-4	49.89	2.70	169.39	14.5	24.33
OC-5	49.09		160.21	14.6	26.81
OC-6	48.81		171.24	17.0	26.18
OC-1F	51.48		212.44	19.8	27.83
OC-2F	52.80		244.81	20.5	28.61
OC-3F	51.76		219.83	16.3	27.26
OC-73M	52.88		200.55	16	24.72
OC-83M	53.26		193.94	17.7	25.51
OC-93M	53.54		204.26	18.4	23.13
OC-10M	49.47		213.29	16.2	27.24
OC-11M	51.73		249.87	16	27.54
OC-12M	50.19		242.13	15.2	25.91
OC-13RS	53.79		210.51	15.8	26.24
OC-14RS	51.20		193.10	15.5	27.04
OC-15RS	51.54		177.90	18.9	26.60
OC-16T2	51.25		191.87	14.5	23.93
OC-17T2	51.89		205.44	16.3	26.82
OC-18T2	50.41		221.35	14.6	25.34
OC-19T0	53.16		195.35	16.2	27.27
OC-20T0	50.43		185.12	16.1	24.26
OC-21T0	52.04		200.62	17.3	24.53
OC-22D1	50.01		181.16	16.4	24.92
OC-23D2	51.18		179.15	21.8	23.16
OC-24D3	51.23		194.07	15.8	23.07

NOTE: F = FUSOR, M = MARASET, RS = RESIN SERVICES,
T2 = TCC205, T0 = TCC067, D = DOW DERAKANE.

Table 6.4a Cumulative Tension Testing Data

SPECIMEN ID	WIDTH (mm)	THICKNESS (mm)	MAX. STRESS (MPa)	MAX. LOAD (KN)	COMMENTS
OCTEN1			119.2	18.66	NO REPAIR
OCTEN2			143.0	22.04	
OCBJ-10	50.50	3.02	87.82	13.39	BUTT-JOINT
OCBJ-11	49.98	3.07	77.38	11.87	
OCBJ-14	50.30	3.09	81.80	12.71	
OCBJ-15	50.86	3.00	73.49	11.21	
OCSJ-9	52.45	3.02	68.39	10.83	S-JOINT
OCSJ-11	51.53	3.00	82.82	12.80	
OCSJ-14	52.23	3.07	77.79	12.47	
OCSJ-16	51.81	2.98	73.99	11.42	
86TEN1			142.5	22.40	NO REPAIR
86TEN2			176.4	27.84	
86BJ-6	53.00	3.02	72.87	11.66	BUTT-JOINT
86BJ-7	52.43	3.04	75.18	11.98	
86BJ-17	51.39	2.97	82.84	12.64	
86BJ-18	50.85	3.00	67.27	10.26	
86SJ-6	53.49	3.09	61.61	10.18	S-JOINT
86SJ-8	53.39	3.08	85.71	14.09	
86SJ-17	53.37	3.04	69.11	11.21	
86SJ-18	53.40	3.04	73.75	11.97	

Table 6.4b Cumulative Tension Testing Data

SPECIMEN ID	WIDTH (mm)	THICKNESS (mm)	MAX. STRESS (MPa)	MAX. LOAD (KN)	COMMENTS
24FTEN1			244.5	35.49	NO REPAIR
24FBJ-6	48.76	2.81	91.76	12.57	BUTT-JOINT
24FBJ-7	49.21	2.84	83.74	11.70	
24FBJ-17	51.04	2.81	99.66	14.29	
24FBJ-18	52.03	2.89	74.77	11.24	
24FSJ-1	50.78	2.89	70.98	10.40	S-JOINT
24FSJ-16	53.00	2.81	81.80	12.18	
24FSJ-17	53.25	2.84	80.03	12.10	
24FSJ-18	53.86	2.84	70.37	10.75	
24WTEN1			177.6	24.39	NO REPAIR
24WBJ-7	49.55	2.67	77.19	10.21	BUTT-JOINT
24WBJ-11	49.18	2.64	107.2	13.92	
24WBJ-12	49.55	2.69	90.50	12.06	
24WBJ-15	51.39	2.93	79.12	11.91	
24WSJ-6	53.20	2.55	91.21	12.37	S-JOINT
24WSJ-7	51.54	2.61	71.94	9.68	
24WSJ-8	48.23	2.60	89.18	11.18	
24WSJ-12	50.58	2.76	84.48	11.79	

Table 6.5a Out-Of-Plane Curvature Study on Rockwell SMC.

SPECIMEN ID	WIDTH (mm)	THICK (mm)	MAX. LOAD (KN)	MAX. σ (MPa)	COMMENTS
R-1 RR-1	51.56	2.54	174.5 902.0	78.71 406.8	FLAT PANEL-NO REPAIR REPAIRED W/BOND LINE PRESSURE
R-2 RR-2	50.95	2.51	327.5 1077	153.1 503.4	FLEX AT FAILURE OF SPECIMEN WAS OVER 1"
R-3 RR-3	51.79	2.64	416.1 1275	173 530	" " " "
R-4 RR-4	51.25	2.43	343.6 1066	170.4 528.5	FLAT PANEL-NO REPAIR REPAIRED W/O BOND LINE PRESSURE
R-5 RR-5	51.58	2.41	349 1034	174.8 517.9	" " " "
R-6 RR-6	50.66	2.40	319.5 1195	164.3 614.4	" " " "
R1-1 RR1-1	57.68	2.47	1248 1256	532.1 535.5	CURVATURE #1-NO REPAIR REPAIRED
R1-2 RR1-2	60.73	2.62	1128 1154	406 415.3	" " " "
R2-1 RR2-1	68.05	2.64	942.3 1468	298.1 464.4	CURVATURE #2-NO REPAIR REPAIRED
R2-2 RR2-2	72.13	2.51	1146 1565	378.4 516.7	" " " "
R3-1 RR3-1	56.48	2.70	614.8 1195	224 435.5	CURVATURE #3-NO REPAIR REPAIRED
R3-2 RR3-2	59.46	2.70	601.3 923.5	208.1 319.1	" " " "

Table 6.5b Out-Of-Plane Curvature Study on Rockwell SMC.

SPECIMEN ID	WIDTH (mm)	THICK (mm)	MAX. LOAD (KN)	MAX. σ (MPa)	COMMENTS
R4-1 RR4-1					CURVATURE #4-NO REPAIR REPAIRED
R4-2 RR4-2	60.97	2.90	730.2 706	213.7 206.6	
R4-4 RR4-4	54.36	2.56	350.3 1187	350.3 499.9	
R5-1 RR5-1	54.96	3.03	303.4 1501	90.22 446.3	CURVATURE #5-NO REPAIR REPAIRED
R5-2 RR5-2	54.16	3.18	263.1 1071	72.08 293.4	
R5-3 RR5-3	49.78	2.98	217.5 848.3	76.36 297.8	
R6-1 RR6-1	52.15	2.81	153 542.3	55.75 197.6	CURVATURE #6-NO REPAIR REPAIR
R6-2 RR6-2	51.63	3.00	131.6 477.9	42.49 154.3	
R6-3 RR6-3	51.67	3.06	174.5 426.9	54.11 132.4	

Table 7.1a OWENS CORNING: TORSIONAL TESTING RESULTS, STANDARD REPAIR
REFERENCE DIMENSIONS: THICKNESS=0.122in, $W_{1,2,3}$= 1.41,1.39,1.46
REPAIRED DIMENSIONS: THICKNESS=0.142, $W_{1,2,3}$= 1.42,1.39,1.40
SPECIMEN ID: OCND-B, OCNB-BR: REFERENCE,REPAIRED RESPECTIVELY

ROTATION (°)	REFERENCE TORQUE (in-lbs)	REPAIRED TORQUE (in-lbs)	COMMENTS
5	45	48	FAILURE BEGAN BY CRACKING
7.5	65	66	ALONG THE SIDES OF THE
10	81	84	SPECIMEN. THE CRACKS
12.5	93	100	THEN PROPAGATED ACROSS
15	102	115	THE SPECIMEN SIDES. THE
16	107	119	FAILURE MODE WAS SEVERE
17	109	125	THROUGH-THE-THICKNESS
18	113	128	DELAMINATION. ALSO, THE
19	107	130	REPAIRED SPECIMEN FAILED
20	105	133	IN THE SAME ZONE AS THE
21	106	132	REFERENCE SPECIMEN.
22	108	134	
23	107	129	
24	98	121	
25	95	95	
26	89	89	
27	72	76	
28	63	78	
29	55	71	
30	51	66	
31	50	66	
32	46	67	
33	45	64	
34	40	64	
35	38	62	
40	26	55	
44	19	52	
48	12	51	
50	11	47	

Table 7.1b OWENS CORNING: TORSIONAL TESTING RESULTS, STANDARD REPAIR
REFERENCE DIMENSIONS: THICKNESS=0.118in, $W_{1,2,3}$= 1.39,1.37,1.40
REPAIRED DIMENSIONS: THICKNESS=0.147, $W_{1,2,3}$= 1.41,1.41,1.38
SPECIMEN ID: OCND-C, OCNB-CR: REFERENCE,REPAIRED RESPECTIVELY

ROTATION (°)	REFERENCE TORQUE (in-lbs)	REPAIRED TORQUE (in-lbs)	COMMENTS
5	37	41	FAILURE BEGAN BY CRACKING
7.5	55	58	ALONG THE SIDES OF THE
10	71	72	SPECIMEN. THE CRACKS
12.5	84	87	THEN PROPAGATED ACROSS
15	94	99	THE SPECIMEN SIDES. THE
16	98	102	FAILURE MODE WAS SEVERE
17	103	109	THROUGH-THE-THICKNESS
18	105	113	DELAMINATION. ALSO, THE
19	107	118	REPAIRED SPECIMEN FAILED
20	110	121	IN THE SAME ZONE AS THE
21	111	112	REFERENCE SPECIMEN.
22	113	101	
23	117	96	
24	122	102	
25	124	107	
26	127	112	
27	134	115	
28	132	116	
29	134	105	
30	138	102	
31	138	93	
32	134	96	
33	131	89	
34	129	83	
35	127	83	
40	84	72	
44	69	59	
48	50	49	
50	46	44	

Table 7.1c EXCEL 8610: TORSIONAL TESTING RESULTS, STANDARD REPAIR
REFERENCE DIMENSIONS: THICKNESS=0.115in, $W_{1,2,3}$= 1.37,1.35,1.41
REPAIRED DIMENSIONS: THICKNESS=0.138, $W_{1,2,3}$= 1.36,1.35,1.35
SPECIMEN ID: 86ND-A, 86ND-AR: REFERENCE,REPAIRED RESPECTIVELY

ROTATION (°)	REFERENCE TORQUE (in-lbs)	REPAIRED TORQUE (in-lbs)	COMMENTS
5	38	41	FAILURE BEGAN BY CRACKING
7.5	56	59	ALONG THE SIDES OF THE
10	74	74	SPECIMEN. THE CRACKS
12.5	92	91	THEN PROPAGATED ACROSS
15	111	105	THE SPECIMEN SIDES. THE
16	119	109	FAILURE MODE WAS SEVERE
17	126	115	THROUGH-THE-THICKNESS
18	134	118	DELAMINATION. ALSO, THE
19	141	119	REPAIRED SPECIMEN FAILED
20	149	115	IN THE SAME ZONE AS THE
21	158	87	REFERENCE SPECIMEN.
22	167	70	
23	175	66	
24	182	71	
25	190	71	
26	195	64	
27	202	63	
28	203	56	
29	206	50	
30	192	47	
31	137	47	
32	122	42	
33	116	42	
34	100	42	
35	82	37	
40	27	35	
44	17	34	
48	14	29	
50	12	28	

Table 7.1d EXCEL 8610: TORSIONAL TESTING RESULTS, STANDARD REPAIR
REFERENCE DIMENSIONS: THICKNESS=0.123in, $W_{1,2,3}$= 1.35,1.31,1.33
REPAIRED DIMENSIONS: THICKNESS=0.153, $W_{1,2,3}$= 1.33,1.31,1.34
SPECIMEN ID: 86ND-B, 86ND-BR: REFERENCE,REPAIRED RESPECTIVELY

ROTATION (°)	REFERENCE TORQUE (in-lbs)	REPAIRED TORQUE (in-lbs)	COMMENTS
5	39	53	FAILURE BEGAN BY CRACKING
7.5	58	76	ALONG THE SIDES OF THE
10	77	94	SPECIMEN. THE CRACKS
12.5	97	111	THEN PROPAGATED ACROSS
15	116	81	THE SPECIMEN SIDES. THE
16	123	86	FAILURE MODE WAS SEVERE
17	132	93	THROUGH-THE-THICKNESS
18	140	98	DELAMINATION. ALSO, THE
19	148	98	REPAIRED SPECIMEN FAILED
20	156	98	IN THE SAME ZONE AS THE
21	164	93	REFERENCE SPECIMEN.
22	174	89	
23	182	71	
24	190	71	
25	198	59	
26	207	57	
27	217	57	
28	225	56	
29	234	52	
30	243	51	
31	251	51	
32	258	53	
33	161	49	
34	153	49	
35	152	48	
40	36	44	
44	26	42	
48	23	38	
50	21	38	

Table 7.1e EXCEL 2415-FILL: TORSIONAL TESTING RESULTS, STANDARD REPAIR
REFERENCE DIMENSIONS: THICKNESS=0.114in, $W_{1,2,3}$= 1.33,1.28,1.36
REPAIRED DIMENSIONS: THICKNESS=0.146, $W_{1,2,3}$= 1.31,1.30,1.31
SPECIMEN ID: 24FND-A, 24FND-AR: REFERENCE,REPAIRED RESPECTIVELY

ROTATION (°)	REFERENCE TORQUE (in-lbs)	REPAIRED TORQUE (in-lbs)	COMMENTS
5	27	34	FAILURE BEGAN BY CRACKING
7.5	40	46	ALONG THE SIDES OF THE
10	51	59	SPECIMEN. THE CRACKS
12.5	60	71	THEN PROPAGATED ACROSS
15	74	80	THE SPECIMEN SIDES. THE
16	80	83	FAILURE MODE WAS SEVERE
17	84	87	THROUGH-THE-THICKNESS
18	89	90	DELAMINATION. ALSO, THE
19	95	93	REPAIRED SPECIMEN FAILED
20	98	96	IN THE SAME ZONE AS THE
21	102	92	REFERENCE SPECIMEN.
22	108	99	
23	112	102	
24	117	104	
25	120	107	
26	119	108	
27	125	106	
28	128	107	
29	133	107	
30	137	102	
31	139	102	
32	137	102	
33	141	105	
34	145	104	
35	150	106	
36	153	92	
37	155	88	
40	109	86	
50	53	60	

Table 7.1f EXCEL 2415-FILL: TORSIONAL TESTING RESULTS, STANDARD REPAIR
REFERENCE DIMENSIONS: THICKNESS=0.113in, $W_{1,2,3}$= 1.34,1.31,1.33
REPAIRED DIMENSIONS: THICKNESS=0.136, $W_{1,2,3}$= 1.35,1.32,1.33
SPECIMEN ID: 24FND-B, 24FND-BR: REFERENCE,REPAIRED RESPECTIVELY

ROTATION (°)	REFERENCE TORQUE (in-lbs)	REPAIRED TORQUE (in-lbs)	COMMENTS
5	26	33	FAILURE BEGAN BY CRACKING
7.5	38	47	ALONG THE SIDES OF THE
10	50	59	SPECIMEN. THE CRACKS
12.5	62	69	THEN PROPAGATED ACROSS
15	73	78	THE SPECIMEN SIDES. THE
16	78	82	FAILURE MODE WAS SEVERE
17	83	86	THROUGH-THE-THICKNESS
18	87	90	DELAMINATION. ALSO, THE
19	93	91	REPAIRED SPECIMEN FAILED
20	97	94	IN THE SAME ZONE AS THE
21	102	96	REFERENCE SPECIMEN.
22	108	98	
23	114	99	
24	120	98	
25	125	99	
26	131	82	
27	138	77	
28	143	56	
29	147	55	
30	148	57	
31	153	53	
32	161	53	
33	165	52	
34	173	52	
35	178	50	
36	183	49	
37	163	48	
40	107	47	
50	18	45	

Table 7.1g EXCEL 2415-WARP: TORSIONAL TESTING RESULTS, STANDARD REPAIR
REFERENCE DIMENSIONS: THICKNESS=0.108in, $W_{1,2,3}$= 1.40,1.39,1.38
REPAIRED DIMENSIONS: THICKNESS=0.143, $W_{1,2,3}$= 1.43,1.42,1.42
SPECIMEN ID: 24WND-A, 24WND-AR: REFERENCE,REPAIRED RESPECTIVELY

ROTATION (°)	REFERENCE TORQUE (in-lbs)	REPAIRED TORQUE (in-lbs)	COMMENTS
5	29	38	FAILURE BEGAN BY CRACKING
7.5	43	50	ALONG THE SIDES OF THE
10	56	64	SPECIMEN. THE CRACKS
12.5	68	77	THEN PROPAGATED ACROSS
15	87	90	THE SPECIMEN SIDES. THE
16	93	95	FAILURE MODE WAS SEVERE
17	101	100	THROUGH-THE-THICKNESS
18	108	106	DELAMINATION. ALSO, THE
19	115	109	REPAIRED SPECIMEN FAILED
20	121	115	IN THE SAME ZONE AS THE
21	129	118	REFERENCE SPECIMEN.
22	137	123	
23	144	126	
24	153	109	
25	162	109	
26	167	109	
27	177	113	
28	185	109	
29	193	107	
30	198	105	
31	195	92	
32	202	81	
33	212	78	
34	220	75	
35	226	69	
36	190	68	
37	173	68	
40	128	64	
50	50	37	

Table 7.1h EXCEL 2415-WARP: TORSIONAL TESTING RESULTS, STANDARD REPAIR
REFERENCE DIMENSIONS: THICKNESS=0.108in, $W_{1,2,3}$= 1.35,1.31,1.30
REPAIRED DIMENSIONS: THICKNESS=0.130, $W_{1,2,3}$= 1.41,1.39,1.38
SPECIMEN ID: 24WND-B, 24WND-BR: REFERENCE,REPAIRED RESPECTIVELY

ROTATION (°)	REFERENCE TORQUE (in-lbs)	REPAIRED TORQUE (in-lbs)	COMMENTS
5	31	29	FAILURE BEGAN BY CRACKING
7.5	44	43	ALONG THE SIDES OF THE
10	56	56	SPECIMEN. THE CRACKS
12.5	69	68	THEN PROPAGATED ACROSS
15	80	87	THE SPECIMEN SIDES. THE
16	85	93	FAILURE MODE WAS SEVERE
17	90	101	THROUGH-THE-THICKNESS
18	95	108	DELAMINATION. ALSO, THE
19	100	115	REPAIRED SPECIMEN FAILED
20	105	121	IN THE SAME ZONE AS THE
21	105	129	REFERENCE SPECIMEN.
22	106	137	
23	109	144	
24	114	153	
25	114	162	
26	118	167	
27	122	177	
28	122	185	
29	124	193	
30	125	198	
31	127	195	
32	123	202	
33	72	212	
34	63	220	
35	62	226	
36	59	190	
37	59	173	
40	56	128	
50	43	50	

Table 7.2a OWENS CORNING-BUTT JOINT: TORSIONAL TESTING RESULTS, STANDARD REPAIR REPAIRED DIMENSIONS: THICKNESS=0.120, W_1=2.00,THICKNESS=0.121, W_1= 2.00 SPECIMEN ID: OCBJ-12, OCBJ-13: REPAIRED

ROTATION (°)	OCBJ-12 TORQUE (in-lbs)	OCBJ-13 TORQUE (in-lbs)	COMMENTS
5	56	53	FAILURE BEGAN BY RIPPING
7.5	105	80	OF THE PATCH ALONG THE
10	105	97	EDGE OF THE BOND LINE.
12.5	130	130	THEN PROPAGATED ACROSS
15	130	135	THE SPECIMEN. THE
16	131	138	FAILURE MODE WAS DUE TO
17	132	141	PATCH FAILURE, THOUGH
18	133	142	UTILIZATION OF A LARGE
19	133	143	AMOUNT OF PATCH AREA
20	134	144	BEFORE FAILURE OCCURED.
21	139	95	
22	128	98	
23	117	99	
24	114	94	
25	102	90	
26	106	92	
27	106	95	
28	112	92	
29	111	87	
30	106	90	
31	111	60	
32	116	52	
33	115	47	
34	96	44	
35	87	36	
36	60	34	
37	54	30	
40	47	26	
50	23	14	

Table 7.2b

OWENS CORNING-S-JOINT: TORSIONAL TESTING RESULTS, STANDARD REPAIR REPAIRED DIMENSIONS: THICKNESS=0.137, W_1= 2.15,THICKNESS=0.146, W_1= 2.09 SPECIMEN ID: OCSJ-10, OCSJ-13: REPAIRED

ROTATION (°)	OCSJ-10 TORQUE (in-lbs)	OCSJ-13 TORQUE (in-lbs)	COMMENTS
5	50	60	FAILURE BEGAN BY RIPPING
7.5	75	100	OF THE PATCH ALONG THE
10	98	112	EDGE OF THE BOND LINE.
12.5	125	160	THEN PROPAGATED ACROSS
15	148	167	THE SPECIMEN. THE
16	150	170	FAILURE MODE WAS DUE TO
17	170	188	PATCH FAILURE, THOUGH
18	176	188	UTILIZATION OF A LARGE
19	184	189	AMOUNT OF PATCH AREA
20	205	189	BEFORE FAILURE OCCURED.
21	190	193	EXCLUSIVELY FOR THE
22	166	202	S-JOINT: GOOD USE OF THE
23	155	209	BOND LINE LENGTH, AND A
24	161	216	LOT OF PATCH DELAMINATION
25	164	159	
26	169	160	
27	167	159	
28	152	162	
29	146	165	
30	136	164	
31	133	113	
32	125	82	
33	110	72	
34	25	61	
35	23	58	
36	22	49	
37	17	43	
40	7	41	
50	0	26	

Table 7.2c EXCEL 8610 BUTT-JOINT: TORSIONAL TESTING RESULTS, STANDARD REPAIR REPAIRED DIMENSIONS: THICKNESS=0.152, W_1= 2.06,THICKNESS=0.142, W_1= 2.00 SPECIMEN ID: 86BJ-13, 86BJ-16: REPAIRED

ROTATION (°)	86BJ-13 TORQUE (in-lbs)	86BJ-16 TORQUE (in-lbs)	COMMENTS
5	55	45	FAILURE BEGAN BY RIPPING
7.5	76	60	OF THE PATCH ALONG THE
10	105	88	EDGE OF THE BOND LINE.
12.5	130	108	THEN PROPAGATED ACROSS
15	147	134	THE SPECIMEN. THE
16	150	134	FAILURE MODE WAS DUE TO
17	160	144	PATCH FAILURE, THOUGH
18	170	152	UTILIZATION OF A LARGE
19	140	159	AMOUNT OF PATCH AREA
20	114	158	BEFORE FAILURE OCCURED.
21	112	162	
22	112	133	
23	105	132	
24	100	105	
25	104	89	
26	89	86	
27	85	89	
28	86	90	
29	64	77	
30	42	70	
31	38	50	
32	36	40	
33	34	40	
34	36	40	
35	29	31	
36	19	31	
37	17	25	
40	15	25	
50	6	10	

Table 7.2d EXCEL 8610 S-JOINT: TORSIONAL TESTING RESULTS, STANDARD REPAIR REPAIRED DIMENSIONS: THICKNESS=0.144, W_1= 2.12,THICKNESS=0.142, W_1= 1.98 SPECIMEN ID: 86SJ-9, 86SJ-16: REPAIRED

ROTATION (°)	86SJ-9 TORQUE (in-lbs)	86SJ-16 TORQUE (in-lbs)	COMMENTS
5	54	35	FAILURE BEGAN BY RIPPING
7.5	100	60	OF THE PATCH ALONG THE
10	108	68	EDGE OF THE BOND LINE.
12.5	135	86	THEN PROPAGATED ACROSS
15	163	107	THE SPECIMEN. THE
16	169	111	FAILURE MODE WAS DUE TO
17	176	121	PATCH FAILURE, THOUGH
18	184	130	UTILIZATION OF A LARGE
19	153	138	AMOUNT OF PATCH AREA
20	161	148	BEFORE FAILURE OCCURED.
21	154	159	
22	158	168	
23	148	172	
24	148	180	
25	50	163	
26	49	162	
27	48	173	
28	48	181	
29	40	185	
30	40	173	
31	38	170	
32	35	164	
33	35	164	
34	30	130	
35	26	124	
36	24	124	
37	24	104	
40	17	94	
50	8	40	

Table 7.2e EXCEL 2415-FILL BUTT-JOINT: TORSIONAL TESTING RESULTS, STANDARD REPAIR REPAIRED DIMENSIONS: THICKNESS=0.134, W_1=2.00,THICKNESS=0.137, W_1= 2.00 SPECIMEN ID: 24FBJ-15, 24FBJ-16: REPAIRED

ROTATION (°)	24FBJ-15 TORQUE (in-lbs)	24FBJ-16 TORQUE (in-lbs)	COMMENTS
5	54	36	FAILURE BEGAN BY RIPPING
7.5	60	50	OF THE PATCH ALONG THE
10	65	69	EDGE OF THE BOND LINE.
12.5	80	87	THEN PROPAGATED ACROSS
15	99	107	THE SPECIMEN. THE
16	108	114	FAILURE MODE WAS DUE TO
17	115	122	PATCH FAILURE, THOUGH
18	123	131	UTILIZATION OF A LARGE
19	132	139	AMOUNT OF PATCH AREA
20	135	149	BEFORE FAILURE OCCURED.
21	130	160	
22	135	166	
23	133	104	
24	104	40	
25	94	17	
26	78	-	
27	70	-	
28	67	-	
29	66	-	
30	34	8	
31	30	0	
32	27	0	
33	26	0	
34	20	0	
35	15	0	
36	10	0	
37	9	0	
40	8	0	
50	3	0	

Table 7.2f EXCEL 2415-FILL S-JOINT: TORSIONAL TESTING RESULTS, STANDARD REPAIR REPAIRED DIMENSIONS: THICKNESS=0.134, W_1= 2.07,THICKNESS=0.129, W_1= 2.02 SPECIMEN ID: 24FSJ-11, 24FSJ-15: REPAIRED

ROTATION (°)	24FSJ-11 TORQUE (in-lbs)	24FSJ-15 TORQUE (in-lbs)	COMMENTS
5	36	33	FAILURE BEGAN BY RIPPING
7.5	70	60	OF THE PATCH ALONG THE
10	71	67	EDGE OF THE BOND LINE.
12.5	89	86	THEN PROPAGATED ACROSS
15	110	106	THE SPECIMEN. THE
16	118	114	FAILURE MODE WAS DUE TO
17	127	122	PATCH FAILURE, THOUGH
18	136	130	UTILIZATION OF A LARGE
19	145	140	AMOUNT OF PATCH AREA
20	147	148	BEFORE FAILURE OCCURED.
21	151	153	
22	161	133	
23	172	139	
24	138	138	
25	145	146	
26	151	154	
27	158	162	
28	167	168	
29	124	164	
30	128	168	
31	132	171	
32	100	172	
33	98	178	
34	40	118	
35	39	115	
36	38	119	
37	38	123	
40	37	103	
50	35	25	

Table 7.2g EXCEL 2415-WARP BUTT-JOINT: TORSIONAL TESTING RESULTS, STANDARD REPAIR REPAIRED DIMENSIONS: THICKNESS=0.129, W_1=1.94,THICKNESS=0.141, W_1= 1.94 SPECIMEN ID: 24WBJ-13, 24WBJ-14: REPAIRED

ROTATION (°)	24WBJ-13 TORQUE (in-lbs)	24WBJ-14 TORQUE (in-lbs)	COMMENTS
5	30	37	FAILURE BEGAN BY RIPPING
7.5	40	60	OF THE PATCH ALONG THE
10	59	69	EDGE OF THE BOND LINE.
12.5	75	86	THEN PROPAGATED ACROSS
15	89	104	THE SPECIMEN. THE
16	100	115	FAILURE MODE WAS DUE TO
17	106	123	PATCH FAILURE, THOUGH
18	108	125	UTILIZATION OF A LARGE
19	115	140	AMOUNT OF PATCH AREA
20	123	142	BEFORE FAILURE OCCURED.
21	130	148	
22	137	157	
23	144	162	
24	150	150	
25	156	150	
26	158	121	
27	128	120	
28	115	123	
29	99	90	
30	71	76	
31	70	71	
32	66	40	
33	61	38	
34	47	32	
35	38	27	
36	30	26	
37	27	24	
40	18	22	
50	8	14	

Tab

Table 7.2h EXCEL 2415-WARP S-JOINT: TORSIONAL TESTING RESULTS, STANDARD REPAIR REPAIRED DIMENSIONS: THICKNESS=0.132, W_1= 2.00,THICKNESS=0.131, W_1= 2.00 SPECIMEN ID: 24WSJ-13, 24WSJ-14: REPAIRED

ROTATION (°)	24WSJ-13 TORQUE (in-lbs)	24WSJ-14 TORQUE (in-lbs)	COMMENTS
5	37	40	FAILURE BEGAN BY RIPPING
7.5	40	60	OF THE PATCH ALONG THE
10	71	78	EDGE OF THE BOND LINE.
12.5	90	86	THEN PROPAGATED ACROSS
15	105	118	THE SPECIMEN. THE
16	110	120	FAILURE MODE WAS DUE TO
17	126	142	PATCH FAILURE, THOUGH
18	120	145	UTILIZATION OF A LARGE
19	122	160	AMOUNT OF PATCH AREA
20	122	162	BEFORE FAILURE OCCURED.
21	121	134	
22	126	140	
23	133	146	
24	140	154	
25	149	128	
26	112	134	
27	99	141	
28	96	126	
29	100	115	
30	103	111	
31	102	106	
32	96	100	
33	95	97	
34	96	97	
35	93	96	
36	91	96	
37	91	99	
40	90	34	
50	12	21	

Table 7.3a OWENS CORNING: TORSIONAL REPAIR STUDY, STITCHING REPAIR
REFERENCE DIMENSIONS: THICKNESS = 0.120, $W_{1,2,3}$= 1.22,1.20,1.23
SPECIMEN ID: OCT-1, REPAIRED WITH (3X6) DENSITY NYLON THREAD

ROTATION (°)	REFERENCE TORQUE (in-lbs)	REPAIRED TORQUE (in-lbs)	COMMENTS
5	62	24	FAILURE BEGAN BY CRACKING
7.5	77	34	OF THE MATRIX ALONG THE
10	87	45	EDGE OF THE SPECIMEN.
12.5	92	53	THEN PROPAGATED ACROSS
15	94	60	THE SPECIMEN. THE
16	94	61	FAILURE MODE WAS DUE TO
17	97	66	SEVERE DELAMINATION OF
18	99	69	THE MATRIX. THE
19	102	73	REPAIRED SPECIMEN FAILED
20	104	75	IN THE SAME ZONE.
21	107	78	
22	109	79	STITCHING IS A CRITICAL
23	109	82	ALONG BOTH EDGES
24	110	84	
25	109	87	
26	109	84	
27	110	86	
28	111	89	
29	111	90	
30	111	86	
31	112	85	
32	112	79	
33	112	66	
34	112	62	
35	110	61	
36	102	62	
37	100	59	
40	95	58	
50	68	42	

Table 7.3b OWENS CORNING: TORSIONAL REPAIR STUDY, STITCHING REPAIR
REFERENCE DIMENSIONS: THICKNESS = 0.118, $W_{1,2,3}$= 1.21,1.20,1.26
SPECIMEN ID: OCT-2, REPAIRED WITH (4X7) DENSITY NYLON THREAD

ROTATION (°)	REFERENCE TORQUE (in-lbs)	REPAIRED TORQUE (in-lbs)	COMMENTS
5	34	22	FAILURE BEGAN BY CRACKING
7.5	49	32	OF THE MATRIX ALONG THE
10	61	40	EDGE OF THE SPECIMEN.
12.5	68	48	THEN PROPAGATED ACROSS
15	72	56	THE SPECIMEN. THE
16	75	57	FAILURE MODE WAS DUE TO
17	80	60	SEVERE DELAMINATION OF
18	84	63	THE MATRIX. THE
19	81	66	REPAIRED SPECIMEN FAILED
20	84	68	IN THE SAME ZONE.
21	89	71	
22	92	75	STITCHING IS CRITICAL
23	95	77	ALONG BOTH EDGES
24	97	79	
25	98	81	
26	102	82	
27	106	84	
28	106	84	
29	108	86	
30	108	84	
31	109	81	
32	105	82	
33	105	78	
34	90	75	
35	88	72	
36	86	67	
37	80	66	
40	71	56	
50	31	38	

Table 7.3c OWENS CORNING: TORSIONAL REPAIR STUDY, STITCHING REPAIR
REFERENCE DIMENSIONS: THICKNESS = 0.120, $W_{1,2,3}$= 1.24,1.20,1.24
SPECIMEN ID: OCT-3, REPAIRED WITH (2X4) DENSITY NYLON THREAD

ROTATION (°)	REFERENCE TORQUE (in-lbs)	REPAIRED TORQUE (in-lbs)	COMMENTS
5	34	29	FAILURE BEGAN BY CRACKING
7.5	48	40	OF THE MATRIX ALONG THE
10	60	49	EDGE OF THE SPECIMEN.
12.5	66	59	THEN PROPAGATED ACROSS
15	72	68	THE SPECIMEN. THE
16	74	70	FAILURE MODE WAS DUE TO
17	77	74	SEVERE DELAMINATION OF
18	79	76	THE MATRIX. THE
19	82	80	REPAIRED SPECIMEN FAILED
20	86	83	IN THE SAME ZONE.
21	87	86	
22	90	87	STITCHING IS CRITICAL
23	92	89	ALONG BOTH EDGES
24	93	89	
25	95	86	
26	94	88	
27	94	88	
28	90	89	
29	91	86	
30	91	89	
31	92	85	
32	93	87	
33	93	85	
34	93	86	
35	94	85	
36	89	85	
37	90	80	
40	83	72	
50	39	37	

Table 7.3d OWENS CORNING: TORSIONAL REPAIR STUDY, STITCHING REPAIR
REFERENCE DIMENSIONS: THICKNESS = 0.120, $W_{1,2,3}$= 1.14,1.12,1.12
SPECIMEN ID: OCT-4, REPAIRED WITH (3X6) DENSITY STEEL THREAD

ROTATION (°)	REFERENCE TORQUE (in-lbs)	REPAIRED TORQUE (in-lbs)	COMMENTS
5	31	27	FAILURE BEGAN BY CRACKING
7.5	45	36	OF THE MATRIX ALONG THE
10	56	45	EDGE OF THE SPECIMEN.
12.5	63	53	THEN PROPAGATED ACROSS
15	70	60	THE SPECIMEN. THE
16	70	60	FAILURE MODE WAS DUE TO
17	72	63	SEVERE DELAMINATION OF
18	73	66	THE MATRIX. THE
19	75	68	REPAIRED SPECIMEN FAILED
20	70	70	IN THE SAME ZONE.
21	72	71	
22	73	73	STITCHING IS CRITICAL
23	74	73	ALONG BOTH EDGES
24	75	76	
25	76	78	
26	77	78	
27	79	80	
28	79	82	
29	80	83	
30	81	84	
31	83	82	
32	84	78	
33	85	76	
34	84	76	
35	82	76	
36	78	76	
37	69	76	
40	65	71	
50	27	62	

Table 7.3e OWENS CORNING: TORSIONAL REPAIR STUDY, STITCHING REPAIR
REFERENCE DIMENSIONS: THICKNESS = 0.120, $W_{1,2,3}$= 1.20,1.19,1.20
SPECIMEN ID: OCT-6, REPAIRED WITH (4X7) DENSITY STEEL THREAD

ROTATION (°)	REFERENCE TORQUE (in-lbs)	REPAIRED TORQUE (in-lbs)	COMMENTS
5	35	28	FAILURE BEGAN BY CRACKING
7.5	51	40	OF THE MATRIX ALONG THE
10	64	50	EDGE OF THE SPECIMEN.
12.5	75	60	THEN PROPAGATED ACROSS
15	80	69	THE SPECIMEN. THE
16	82	71	FAILURE MODE WAS DUE TO
17	84	76	SEVERE DELAMINATION OF
18	85	78	THE MATRIX. THE
19	86	82	REPAIRED SPECIMEN FAILED
20	87	84	IN THE SAME ZONE.
21	86	86	
22	89	90	STITCHING IS CRITICAL
23	90	93	ALONG BOTH EDGES
24	91	96	
25	91	99	
26	89	100	
27	88	103	
28	87	104	
29	88	107	
30	85	109	
31	83	111	
32	83	114	
33	79	112	
34	77	115	
35	77	116	
36	77	118	
37	76	120	
40	74	121	
50	41	93	

Table 7.3f OWENS CORNING: TORSIONAL REPAIR STUDY, STITCHING REPAIR
REFERENCE DIMENSIONS: THICKNESS = 0.120, $W_{1,2,3}$ = 1.27,1.22,1.24
SPECIMEN ID: OCT-7, REPAIRED WITH (2X4) DENSITY STEEL THREAD

ROTATION (°)	REFERENCE TORQUE (in-lbs)	REPAIRED TORQUE (in-lbs)	COMMENTS
5	35	32	FAILURE BEGAN BY CRACKING
7.5	51	44	OF THE MATRIX ALONG THE
10	62	54	EDGE OF THE SPECIMEN.
12.5	68	63	THEN PROPAGATED ACROSS
15	72	73	THE SPECIMEN. THE
16	75	75	FAILURE MODE WAS DUE TO
17	76	79	SEVERE DELAMINATION OF
18	79	81	THE MATRIX. THE
19	82	84	REPAIRED SPECIMEN FAILED
20	86	86	IN THE SAME ZONE.
21	89	89	
22	91	91	STITCHING IS CRITICAL
23	94	93	ALONG BOTH EDGES
24	96	94	
25	98	96	
26	99	95	
27	101	96	
28	103	96	
29	106	97	
30	106	95	
31	104	78	
32	102	78	
33	103	75	
34	100	73	
35	99	73	
36	94	70	
37	83	70	
40	60	70	
50	45	69	

Table 7.3g OWENS CORNING: TORSIONAL REPAIR STUDY, STITCHING REPAIR
REFERENCE DIMENSIONS: THICKNESS = 0.120, $W_{1,2,3}$= 1.21,1.19,1.25
SPECIMEN ID: OCT-8, REPAIRED WITH 4/WIRE GRID STEEL STRANDS PER SIDE

ROTATION (°)	REFERENCE TORQUE (in-lbs)	REPAIRED TORQUE (in-lbs)	COMMENTS
5	34	21	FAILURE BEGAN BY CRACKING
7.5	49	30	OF THE MATRIX ALONG THE
10	60	38	EDGE OF THE SPECIMEN.
12.5	66	45	THEN PROPAGATED ACROSS
15	69	53	THE SPECIMEN. THE
16	71	54	FAILURE MODE WAS DUE TO
17	73	58	SEVERE DELAMINATION OF
18	75	60	THE MATRIX. THE
19	77	63	REPAIRED SPECIMEN FAILED
20	79	66	IN THE SAME ZONE.
21	81	69	
22	84	72	STITCHING IS CRITICAL
23	86	75	ALONG BOTH EDGES
24	88	76	
25	90	80	
26	92	80	
27	94	82	
28	96	84	
29	97	88	
30	98	88	
31	97	89	
32	96	86	
33	94	86	
34	91	85	
35	80	78	
36	68	75	
37	64	72	
40	56	62	
50	32	34	

Table 7.4 Cumulative S-Joint Results for Three-Point Bending Repair

SPECIMEN ID	WIDTH (mm)	THICK (mm)	MAX. STRESS (MPa)	MAX. LOAD (KN)	FLEX (mm)	COMMENTS
OCSJ-1	51.44	3.00	358.4	1.106		0-DEGREES
OCSJ-2	51.68	3.02	417.0	1.310		
OCSJ-3	51.14	3.02	423.0	1.315		
OCSJ-4	50.62	2.89	427.6	1.205	16	45-DEGREES
OCSJ-5	50.46	3.10	352.1	1.138	11	
OCSJ-6	51.25	3.06	313.9	1.004	10	
OCSJ-7	98.62	3.06	285.3	1.756	12	90-DEGREES
OCSJ-8	99.18	3.06	268.5	1.662	12	
OCSJ-9	99.26	3.06	260.1	1.611	13	
24FSJ-4	51.70	2.87	533.4	1.514	11	0-DEGREES
24FSJ-5	51.77	2.88	456.0	1.305	9.5	
86SJ-10	54.47	3.09	412.0	1.428	9.8	
86SJ-11	52.70	3.11	427.4	1.452	11	
86SJ-15	51.65	3.08	467.9	1.528	12	
24WSJ-1	48.92	2.70	587.3	1.396	13	
24WSJ-2	48.38	2.70	515.2	1.211	12	
24WSJ-3	48.23	2.70	529.1	1.240	12	
24WSJ-4	48.36	2.70	450.3	1.058	11	45-DEGREES
24WSJ-5	49.55	2.70	418.3	1.007	13	
24WSJ-6	49.41	2.70	374.6	.8993	16	

Table 7.5a Tension Layer Study for S-, Butt-, and WW-Joints

SPECIMEN ID	WIDTH[1] (mm)	THICK[1] (mm)	WIDTH[2] (mm)	THICK[2] (mm)	STRENGTH (MPa)	MAX LOAD (KN)	NOTE
OCBJL-1	51.37	2.90	52.43	4.39	160.5	24.40	4 PLY PER SIDE
OCBJL-2	50.66	3.04	50.68	3.73	73.88	11.38	2 PLY
OCBJL-3	51.38	3.06	51.58	3.53	76.11	12.01	
OCBJL-4	51.35	3.04	51.71	3.79	98.94	15.55	3 PLY
OCBJL-5	50.74	3.04	50.69	4.20	129.3	19.92	
OCBJL-6	51.32	3.09	52.29	4.06	104.4	16.87	GAP @ BOND LINE
OCBJL-7	50.69	3.06	51.56	4.08	129.2	20.38	4 PLY
OCBJL-8	51.56	3.03	51.84	4.57	157.4	24.72	
OCBJL-9	51.35	3.08	51.51	4.45	122.9	19.50	
OCSJL-15	50.88	2.94	52.65	3.64	75.99	11.76	2 PLY PER SIDE
OCSJL-18	50.58	2.92	51.76	3.41	80.08	12.10	
OCSJL-19	50.46	2.97	53.21	3.63	76.14	12.03	
OCSJL-1	51.47	3.07	52.29	3.77	87.86	14.10	
OCSJL-A	51.42	3.02	52.67	4.24	107.8	17.15	3 PLY
OCSJL-B	51.24	3.06	52.87	3.81	113.0	18.27	
OCSJND15	49.87	2.95	51.84	3.96	124.0	18.96	
OCSJL-7	51.52	3.04	52.32	4.64	135.3	21.52	4 PLY
OCSJL-8	51.94	3.04	53.73	4.26	114.4	18.68	
OCSJL-9	51.05	3.08	52.47	4.09	138.6	22.40	CAT. FAIL

NOTE: ALL BUTT-JOINTS AND WW-JOINTS EXIBITED CATASTROPHIC FAILURE, THE S-JOINTS WERE NON-CATSTROPHIC EXCEPT FOR SOME OF THE 4 PLY SPECIMEN

Table 7.5b Tension Layer Study for S-, Butt-, and WW-Joints

SPECIMEN ID	WIDTH[1] (mm)	THICK[1] (mm)	WIDTH[2] (mm)	THICK[2] (mm)	STRENGTH (MPa)	MAX LOAD (KN)	NOTE
OCWJL-2	50.27	3.02	51.05	3.84	115.9	22.71	2 PLY PER SIDE
OCWJL-3	51.53	3.06	52.60	3.59	128.1	20.62	
OCWJL-4	51.00	3.04	51.90	3.47	147.1	23.21	
OCWJL-5	50.87	3.04	51.96	4.27	146.3	23.10	3 PLY
OCWJL-6	51.06	3.09	52.60	4.40	192.8	31.33	
OCWJL-7	50.67	3.02	51.61	3.87	163	25.40	
OCWJL-8	51.44	3.06	52.22	4.08	211.1	33.73	4 PLY
OCWJL-9	51.06	3.06	52.62	4.48	226.4	36.44	

NOTE: ALL BUTT-JOINTS AND WW-JOINTS EXIBITED CATASTROPHIC FAILURE, THE S-JOINTS WERE NON-CATSTROPHIC EXCEPT FOR SOME OF THE 4 PLY SPECIMEN

Table 7.6a Comparison of All Materials for Each Testing Procedure. All of the Values in the Table are Average Values.

	OWENS CORNING		EXCEL 8610		EXCEL 2415 FILL-DIRECTION		EXCEL 2415 WARP-DIRECTION	
TESTING ID	MAX σ (MPa)	MAX Load (KN)	MAX σ (MPa)	MAX Load (KN)	MAX σ (MPa)	MAX Load (KN)	MAX σ (MPa)	MAX Load (KN)
TENSION								
NO DAMAGE	131.1	20.35	159.5	25.14	178	24.39	245	35.49
BUTT-JOINT	80.12	12.30	74.50	11.64	88.5	12.03	87.5	12.45
S-JOINT	75.75	11.88	72.5	11.86	84.2	11.26	75.8	11.36
COMPRESSION								
NO DAMAGE	-	24.83	-	27.4	-	28.93	-	32.49
BUTT-JOINT	-	25.81	-	24.9	-	23.14	-	23.32
S-JOINT	-	-	-	-	-	-	-	-
BUCKLING								
NO DAMAGE	54.40	7.83	53	7.80	52	74.05	69.2	9.39
BUTT-JOINT	87.42	13.26	121.5	20.5	98.4	12.94	99	12.37
S-JOINT	134.7	20.47	108.5	15.49	108	14.99	130.3	17.76
TORSION		TORQ in-lbs		TORQ in-lbs		TORQ in-lbs		TRQ in-#
NO DAMAGE	-	125.5	-	232	-	169	-	203.5
REPAIRED	-	127.5	-	115	-	103.5	-	124.5
BUTT-JOINT	-	141.5		164.5	-	150.5	-	160
S-JOINT		210.5		182	-	175	-	153.5

Table 7.6b Comparison of All Materials for Each Testing Procedure. All of the Values in the Table are Average Values.

	OWENS CORNING		EXCEL 8610		EXCEL 2415 FILL-DIRECTION		EXCEL 2415 WARP-DIRECTION	
TESTING ID	MAX σ (MPa)	MAX Load (KN)	MAX σ (MPa)	MAX Load (KN)	MAX σ (MPa)	MAX Load (KN)	MAX σ (MPa)	MAX Load (KN)
FATIGUE CYCLES								
NO DAMAGE								
100	278.6	0.671	299.1	1.001	362	1.494	484.1	1.272
1,000	232.2	0.695	302.7	1.032	377	0.976	501.3	1.356
10,000	247.9	0.751	293.7	1.002	372	1.003	531	1.408
BUTT-JOINT								
100	300.9	0.885	281.6	0.872	350	0.863	335	0.710
1,000	294.6	0.899	271	0.862	332	0.859	287.1	0.652
10,000	156.7	0.493	237.4	0.768	300	0.804	264	0.681
S-JOINT								
100	416.8	1.285	438.1	1.457	402	1.176	568	1.451
1,000	459.8	1.477	310.1	1.076	468	1.234	434	1.179
10,000	416.1	1.340	441.9	1.548	349	0.992	437	1.027

LIST OF REFERENCES

LIST OF REFERENCES

BOOKS

1. Engineered Materials Handbook, Vol. #1, Composites, ASM Inter., August 1989.

2. Composite Repairs, ed. Henry Brown, SAMPE Monograph, No. 1, 1985.

3. Baker, A.A. and Jones, R., Bonded Repair of Aircraft Structures, Martinus Nijhoff Publishers, 1988.

4. Bonding and Repair of Composites, ed. John Herriot, Butterworths, 1989.

5. "Joining of Composite Materials," Kedward, K.T., Ed., ASTM STP 749, PCN = 04-749000-33, April, 1980.

6. "Composites," The International Journal of the Science and Technology of Reinforced Materials, Butterworth-Heinemann, Vol. 22, No. 2, March 1991.

PAPERS

7. "Field-Level Repair Materials and Processes," Stone, Robert H., 28th Nat. SAMPE Symp., 1983.

8. "Repair of Damaged Composite Materials," Zimmerman, K., Liu, D., Proc. 1992 Joint ASM/ASC Inter. Conf. on Composites, with Japan, Orlando, FL, June 1992.

9. "Further Developments in the Design and Analysis of Adhesively-Bonded Structural Joints," Hart-Smith, L.J., Joining of Composite Materials, ASTM STP 749, K.T. Kedward, Ed., American Society for Testing and Materials, 1981, pp. 3-31.

10. "From 49-1 to HX1567-Development of a Low Energy Composite Repair System," Lee, F., Brinkerhoff, S., McKinney, S., Hexcel Corp., 35th Inter. SAMPE Symp., April, 1990.

11. "Repair Adhesives: Development Criteria for Field Level Repair," Cichon, M.J.,Hysol Aerospace Products, 34th Inter. SAMPE Symp., May, 1989.

12. "Rapid Low-Temperature Cure Patching System for Field Repair," Sivy, G.T., ITW Adhesive Systems, 34th Inter. SAMPE Symp., May, 1989.

13. "Composite Repair Concepts for Depot Level Use," Labor, James D., 26th Nat. SAMPE Symp., 1981.

14. " Field-Level Repair Materials and Processes," Stone, Robert H., 28th Nat. SAMPE Symp., April 12-14, 1983.

15. " Field Repairs For The AH-1 Composite Main Rotor Blade," Falcone, Alfred S., 28th Nat. SAMPE Symp., April 12-14, 1983.

16. " Repair Procedures For Composite Sinewave Substructure," Labor, James D., 16th Nat. SAMPE Tech. Conf., Oct. 9-11, 1984.

17. "Bolted Field Repair of Graphite/Epoxy Wing Skin Laminates," Bohlmann, R.E., Renieri, G.D., Libeskind, M., Joining of Composite Materials, ASTM STP 749, 1980.

18. " Acousto-Ultrasonic Evaluation of Impact-Damaged Graphite/Epoxy Composites," Green, James E., Rodgers, John, 27th Nat. SAMPE Symp., May 4-6, 1982.

19. "Nondestructive Testing of Composite Bonds," Cawley, P, Bonding and Repair of Composites, 1989.

20. "A Nondestructive Method of Evaluating Adhesive Bond Strength in Fiberglass Reinforced Plastic Assemblies," Chapmen II, G.B., Joining of Composite Materials, ASTM STP 749, 1980.

21. Effect of Manufacturing Defects and Service-Induced Damage on the Strength of Aircraft Composite Structures," Garrett, R.A., 28th Nat. SAMPE Symp. April 1983.

22. "A Review of Defect Types and Nondestructive Testing Techniques for Composites and Bonded Joints," Cawley, P., Adams, R.D., Bonding and Repair of Composites, 1989.

23. "The Study on the Composite-Patching Repairs for Metallic Aircraft Structures," Ong, C.L., Shen, S.B., Aeronautical Research Lab/AIDC, 36th Inter. SAMPE Symp., April 1991.

24. "The Competitive Position of Selected Composite Fabrication Technologies for Automotive Applications," Krolewski, S., Busch, J., IBIS Associates, Inc., 35th Inter. SAMPE Symp., April 1990.

25. "Adhesive-Bonded Composite-Patching Repair of Cracked Aircraft Structures," Ong., C.L., Shen. S., 34th Inter. SAMPE Symp., May 1989.

26. "Repairs to Damage Tolerant Aircraft," Swift, T., Federal Aviation Administration,

Inter. Symp. on Structural Integrity of Aging Airplanes, Atlanta GA, March 1990.

27. "Development of Repair Procedures for Graphite/Epoxy Structures on Commercial Transports," Stone, Robert H., 26th Nat. SAMPE Symp., April 28-30, 1981.

28. "Demonstration of Repairability and Repair Quality on Graphite/Epoxy Structural Subelements," Knauss, James F., Stone, Robert H., 27th Nat. SAMPE Symp., May 4-6, 1982.

29. "Repairing The Damage," Armstrong, K.B., Bonding and Repair of Composites, 1989.

30. "Analysis of the Joggle-Lap Joint for Automotive Applications," Givler, R.C., Pipes, R.B., Joining of Composite Materials, ASTM STP 749, 1980.

31. "Crack Patching: Design Aspects," Jones, R., Bonded Repair of Aircraft Structures, pgs 49-76, 1988.

32. "Theoretical Analysis of Crack Patching," Rose, L.R.F., Bonded Repair of Aircraft Structures, pgs 77-106, 1988.

33. "Crack Patching: Experimental Studies, Practical Applications," Baker, A.A., Bonded Repair of Aircraft Structures, pgs 107-174, 1988.

34. "High Performance Epoxy Adhesives," Behm, D.T., Clark, E., Ciba-Geigy Corp., 34th Inter. SAMPE Symp., May 1989.

35. "Damage Tolerance of Laminated Composites Containing A Hole and Subjected to Tension or Compression," Chang, F.K., Lessard, L., Chang, K.Y., Liu, S., 34th Inter. SAMPE Symp., May, 1989.

36. "Viscoelastic Relaxation in Bolted Thermoplastic Composite Joints," Schmitt, R.R., Boeing Military Airplanes, Horn, W.J., 35th Inter. SAMPE Symp., April 1990.

37. "Induction Heating Development for Aircraft Repair," Border, J., Salas, R., Black, M., PDA Engineering, 35th Inter. SAMPE Symp., April 1990.

38. "An Apparatus to Prepare Composites for Repair," Westerman, E.A., Roll, P.E., Boeing Advanced Systems, 34th Inter. SAMPE Symp., May 1989.

39. "The Repair of Thermoplastic Composites After Impact," Ong, C.L., Sheu, M.F., Liou, Y.Y., 34th Inter. SAMPE Symp., May 1989.

40. "Repair Technology for Thermoplastic Aircraft Structures (REPTAS),"

Heimerdinger, M.W., Northrop Corp., Aircraft Division, Hawthorn, CA 90250-3277.

41. "Analysis and Repair of Damaged Composite Laminates," Bair, D.L., Hudson, P.O., 36th Inter. SAMPE Symp., April 1991.

42. "Resin Requirements for Successful Repair of Delaminations," Russell, A.J., Bowers, C.P., Defense Research Establishment Pacific, 36th Inter. SAMPE Symp., April 1991.

43. "Tensile Strength of Stitching Joint in Woven Glass Fabrics," Lee C., Liu, D., ASME, May 1989.

44. "Impact Energy Absorption of Continuous Fiber Composite Tubes," Wickliffe, L.E., Schmueser, D.W., General Motors Research Lab, ASME Annual Meeting, Paper no. 85-WA/Mats-11, November 1985.

45. "Advanced Composite Repair--Recent Developments and Some Problems," Myhre, S.M., 26th Nat. SAMPE Symp., April 28-30, 1981.

46. " Constant Temperature Heaters For the Repair of Composite Structures," Walty, Robert J., 30th Nat. SAMPE Symp., March 19-21, 1985.

47. " Elevated Temperature Repairs of Advanced Composite Structures," Roberts, Larry, 30th Nat. SAMPE Symp., March 19-21, 1985.

48. " Improved Resins For Wet Layup Repair of Advanced Composite Structure," Scott, James R., Mashiba, Charlene K., 16th Nat. SAMPE Tech. Conf., Oct. 9-11, 1984.

49. " Repair Investigation of Bismaleimide Structure," Knight, Ronald C., 28th Nat. SAMPE Symp., April 12-14, 1983.

50. " Preliminary Evaluation Of Large Area Bonding Processes For Repair of Graphite/Polyamide Composites," Deaton, Jerry W., Mosso, Nancy A., 28th Nat. SAMPE Symp., April 12-14, 1983.

51. " Structural Repair Systems For Thermoplastic Composites," Weider, S.M., Lause, H.J., Fountain, R., 16th Nat. SAMPE Tech. Conf., Oct. 9-11, 1984.

52. " Development of Large-Area Damage Repair Procedures For The F-14A Horizontal Stabilizer Phase I-Repair Development," Mahon, John, Candella, James, 26th Nat. SAMPE Symp., April 28-30, 1981.

53. " Repair Of Post-Buckled Advanced Composite Fuselage Structure," 28th Nat. SAMPE Symp., April 12-14, 1983.

54. " Surface Treatments for Bonded Repair of Metals," Reinhart, Theodore, Bonded Repair of Aircraft Structures, pgs 19-30, 1988.

55. "Design and Analysis of Bonded Repairs for Metal Aircraft Structures," Hart-Smith, L.J., Bonded Repair of Aircraft Structures, pgs 31-48, 1988.

56. "Repair of Composite Aircraft," Williams, J.G., Donnellan, T.M., Trabocco, R.E., Repair of Aircraft Structures, pgs 175-211, 1988.

57. "Adhesives for Composite Joints," Lees, W.A., Bonding and Repair of Composites, 1989.

58. "Frictional Coupling for Bonding of Composites," Gradin, P.A., Boning and Repair of Composites, 1989.

59. "Bondability of Carbon Fibre Composites," Parker, B.M., Bonding and Repair of Composites, 1989.

60. "Structural Adhesive Bonding of Thermoplastic Fibre Composites," Kinloch, A.J., Kodokian, G.K.A., Bonding and Repair of Composites, 1989.

61. "Durability of Composite Joints Using Cold-Setting Adhesives," Matthews, F.L., Kinloch, A.J., John, S.J., Bonding and Repair of Composites, 1989.

62. "Low Energy Cured Composite Repair Systems," Lee, F., Brinkerhoff, S, McKinney, S., Bonding and Repair of Composites, 1989.

63. "A New Low-Temperature Rapid Curing Composite Material for Structural Repair," Subrahmanian, K.P., Davis, J.W., Marteness, B.A., Bonding and Repair of Composites, 1989.

64. "Feasibility of Welding Thermoplastic Composite Materials," Taylor, N.S., Jones, S.B., Bonding and Repair of Composites, 1989.

65. "Thermoplastic Interlayer Bonding of Aromatic Polymer Composites," Cogswell, F.N., Meakin, P.J., Smiley, A.J., Harvey, M.T., Booth, C., Bonding and Repair of Composites, 1989.

66. "Adhesive Bonded Joint Between a Fibre Composite Wing Blade and the Steel Hub of a Wind Turbine," Lystrup, A., Anderson, S.I., Bonding and Repair of Composites, 1989.

67. "FDEMS Sensors:In-Situ Monitoring of Adhesive Bondline and Resin Cure During Repair," Kranbuehl, D.E., Eichinger, D., Hamilton, T., Clark, R., Koury, J., Freeman,

T., Bonding and Repair of Composites, 1989.

68. "Further Developments in the Design and Analysis of Adhesively-Bonded Structural Joints," Hart-Smith, L.J., Joining of Composite Materials, ASTM STP 749, 1980.

69. "Improving Composite Bolted Joint Efficiency by Laminate Tailoring," Eisenmann, J.R., Leonhardt, J.L., Joining of Composite Materials, ASTM STP 749, 1980.

70. "Bolt Bearing Fatigue of a Graphite/Epoxy Laminate," Crews, J.H., Joining of Composite Materials, ASTM STP 749, 1980.

71. "Failure Analysis of Composite Laminates with a Fastener Hole," Soni, S.R., Joining of Composite Materials, ASTM STP 749, 1980.

72. "Static and Fatigue Strength of High Load Intensity Steel Hybrid Composite Bonded Scarf Joints," Macander, A.B., Joining of Composite Materials, ASTM STP 749, 1980.

73. "Design Data for Graphite Cloth Epoxy Bolted Joints at Temperatures up to 450K," Bailie, J.A., Duggan, M.F., Bradshaw, N.C., McKenzie, T.G., Joining of Composite Materials, ASTM STP 749, 1980.

REPAIR MANUALS

74. Boeing 767-200 Structural Repair Manual, Boeing Commercial Aircraft Co., P.O. Box 3707, Ms73-43, Seattle, WA, U.S.A.

75. Boeing 737-300 Structural Repair Manual, Boeing Commercial Aircraft Co., P.O. Box 3707, MS73-43, Seattle, WA, U.S.A.

76. "FRP Truck-Trailer Repair," Owens/Corning Fiberglas Repair Manual, 1975.

77. "Fiber Glass Repairability," A Guide and Directory to the Repair of Fiber Glass Commercial Fishing Boats," Owens/Corning Fiberglas, 1972.

78. "Repair of Fiberglas Boats," Owens/Corning Fiberglas, 1972.

U.S. PATENTS

79. "Method of Repairing Discontinuity in Fiberglass Structures," Fletcher, J.C., U.S. Patent, Patent # 3,814,645, February 1974.

80. "Process for Repairing Body Parts on Vehicles or the Like," Griffith, F.L.F., U.S.

Patent, Patent # 4.430,133, February 1984.

81. "Method of Repairing Ballistic Damage," Miller, R.W., U.S. Patent, Patent # 4,517,038, May, 1985.

82. "Method for Repairing Glass Fiber Reinforced Plastic Parts and Product," Faber, D.D., Holmes, R.G., Varano, J.J., U.S. Patent, Patent # 4,409,270, October 1983.

83. "Repair Laminate Sheet for Acrylic and Fiberglass Tubs," Thomas, W., Lucatuorto, P., U.S. Patent, Patent # 4,511,621, April 1985.

84. "Conductive Joint Seals for Composite Aircraft," Bannink Jr., E.T., U.S. Patent, Patent # 4,556,592, December 1985.

85. "Multiple Lap-Joint for Thermoplastic Laminates," Ritter, J.D., U.S. Patent, Patent # 4,564,543, January 1986.

86. "Aerospace Structure Having a Cast-In-Place Noncompressible Void Filler," Scollard, C.Y., U.S. Patent, Patent # 4,861,643, August 1989.

JOURNALS

87. "Static and Vibration Analysis of Laminated Composite Beams with an Interlaminar Shear Stress Continuity Theory," Lee, C.Y., Liu, D., Lu, X, Inter. Journal for Numerical Methods in Engineering, vol. 33, 409-424, 1992.

88. "The Crush Behavior of Pultruded Tubes at High Strain Rates," Thornton, P.H., Ford Motor Company, Journal of Composite Materials, Vol. 24, June 1990.

89. "The Strength of Composite Repair Patches: A Laminate Analysis Approach," Matthews, F.L., Robson, J.E., Kinloch, A.J., Journal of Reinforced Plastics and Composites, Vol. 11, July 1992.

90. "Energy Absorption of Composite Materials," Farley, G.L., Journal of Composite Materials, Vol. 17, May 1983.

91. "Energy Absorption in Composite Tubes," Thornton, P.H., Ford Motor Company, Journal of Composite Materials, Vol. 16, p.p. 521-545, November 1982.

92. "Energy Absorption in Composite Structures," Thornton, P.H., Ford Motor Company, Journal of Composite Materials, Vol. 13, p.p. 247-260, July 1979.

NASA TECHNICAL MEMOS

93. "Adhesively Bonded Double-Lap Joints," Hart-Smith L.J., Nasa Langley Research Centre, Rept. Nasa CR-112235, January 1973.

94. "Simplified Procedures For Designing Adhesively Bonded Composite Joints," Chamis, C.C., Murthy, P.L.N., Lewis Research Center, Tech. Memo #102120, 1989.

95. "Preliminary Design of Adhesively Bonded Composite Joints," Chamis, C.C., Murthy P.L.N., Nasa Lewis Research Center, Nasa Tech Briefs, October 1992.

96. "Damage-Tolerant Composites Made by Stitching Carbon Fabrics," Dow, M.B., Nasa Langley Research Center, Smith, D.L., Planning Research Corp., Nasa Tech Briefs, November 1992.

97. "Stiff, Strong Splice for a Composite Sandwich Structure," Nasa Ames Research Center, Nasa Tech Briefs, ARC-11743.

98. "The effects of Crushing Speed on the Energy-Absorption Capability of Composite Material," Nasa Langley Research Center, Nasa Technical Memo 89122, March 1987.

ANNUAL REPORTS

99. R.E. Robertson, "A Repair Methodology for Fiber-Reinforced Composite Structures," Final Report submitted to Michigan Materials and Processing Institute, July 1992.

100. Dahsin Liu, C.Y. Lee, X. Lu, "Repairability of Damaged Structural Composites," an Annual Report submitted to Michigan Materials and Processing Institute, September 1991.

101. K. Zimmerman and D.Liu, "An Experimental Investigation on the Repairability of Damaged Structural Composites, an Annual Report submitted to Michigan Materials Processing Institute, September 1992.

ADDITIONAL PAPERS

102. D. Liu, "Delamination Resistance in Stitched and Unstitched Composite Plates Subjected to Impact Loading," Journal of Reinforced Plastics and Composites, 9(1), pp59-69, 1990.

103. Lee, C.Y., and Liu, D., "An Interlaminar Stress Continuity Theory for Laminated

Composite Analysis," Computers and Structures, 42(1), pp 68-78, 1992.